Technical and Cost Assessment of the PCAST Machine

Final Report

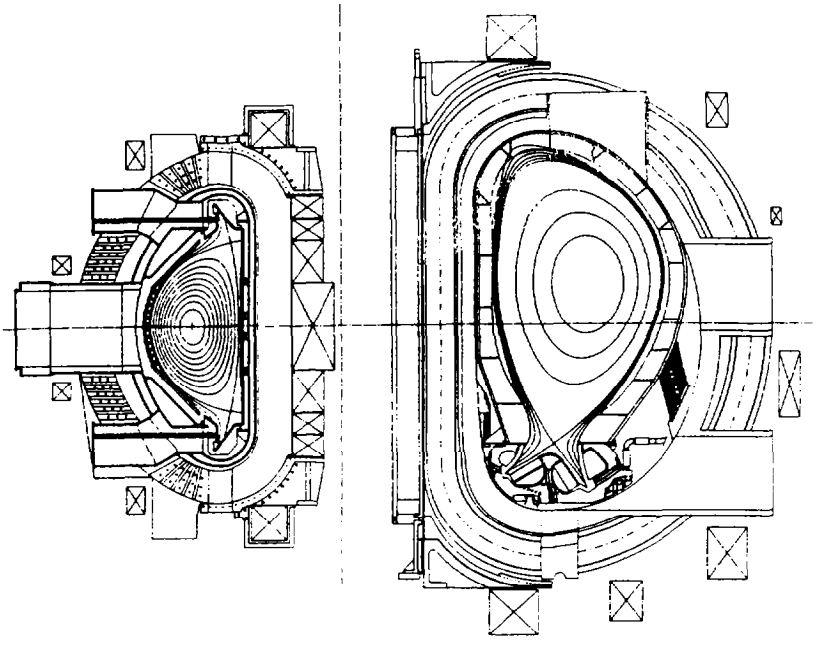

PCAST ITER

Volume II

Chapter 3.0 Engineering

prepared by
PCAST Study Group
December, 1995

91-951208-MIT/DBMontgomery-01

Technical and Cost Assessment of the PCAST Machine

— Final Report —

Volume II

Chapter 3.0 — Engineering

Chapter 4.0 — Cost

Contents

Chapter 3 — Engineering

Chapter 3

Engineering Design of the PCAST Machine

Introduction (J. Schmidt, J. Sinnis and T. Brown):

This chapter describes a tokamak design selected to meet the objectives set forth in the PCAST report. Namely, to see if there is a device that could meet the ITER physics mission of ignition and sustained burn at a fraction of the cost of ITER by eliminating the technology requirement of neutron fluence, breeding blankets and 1,000 second pulse lengths.

Time and funding were not available to fully optimize the design point selected. However, the trade studies discussed in Chapter 2 were carried out to assess the sensitivity of the design point to optimization factors.

Based on ITER physics rules and experience with previous designs, a five meter major radius, higher field (B_t=7 T, Ip=15.3 MA) design point was selected. Increased plasma current and associated performance are achieved by stronger shaping (kappa_95=1.75 and delta_95=0.45) than employed in the ITER design. This increase in plasma shaping relative to ITER is facilitated by the copper magnet configuration.

The design incorporates cryogenically cooled copper coils that depend on their thermal inertia to achieve the required pulse length. With the exception of one pair of central solonoid coils the magnets are cooled to 80° K with helium gas to limit end of pulse temperatures and power consumption. A pair of high current density CS coils are further precooled to 30°K with helium gas to provide the required pulse length.

The fusion power of 400 MW is sustained for three helium accumulation times (~120 seconds). The plasma current is ramped up to 15.3 MA in 25 seconds, 15 seconds is provided for heating to ignition and 120 seconds is provided for the burn duration.

Strong shaping leads naturally to a double null divertor design which was adopted for this study. The double null configuration is provided by a poloidal field (PF) magnet set that is symmetrical about the midplane. The PF consists of fourteen coils (PF#1-#7 upper and lower), that are powered in pairs to provide shaping and the required flux swing of 217 webers. PF#1 in the central solenoid is sub-cooled to 30° K (with gaseous helium) to limit its peak temperature and energy consumption.

As in the ITER design, the TF centering force is reacted by "bucking" against the central solenoid. However, the stronger shaping requirements of the PCAST Machine result in fringing fields from the central solenoid that produce increased out of plane loads on the inner leg of the TF coil. A compensating feature of this design is the relatively thick cross-section of the TF magnet which provides the required stiffness to support the increased loads.

The TF magnet consists of 16 coils. It is supported against out of plane loads by an ITER type "crown/rail" system at the top and bottom of the coil and, on the outboard side, by intercoil structure between the coil cases. The TF winding pack consists of two 25 turn pancakes with a coolant tube soldered into the edge of each turn. The current per turn is 219 kilo amperes. The loads on PF#1 are such that the TF must be at full field to help react the loads at initial magnetization. This, plus the current ramp, heating and burn times result in a 160 second requirement for the TF flat-top time. Starting at 80°K, the TF reaches a peak temperature of 244°K at the end of the pulse. (*Note*: This does not include magneto resistive effects which are estimated to increase the peak temperature by less than 15 degrees.)

Structural analysis of the magnet show acceptable stresses based on both static and fatigue considerations. A full fracture mechanics analysis has not been performed.

All plasma facing components are carbon based, actively cooled, and are supported off of the vacuum vessel wall. The divertor is a double null with a 0.93 m "deep Vee" configuration, it is designed to accommodate the 4.4 MW/m^2 power density of the high recycling mode of operation. The divertors are pumped through sixteen pump ducts (eight top and eight bottom) which employ

turbomolecular pumps All internal components are of modular construction to facilitate remote maintenance.

The remote maintenance system has been modeled after ITER's with modest changes to account for the differences in the scale of the two facilities and the large differences in fusion energy production. The PCAST in-vessel RM system incorporates relatively short (90° reach), stiff articulated booms. Port access to the interior of the vessel is provided at four toroidal locations spaced symmetrically in each quadrant of the vessel. This arrangement permits two booms to work on a given maintenance task simultaneously. The strategy is to have one function as a dexterous manipulator and the other to provide the lifting capability.

The vacuum vessel is a double walled structure, the vessel material is Inconel 625. A steel-water neutron shield fills the space between the walls to reduce the nuclear heating of the magnets and limit the radiation dose to the magnet insulation. This shield, combined with intervening structure, reduce the neutron heat load to the TF magnet to 5% of the 320 MW of neutron power produced. The vessel wall incorporates close fitting structure to slow down the vertical instability of the plasma. Sets of internal control coils are used to provide stability on longer (~10 ms) time scales. The vessel design includes 16 large mid-plane ports with dimensions (w X h) of 1.4m X 2.6m. Two ports are allocated to ICH launchers, two to NINB (each neutral beam port can accommodate two injectors), one port is provided for a possible RF upgrade and four locations are assigned to remote maintenance. The remote maintenance port locations combine the functions of tangential viewing access for diagnostics and tangential injection for beams with radial access for maintenance. The operating temperature of the vessel is 100°C with a 350°C bake-out temperature. The tokamak is enclosed in a stainless steel vacuum cryostat.

The auxiliary heating systems consist of a combination of ion cyclotron heating (ICH) and negative ion neutral beams (NINB). The two ICH launchers are similar to the ITER design, each consisting of eight current straps in a four by two array. The frequency and current strap phasing capability of the system permits direct ion heating of either deuterium or tritium ions, and electron

heating (with the option of on axis current drive). Each launcher provides 15 MW to the plasma.

The 30 MW NINB system consists of three 500 kV JT-60U type injectors modified for long (135 second) operation. They are arranged in a two co, one counter direction aimed at $R=R_0-2a/3$.

Primary power requirements are met by utilizing a combination of motor generator sets and utility power. The operating scenario meets the ITER site criterion of 650 MW maximum utility power with power level changes limited to 200 MW/s. The configuration includes 4 MG sets to augment the utility capacity and 295 MVA of reactive power compensation to meet the utility constraint of 500 MVAR. A set of switched rectifiers are employed in the PF circuit to meet the high peak power requirement at the beginning of the pulse and the large energy requirement during the 120 second burn. These rectifiers are fed from the MG sets when high power is required and are switched to the utility grid during the burn phase.

The cryogenic plant required to support experimental operations consists of a 7.5 MW liquid nitrogen plant and an 80 kW 30°K helium gas refrigerator to provide the subcooling for PF#1. To minimize the capital cost of the refrigeration system, the plants will operate 24 hours per day with the machine pulses spaced at approximately equal intervals during this period. This simplifies the design of the magnet cooling by providing over four hours for cool-down between pulses.

The site and facility requirements have been modeled after ITER's with adjustments made to reflect the differences in scale and mission as well as in design. The smaller size of the PCAST Machine permits a reduction in the size of the Tokamak, Assembly and Laydown halls while the use of MG sets requires the addition of this facility. Compared to the overall machine size, relatively more space has been provided in the PCAST test cell and assembly halls for ancillary equipment and laydown space. This has resulted in a facilities cost that is higher than would be expected from machine size considerations. The large facility costs in general and the modest (35%) reduction from ITER in particular suggest the existence of sizable cost

improvements that can be identified through future value engineering.

This study is at a pre-conceptual level of detail and maturity, time did not permit optimization of the design or more thorough investigation of alternative approaches. However, two alternate magnet configurations were considered, a beryllium copper plate type magnet in a wedged configuration and a C-mod type sliding joint TF design. The BeCu magnet suffered from excessive power dissipation while the C-mod approach was considered to be too avant-garde for a device of this scale.

The following sections of this chapter provide more detail on the illustrative example selected for this study.

Section 1.0 Configuration Framework

The primary configurational features for the PCAST design point were discussed in the preceeding section. Additional configuration related design choices are as follows:

- As summarized in the preceeding section the ITER bucked magnet configuration was adopted using the solenoid as a bucking cylinder and supporting the out-of-plane magnetic forces with a combination of intercoil structure, upper and lower crown structures and the stiffness of the coil case.

- The configuration is designed for remote maintainability, allowing components to be maintained using existing or near-term remote maintenance equipment.

- Sufficient access to the plasma chamber is provided to meet operational objectives (tangential injection, divertor pumping, diagnostic access, invessel service access, maintenance).

- A minimum set of TF coils are configured to allow near tangential beam access with adequate port space to meet remaining heating, maintenance and diagnostic requirements.

- The vacuum pumping system is configured to be in a hands-on environment.

- The TF coil bore is sized to allow vacuum vessel port/weld interfaces to be rotated within the TF enclosure.

- The invessel services and diagnostics are configured to optimize interfaces with external facilities.

- The diagnostics and services from the cryostat dome are restricted to enhance ease of access to the tokamak core components.

Tokamak Build

The radial build dimensions established for key components and the gaps set for assembly tolerances are summarized in Table 1.0-1. Starting from a physics specified 10 cm inboard plasma scrape-off, 9.5 cm was allocated to the inboard first wall components (first wall tile and support plate structure) and 12.7 cm set aside for first wall alignment space, coolant connections and invessel diagnostics. 25.4 cm was allocated to the inboard double wall vacuum vessel structure; 4.45 cm per shell wall and 16.5 cm shielding space. TF analysis set the space requirement of the copper winding and case structure for the TF inboard leg. Additional space was added for insulation and assembly tolerances to bring the total inboard TF leg build up to 109.5 cm. 6.6 cm was allocated for thermal insulation, manufacturing and assembly tolerances between the TF and VV. The vacuum vessel space was increased on the outboard side of the plasma to provide added vessel stiffness and increased space for shielding. Space for a larger outboard vacuum vessel build dimension was anticipated given the need to position the TF coil outer leg to meet a near tangential beam access requirement. The placement of the TF outer leg position was checked to assure field ripple requirements were also satisfied. Further breakdown of the radial build can be found in Table 1.0-1.

COMP	COMP BUILD		COMP DIM	TOTAL Build
	Machine Center			0.0
OH	Nominal winding thk	95.51	100.904	65.5
	Total transition space	5.08		
	Total ground wrap	1.58		
	Ext OH structure	1.65	2.159	167.7
	OH TPT	0.25		
	TF TPT	0.25		
	OH/TF gap	0.00		
	OH/TF defl	0.00		
inbd TF	Wedge side case thk	8.00	109.474	169.9
	Winding thk	91.44		
	Total ground wrap	1.14		
	Total coil/case gap	3.81		
	Coolant space	0.00		
	Inner wall thk	5.08		
	Trapezoidal Effect	5.38	13.005	279.4
	TF TPT	0.95		
	Minimum TF/VV gap	2.54		
	VV TPT	0.95		
	Insulation	3.18		
inbd VV	VV shell thk	4.45	25.400	292.4
	Borated water	16.51		
	VV shell thk	4.45		
	TPT	1.27	32.225	317.8
	VV/FW space	11.43		
inbd FW	FW thk	9.53		
	5 cm SOL @ RT	10.00		
	Plasma minor radii	150.00	150.000	350.0
------- --	-------- -- ------- --	------- --	-- -------	500.0
	Plasma minor radii	150.00		
	outbd SOL@ RT	3.00		653.0
PL	Poloidal Limiter thk	7.62		
	PL support post thk	15.24		675.8
	gap	25.40		701.2
outbd VV	VV shell thk	4.45		
	Borated water	29.21		
	VV shell thk	4.45	38.1	739.3
	Insulation	3.81		
	VV/TF outbd gap	56.85		800.0
outbd TF	Inner wall thk	8.00		
	Winding thk	91.44		
	Total ground wrap	1.14		
	Total coil/case gap	3.81		
	Coolant space	0.00		
	Outer wall thk	8.00	112.4	912.4
	TF/Cryostat gap	128.10		
	Cryostat thk	45.72		1086.2

Table 1.0-1 Radial Build Dimensions (cm)

Machine Description

The primary features of the PCAST configuration are highlighted in the plan view of Figure 1.0-1 and elevation view of Figure 1.0-2. A basic core module consists of two TF coils and the included vacuum vessel, as shown in Figure 1.0-3.

Plasma Facing Components (PFC)

As summarized in preceeding sections of this report the Plasma Facing Components include modularized double null divertor sections and additional wall coverage for plasma heat removal and wall protection. Plasma facing surfaces are covered with carbon composite materials. Passive plate structures provide short time scale passive stabilization of plasma motion. Long time scale stabilization of plasma motion is provided by two coils behind located inside the vessel.

The general configuration provides plasma chamber access to extract PFC components through horizontal ports. Divertor modules and their supports are designed to allow divertor modules to be extracted vertically (up or down) to the center of the plasma chamber and then removed out through the large horizontal ports. This arrangement provides the simplest approach for divertor support, alignment and maintenance.

To maximize maintenance feasibility/availability, four vessel ports are allocated to the invessel remote maintenance systems. Removing a divertor module with a 90° rotation, while in its centered horizontal position, allows subdivision of the divertors into 16 modules. Module weight for this segmentation approach may be within the weight limitations of a planned boom mounted manipulator remote maintenance system. However, for this scoping study, a lighter weight, 32 module divertor segmentation approach was developed for the baseline design. Divertor module segmentation is arranged with module gaps aligned to the centerline of the pump ducts. This was done to provide viewing access space, between modules, for diagnostics. Divertor services are routed through horizontal pump ducts where an internal remote disconnect is required, close to the module, prior to its extraction.

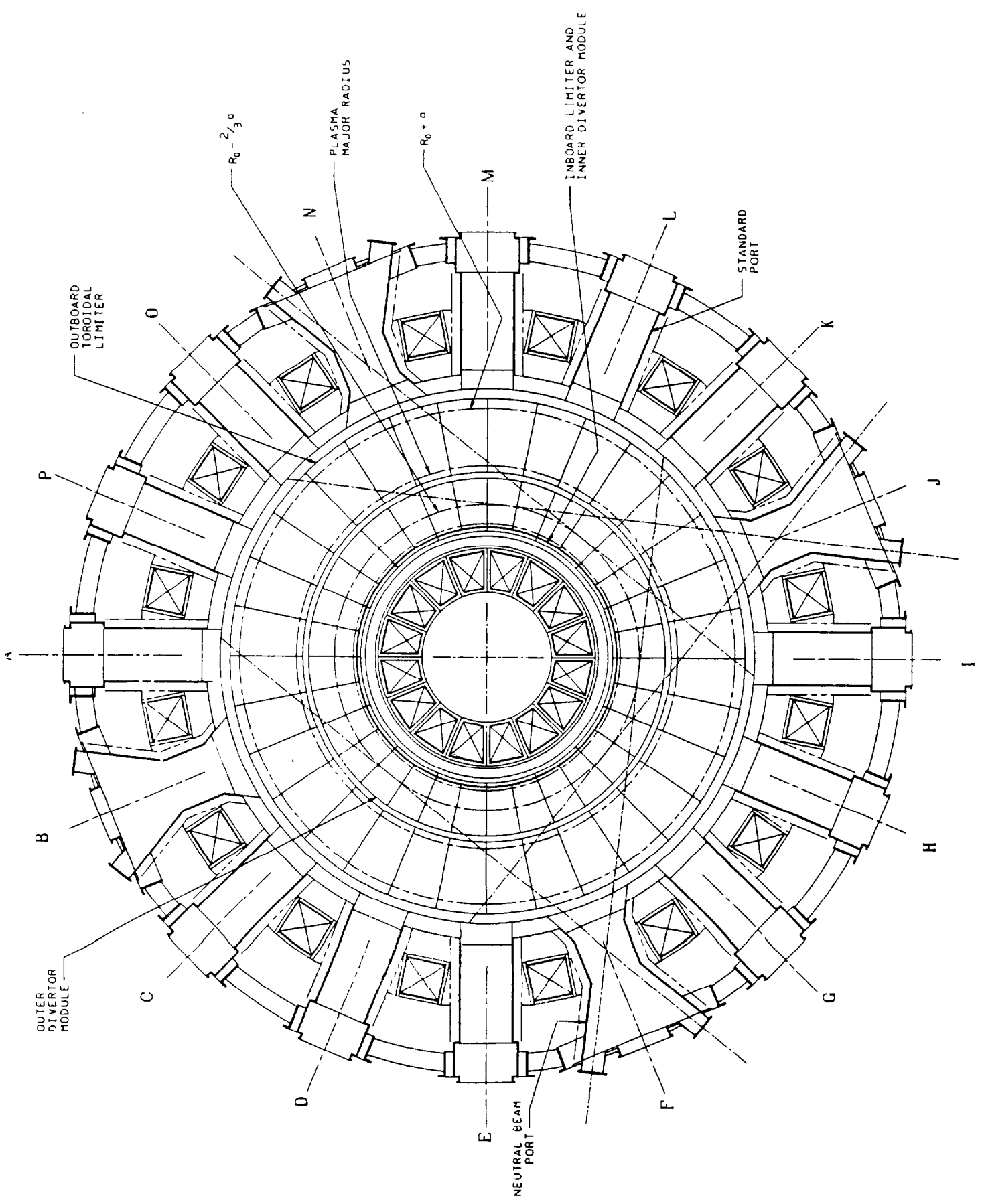

Figure 1.0-1 PCAST Device Plan View

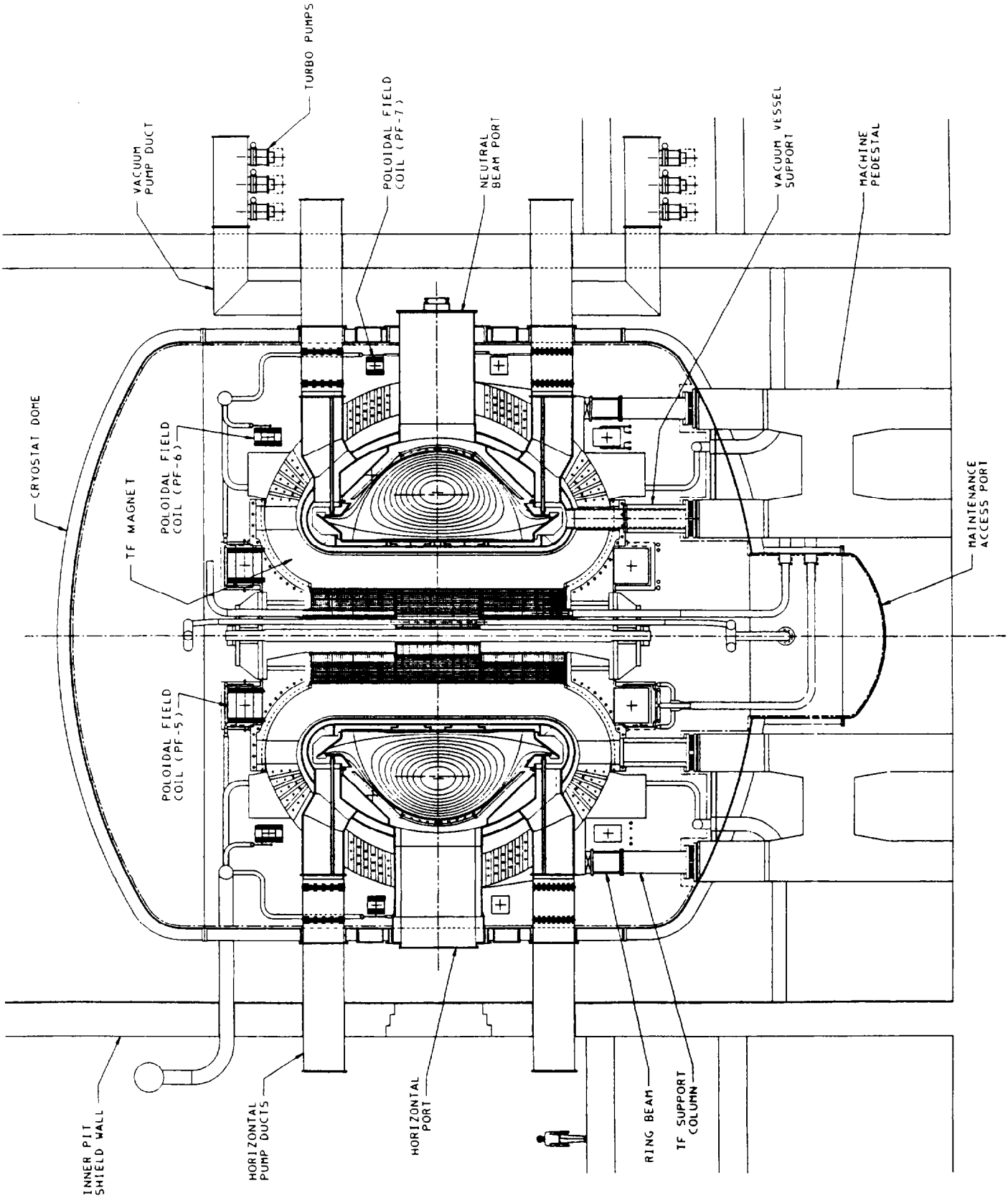

Figure 1.0-2 PCAST Device Elevation View

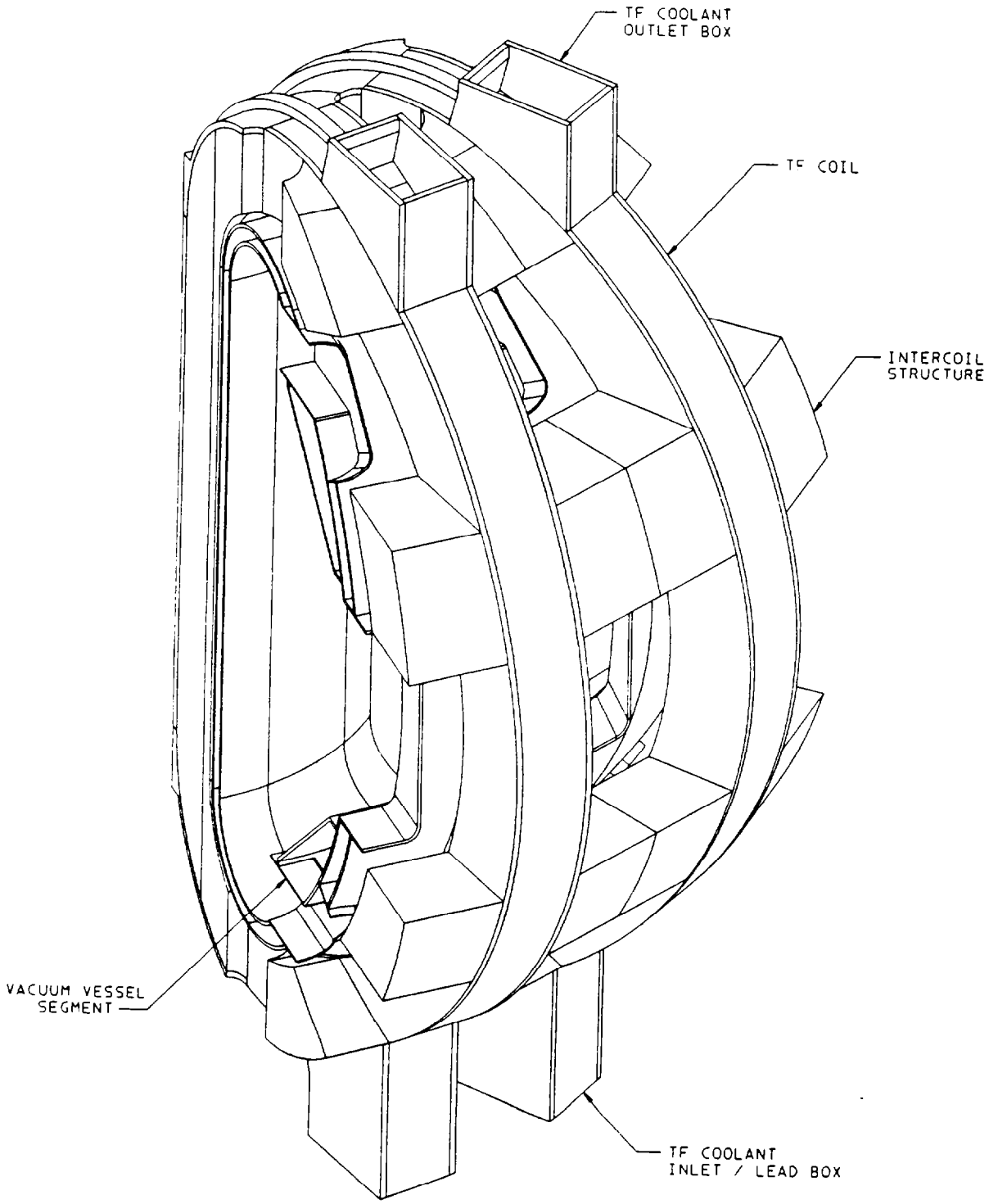

Figure 1.0-3 Two Coil Module Isometric View

Vacuum Vessel

A double wall, inconel, vacuum vessel was configured to provide space for all plasma facing components, their mounting structure and invessel diagnostics. The basic vacuum vessel geometry was formed with a straight inner shell and two circular arcs that enclosed the divertor sections and plasma. A secondary structure was added to the outboard vacuum vessel regions (top and bottom) to improve plasma stabilization and add additional shielding space in front of the divertor pump ducts. The passive plate structure was supported from the inner shell, in close proximity to the plasma, yet provided sufficient space in front of it for first wall tiles, mounting structure, magnetic diagnostics and an internal control coil.

Divertor pumping was provided by horizontal pump ducts, located above and below the horizontal midplane ports. The pump ducts were extended locally into the region of the stabilization structure to provide additional access space to route internal services out of the vacuum vessel.

Two types of horizontal ports have been developed: a standard port, and a neutral beam port. The standard port has a 2.64 m vertical by 1.37 m horizontal clear opening that provides access to insert external components radially into the vacuum vessel port. An additional 20 cm was allocated at the top and bottom of the ports to provide space to route services out of the ports, above the vacuum flange opening. Neutral beam ports are dimensionally the same as the standard port at the ports midsection, but two auxiliary ports are added at the ends to allow negative ion beams to be attached with a near tangential view of the plasma. A center port (dimensionally the same as in the standard port) is located midway between the auxiliary beam ports.

The vacuum vessel will be formed in eight 45° segments with the on-site assembly weld joints located at each end, bisecting standard horizontal ports and upper and lower divertor ports. Vertical diagnostic ports will be restricted to the center region of the 45° vacuum vessel segment.

TF Coils

The TF coil configuration impacts the overall plasma chamber access and maintainability features of the design. A sixteen TF coil configuration was selected and sized to meet near tangential beam access requirements, provide additional space for port shielding and also allow the vacuum vessel (less ports) to be rotated freely within the bore of the coils. Field ripple requirements are also met with this number and size of coils. A twenty coil configuration was evaluated but was found to be more confining, providing less tangential access space as well as reduced vertical access for lower supports and diagnostics.

Space for TF coolant lines were provided at the lower and upper region of the coil just outboard of the TF crown structure. Intercoil structure is located at all spaces not occupied by the horizontal, diagnostic, and vertical ports. Two TF coils and an included vacuum vessel form an assembly module with a combined weight of approximately 781 tonne.

PF

The cryogenically cooled copper PF magnet includes an 8 section solenoid coil and six ring coils that encircle the TF coils. The PF coils are supported from the TF. The outermost ring coil (PF7) was configured with an inner radius that allows the coil to be installed (removed) over the back leg of the TF coil. Coolant services enter the lower cryostat dome and are subdivided into local manifolds that supply coolant to each coil. Returning coolant exits through local return manifolds and return lines that pass through the upper cryostat shell. Installed in the core of the solenoid are tie rods to react the vertical separating force experienced by the solenoid. In addition, the solenoid core contains a structure to react the component of the TF centering force which is not supported by the solenoid magnetic load.

Divertor Pumping

Locating divertor pumps in a hands-on environment was accomplished by moving the pumps outside of the tokamak core area (locating them behind the inner pit wall) and using large pump ducts to meet the pumping

conductance requirements. The PCAST design pumping system incorporates a total of sixteen pump ducts, eight top and eight bottom, located symmetically about the torus. Three turbopumps are attached beneath the 122 cm diameter pump ducts that extend throught the inner pit wall. The pump ducts are vertically offset from the larger horizontal ducts (145 cm diameter) that pass from the vacuum chamber out through the interior pit shield wall, as shown in the elevation view of Figure 1.0-2. To minimize neutron streaming the bend in the pump ducts are placed between the cryostat and inner pit wall to form a labyrinth passageway. The distance between the cryostat and the inner pit wall was set at 2 m to provide the required space for the angled pump duct as well as increase the available space for remote maintenance.

Divertor and vacuum vessel coolant services pass through a local shielded labyrinth plug at the end of all straight radial ducts before exiting the inner pit shield wall. At locations where divertor pumps are located only divertor coolant lines are present, no other vacuum vessel services or diagnostics are allowed.

Cryostat

The cryostat consists of an upper dome structure, an upper and lower shell structure (with openings for divertor pumping and services), a midsection shell structure (containing openings for the large horizontal ports), and a domed base structure. Additional supports have been added to the domed base structure to provide a horizontal platform from which to locate the machine gravity supports. No services penetrate the upper dome but maintenance access ports would be provided to gain quick access to the tokamak core. The cryostat base is supported off the test cell floor from local columns to a height of 7 m.

Machine Support

The TF coils, and those systems supported from it, are supported from a continuous circular ring beam structure and a lower crown structure as shown in the elevation view of Figure 1.0-2. The outer ring structure provides greater seismic stability than a support system with the crown structure

alone. The ring beam can also be used during initial installation for positioning and aligning the coils.

Guide pins, protruding downward from the base of the TF coil structure, will ride in radial slots attached to the support ring. The guide pin will transmit seismic horizontal forces from the TF coil structure into the support ring. Support against upward vertical forces will be provided by vertical restraints attached to the support ring.

The lower crown structure (as in the baseline ITER design) is also used for out-of-plane support. The TF outer ring structure and lower crown structure are supported from the cryostat base using low conductivity titanium structures tied to a Hilman roller support system that allows radial movement but provides support against vertical and tangential motion.

Port Allocation

The general arrangement of heating, diagnostic and auxiliary equipment is shown in the plan view drawing of Figure 1.0-4. Port allocations are schematically represented in the port allocation drawing of Figure 1.0-5 and Figure 1.0-6.

Neutral beam ports are located at four locations, 90° apart (Bays B, F, J and N). The large central opening of each beam port has been designated a remote maintenance port, allowing four RM systems to operate within the vacuum vessel. Bays C and D have been designated ICH ports and bay B an rf upgrade port. Two Negative Ion Beams are located in port J and one on the south side of port F. Capabilities to add a fourth NIB on the north side of port F has been factored into the design. The location of the NIB's and rf equipment has been arranged to eliminate beam shine through onto the rf system.

Diagnostic equipment can be located in the upper and lower divertor ducts at the eight positions where pumping is not located. Vertical ports will be restricted to the center location of all vacuum vessel 45° segments. Off-vertical viewing (into the divertor baffle) may be possible at selected locations. All diagnostic services will be routed through the divertor ducts or local

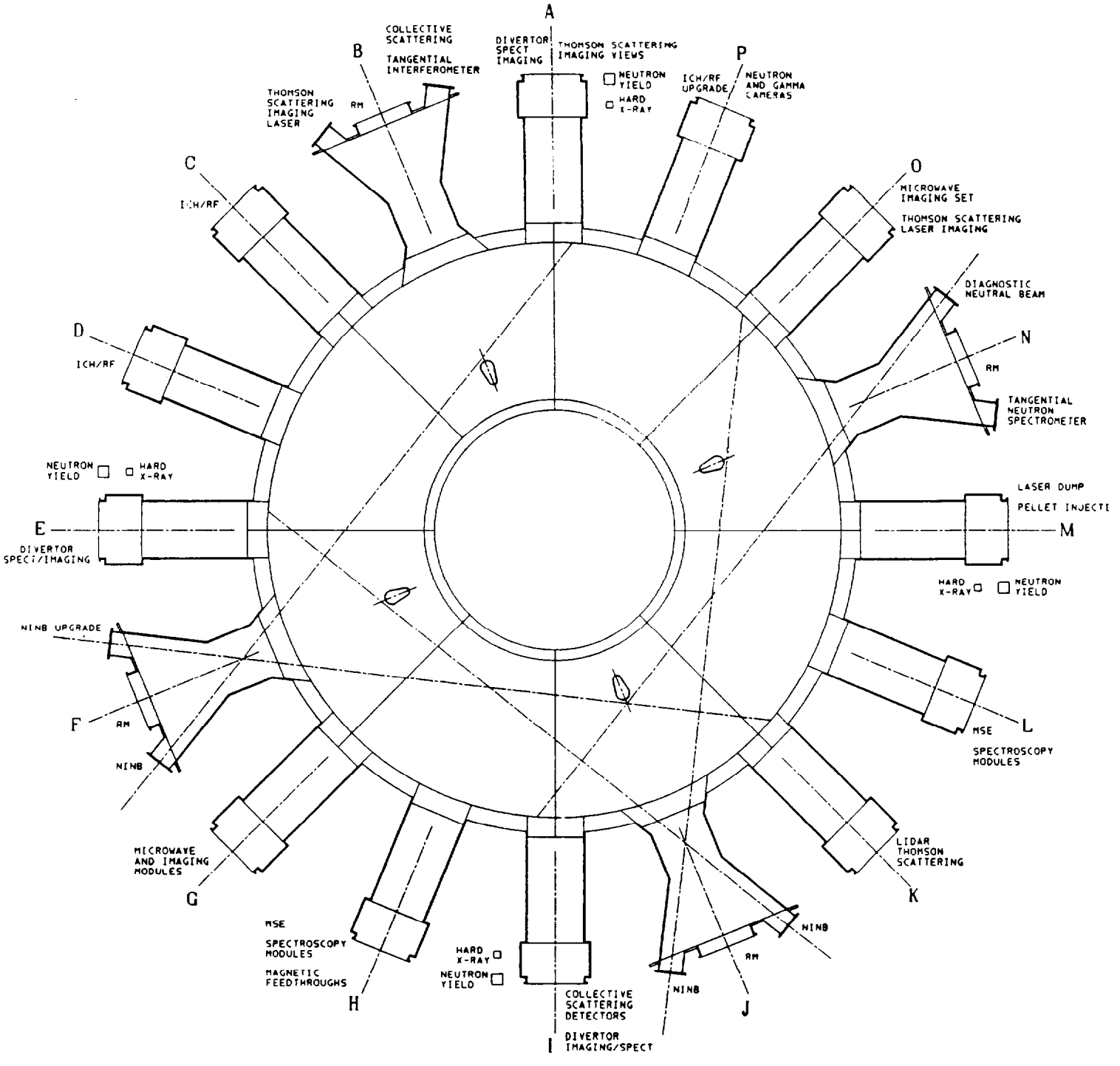

Figure 1.0-4 Equipment General Arrangement

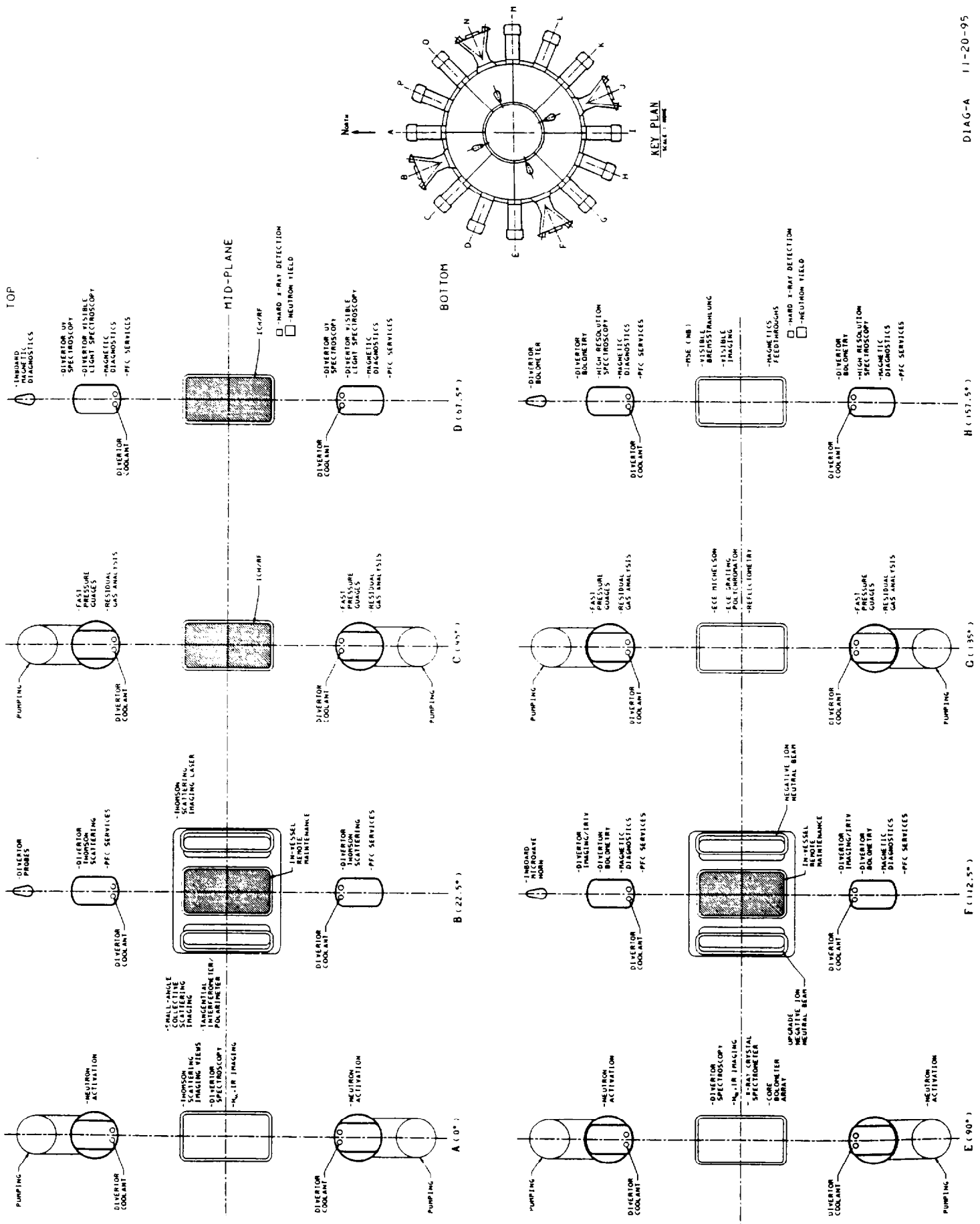

Figure 1.0-5 Port Allocation Schematic (Bays A - H)

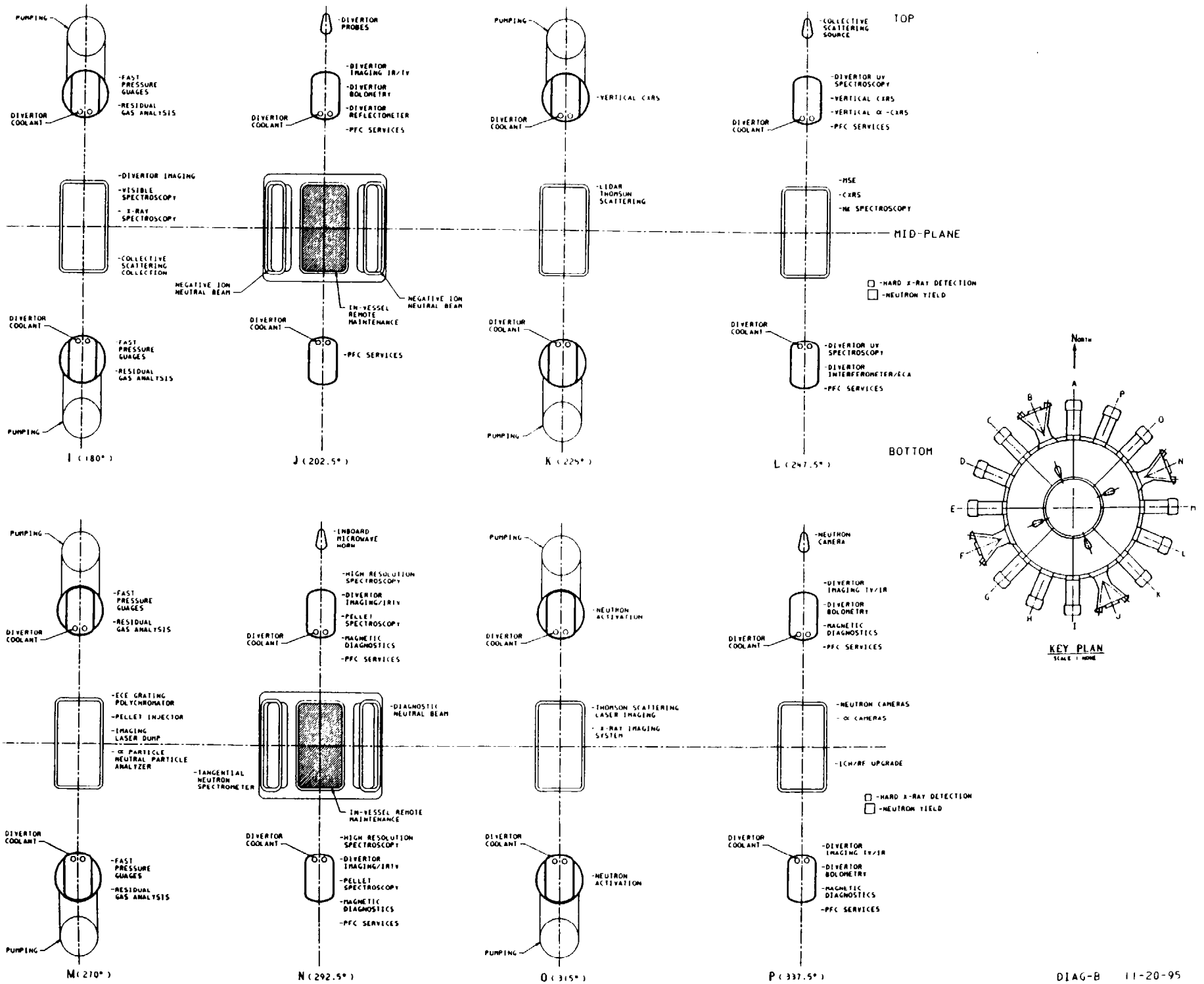

Figure 1.0-6 Port Allocation Schematic (Bays I - P)

horizontal vacuum pipes that pass through the upper and lower cryostat shell.

Test Cell Layout

Plan and elevation views of the PCAST device in the test cell are shown in Figure 1.0-7 and Figure 1.0-8 . The test cell arrangement developed for PCAST follows the ITER building design approach with a few added configuration changes. As stated earlier, the distance between the inner pit wall and cryostat (when compared with ITER) was increased to provide space to develop a labyrinth passageway to the divertor turbopumps, which are located behind the inner pit wall. In addition to the needs of pumping, an increase in cryostat-to-inner pit wall distance was required to provide space to introduce inspection and maintenance equipment, from above, to service/inspect magnet system services and their cryostat penetrations.

The 12.5 m distance between the outside of the inner pit wall and the shield outer wall was maintained in the PCAST test cell arrangement (as in ITER), although four local alcoves were added to accommodate the geometry layout required for the JT-60U negative-ion based neutral beam system. Allocated space for four negative ion beams were established on the test cell south side. Vertical shield walls were added on one side of each NIB to form a shielded containment room, to house two negative ion neutral beams and the included remote maintenance system. The NIB themselves are surrounded with local shield blocks in an effort to minimize the activation within the NIB containment room. With a combination of local shielding added within the NIB horizontal port, local shield blocks surrounding the NIB pumping units and with the sources located away from the device (per the JT-60U design), it is hoped that hands-on-maintenance (some period after shut down) might be possible at the NIB sources. In any case, the NIB cell would be designed to have full crane access from above.

It is expected that components that access the remaining horizontal ports would have sufficient local shielding that will allow hands-on maintenance outside the inner pit shield wall.

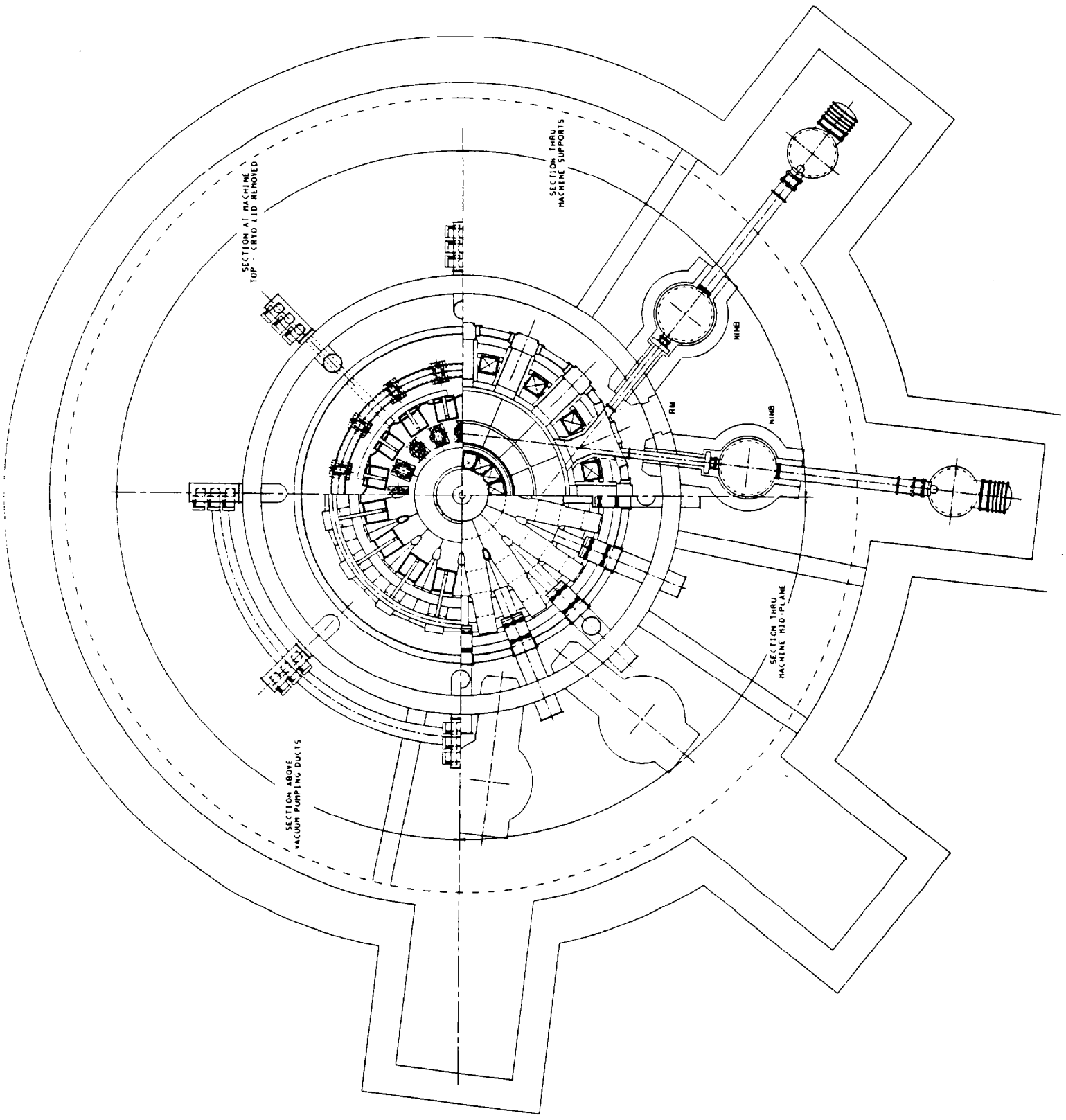

Figure 1.0-7 Plan View of the PCAST device within the Test Cell

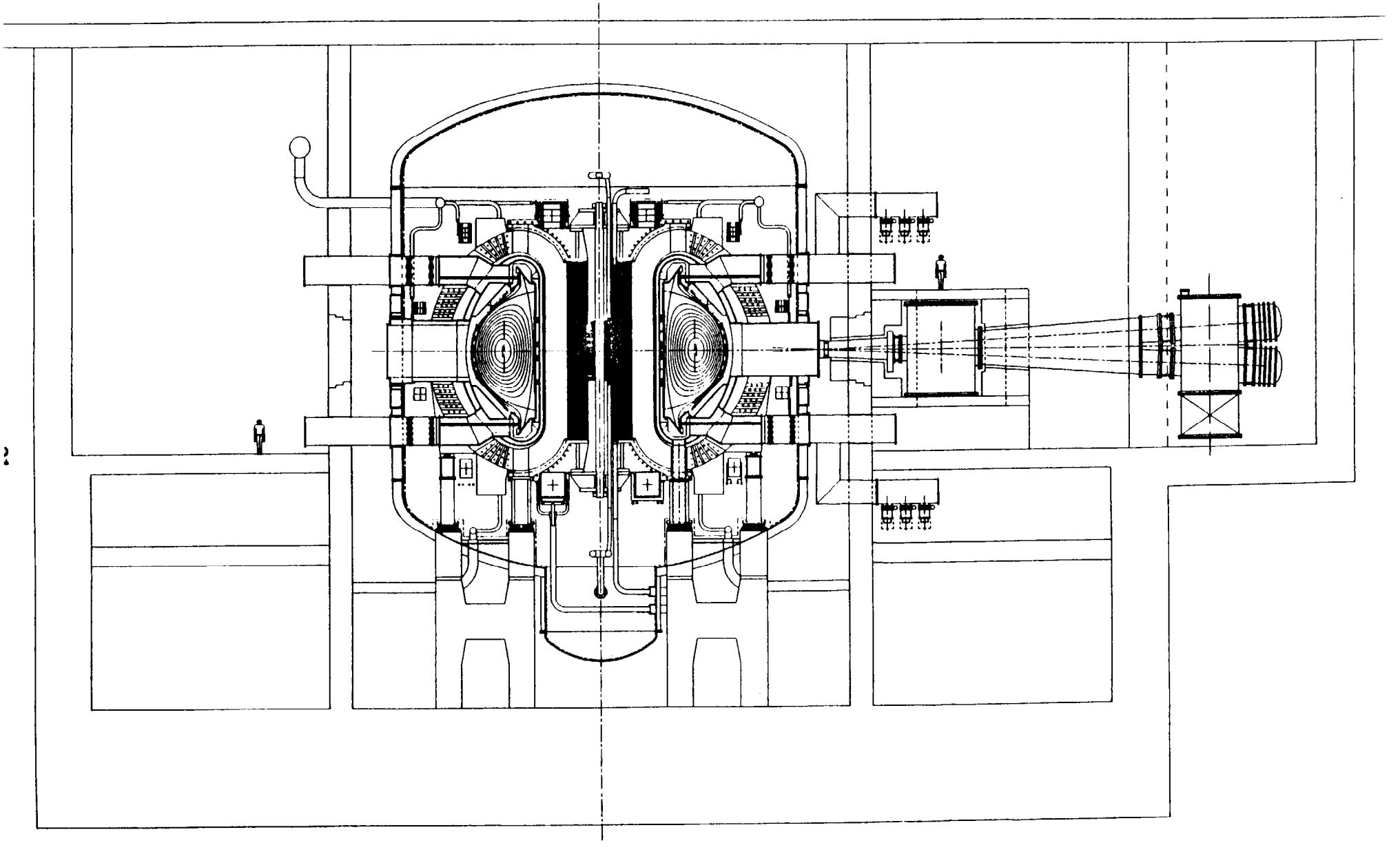

Figure 1.0-8 Elevation View of the PCAST device within the Test Cell

Section 1.1: Magnet System Overview (J. Citrolo)

The PCAST Machine magnet system consists of a set of 16 Toroidal Field (TF) coils, a Central Solenoid (CS) with a symmetric set of 4 coils (PF's 1 thru 4), and 3 sets of symmetric ring coils (PF's 5 thru 7), encircling the TF coils. In addition, there are two sets of control coils located within the vacuum vessel. Figure 1.1-1 is an elevation view of the PCAST Machine magnet system.

All the coils are normal resistive copper coils cryogenically cooled between pulses. All coils heat up adiabatically during the pulse. The TF current waveform is such to provide a flattop time of 160 seconds for a plasma burn time of 120 seconds. All the TF coils and all the PF coils except PF - 1 start from an initial temperature of 80°K and are cooled with gaseous helium. The maximum temperature reached by the TF coils is 244°K. Cooldown time between pulses for the TF is approximately 4.8 hours.

PF's 1 Upper and Lower start from an initial temperature of 30°K and are cooled with gaseous helium. They reach a maximum temperature 216°K and also require 4.8 hours to cool down. PF 1 starts at 30°K to take advantage of the low resistance of copper at these temperatures and minimize electric power, total energy and cooldown time and to limit the maximum coil temperatures.

Poloidal Field coils 2 thru 7 Upper and Lower, start at an initial temperature of 80°K. The hottest coil at the end of the pulse is PF 5 with a maximum temperature of 141°K.

Helium is used as the cooling fluid regardless of starting temperature to avoid the high pressures that would be needed to avoid the two phase and film boiling problems that would be present in a liquid nitrogen system.

The structural support concept for the TF coils and the Central Solenoid is an adaptation of the ITER design modified for copper coils. The TF coils are in stainless steel 316 LN cases which provide support to the winding pack for both in plane loads due to the TF centering forces and out of plane loads from the interaction of the TF current with the poloidal field. As in ITER, the coil cases

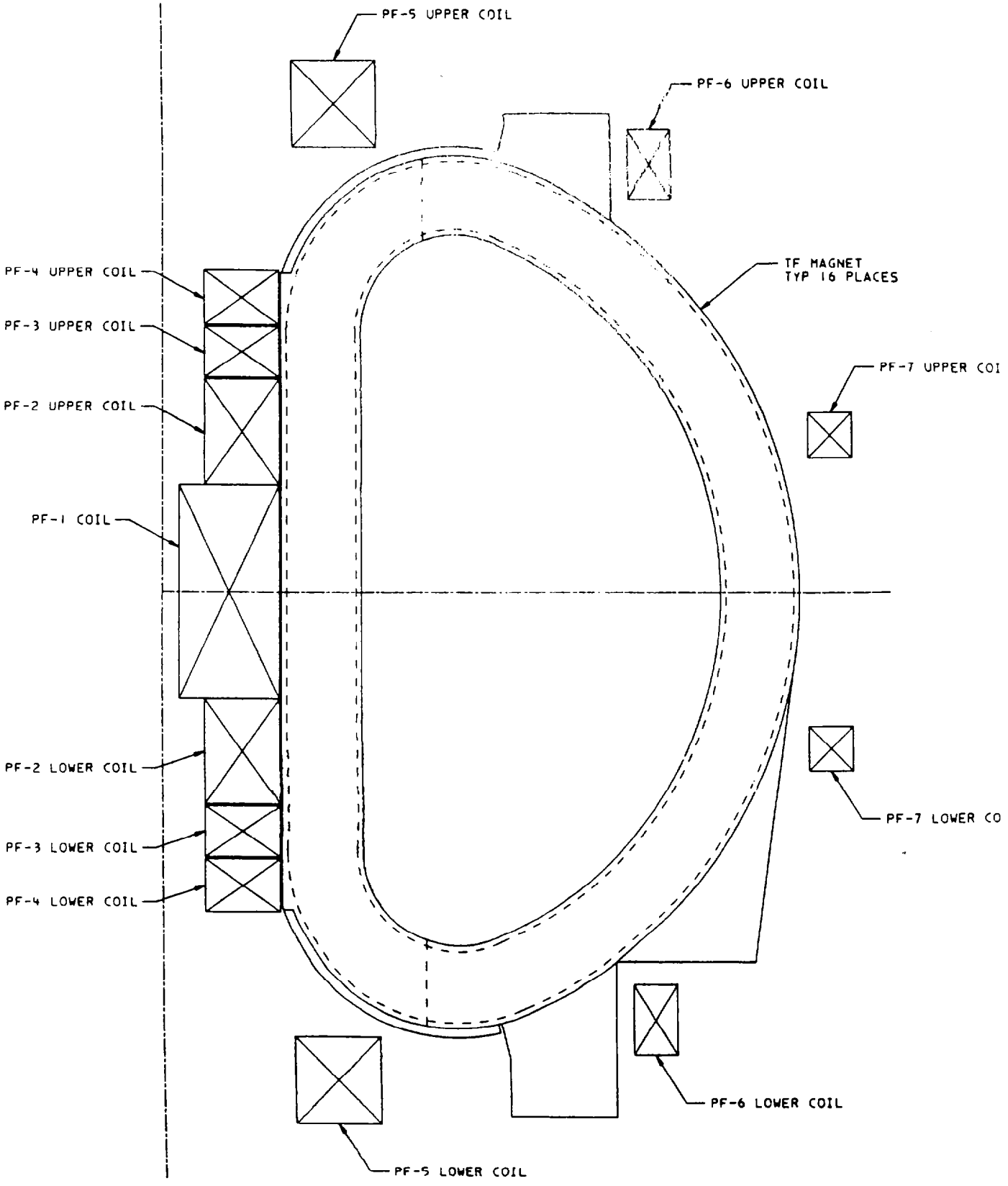

HALEEL-TFPF 11-20-95

Figure 1.1-1
Machine Elevation Showing Location of Coils

are bucked against the central solenoid. The TF cases receive in plane support from both the central solenoid and the intercoil structure. Out of plane loads are reacted by the coil case, the intercoil structure and the crowns, an element also adapted from the ITER design.

A bucking cylinder and tie rod are in the center bore of the central solenoid. The bucking cylinder aspect of this element is necessary when the CS currents swing through zero while the TF is at full field. The tierod is necessary to resist the separating forces (launching loads) on the central solenoid stack, particularly at the time of X point creation.

The ring coils PF's 5, 6 and 7 are supported vertically by the TF coils and radially by their own hoop tension. At this time the coils are envisioned as not having coil cases. However, detailed analysis of these coils including the fixity to the TF coils, has not been performed. It is assumed that need for a coil case, when established, and the proper mounting to the TF can be accommodated at a later time.

Toroidal Field Coil Description

The toroidal field coil conductor is OFHC copper rolled to a hardness with a yield strength of 300 MPa. and 100% IACS conductance. There are two pancakes of strip wound conductor with 25 turns in each pancake. See Figure 1.1-2. The thickness of each turn varies to provide a uniform current density in the inboard leg. The thickest turn, at the nose, is 54 mm. The thinnest turn is 28 mm. The weight of a single TF coil winding pack is 171 metric tons.

The cooling passages in the conductor are formed by tubes which are soldered into grooves milled in the outer edges of the conductor. These channels provide a flow area of 200 mm^2. The helium coolant is introduced to each turn in a manifold at the bottom of the coil and exits at a manifold at the top. See Figure 1.1-3. Coolant flow splits as it enters the passage so that there is fresh coolant for both the inner and outer legs. The length of each passage is approximately 20 m. The coolant manifolds, headers, insulators and flow controllers are located within box like structures that are an integral part of the coil case.

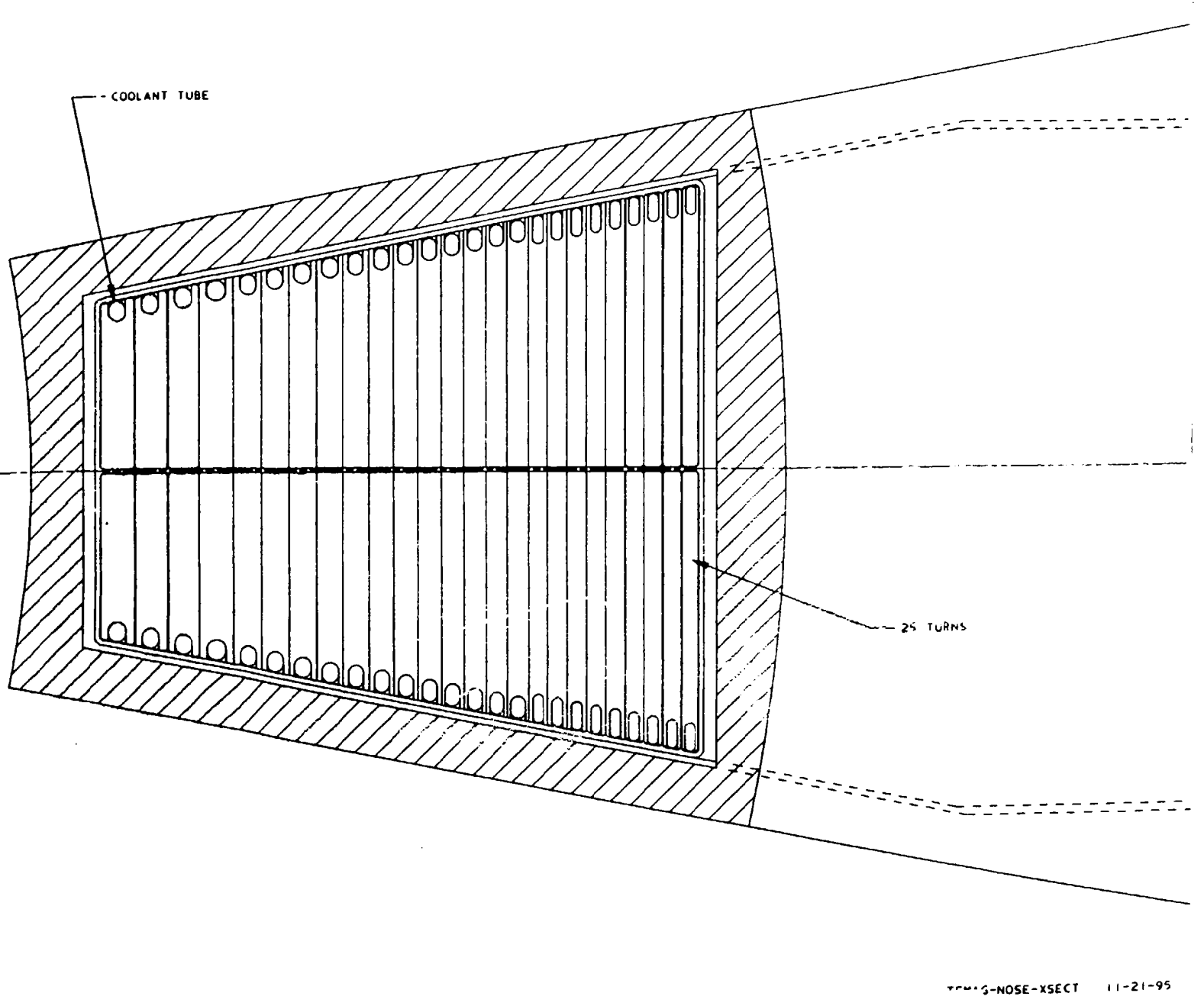

Figure 1.1-2
Toroidal Field Coil Inner Leg Cross Section

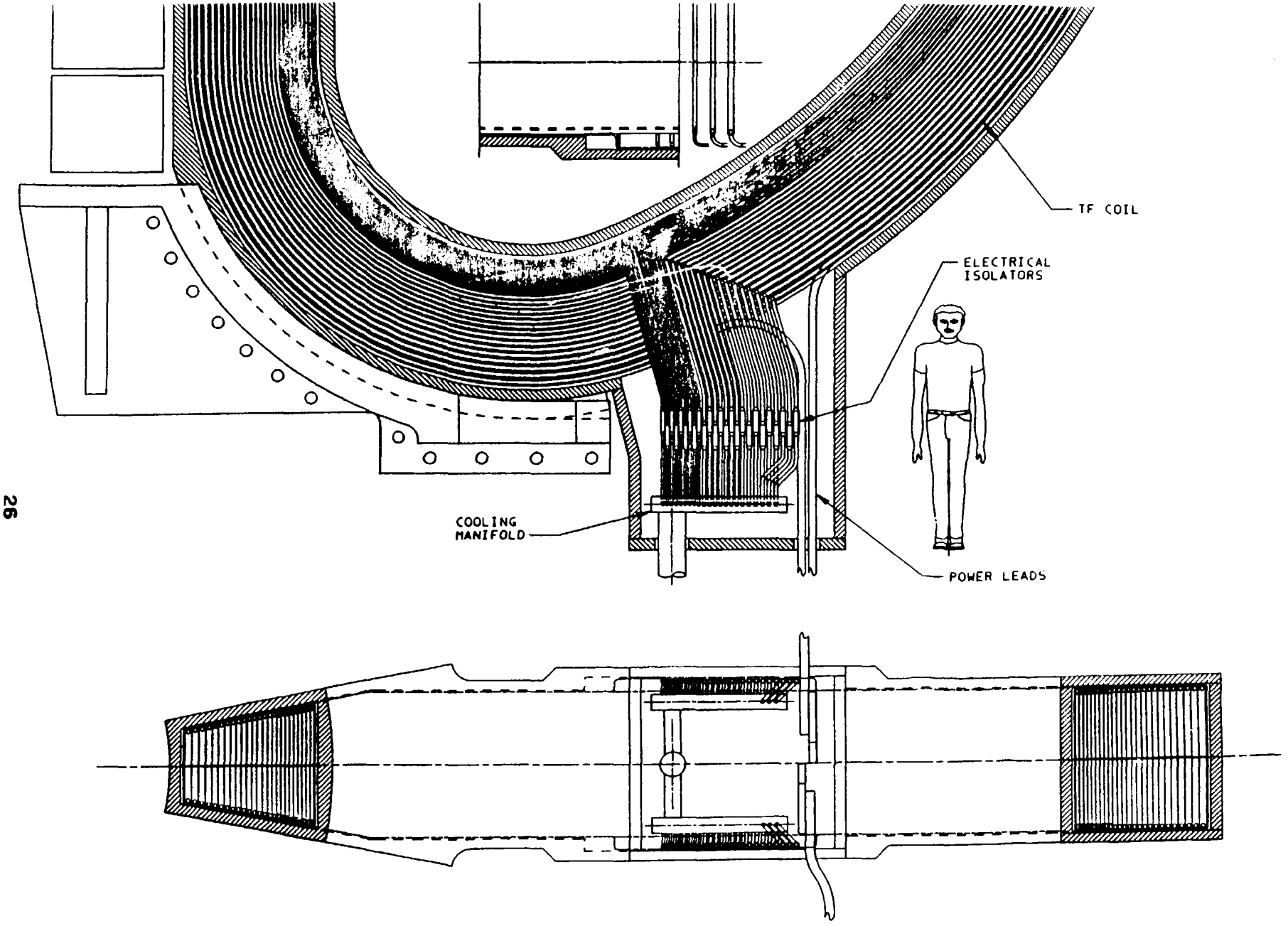

Figure 1.1-3
Toroidal Field Coil Cooling Manifold Arrangement

Two options are being considered for the TF coil insulation system. The voltage between turns is a modest 4 V. The choice will depend upon detailed shear stress analysis of the coil. The first option consists of multiple layers of Kapton tape followed by layers of glass tape wrapped around each conductor to a total thickness of .6 mm. After completion of winding the coil will be impregnated with epoxy in a VPI treatment. This method would result in a slip plane at the interface between the conductor and the insulation and would be chosen if detailed analysis shows that there are high shear stresses developed at a bonded interface. These stresses would be due to the mismatch of the coefficient of thermal expansion of conductor and the insulation or the anisotropy of thermal expansion inherent in an all glass epoxy system. This effect which has been found to be critical at 5° K may not be at 80° K.

If analysis indicates that detailed insulation shear due to thermal stresses is not a problem; but global shear strength of the winding pack as governed by out-of-plane loads is a problem, then an all glass epoxy system with VPI will be chosen. In both cases a rigid sheet of G-10 will be used as a barrier between pancakes. A third system using Kapton and prepreg tape, while a possibility, is considered to be too difficult to use because of the high pressure required if curing is performed after winding the coil or the complications of winding the coil after applying the insulation.

The ground insulation will be multiple layers of Kapton and glass, impregnated in a VPI process and would be 1 cm. thick. This may be a one or two step process with the rest of the coil impregnation and the determination would be made as the details of the manufacturing design progresses.

The toroidal field coil cases are made of type 316LN stainless steel. The nominal thickness of the coil case side wall is 80 mm. The inner and outer rings of the case are also 80 mm. thick (Figure 1.1-4). The coolant manifolds as previously noted are within the coil cases. The coil cases are supported from an outer ring structure and a lower crown structure. The outer ring structure provides seismic stability and is used during installation for positioning the coils. The TF outer ring structure and lower crown structures are supported from the cryostat base with low conductivity titanium pedestals tied to a roller support

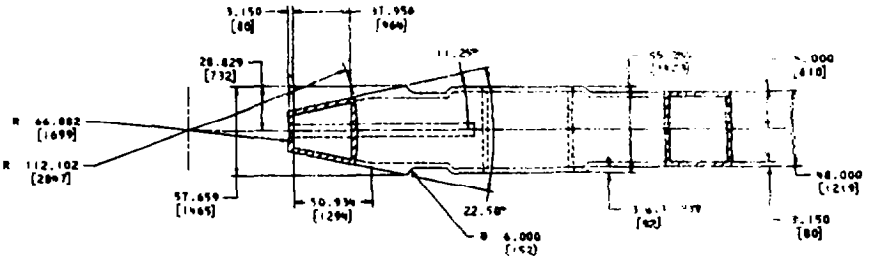

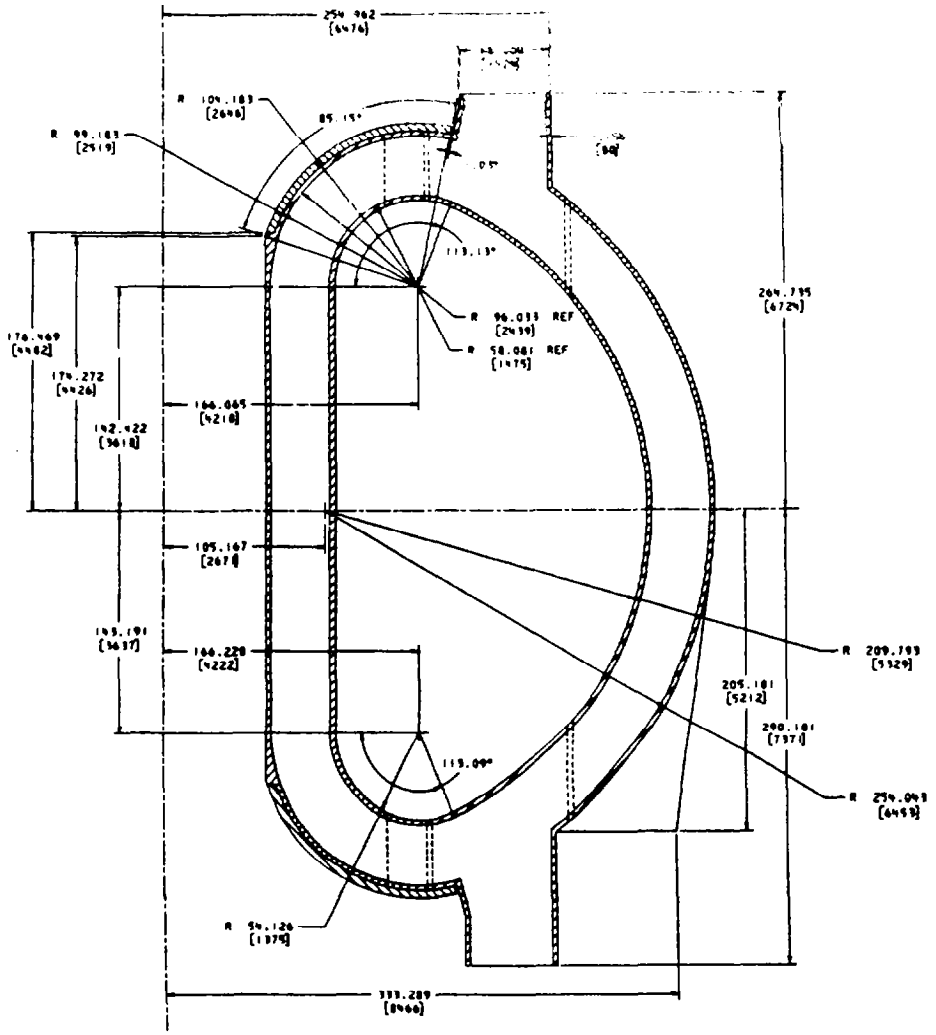

Figure 1.1-4
Coilcase -TF Coil

system that allows radial movement but provides support against radial and tangential motion. The weight of each TF case is 75 metric tons.

The crown structure is positioned at the top and bottom of the inner leg of each coil. It is keyed to the coil case and functions as an out of plane restraint by locking together local coil rotations at the ends of the inner legs. The crown structure pieces have an insulated break located at the plane between coil faces to break up eddy current loops. The crowns also support the central solenoid and PF5.

Table 1.1-1

Toroidal Field Coil Characteristics

Major Radius	5.0 m
Field on Axis	7.0 T
Total Ampere Turns	175 MAT
Number of Coils	16
Number of Turns per coil	50
Conductor Current	218.8 kA
Current Density, Inner Leg	17.0 MA/m^2
TF total Resistance @ 80° K	3.66E-03 Ω
TF total Inductance	1.46 H
$\int I^2 dt$ per coil per pulse	1.18E+13 A^2s
Temp rise per pulse	244° K
Max. System Resistive Power per Pulse	560 MW
Total System Energy per pulse	85 GJ

PF Coil Description

The current time history of each of the poloidal field coils and the TF coils is shown in Figure 1.1-5. The characteristics of the PF coils are tabulated in table 1.1-2. PF coils 1 thru 4, upper and lower, make up the central solenoid and are shown in Figure 1.1-6. The orientation of conductors, general cooling arrangement and construction of these coils is similar and dictated by the high coolant flow rates of PF 1. PF Coils 5, 6 and 7 are stripwound coils of similar construction. PF 5 and is representative of these coils. A crossection of PF 5 is shown in Figure 1.1-7.

Poloidal Field Coil 1

Poloidial Field coils 1 Upper and 1 Lower, while considered in magnetic and cooling calculations as two separate coils symmetric about the mid plane and electrically connected in series, are actually one coil. This is necessary

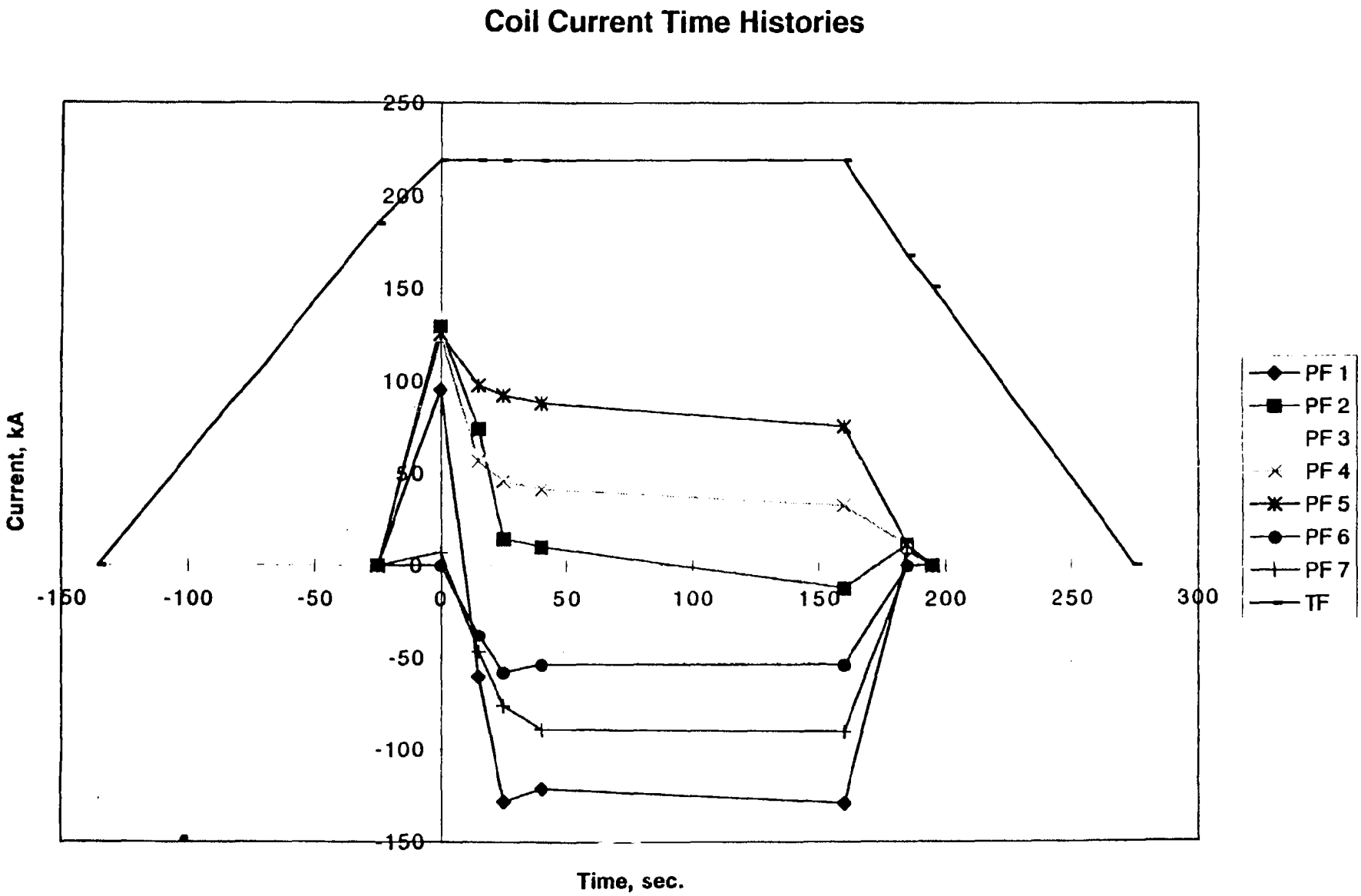
Coil Current Time Histories
Current, kA
Time, sec.
250
200
150
100
50
0
-50
-100
-150
-150
-100
-50
0
50
100
150
200
250
300
PF 1
PF 2
PF 3
PF 4
PF 5
PF 6
PF 7
TF

Figure 1.1-5

Table 1.1-2
Poloidal Field Coil System Characteristics

	PF 1	PF 2	PF 3	PF4	PF 5	PF 6	PF 7
R,m	1.16	1.286	1.286	1.286	2.483	7.036	9.566
Z,m	0.723	2.278	3.374	4.114	6.858	6.012	2.204
ΔR,m	0.945	0.693	0.693	0.693	1.225	0.608	0.608
ΔZ,m	1.448	1.426	0.714	0.714	1.216	0.961	0.612
Max. MAT	38.73	28.52	13.75	30.11	30.11	6.98	5.42
Time of Max.	EOB	SOI	SOI	SOI	SOI	SOF	EOB
No. of Turns per coil	300	220	110	110	240	120	60
No. of Truns Radial	15	11	11	11	60	30	30
No of Pancakes	20	20	10	10	4	4	2
Max. Conductor Current,kA	129.1	129.6	125	125	125.458	58.167	90.33
∫j^2dt per coil,A^2s	1.30E+17	8.89E+15	1.79E+16	1.73E+16	4.13E+16	2.30E+16	3.70E+16
Coil Max. Temp, °K	211.6	85.5	97.1	96.2	140.7	104.8	130.9
Coil Starting Temp,°K	30	80	80	80	80	80	80

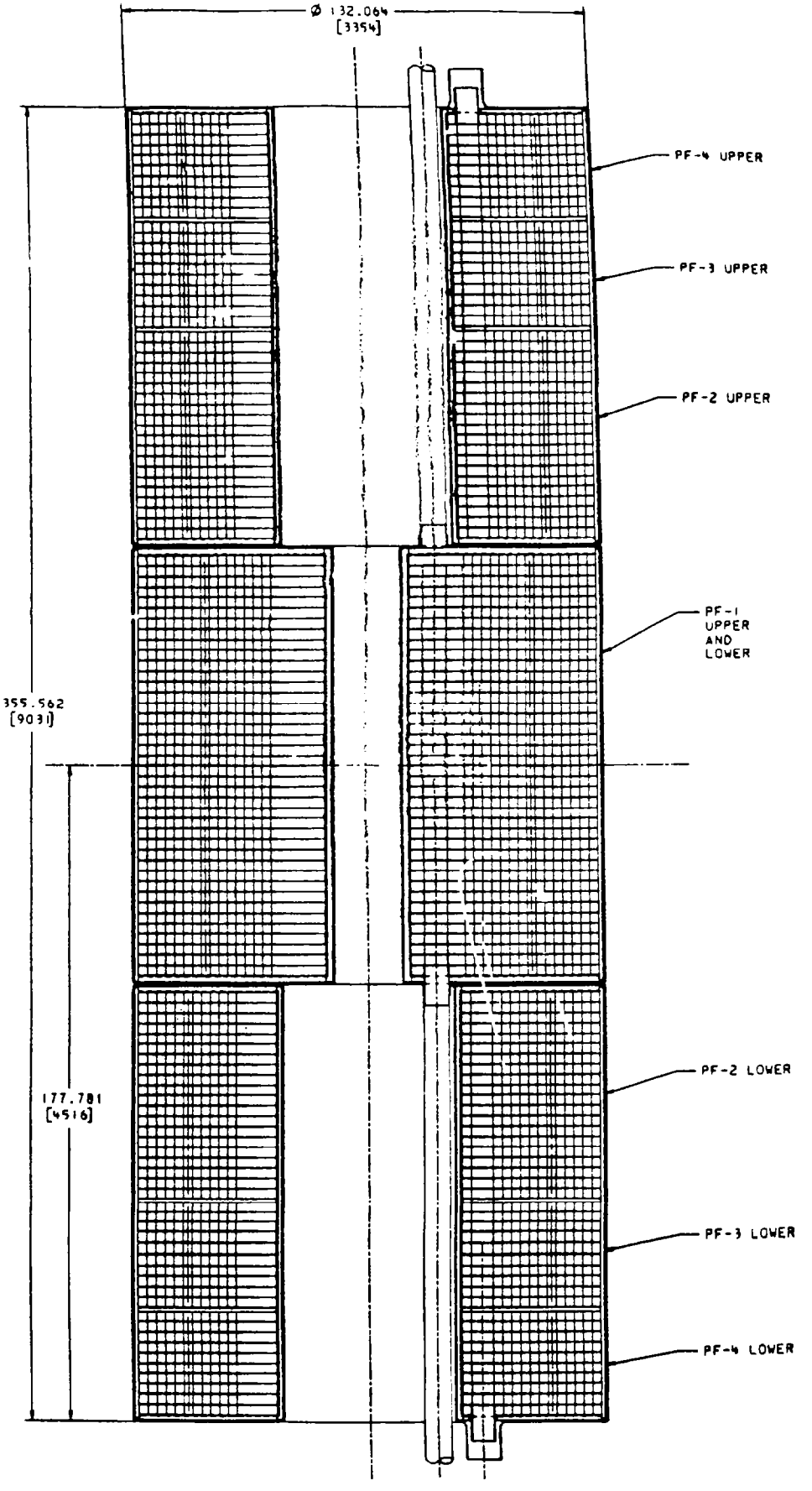

SOLENOID-EL 11-20-95

Figure 1.1-6
Central Solenoid-Arrangement of Coils

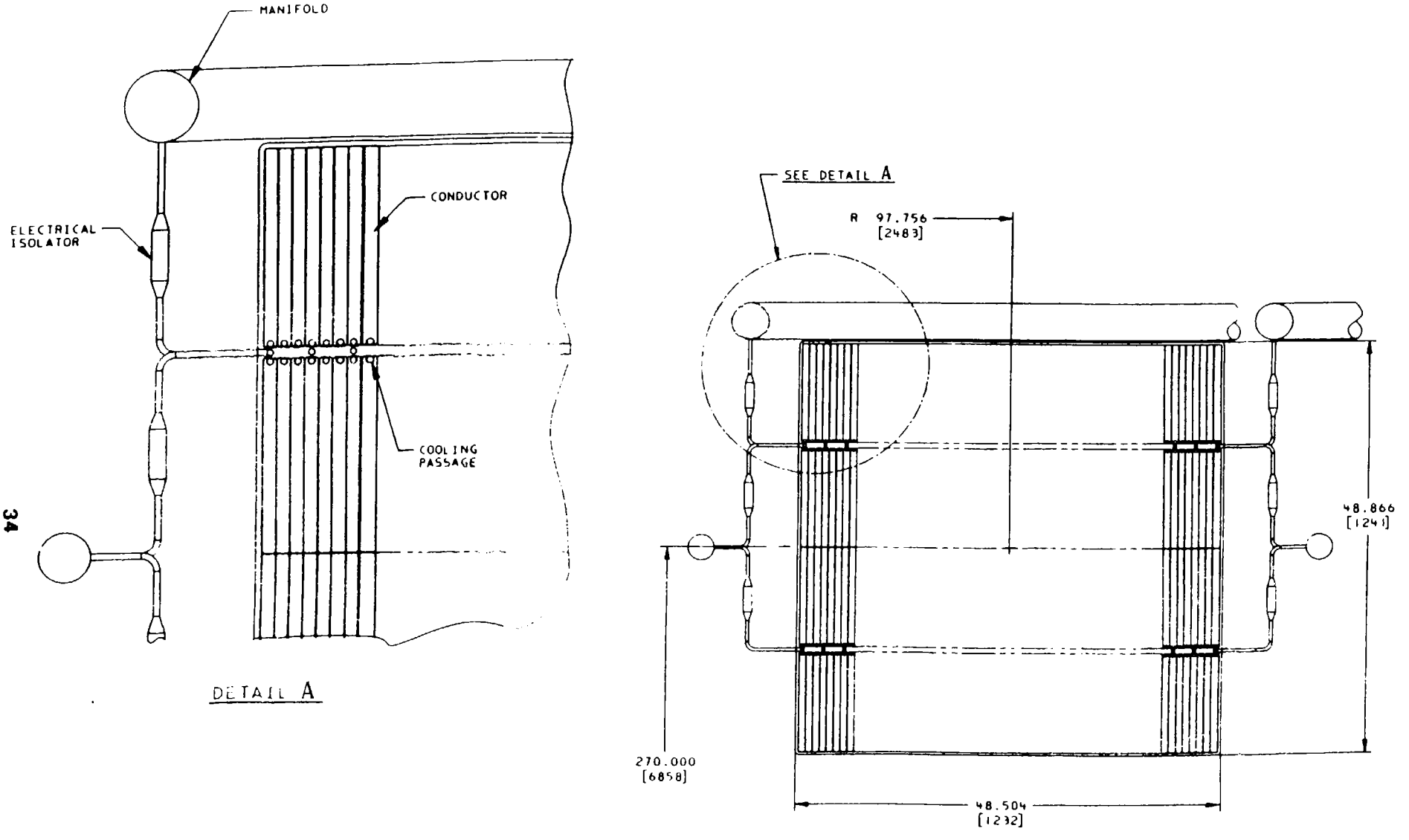

Figure 1.1-7
Poloidal Field Coil No. 5- Cross Section

PF-5 11-17-95

because of the limited space in the bore of the coil. The combining of the two coils eliminates one pair of current leads and cooling pipes.

The arrangement of conductors in P F 1 departs from the stripwound orientation of the TF coils and the PF coils 5, 6 and 7. See Figure 1.1-8. This is due to the higher coolant flow rates required to recool to the 30°K starting temperature. The conductors are arranged in 42 pancakes of 14 spirally wound turns. The turns will be manufactured by water jet cutting 67 mm thick copper plate. The helium coolant flows between pancakes in radial channels cut in the pancake-to-pancake insulation. Coolant is introduced into the coil at the inner bore and flows radially outward through the channels to the outer diameter. The coolant then flows vertically to the top and bottom ends of the coil where it flows in horizontal channels back to the inner bore, as shown in Figure 1.1-9. The complicated manifolding of this cooling arrangement requires the PF 1 coils to be enclosed in a pressurized container. The container is made of high resistance tianium alloy with a wall thicknesss of 6 mm. The total mass flow rate of helium coolant thru each coil is 7.2 kg/s.

The manifolding at the inner bore and the directing of the coolant to the channels between the pancakes is achieved by an arrangement of stainless steel plates. See Figure 1.1-10 The plates are the same thickness as each of the pancakes with insulation between plates and channels in the insulation corresponding to the channels between the pancakes. Flow is directed from the intake into large holes in the plates and then to the channels. The plates also transmit the radial load from the TF coils to the inner bucking cylinder.

Poloidal Coils 2 thru 4

The winding arrangement and the coolant flow in PF coils 2 through 4 of the central solenoid is similar to that of PF-1. The reason for this is not because of the high cooling rates needed, but to eliminate the insulators and multiple feed lines needed in the strip wound coils and relive crowding in the bore. These coils are cooled with helium and start at a prepulse temperature of 80°K. PF coils 2, 3 and 4 upper and 2, 3 and 4 lower are in seperate pressure containers and are cooled with single in and out coolant feed lines as shown in Figure 1.1-11

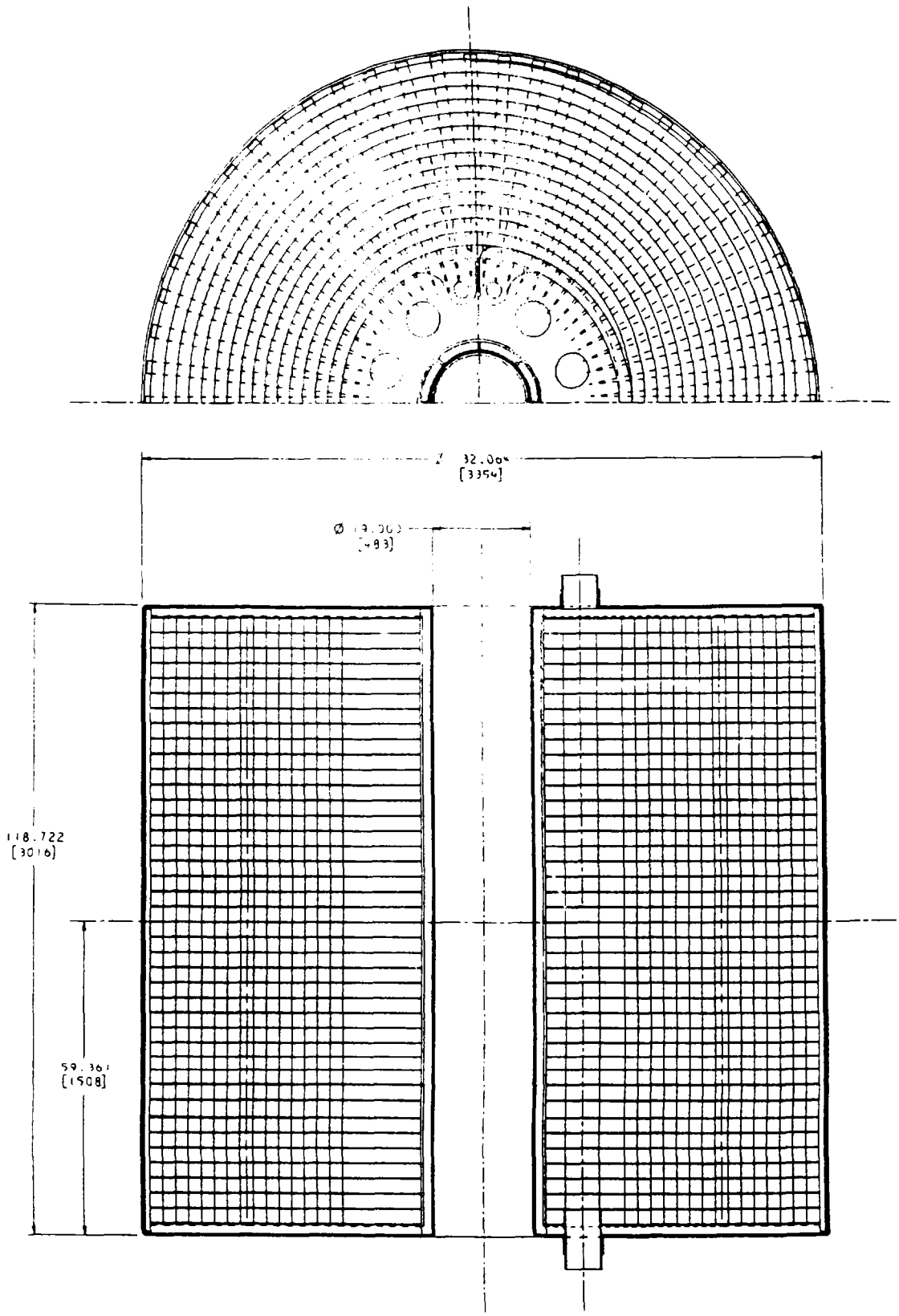

PF 1 11-20-95

Figure 1.1-8
Poloidal Field Coil No. 1-Cross Section

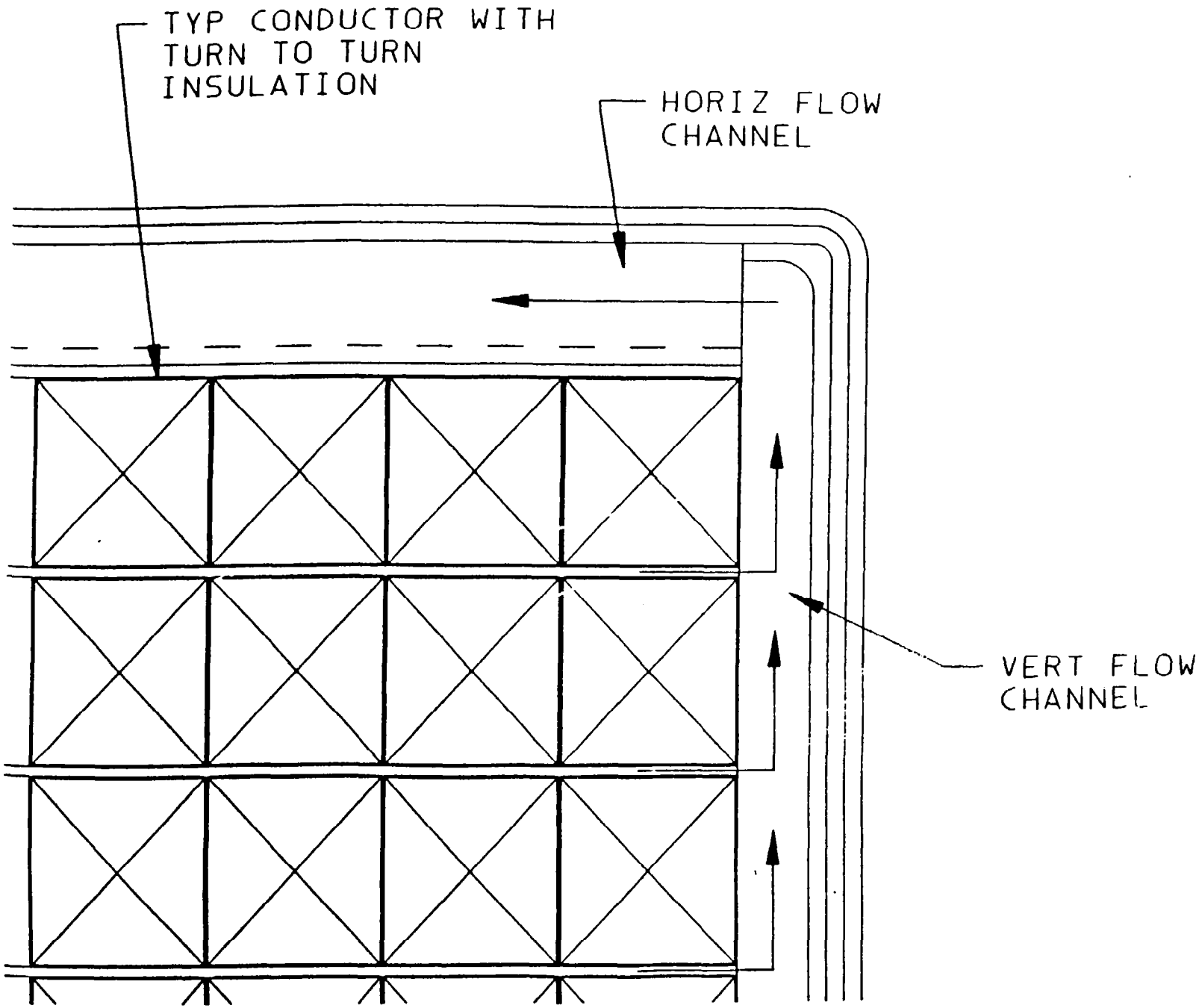

Figure 1.1-9
Conductor Flow Patterns - Typical of all Central Solenoid Coils

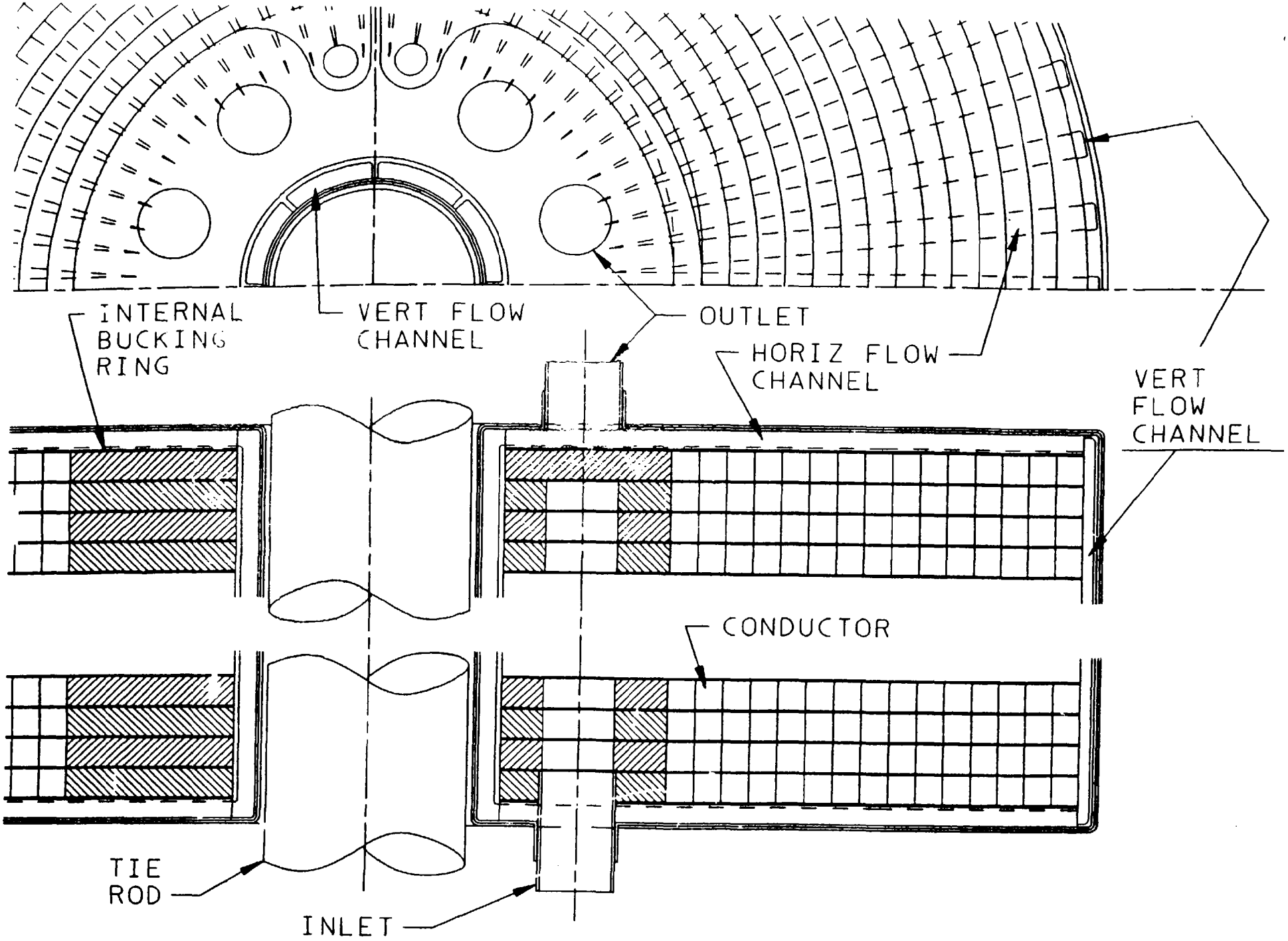

Figure 1.1-10
Cooling and Conductor Arrangement - Typical of all Central Solenoid Coils

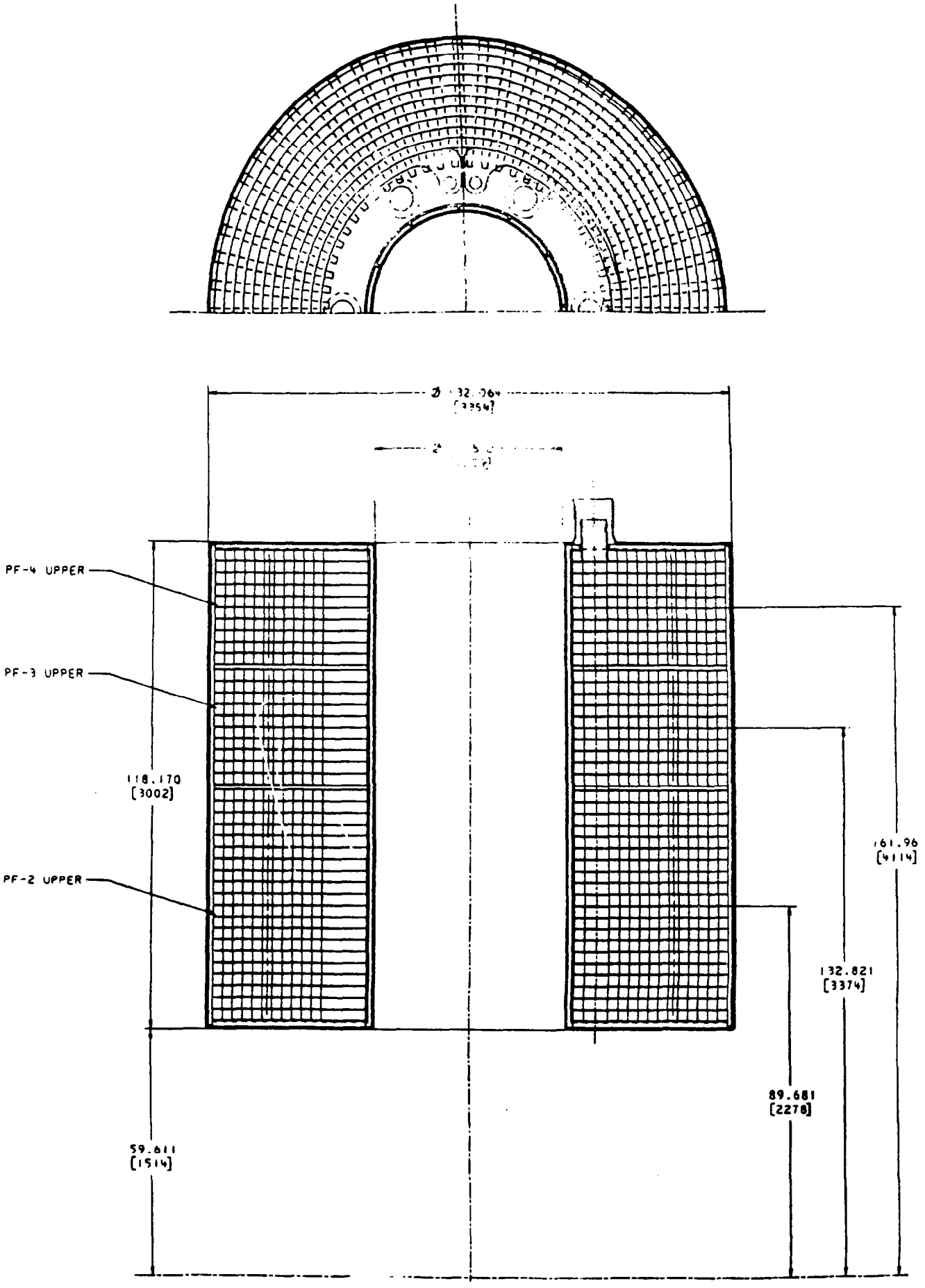

Figure 1.1-11
Poloidal Field Coils 2, 3 and 4 - Cross Section

Polodial Coils 5, 6 and 7

The winding arrangement of these coils is similar to that of the TF coil. These coils are strip wound. All conductor is 50% hard OFHC copper and is 1.9 mm thick. The width of the conductor varies with each coil. The cooling passages in the conductor are formed by tubes soldered into grooves milled in the edges of the conductor as in the TF coil. Unlike the TF the coolant lines run radially between the pancakes and not on the outside. These coils are cooled to 80° K prior to each pulse and are cooled with helium.

Section 1.2: Magnet Cooling Design and Analysis (A. Brooks)

Overview

The Toroidal Field Coils are designed to be pulsed 5 times a day to 7 Tesla for a 160 second flat top. The Poloidal Field Coils must provide the equilibrium fields for plasma burn as well as the startup flux swing. The coils absorb the ohmic heating inertially and are recooled between pulses by a high pressure primary coolant loop of gaseous helium. To maintain low power dissipation the TF coils and PF coils 2 thru 7 are cooled to 80K.

In order to satisfy the higher current density requirements of PF 1 it is necessary to subcooled it to 30K.

The coolant configurations were driven by an initial desire to recool the field coils in 1 to 1.5 hours. Refrigeration and thermal storage limitations have lead to a more drawn out recool cycle. Further simplification of the internal coolant configuration should be possible.

TF Performance

Heating

The TF coils are limited by the temperature rise in the inner leg during a pulse. The 'G' function (Temperature vs Integrated j^2t) for OHFC Copper, Figure 1.2-1 is given relative to a 30K initial temperature. The turns of the TF Coils are sized to provide a uniform current density in the inner leg (consequently, the current density and therefore heating is not uniform in the outer leg). The j^2t for the given geometry is driven by flat top requirements as well as power supply limitations in ramping up and ramping down the field.

The analysis of the TF Coil employed the TF Systems code, TFSYS developed for use with CIT and BPX. The code models the 3D coil geometry (Figure 1.2-2) and solves for the coupled thermal-electral-magnetic response using a simplified representation of the power supplies. Outputted from the code are current and voltage waveforms, power consumption, energies stored and dissipated, and temperature histories.

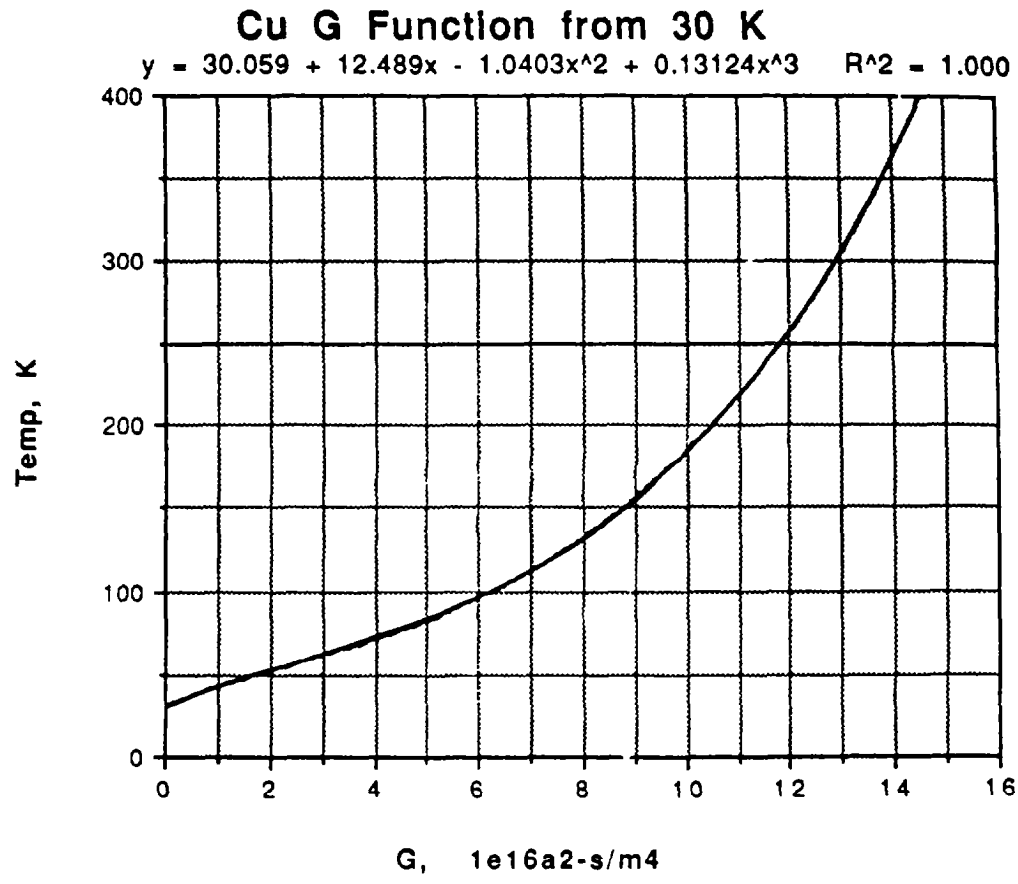

Figure 1.2-1 Temperature Rise verses Integrated j^2t for OFHC Copper

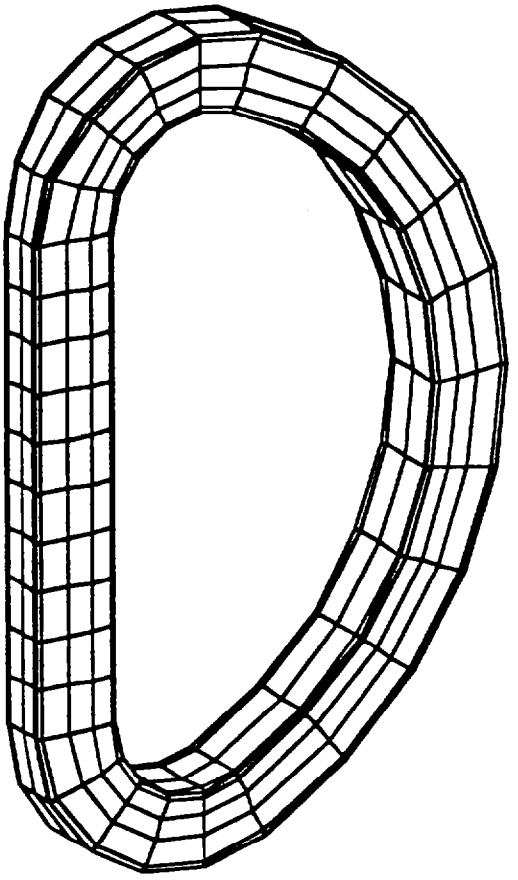

Figure 1.2-2 TF Coil Thermal-Electrical-Magnetics Model

Figures 1.2-3 through 1.2-7 show the TF response with a 3.2 KV maximum driving voltage and a 20% droop in voltage at full current. Rampdown assumes a constant 60% inversion voltage capability. The coil performance is summarized in table 1.2-1 for operation starting at 80K. The coils ramp up to their maximum current of 218.8 KA in 133 seconds. Power requirements peak at the end of ramp at 560 MW, then drop to 220 MW at start of flat top. As the coils heats up, the resistance of the TF builds from 4.6 milliohms at start of flat top to 11.7 milliohms at the end of flat top where power requirements again peak at 560 MW. The end of pulse temperatures reach 244 K, with a total dissipated energy of 85 GJ.

Recool

The cooling configuration provides for edge cooling of the strip wound conductors. Coolant is fed into each of the coils slightly outboard of center at the bottom and removed at the top, providing 2 unequal coolant paths per turn. The longer, inner leg hydraulic paths are 16mm diameter and approximately 20 m long allowing for a modest helium pressure loop of 5 atm. and limiting maximum pressure drops to 20% of inlet pressure (1 atm).

The recool of the TF and other field coils is accomplished by transferring the stored thermal energy from the coils to an 80K refrigeration plant. To minimize the size of the refrigerators, the machine is operated with the 5 pulses spread out evenly over a 24 hour day. During the 4.8 hours between pulses, the heat load to the refrigerators is also maintained constant by extracting heat from the coils at a constant rate. For the five 85 GJ pulses the averaged load is 4.92 MW.

Helium was chosen as the heat transfer fluid because it is easier to control the heat removal rate using a single phase fluid. (Faster cooldowns could be achieved with high pressure LN2, but the refrigerators could not keep up with it and intermediate thermal storage proved to be extremely large and expensive and not warranted). Flow rates are adjusted to maintain a constant value of mass flow times enthalpy change. The coolant passages are sufficiently long that the coolant exits the coil at very near the coil

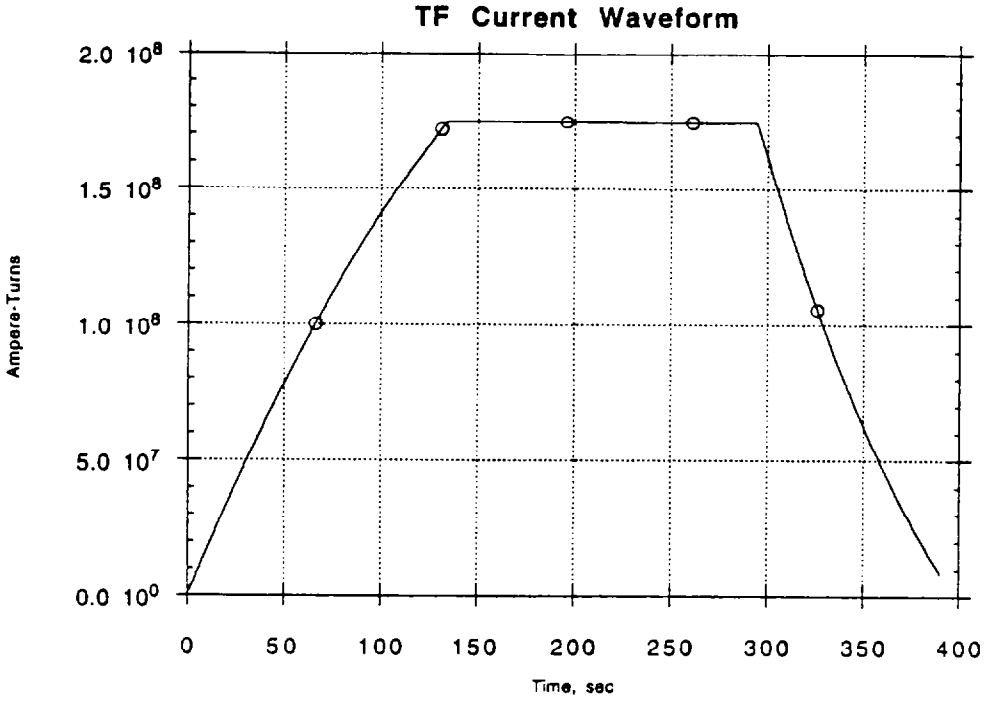

Figure 1.2-3

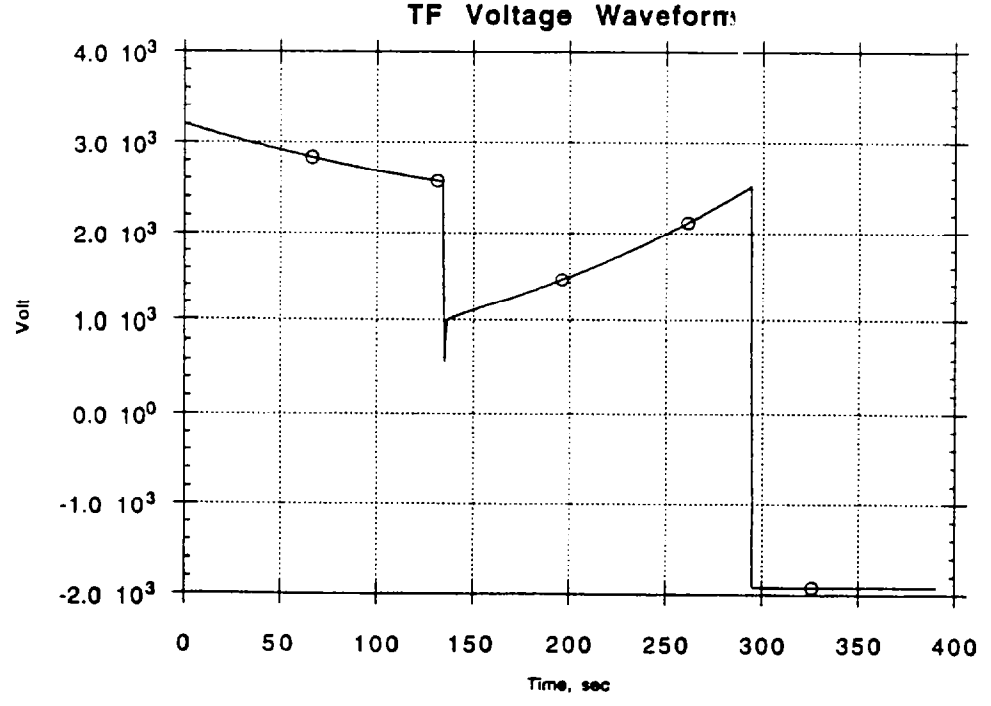

Figure 1.2-4

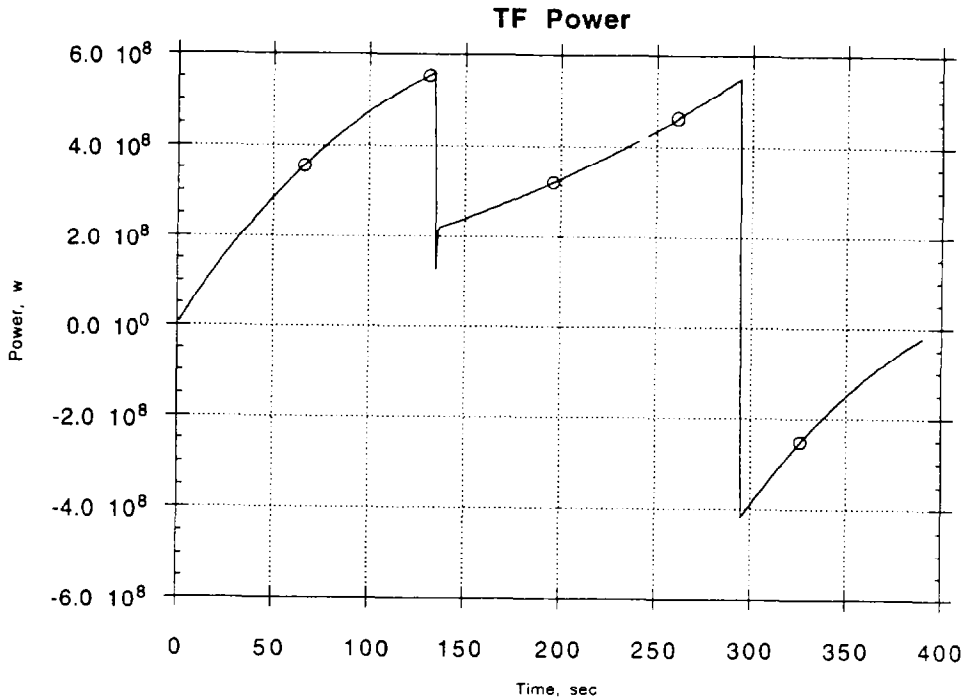
TF Power
6.0 10^8
4.0 10^8
2.0 10^8
0.0 10^0
-2.0 10^8
-4.0 10^8
-6.0 10^8
Power, w
0
50
100
150
200
250
300
350
400
Time, sec

Figure 1.2-5

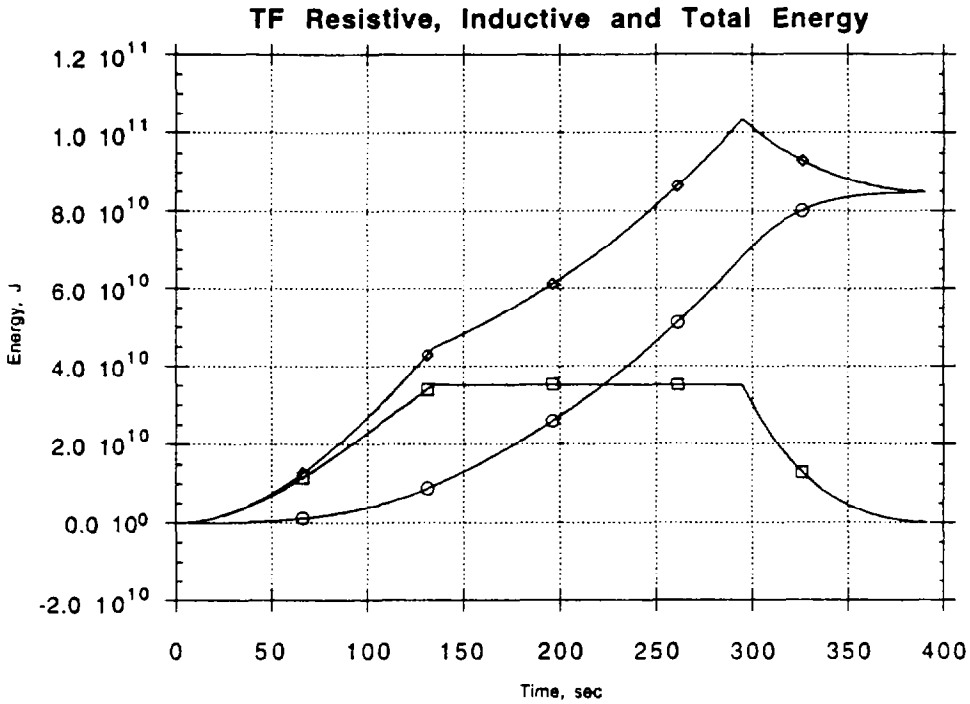

Figure 1.2-6

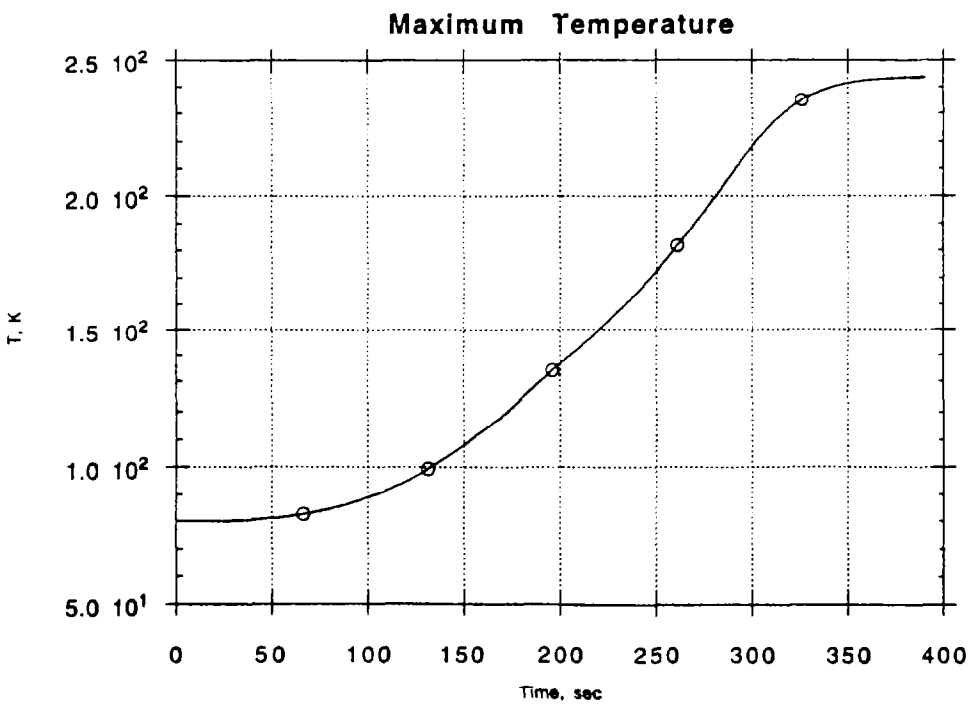

Figure 1.2-7

Table 1.2-1
TF Coil Performance Summary

Major Radius, m		5
TF Field, T		7
Number of Coils		16
Number of Turns per Coil		50
Flat Top Current, KA		218.8
Flat Top Duration, sec		160
Power Supply Voltage, KV		3.2
Voltage Droop, %		20
Rise Time, sec		133
Temp, K	SOP	80
	SOFT	101
	EOFT	212
	EOP (inverting)	244
	EOP (L/R decay)	276
Power, MW	End of Ramp	560
	SOFT	220
	EOFT	560
Energy, GJ, Inductive	FT	35
Energy, GJ, Resistive	SOFT	9
	EOFT	69
	EOP (inverting)	85
	EOP (L/R decay)	104
Voltage, KV	End of Ramp	2.56
	SOFT	1
	EOFT	2.56
TF Resistance, milliohm	SOFT	4.57
	EOFT	11.70
TF Inductance, h		1.46
Decay Time Constant (L/R), sec		125

temperature. Flow is therefore a minimum at the start of cooldown (5.8 kg/s) and increases as the coil cools to a maximum design value of 34.2 kg/s.

The cooldown was simulated using FACOOL, a code developed to analyze the performance of the TFTR TF Coils with alternate coolants. The maximum mass flow rate of 34.2 kg/s (16 m/s) was set by investigating the flow of helium which could be achieved in long passages with heat transfer. The pressure drops were limited to 20% of the inlet pressure to minimize compressor power. Figure 1.2-8 shows the pressure variation along a 244 K channel with various inlet velocities (shown as inlet Mach Numbers) for helium at 80 K and 5 atm. The relationship is very nonlinear for compressible fluid and can lead to choking at channel lengths shorter than needed if flows are increase. Alternately, if channel lengths much longer than chosen are used, mass flow rates must drop significantly, resulting in much longer cooldown times.

Figures 1.2-9 and 1.2-10 shows the transient temperature response and heat removal rate from a single coolant passage in the coil. For most of the cooldown period, the goal of constant heat removal is achieved. Only at the tail end does heat removal fall off, where higher flow rates (or fluid subcooling) would be necessary to sustain it.

Initial Cooldown

The cooling system is capable of cooling the TF Conductors from room temperature to 80 K (200 GJ) in 8 hours. However, refrigeration limitations and/or thermal stress considerations will probably lead much slower cooldown.

PF1 Performance

Heating

The PF coils are also inertially cooled during the pulse. The j^2t for each of coils except PF1 are low enough to permit starting at 80K and still limit peak temperatures to less than 150K and acceptable total energy dissipation (less

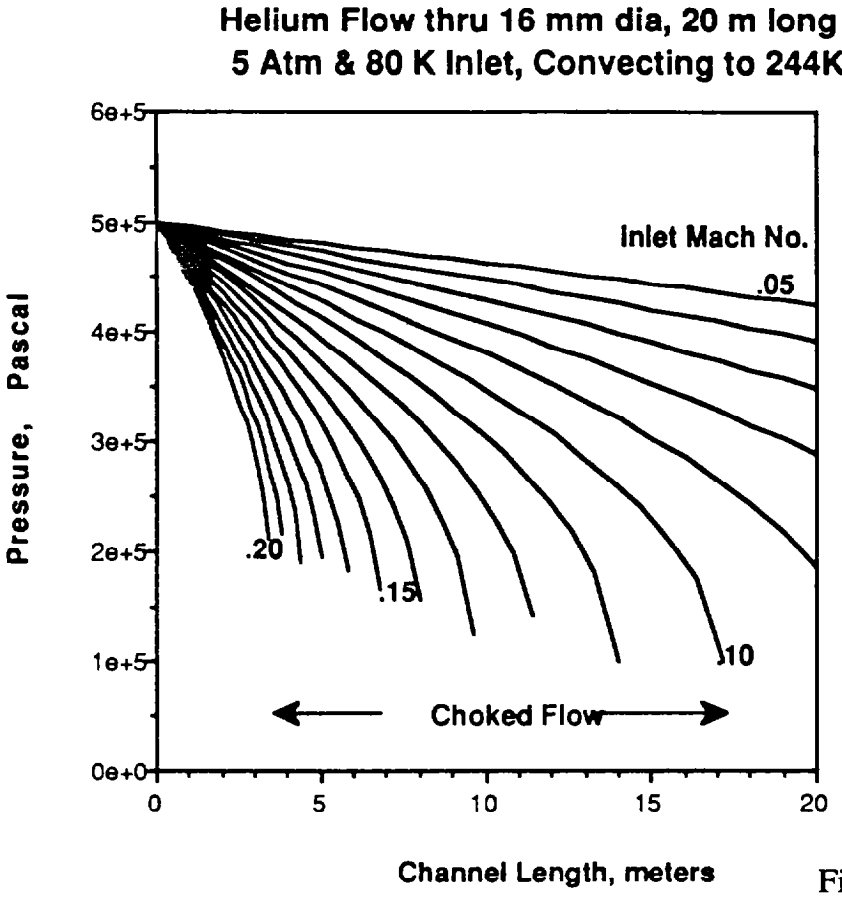
Helium Flow thru 16 mm dia, 20 m long TF Channel
5 Atm & 80 K Inlet, Convecting to 244K Conductor
Pressure, Pascal
6e+5
5e+5
4e+5
3e+5
2e+5
1e+5
0e+0
0
5
10
15
20
Channel Length, meters
Inlet Mach No.
.05
.10
.15
.20
Choked Flow

Figure 1.2-8

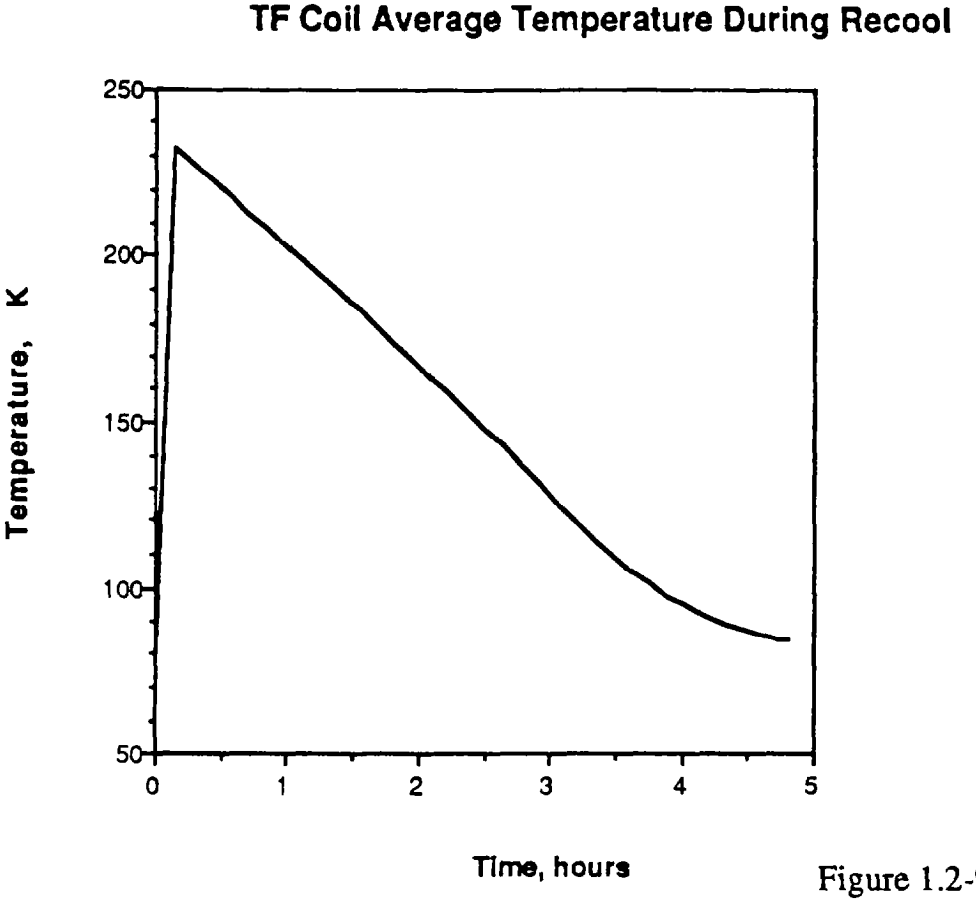
TF Coil Average Temperature During Recool
Temperature, K
250
200
150
100
50
0
1
2
3
4
5
Time, hours

Figure 1.2-9

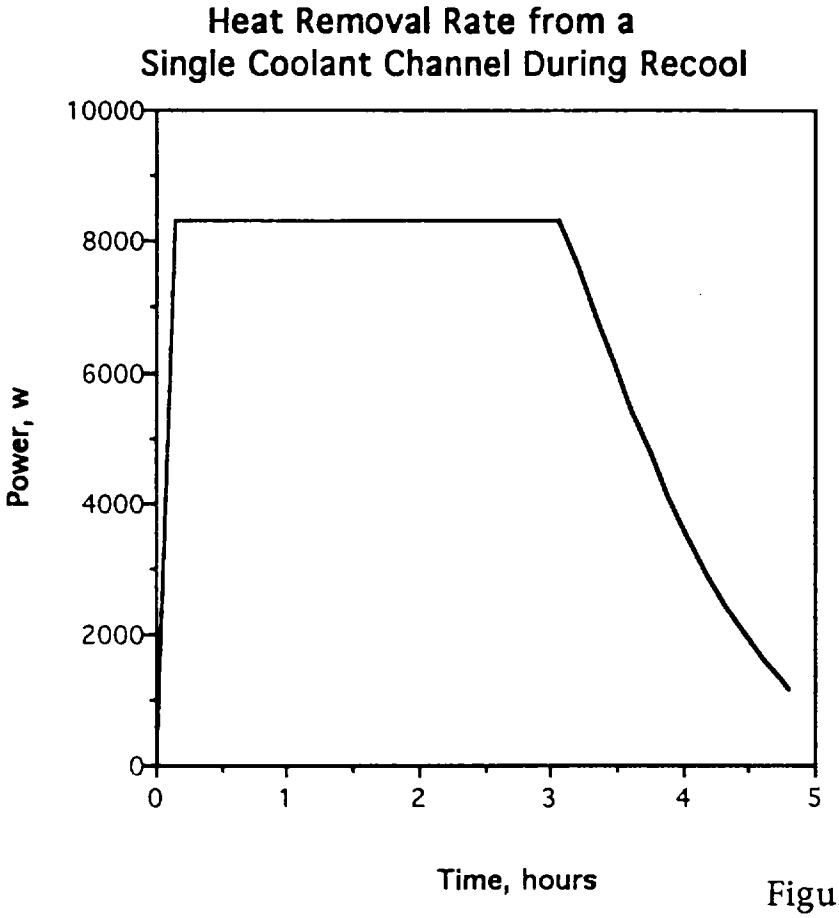
Heat Removal Rate from a
Single Coolant Channel During Recool
10000
8000
6000
4000
2000
0
Power, w
0
1
2
3
4
5
Time, hours

Figure 1.2-10

than 15 GJ per pulse). PF1 requires subcooling to 30 K to keep end of pulse temperatures below 300 K and dissipated energy low (8.2 GJ).

Recool

PF1 is cooled by flowing helium at 5 atm thru radial channels cut in the pancake insulation. The coolant flows radially outward between layers of conductor.

The cooldown is accomplished in two stages. The helium coolant is initially passed through the 80K refrigerators and when most of the heat from the coils has been removed (7.2 GJ) further cooled by the 30K refrigerators. Aggressively cooling the coils during the first stage from their maximum temperature of 216K down to 85 K in 45 minutes allows 4 hours to remove the final 1 GJ.stored below 85 K. This keeps the average heat removal rate at only 0.07 MW for the second stage, significantly reducing the size of the 30 K refrigerators.

A mass flow rate of 7.4 kg/s is required during the first stage to achieve the 45 minute initial cooldown. Heat removal rates are not uniform for PF1 during this stage but will be balanced by varying loads on other systems. To provide a constant heat removal rate during the second stage, flowrates will drop to only 0.25 kg/s when the 30K refrigerators first kick in and the coil is at 85 K, then gradually build up to the full 7.4 kg/s as the coil cools toward 30K.

There are nearly 1300 small channels per coil manifolded together, each 20 mm wide by 3.5 mm high (copper to copper separation) by 2.1 m long. The maximum inlet velocity is 16 m/s, low enough to stay with a 20% pressure drop budget even at the start of cooling when cold gas is fed into a warm coil accompanied by large changes in density and fluid acceleration.

PF 2 thru 7 represent a much easier recool problem and as such have not been analyzed explicitly.

Initial Cooldown

PF1 initial cooldown does not differ significantly from the recool since PF1 heats up to close to room temperature for each pulse.

Alternate Concepts

A number of alternate design concepts were explored, each with their own merit. As the present design matures, changes will necessarily come about, some of which may lead to rethinking previous choices.

Precooling TF to 30K

The power consumption of the TF coils could be reduced significantly by further cooling to 30K at the cost of a much larger refrigeration system. For the pulsed operations foreseen, this did not provide an economic advantage. Since the technical objectives could be achieved with cooling to only 80K, there was no incentive to further precool.

Steady State TF Operation

With a much more aggressive cooling scheme, and significantly larger coolant mass flow rates, the TF Coils could be operated continuously and maintained at or near LN_2 temperature. Two schemes were investigated: multiple coolant channels extruded or imbedded in the strip wound conductor, or large numbers of small channels carved out of the turn to turn insulation, flowing across the conductor and manifolded together. To maintain an average conductor temperature of 95K (and limit power requirements to 246 MW) with 80K LN2 requires 250,000 gpm. The multiple coolant channels per conductor approach lead to complications in bringing large numbers of tubes (12800 total) into the coils. In the second scheme, manifolding the cross conductor coolant channels eats up valuable space in the inner leg region. Large numbers of channels are required to minimize thermal gradients within the conductor.

Steady State operation at 30 K was not investigated fully because of time constraints. It is expected that one could show that enough coolant could be

passed internally though the coils to maintain modest temperature rises, but problems would be encounter supplying and exhausting the large volumes of gaseous helium required to cool the coils.

Section 1.3: Structural Analysis (P. Titus)

Summary

The bucked, copper, cased TF concept for the PCAST machine has acceptable stress levels for the required pulse length, TF field, and PF scenario. Monotonic stress criteria (Primary Membrane, Bending, etc.) are readily met. Fatigue performance for the 5000 cycle life is close to expected allowable levels. Refinements in thermal behavior are recommended. Use of larger TF outer leg cross sections should be considered to reduce case thermal differential induced tension stress and TF copper winding pack thermal differential end of pulse compression stresses. If the TF case/winding pack thermal differential remains high, and case tension stresses remain close to yield, further fracture mechanics investigations will be needed. More strain controlled copper fatigue R&D will be needed as well. Extension of the crown into volume currently taken by PF4 might be considered to reduce the out-of plane loading effects. Case bending stresses and CS torsional shear stress would profit from improvements in out-of plane support. Current analysis results are for 20 coils. There is a small improvement in out-of-plane behavior for 16 coils. A larger improvement is likely if two-coil modules are used.

PCAST Structural Concept

PCAST is modeled after the ITER structural configuration. It is bucked, and it uses similar out-of-plane (OOP) support structures. It shares many similarities, but it is substantially different than ITER as well. It uses normal conductors (copper) which results in non-uniform temperatures and thermal strains. The plasma has a higher triangularity, and the CS is segmented to accomplish this. The TF conductor/case cross section is much larger in proportion to the coil size than the ITER TF coil. This makes it stronger against out of plane (OOP) loads, less flexible in accommodating assembly tolerances, and more sensitive to finite build related deviations from momentless, constant tension form.

Effects of CS Segmentation

The segmentation of the CS with its differential thermal motions and Lorentz force distribution causes substantial differences in in-plane behavior. The TF bucks against a non-uniform surface. Differential thermal and Lorentz force radial displacements create internal stresses, particularly shear stresses in the CS. The highly shaped, high triangularity plasma causes larger OOP loads in the inner leg. The inner leg is poorly supported for OOP loads. The ITER design evolved based on a PF scenario and plasma shape that minimized OOP loads in the inner leg.

Model Description:

The ANSYS computer code is used for the structural analysis. Model geometry and force files are generated outside of ANSYS. R. Bulmer's memo of October 23 1995, RHB:95.32, which included results for 0.8, 1.0, and 1.2 meter diameter CS coils was used as input to the last of the analysis runs. In these runs, the 1 meter CS build was used. Earlier runs used inconsistent current and coil geometry. The model is 3 dimensional cyclically symmetric, and geometrically non-linear. Many gap elements are used. Material properties are linear and the orthotropic properties of the copper winding packs are assumed to have minimal effect. Isotropic properties are used, somewhat reduced to reflect the inclusion of insulation. The model is shown in Figures 1 and 2. Figure 3 is a comparison of the ITER and PCAST global structural models.

Twenty (20) coils are assumed in the model. The TF case and winding pack are chosen to have minimal poloidal variation in cross section. Some variation exists in the model due to the trapezoidal geometry of the inner leg vs. the rectangular cross section of the outer leg. Temperature of the TF winding pack was initially assumed to remain constant poloidally. The goal of this approach was to minimize poloidal slippage of winding pack and case. This is not necessarily unacceptable, but adds some complexity to the behavior of the TF coil, and adds some special concerns for the leads, and crossovers. Large variations in cross

"Exploded" View
Showing Crown
Rail and Slot

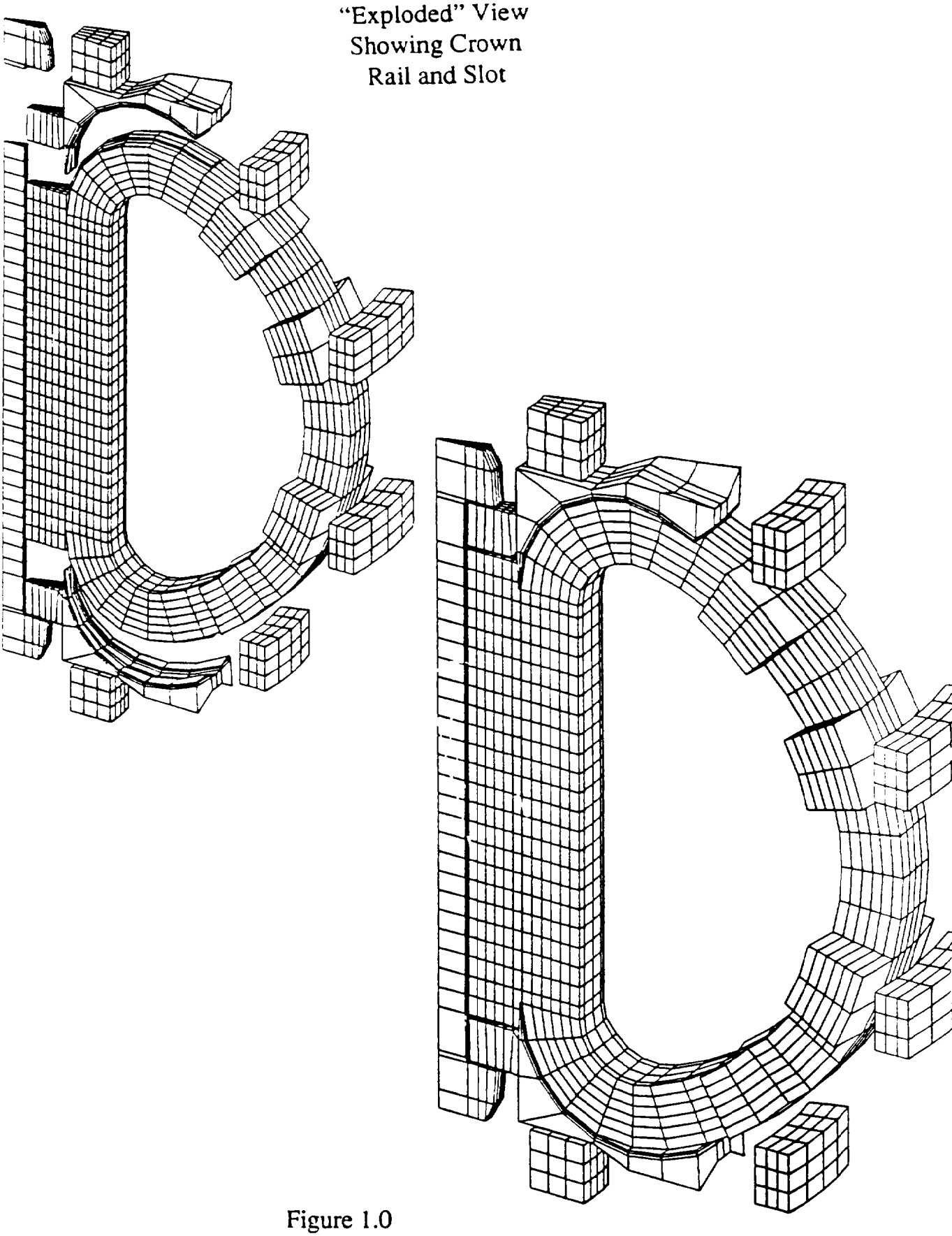

Figure 1.0
Global Structural Model

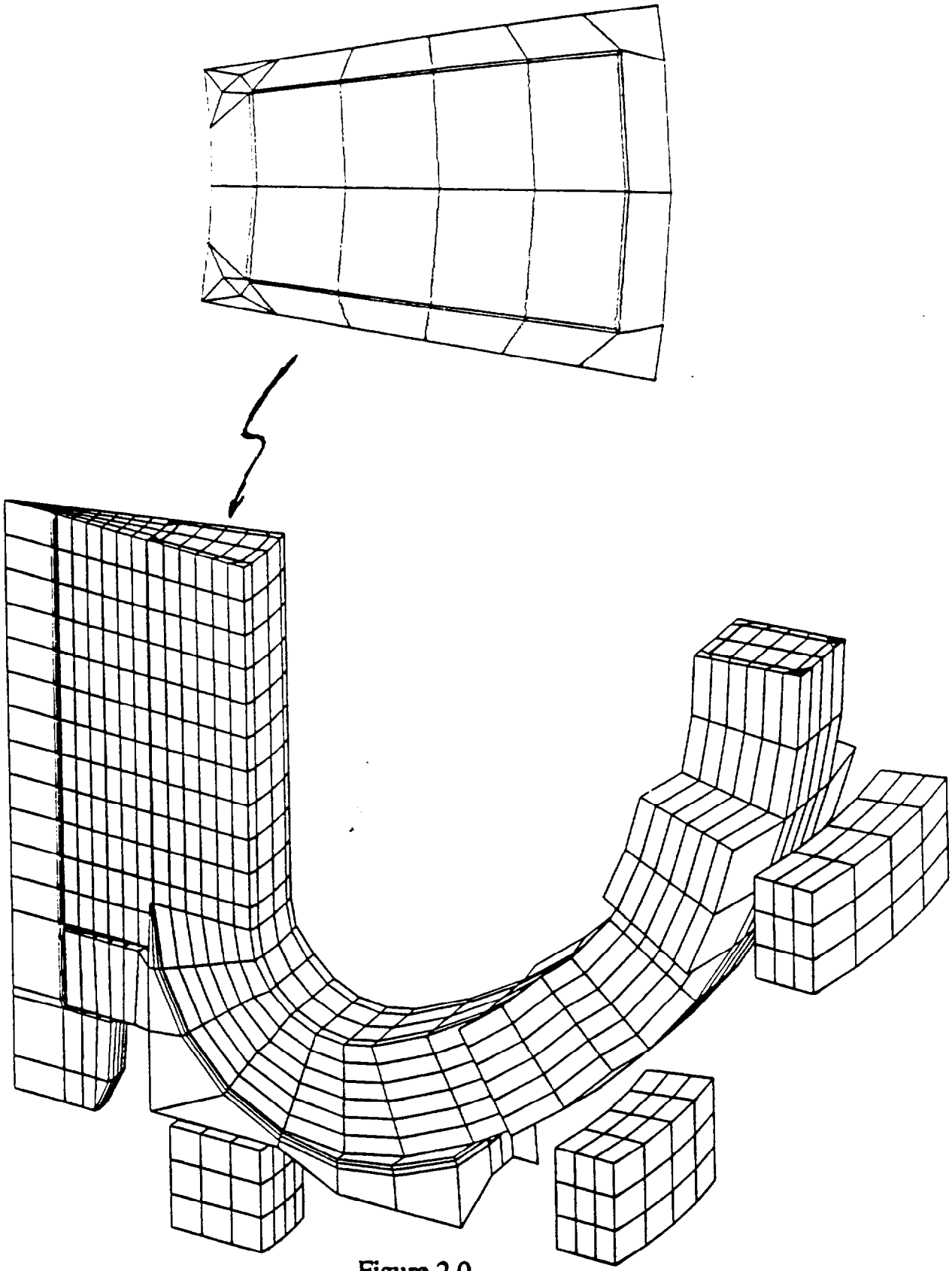

Figure 2.0
Lower Section of Global Model showing TF Case and Winding Pack Sections

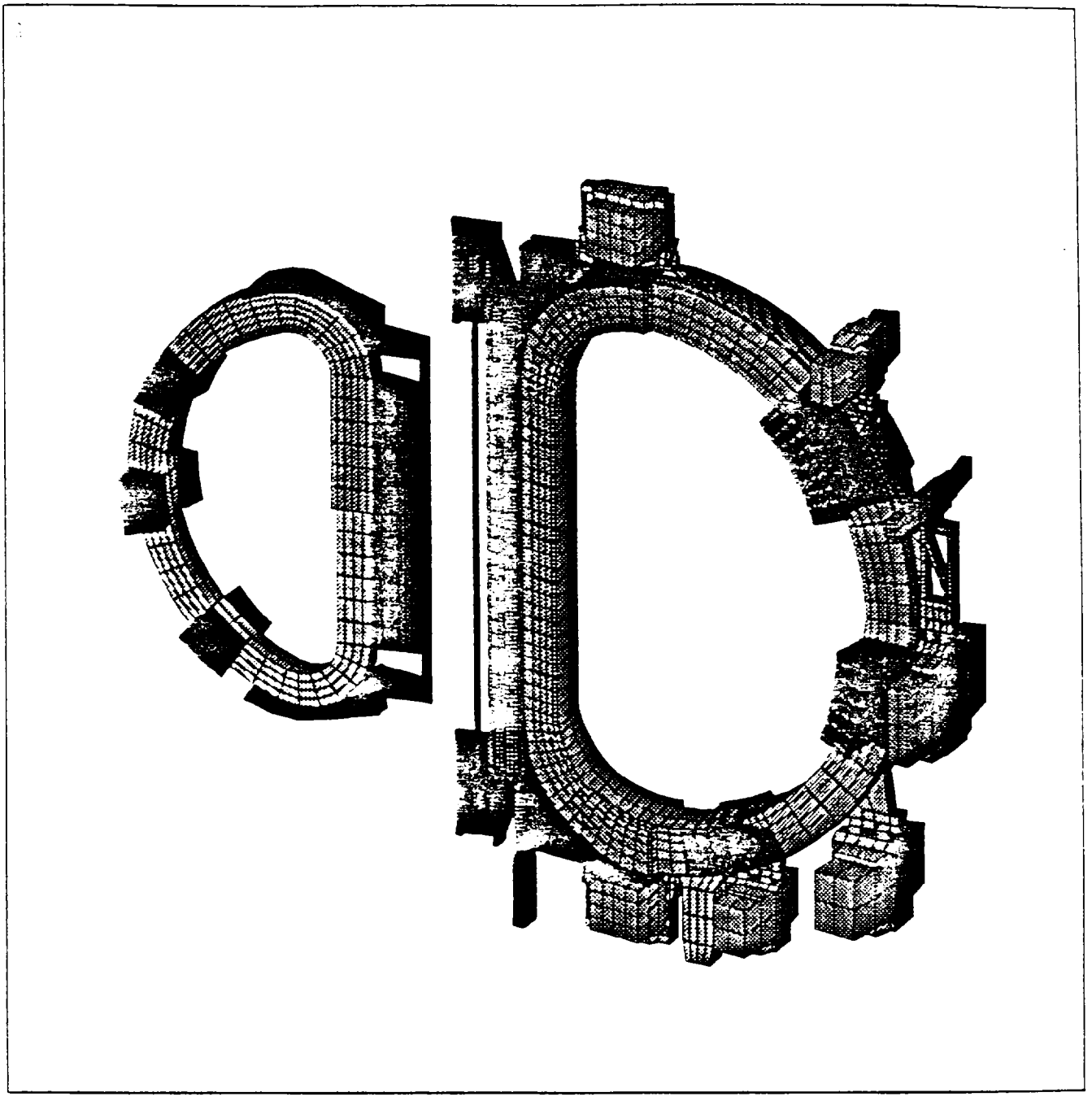

Figure 3.0
Comparison of PCAST and ITER Global Structural Models

section may ultimately be attractive to reduce heat-up, power consumption, and coil stresses.

In early analyses, the heat-up of the TF winding pack produced too high a case poloidal tension stress when uniform poloidal distribution of TF temperature was assumed. It is likely that a cooler outer leg will have to be relied on to improve the temperature related compressions in the copper and the temperature related tensions in the TF case.

Crowns and Intercoil Structure are the major OOP structures. No torque cylinder is used on the inside or outside of the CS. TF Case bending supports inner leg OOP loads. ITER is moving away from using the outer CS cylinder for OOP loading. The PCAST machine has relatively larger inner leg OOP loading and the outer torque cylinder might be more helpful than in ITER. The crown - rail/slot is modeled with toroidal gaps only. The crown is not connected to the TF case vertically except by friction.

PF Coil Support

The PF coils are included in the model, but outside the CS stack, the PF coils are supported via displacement constraints. Their radial loads are taken in hoop tension, vertical loads are taken by displacement constraints, and not the TF case. PF loads applied to the case in the ITER analyses have not proven to be a significant contributor to the case stresses.

Vertical and Torsional Datum for the Model:

Vertical constraint of the model is accomplished via vertical and toroidal displacement constraints at the equatorial plane of the central column. CS bucking cylinder, and TF are constrained. This assumes up-down symmetry consistent with the double null divertor.

Modeling of Interfaces:

The model is non-linear. Gaps with friction capability are used between case and winding pack The assumed friction coefficient is 0.2. Gaps and friction are also

used at TF/CS bucked surface, also with a friction coefficient of 0.2. This is a little on the high side. Friction coefficients lower than this are easily achieved. The choice of bearing material will have an effect on the relative motions of the TF and CS. CS vertical stress, and shear stresses, and TF case out-of-plane bending are affected by interface friction.

Vertical and torsional registration is an important issue with a bucked design. In ITER, a region of higher friction material is used near the equatorial plane, and lower friction bearing material is used at the ends of the CS/TF interface. JET is an example of both the successful application of the concept, and the problems that result if the relative motions across the interface are not well understood. In ITER, frictional simulations using large finite element codes are used, as well as simple special purpose computer simulations. Agreement is good between the two approaches.

Use of a Tierod

Tierod preload is applied to the CS. The launching loads in the CS stack, particularly at the X point creation, must be resisted by a central bolt, or tierod. The total launching load is approximately 200 MN. The tierod doubles as a bucking cylinder for the CS. The exact details of the CS bore will depend on the requirements for cooling passages, the size of the tierod, or assembly of tierods needed to resist the launching forces, and the necessity for improvements in CS shear stress capacity, and the requirements for a bucking cylinder for the CS. Currently, in the model, these functions are satisfied by a single monolithic central bolt, but the actual design will probably be a more complicated multi-purpose structure.

Loading:

A full pulse is analyzed. This consists of the following load steps:

Cooldown

TF on prior to PF energization (TFON), (more reflective of the null point after IM)

Initial Magnetization (IM),

Creation of the X point, or divertor flux shape (XXO or XPF),

Start of Flat Top (SOF)
Start of Burn (SOB)
End of Burn (EOB)
End of Pulse (EOP) prior to cooldown

A plot of in-plane forces at the XPF time point is shown in Figure 4. OOP forces are shown in Figures 5 and 6. These are actually the full load files with the in-plane components zeroed out. TF is assumed at full field at initial magnetization. The full TF centering pressure is needed when the CS current is at a peak.

Temperature Input:

Temperatures are computed outside of ANSYS. The TF temperatures come from a MAP run. The TF winding pack was taken to be at 190 deg K at EOB and at 80 earlier in the pulse. The peak temperature at end of pulse is about 220, with the integrated average being about 180 degrees. A strip wound coil is assumed.

- Strip wound TF coils do not exhibit the coupled thermal electromagnetic current diffusion problem of bitter magnets

- Strip Wound coil develops OOP bending strength without reliance on conductor to conductor bond.

Temperatures are input to the TF winding pack and increase the case tension, and decrease the winding pack tension. Temperatures are also input to PF1 - the rest of the CS/PF coils were assumed to remain cold. PF1 is taken to be at 220 deg K at EOB with the rest of the PF coils remaining near 80 deg K. This roughly corresponds to an initial temperature of 30 deg K in PF1. The temperature input is only applied at EOB and EOP because early in the pulse the temperature differentials are small and can be ignored for this level of study. Many stress components are sensitive to the coil differential temperatures, and some different temperature distributions were investigated to improve the stress state. The CS is fully merged in the earlier models - Differential thermal and Lorentz force load

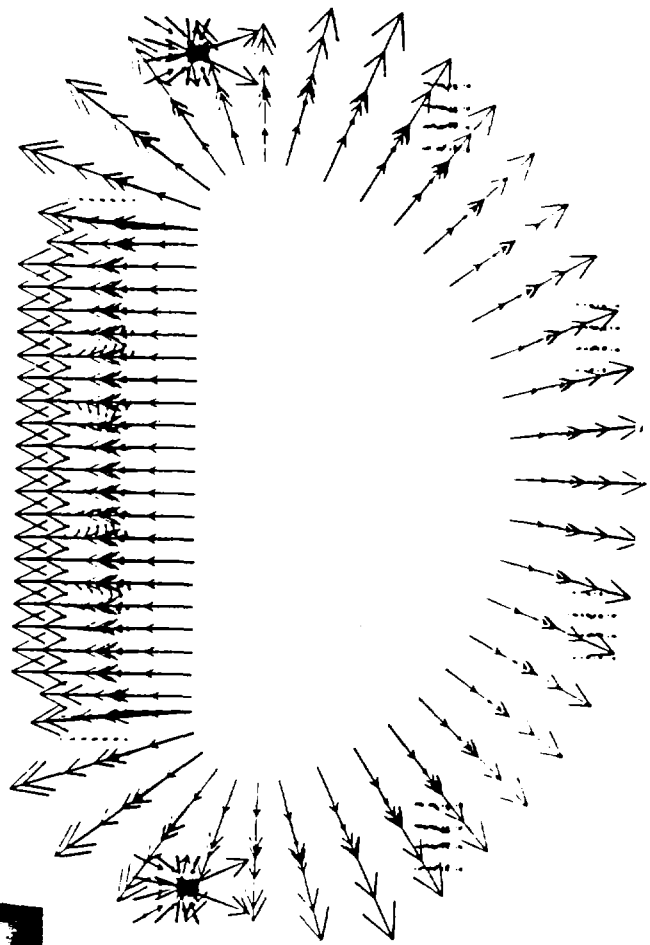

In-Plane TF, CS and PF Forces at XPF

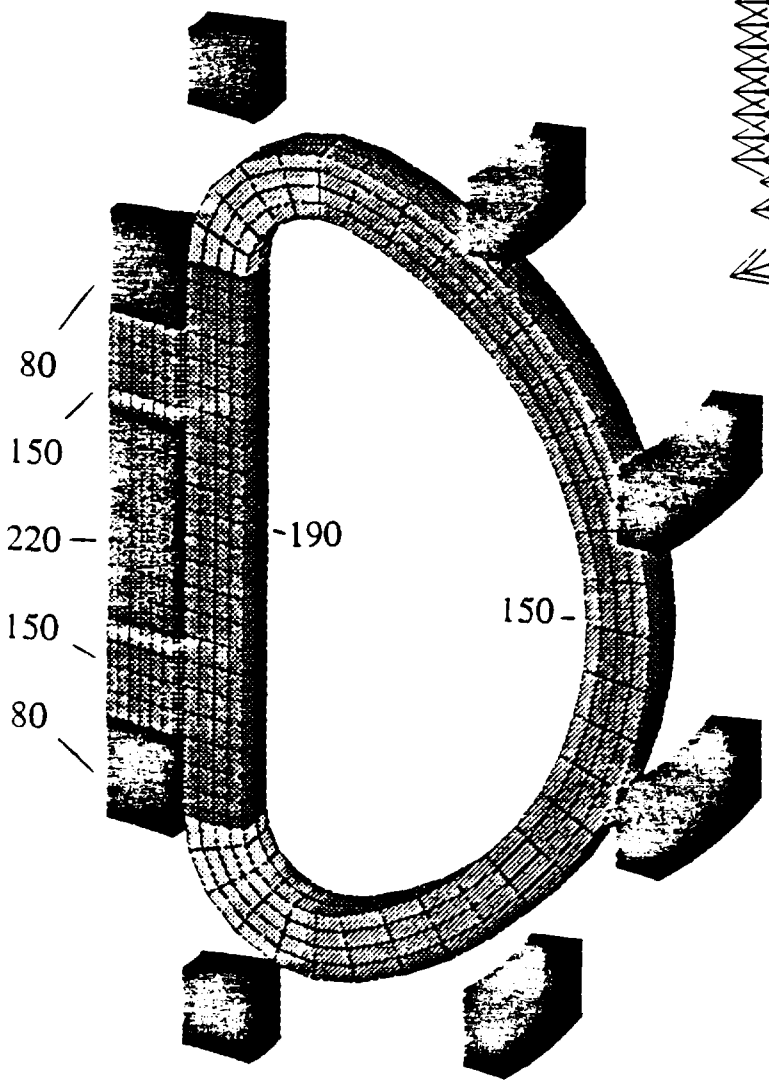

Temperatures at EOB

Figure 4.0
PCAST Structural Analysis Loadi

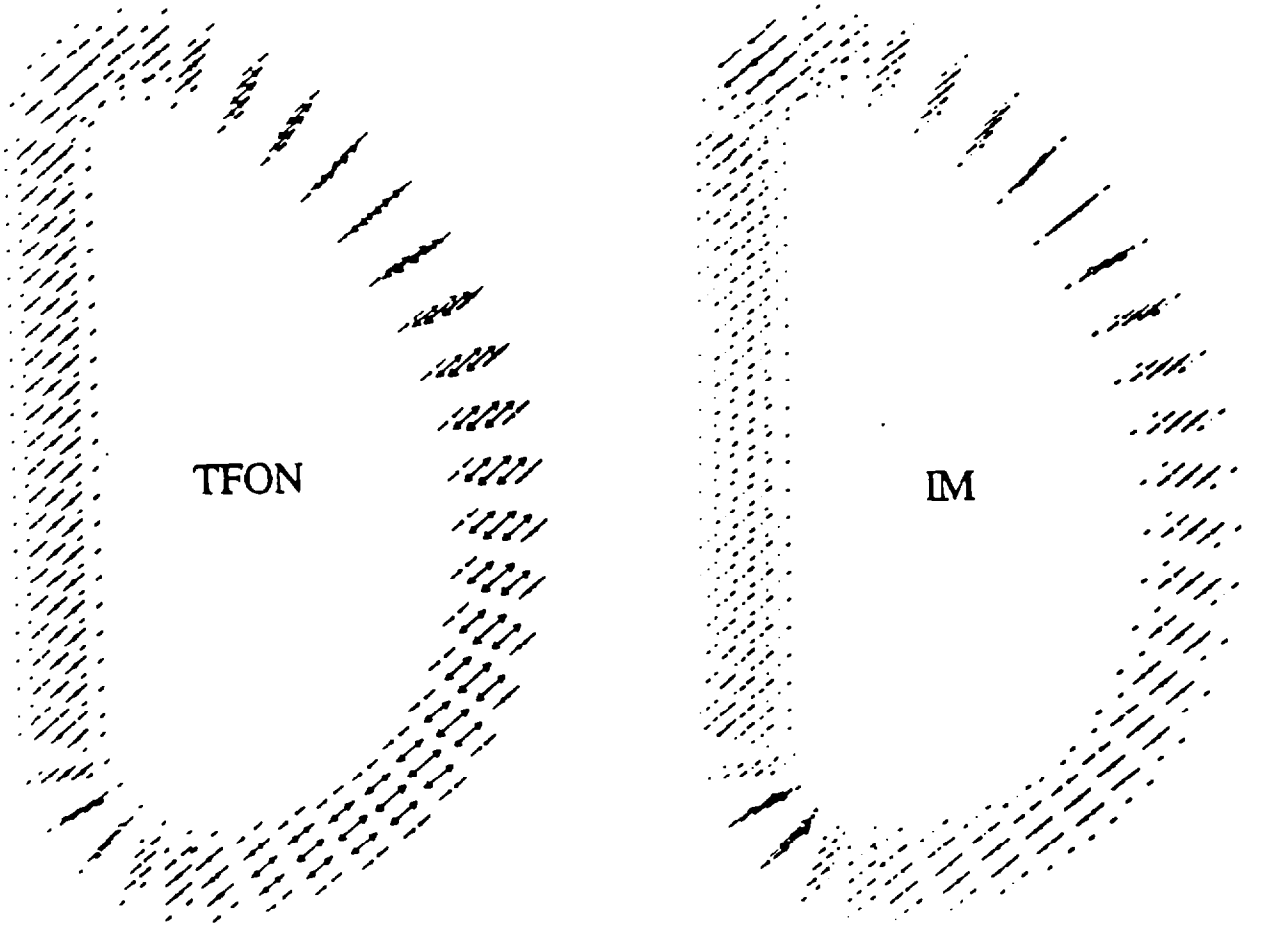

OOP forces (force files with in plane forces zeroed)

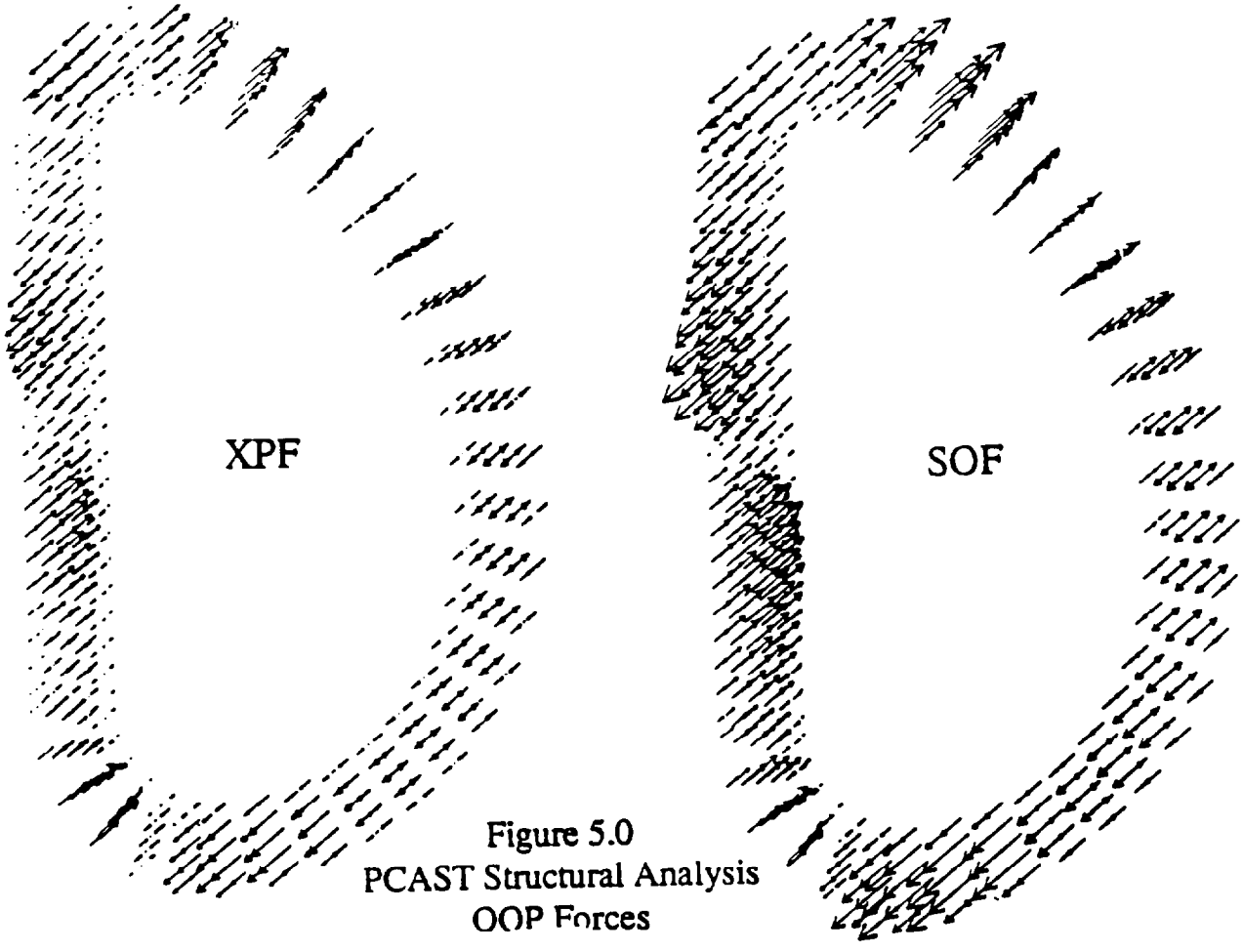

Figure 5.0
PCAST Structural Analysis
OOP Forces

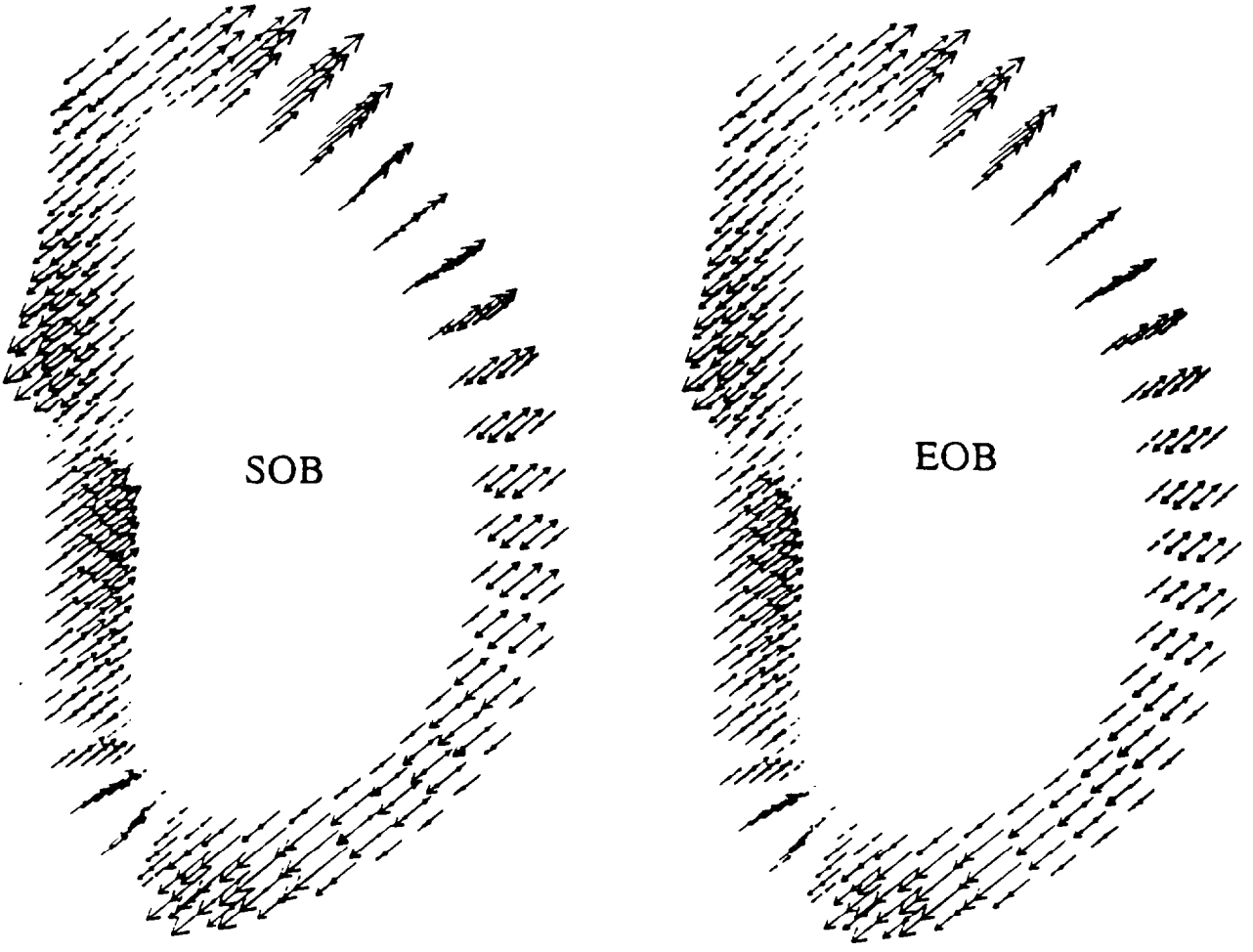

OOP forces (force files with in plane forces zeroed)

Figure 6.0
PCAST Structural Analysis
OOP Forces

strains were absorbed elastically. This should be considered a design goal for a bucked design. The confinement of the CS between the TF and bucking cylinder will help restrain internal CS motions, and minimize shear stresses. The merged modeling is a poor modeling of the launching forces. In later runs, the mesh in PF1 and PF2 was refined and slip planes were added to the interfaces between PFs 2, 3, and 4.

Assembly Logic:

No unfilled TF/CS assembly stand-off or gap is assumed. Use of an epoxy or other filled bladder is assumed at assembly rather than the approach in which an assembly gap is closed via TF energization, as in the current ITER design. Electromagnetic closure of an assembly gap will add bending related poloidal tension stress to the TF case and winding pack. PCAST is stiffer in bending than the larger ITER coil, and would develop larger stresses for the same assembly gap.

Primary Stress Allowables:

The case will remain approximately at liquid Nitrogen temperatures throughout the pulse. Eddy current and nuclear heating may increase the temperature, but for the purpose of the present structural calculation, the steel is assumed to remain at 80 deg. K.

316 SST LN Yield at 80°K	690 to 850 MPa
316 SST LN Ult at 80°K	1200 MPa
316 SST LN Yield at 4°K	980 MPa
316 SST LN Ult at 4°K	1500 MPa
OFHC 60% Hard Copper Yield at 77°K	373 MPa
OFHC 60% Hard Copper Ult at 77°K	474 MPa
OFHC 60% Hard Copper Yield at 292°K	308 MPa
OFHC 60% Hard Copper Ult at 292°K	350 MPa
OFHC 60% Hard Copper Yield at 200°K	328 MPa
OFHC 60% Hard Copper Ult at 200°K	383 MPa

Using the lesser of 2/3 Yield of 1/2 ultimate, produces the primary membrane (PM) and membrane plus bending (PM+B) allowables below:

Stainless Steel at LN2 temperature	
PM	460 MPa
PM+B	680 MPa
Copper at LN2 temperature	
PM	237 MPa
PM+B	355 MPa
Copper at 200 deg K	
PM	191 MPa
PM+B	287 MPa

Fatigue:

The design life of the reactor is 5000 full power shots. The copper peak stresses are for the most part, strain controlled with more favorable R values than -1. Life will have to be calculated based on the specific stress cycle, and thermal history. Some of the load history is at LN2 temperatures, with more favorable fatigue properties of the material, and some of the load cycle is at higher temperatures. For the present study, peak copper stresses were kept at or below the 200 MPa level which would yield thousands of cycles for a room temperature, load controlled R=-1 loading, but with no margin. More careful analysis including strain controlled effects is expected to yield adequate margins. Some strain controlled data is shown in Figure 16. This indicates that much larger strains than that corresponding to 200 MPa stress are allowable if strains are confined. The type of stress experienced by the copper winding is somewhere between strain and load control. The multiple winding composite nature of the coil yields one level of constraint. Flaws in one plate will be constrained by intact material in neighboring plates. The case provides another level of constraint for the whole winding pack. Copper creep and cyclic softening will shed load to the case, at the expense of the case fatigue life. R&D relating to the specific stress state of the copper in the PCAST machine will be needed to demonstrate margin. The more restrictive of a factor of 2 on stress and 20 on cycles is the usual criteria for smooth specimen S-N type criteria and should be reviewed given the specific

range of loading, and the failure mechanism which is not a catastrophic burst as in the case of a boiler .

Analysis Runs:

Run#1

Initial sizing run, monolithic CS with assumed currents calculated from the required volt-sec.

Run#2

Merged CS stack, 6X2 grid in PF1,2,3,and 4, .3m radius tierod, 190 deg TF at EOB, 220 deg PF1 at EOB, all others at 80 degK 1.2 meter CS build, but with Sept 26 PF Scenario based on a .8 meter build

Run#3

Merged PF1 and 2, Gaps between PF2,3,and 4 6X4 grid in PF1 and 2 1.0 Meter CS build, with 1m PF scenario, larger tierod, doubles as a bucking cylinder, 1.14m diameter tierod/BC small tierod pretension.

Run#4

Same as run #2 but with 220 deg PF1 at EOB, and 150 deg PF2 at IM

Run #5

Same a run #4, but the IM temperature of PF2 is returned to 80 deg. and a non-uniform EOB temperature is assumed - 190 at the inner leg and 150 in the outer leg. . A final load step was added that represents the fully off, but hot tokamak. The PF1 temperature is assumed at 220 deg, and the TF winding pack is assumed at 180 deg. 1.14m diameter tierod/BC 390 MN pretension. (tierod preload gap=.012m)

Run #6

Same as Run#5 but with improved knife edge in the crown, and a tierod preload of 195MN

Run #7

Same as Run#6 but the distribution of the friction coefficients at the CS/TF interface was changed. The friction coefficient at the edges of the TF case were set at .1. The upper and lower ends of the interface also had a friction coefficient of .1 leaving a patch at the center region of the contact "patch" at .2 to hold vertical and torsional registration. The intent of this analysis was to reduce the "scuffing" shear on the CS at the mid-plane.

Results:

General Behavior:

TF case poloidal tension is a major indicator of the design adequacy. The bursting force, and the OOP loads are supported by direct tension, and bending tension respectively. These add to contribute to a peak tensile stress typically where the inner straight leg meets the inner curves of the "D". Both these components are resisted by the case and the winding pack. The load share is a function of the relative cross sections, moduli, temperatures, and moments of inertia of the case and winding pack. The CS also participates in carrying OOP loads via friction at the CS/TF interface. At TFON the cold WP reduces case tension, and increases winding pack tension. At EOB, the "warm" WP increases case tension, but the winding pack tension is offset by the thermal compression, which subsequently appears when all the magnets are turned off.

There is a nonuniform bearing at the CS/TF interface. This is partly a result of the TF inner leg twists due to OOP loads, but it is largely the result of the radial expansion of the warmer central region of the CS. This may be seen in the radial displacement plot, Figure 7.

The CS is in hoop tension, when it is fully energized. The large radial build of the CS and an insufficiency of TF pressure produces inner radius tension in the CS. In bucked designs such as ITER, CS hoop tension usually does not develop. The thermal differentials add to the hoop tensions as well. The "warmer" PF1 moves outward at EOB. This increases the radial pressure at the surface of PF1 and reduces its ID hoop tension, but adds to the hoop tension in PF2, and adds vertical bending components. PF1 differential radial motion causes higher nose pressure and causes PF1/PF2 in-plane shear at EOB.

Figure 8 is a vertical displacement plot of the whole model. The relative vertical slippage between CS and TF may be seen. At the ends of the CS, the relative motion is approximately 3.5mm. This will have to be accommodated with low friction bearing materials at the interface.

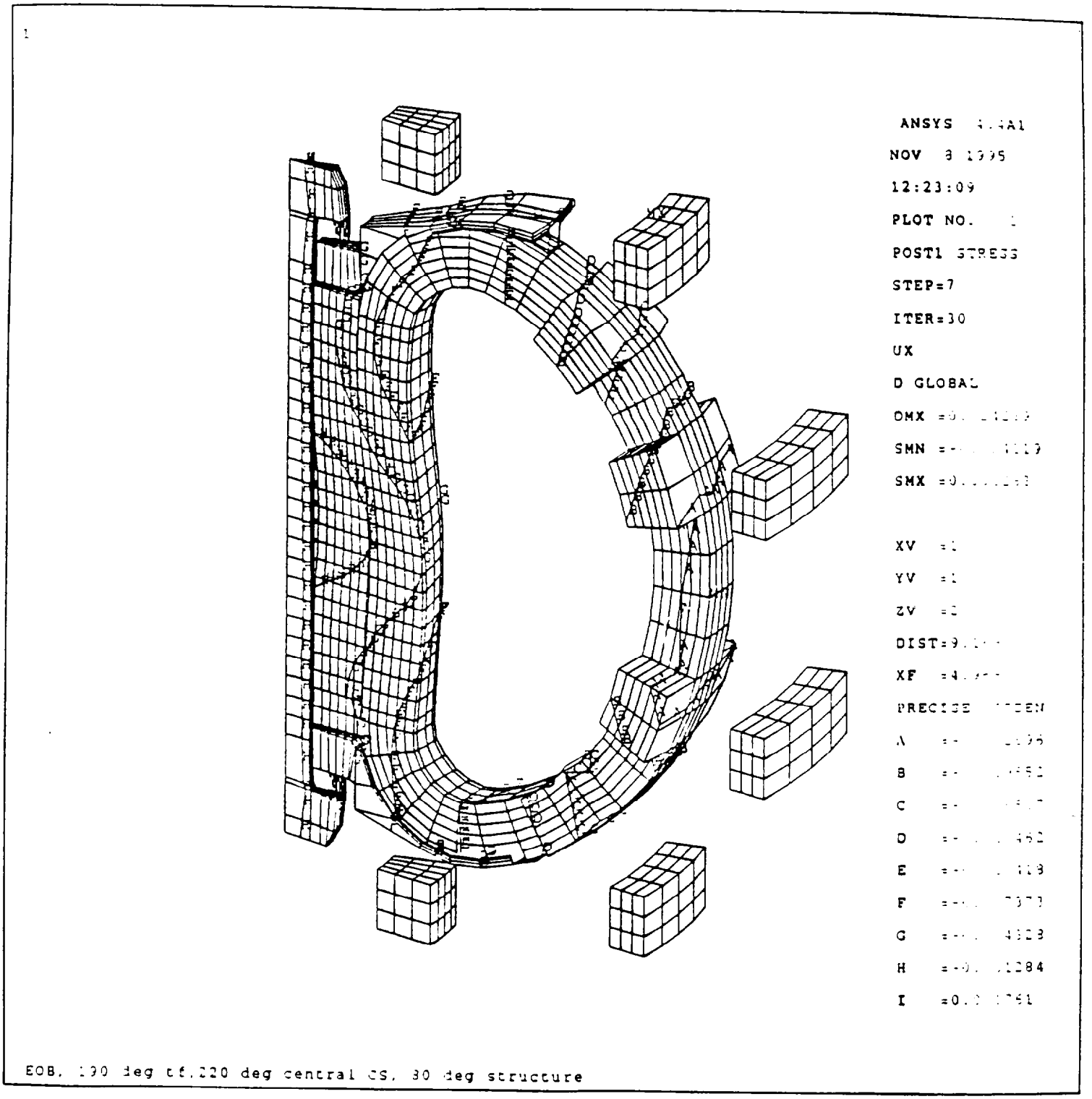

Figure 7
Global Radial (UX) displacement contours
Run #5 EOB

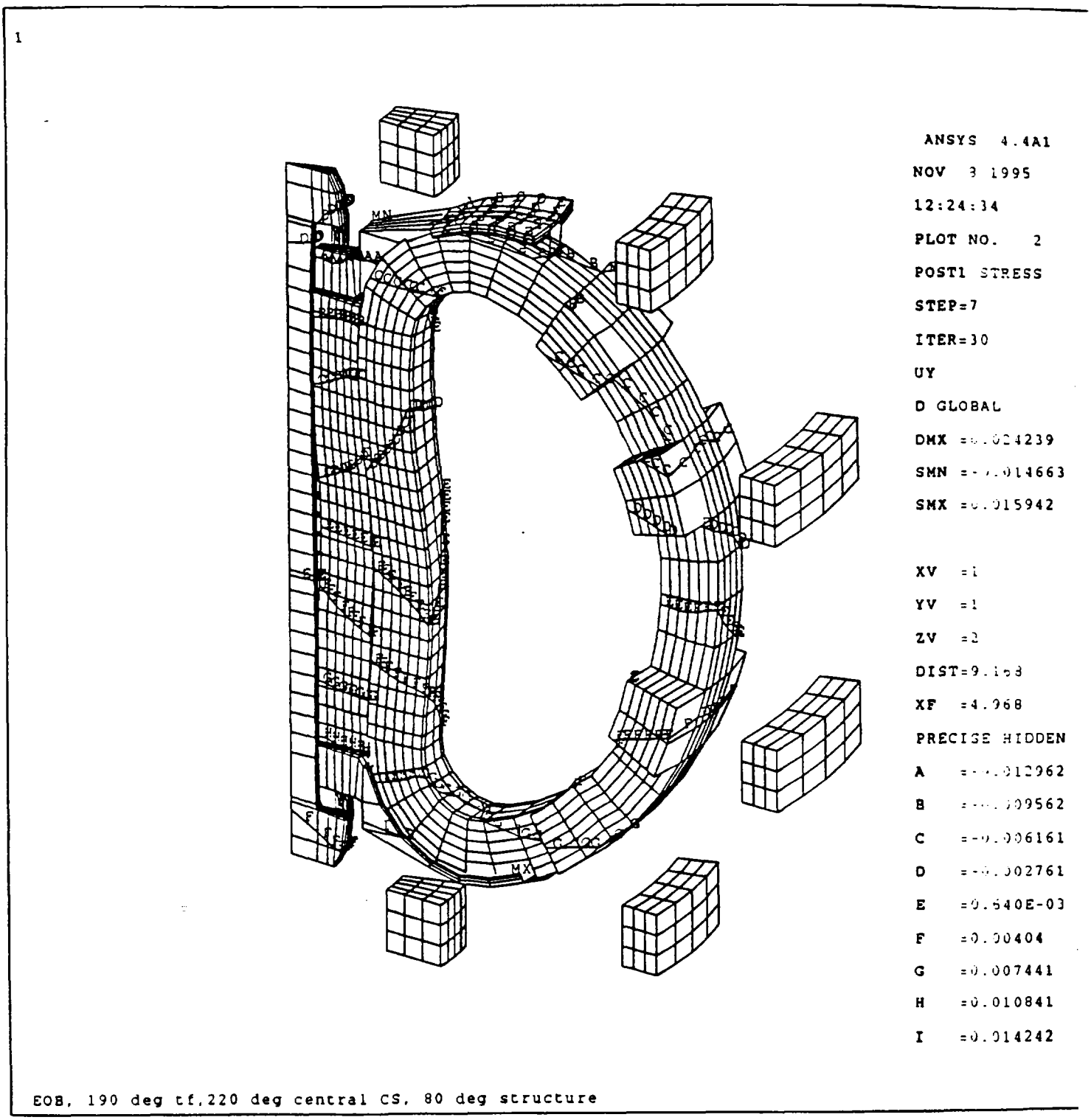

Figure 8
Global Vertical (UY) Displacement Contours
Run #5 EOB

Figure 9 is a toroidal displacement (global UZ) contour plot. The CS is seen to be well coupled toroidally with the TF. The CS is then a participant in the OOP behavior of the machine. In this analysis a friction coefficient of .2 was assumed, lower friction coefficients are possible, and reductions in CS torsional shear could be achieved, but at the expense of an increase in case tension.

TF Case Poloidal Tension

The peak poloidal tension stress in the case is essentially the same as the max principal stress and is the appropriate stress component input to fracture mechanics calculations. It is a measure of the design's fatigue resistance. Initial indications from fracture mechanics calculations indicate this stress component should be ideally less than 450 MPa and possibly as high as 700 MPa may be acceptable pending further fracture mechanics calculations.

Peak Poloidal Tension (in MPa)

	Run#2	Run #3	Run #4	Run #5	Run#7
Cooldown			-2.6	-2.6	-1.95
TFON			222	222	222
IM	350	224	205	205	205
XPF			248	248	283
SOF			320	320	367
SOB			320	320	346
EOB	681	573	628	587	606
EOP					301

The temperature input is applied only at EOB, and it is evident in run #4 that this has a large effect on the case tension stress. SOB and EOB OOP loads are not substantially different, yet the case tension takes a big jump at EOB. In run #5, the outer leg temperature was modeled more realistically as cooler than the inner leg. The outer leg was taken as 150 deg. with the inner leg remaining at 190 deg. An improvement in case tension stress is seen. Plots of the case poloidal tension is shown in Figures 10 and 11.

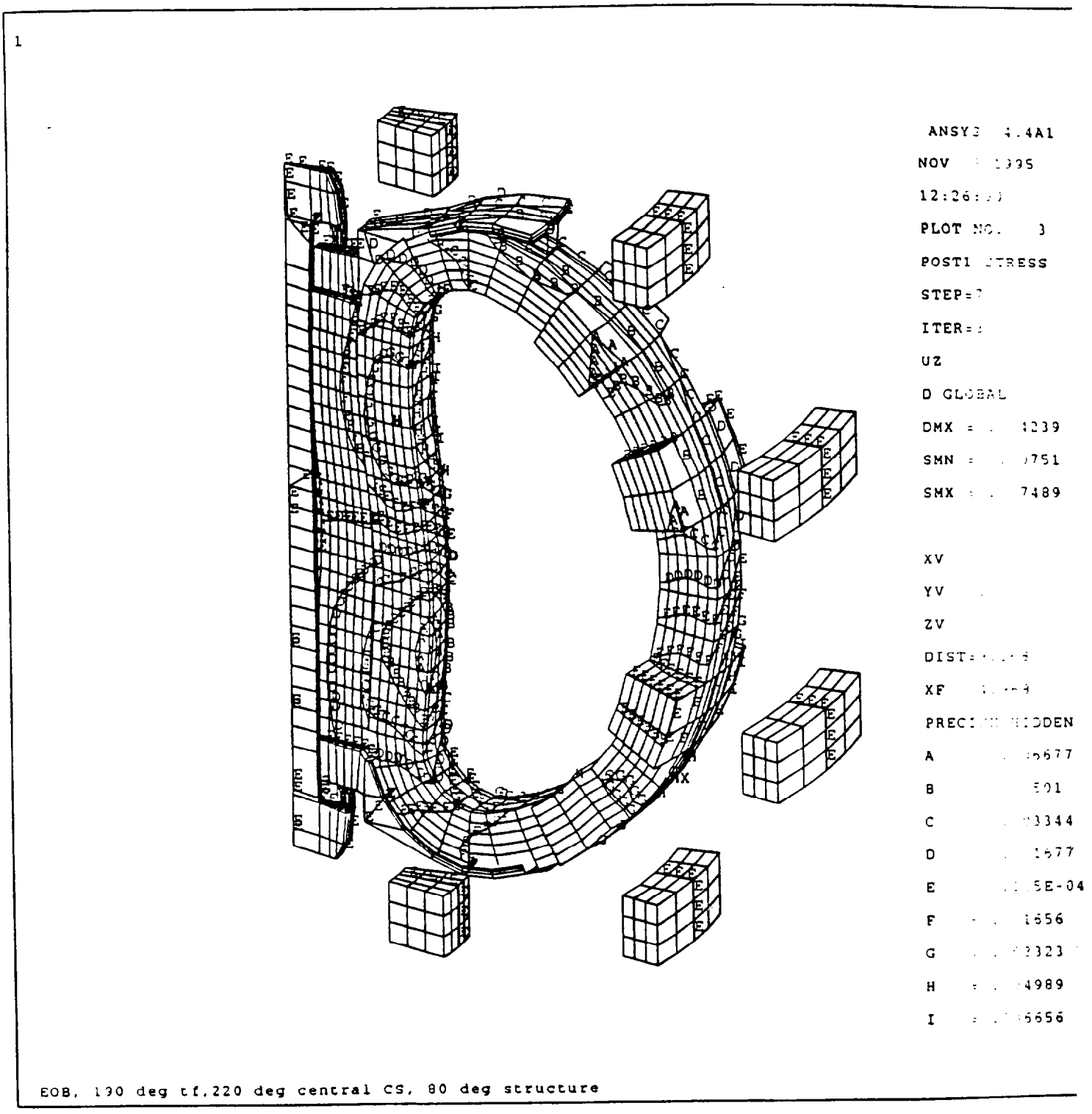

Figure 9
Global Toroidal (UZ) Displacement Contours
Run #5, EOB

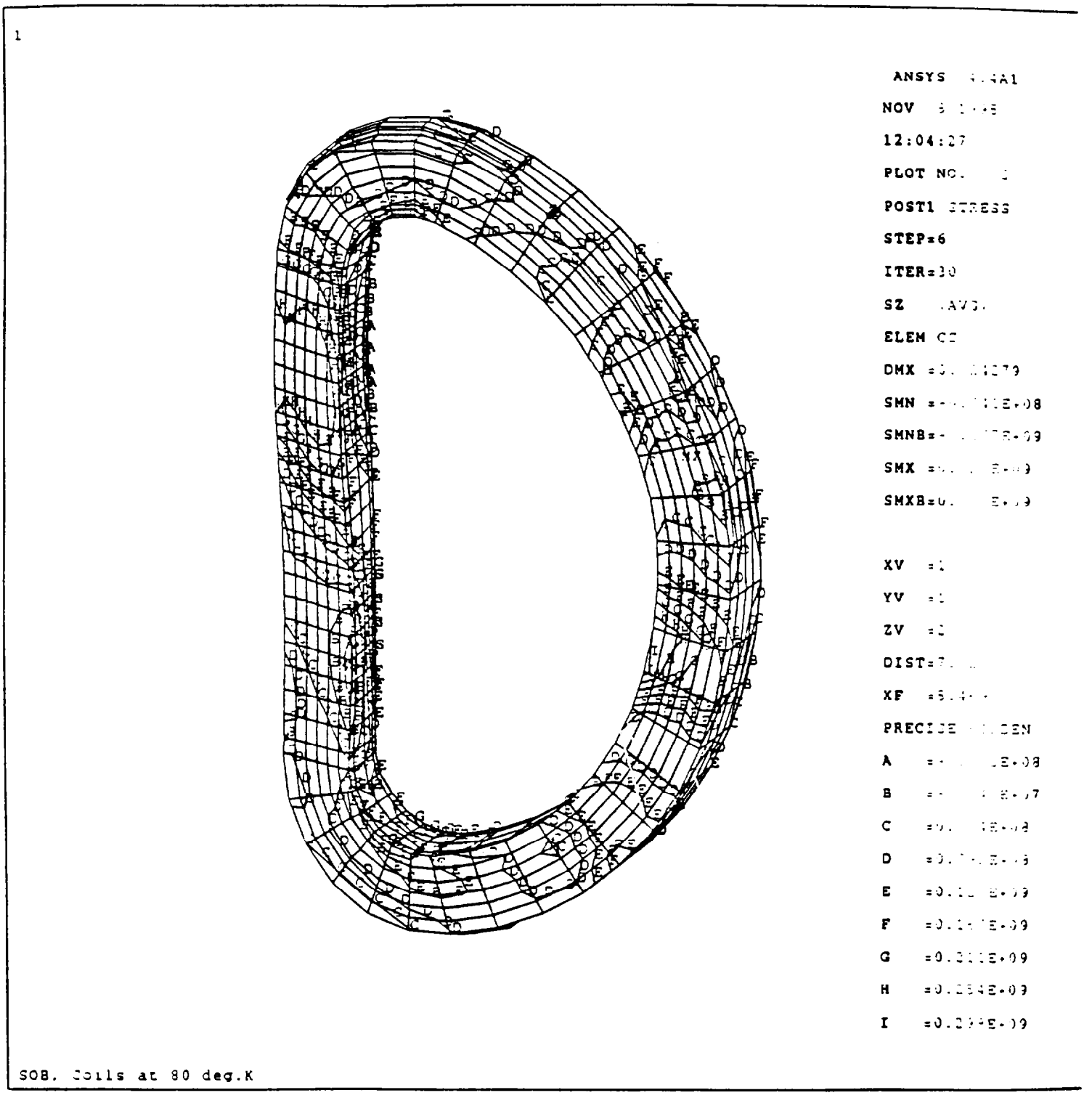

Figure 10
Case Poloidal Tension Stress
(Element Local SZ)
Run #5 SOB

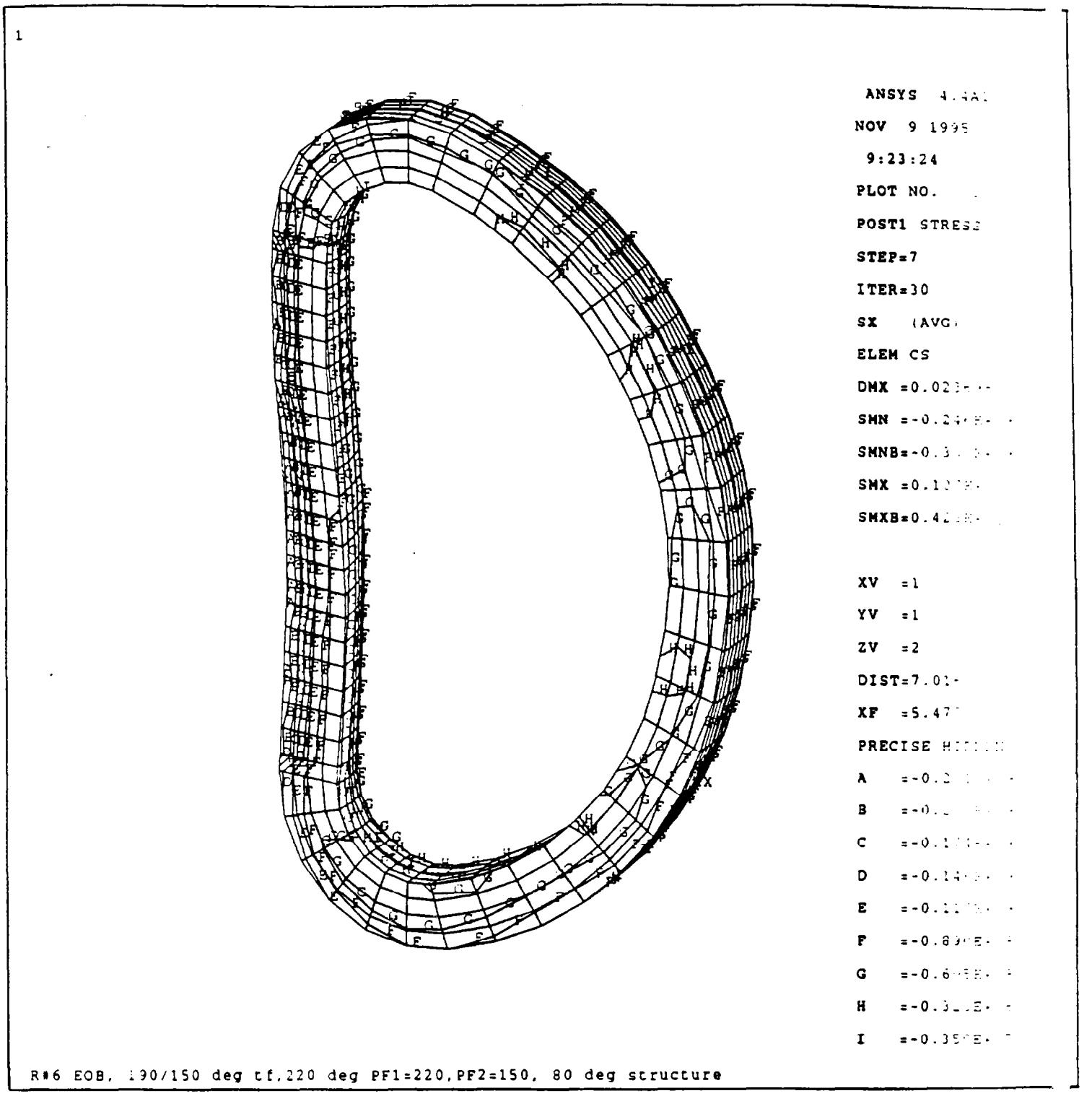

Figure 12
Winding Pack Radial Compression Stress
(Element Local SX)
Showing Higher Compression Bearing Against PF1
Run #5 EOB

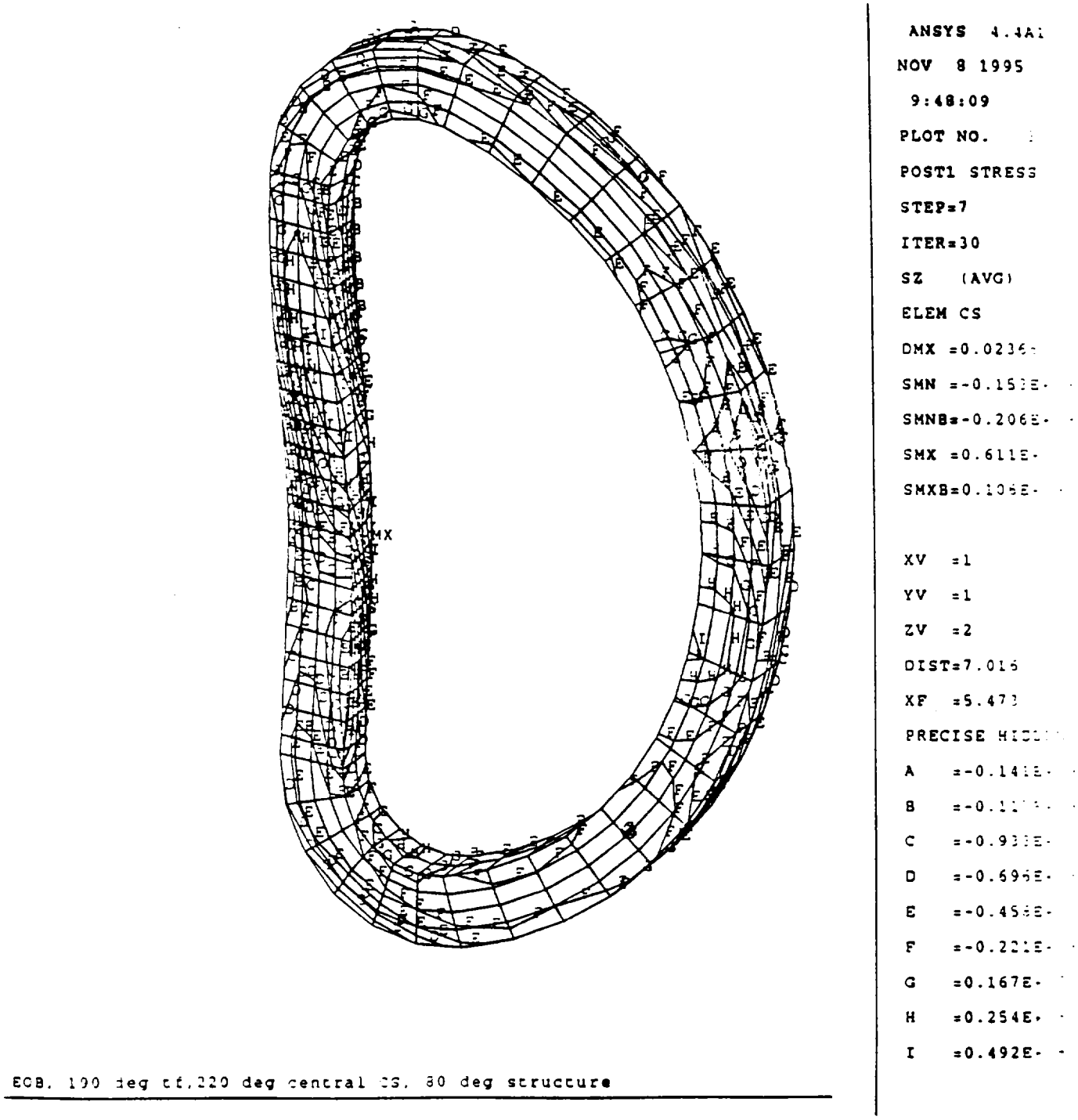

Figure 13
Winding Pack Poloidal Tension Stress
(Element Local SZ)
Run #5 EOB

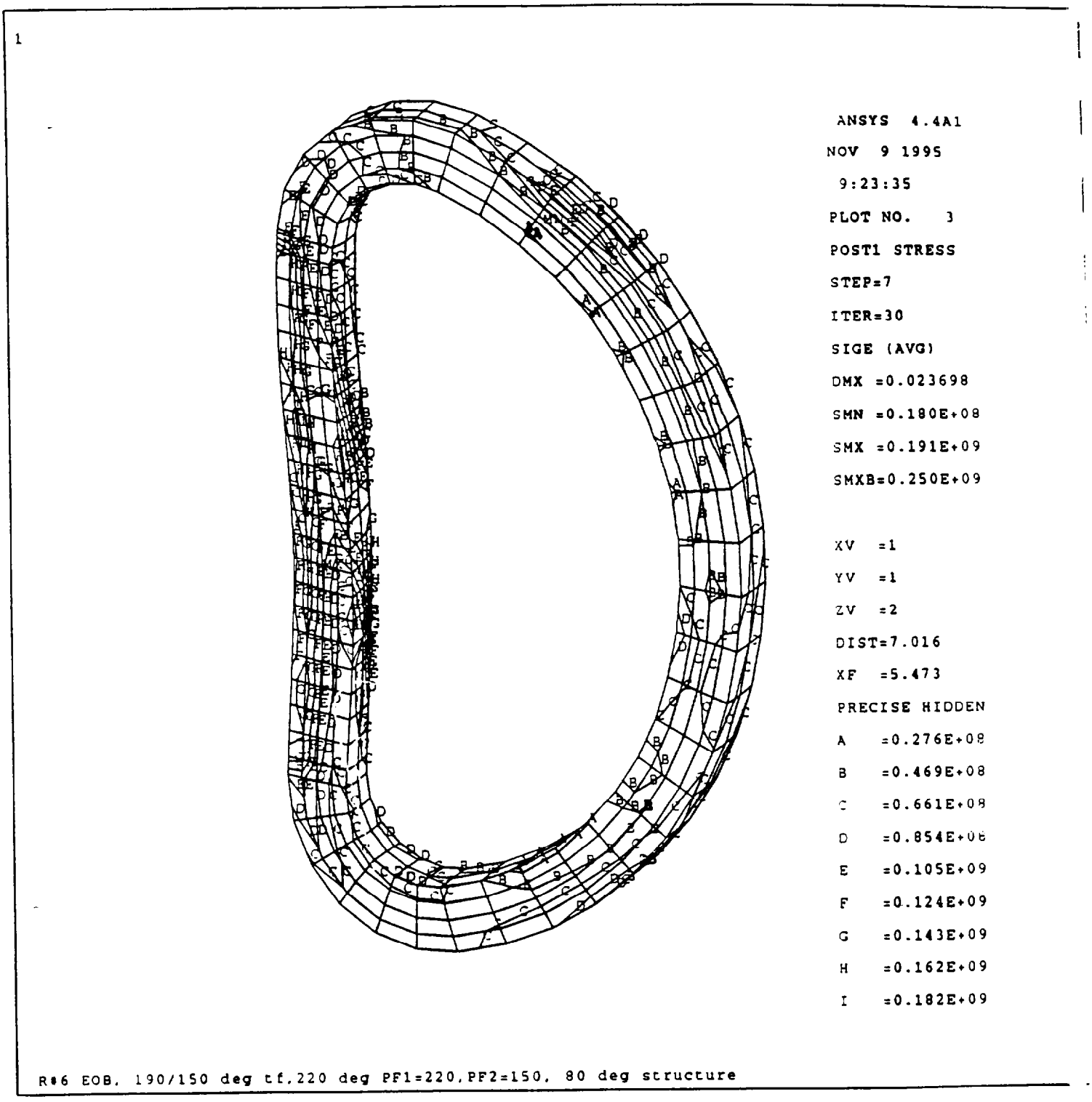

Figure 14
Winding Pack Von Mises Stress
Run #5 EOB

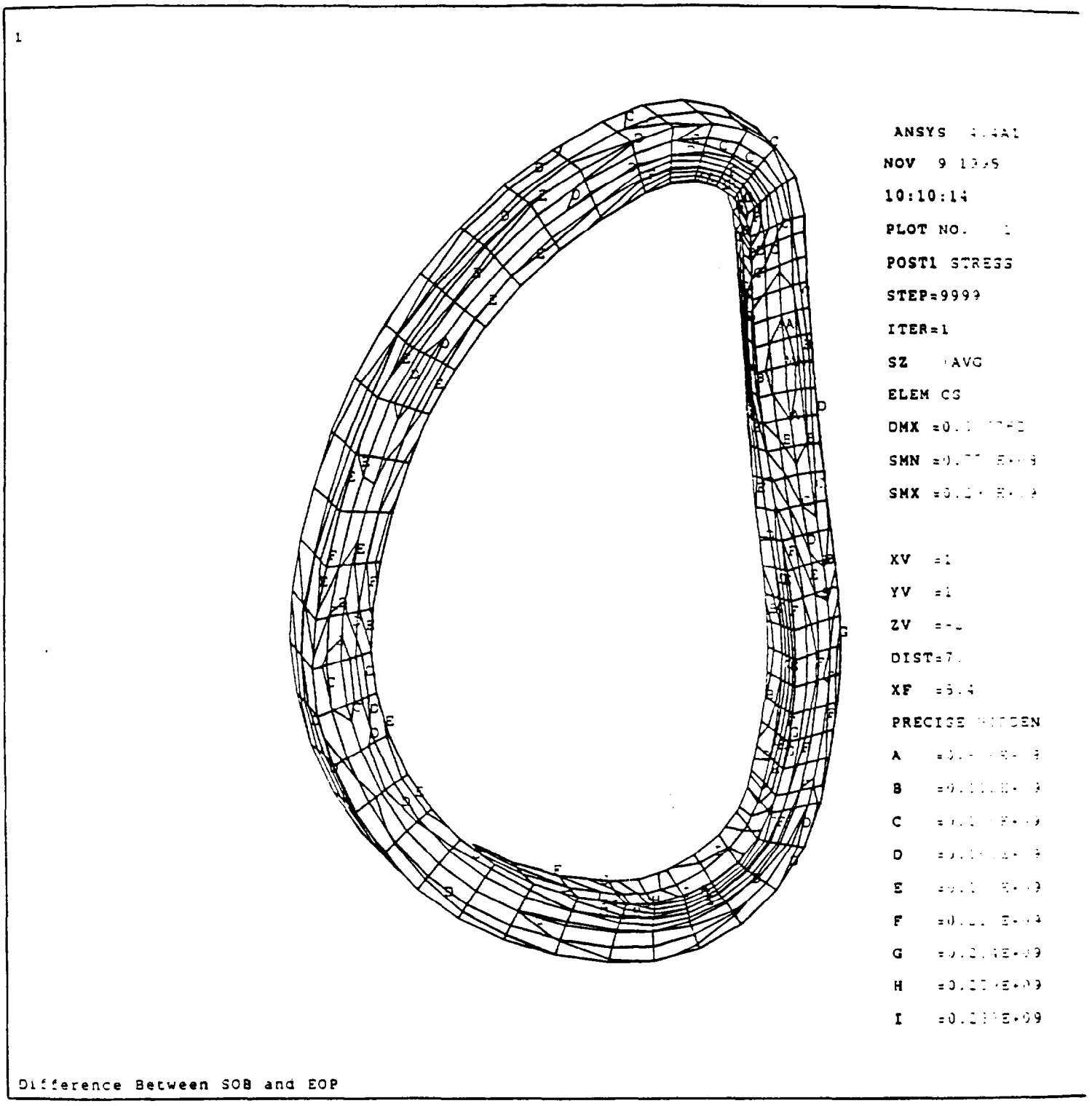

Figure 15
Winding Pack
Tensile - Compressive Stress Range
Run #6 Difference of
SOB and EOP

Figure - 17
Central Solenoid
Stress
Components
Vertical,
Hoop, and
Von Mises
Run #5 EOB

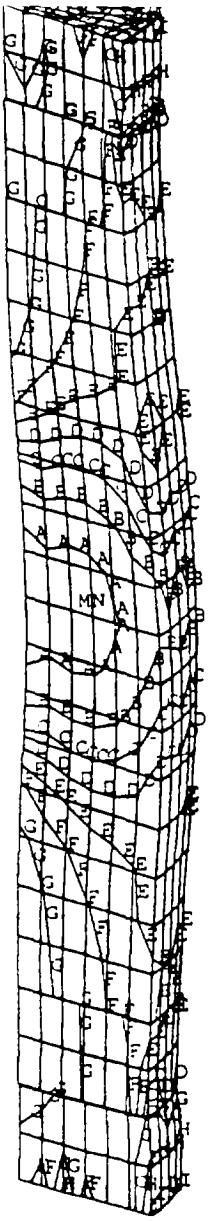

SY (AVG)
ELEM CS
DMX =0.012275
SMN =-0.228E+09
SMNB=-0.256E+09
SMX =0.358E+08
SMXB=0.777E+08
A =-0.213E+09
B =-0.184E+09
C =-0.155E+09
D =-0.125E+09
E =-0.960E+08
F =-0.668E+08
G =-0.375E+08
H =-0.817E+07
I =0.211E+08

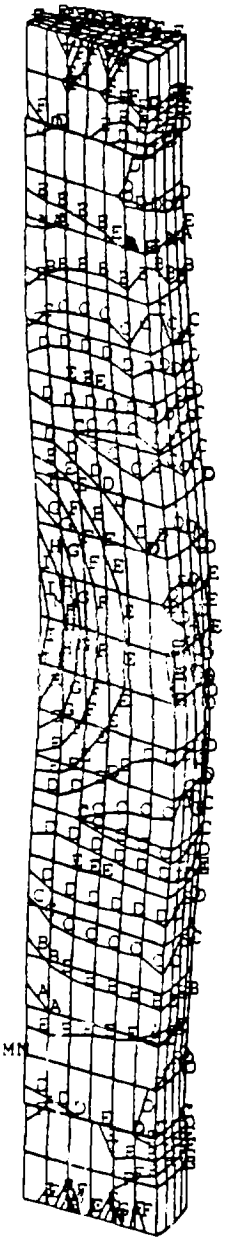

SZ (AVG)
ELEM CS
DMX =0.012275
SMN =-0.196E+09
SMNB=-0.217E+09
SMX =0.104E+09
SMXB=0.132E+09
A =-0.179E+09
B =-0.146E+09
C =-0.113E+09
D =-0.793E+08
E =-0.460E+08
F =-0.127E+08
G =0.205E+08
H =0.538E+08
I =0.871E+08

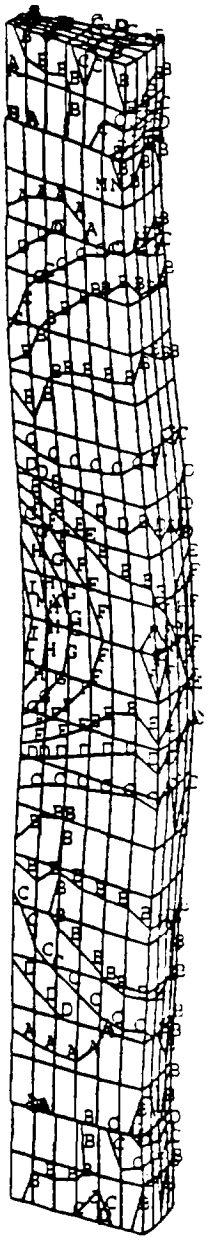

SIGE (AVG)
DMX =0.012275
SMN =0.112E+09
SMX =0.290E+09
SMXB=0.318E+09
A =0.267E+08
B =0.577E+08
C =0.886E+08
D =0.120E+09
E =0.151E+09
F =0.182E+09
G =0.212E+09
H =0.243E+09
I =0.274E+09

CS Radial Pressure Distribution

These are shown in Figure 18. The increase in radial pressure due to the combined effects of heat up and higher currents in PF1. These pressures are similar to ITER at precharge and larger than ITER at EOB.

CS Vertical Stress

These are shown in Figure 19. There are some persistent vertical tensions at the interface between PF1 and PF2. In the model these coils are "glued", or fully merged. The bonded impregnated coil, would not be able to support these stresses. A parting plane will have to be provided.

CS In-Plane Shear (within PF1 and PF2):

	Run #2	Run #3	Run #4	Run #5	Run #7
TFON					.5
IM	-22/18	-17/16	-22/22	-22/22	-8.3/10
XPF				-8/8	0.0
SOF				-15/15	-15/15
SOB					-10/10
EOB	-33/32	-51/49	-21/30	-37/46	-26/25

CS Torsional Shear at mid plane:

	Run#5	Run#6	Run#7
SOF	111		
SOB	106(2)	101	102
EOB	100(1)	96	95.5

(1) with 169 MPa compression, and zero in-plane shear
(2) with 70 MPa compression and zero in-plane shear

CS Required Bond Strength:

	Run#5	Run#6
SOB	106-70*.5= 71	101-48*.5=77
EOB	100-169*.5=15.5	96-157*.5=17.5

(Postprocess of vector sum of shears on a given face minus the compressive stress multiplied by .5). This should be close to 25 MPa.

This could be a potential problem area. Some of the support for the TF OOP loads is coming from the CS. In Run #6, the crown was extended as far as possible into the gap between PF4 and the TF, and the torsional shear at EOB was only

Figure - 18
Central Solenoid
Radial
Stress
Run #7

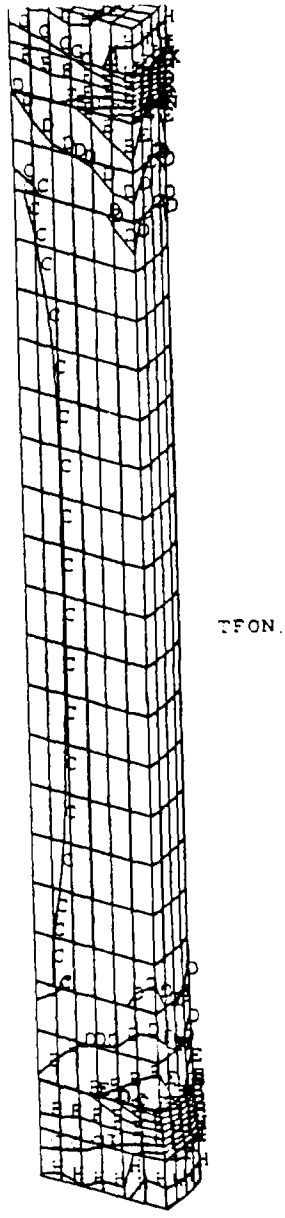

TFON.

SX (AVG)
S GLOBAL
DMX =0.012502
SMN =-0.183E+09
SMNB=-0.219E+09
SMX =0.397E+08
SMXB=0.747E+08

A =-0.171E+09
B =-0.146E+09
C =-0.121E+09
D =-0.965E+08
E =-0.718E+08
F =-0.470E+08
G =-0.222E+08
H =0.257E+07
I =0.273E+08

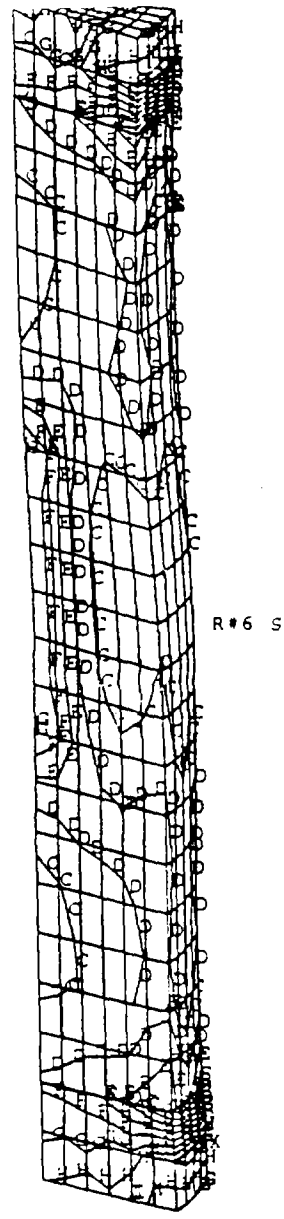

R#6 SOB.

SX (AVG)
S GLOBAL
DMX =0.01369
SMN =-0.182E+09
SMNB=-0.212E+09
SMX =0.418E+08
SMXB=0.715E+08

A =-0.169E+09
B =-0.145E+09
C =-0.120E+09
D =-0.949E+08
E =-0.700E+08
F =-0.452E+08
G =-0.203E+08
H =0.456E+07
I =0.294E+08

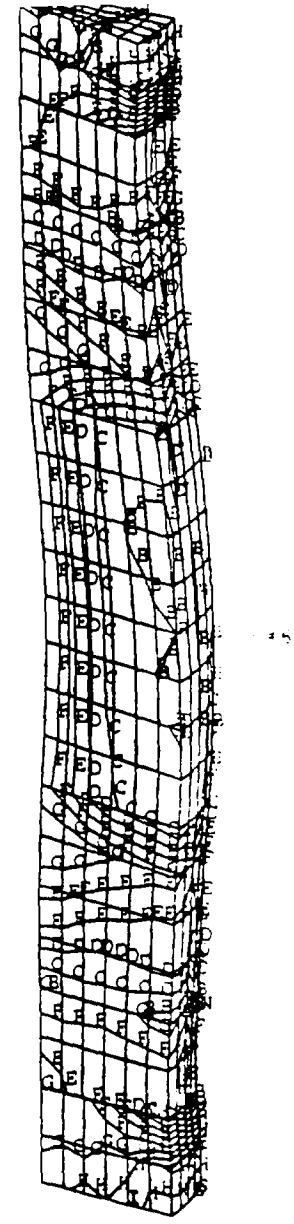

SX (AVG)
S GLOBAL
DMX =0.011467
SMN =-0.199E+09
SMNB=-0.229E+09
SMX =0.433E+08
SMXB=0.878E+08

A =-0.186E+09
B =-0.159E+09
C =-0.132E+09
D =-0.105E+09
E =-0.779E+08
F =-0.510E+08
G =-0.240E+08
H =0.291E+07
I =-0.299E+08

Figure - 19
Central Solenoid
Vertical
Stress
Run #7

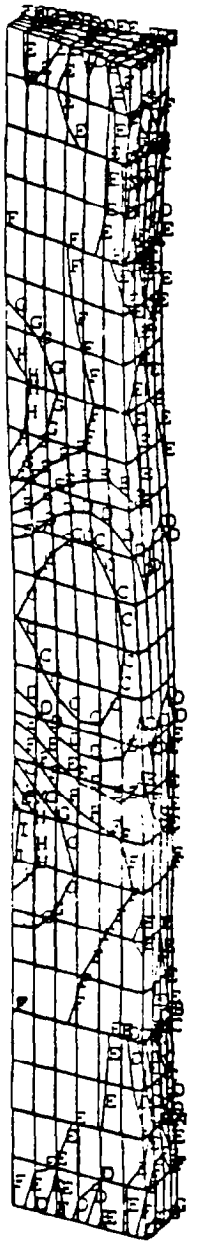

R#6 SOF

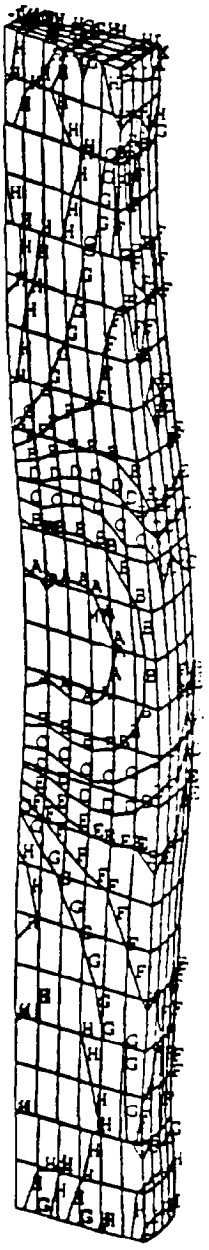

SY (AVG)
S GLOBAL
DMX =0.013723
SMN =-0.121E+09
SMNB=-0.164E+09
SMX =0.783E+08
SMXB=0.117E+09

A =-0.110E+09
B =-0.875E+08
C =-0.654E+08
D =-0.433E+08
E =-0.212E+08
F =914770
G =0.230E+08
H =0.451E+08
I =0.672E+08

SY (AVG)
S GLOBAL
DMX =0.011467
SMN =-0.209E+
SMNB=-0.238E+
SMX =0.275E+0
SMXB=0.684E+0

A =-0.196E+
B =-0.170E+
C =-0.144E+
D =-0.117E+
E =-0.909E+
F =-0.646E+
G =-0.383E+
H =-0.120E+
I =0.143E+0

reduced to 96 MPa. In this run the tierod preload was halved to reduce the CS vertical compression, which went down about 20 MPa. However, the shear component cited here is not pure global torsional twist. Up to 30 MPa of this is from what might be called "scuffing" of the TF nose locally rotating against the CS. This can be seen in the nonuniform toroidal distribution of the shear stress. This can be reduced, or eliminated via reduction in the friction coefficients at the edges of the TF case, or with the addition of a bearing cylinder at the TF/CS interface. With the elimination of this "scuffing" component. The required bond strength is more like 40 MPa for the SOB time point, which is approaching the target of 25 MPa.

An attempt was made to reduce the "scuffing" shear by selectivly positioning the lowest friction coefficient bearing material in run #7. This was not very successful. Further design and analysis work will be needed.

Effect of 20 vs. 16 Coils:

Where OOP bending is important in the TF case, the larger section properties improve the stress state. Ripple requirements usually necessitate moving the outer leg outward away from the plasma. This increases the vertical separating force and direct tension on the inner leg. In going from 20 to 16 coils, there is an improvement in section properties beyond the increase in loads which comes from the increase in current. The improvement is small for the section modulus, and more significant for moment of inertia. When ITER switched from 24 to 20 coils, there were some adjustments in the radial build, and the case tension stress remained about the same. In October, 1994 there were some studies of improvements in OOP support structures, which led to the adoption of the upper and lower crown. Pairing of the inner leg case was investigated, this is analogous to switching from 20 to 10 coils. This would have yielded a noticeable improvement, but was dropped because of the extremely large magnet structure that would have resulted. Such a solution might be attractive for a PCAST scale machine.

CS/TF Interface

ITER has accepted the feasibility of using teflon/fiberglas bearing materials at the CS/TF interface. This confidence stems largely from the positive experience

positive experience at JET. Use of a bucked vs. wedged design was argued extensively prior to, and during the Oct. 1994 ITER design review. There was concern over the interface issue then. It was successfully countered by analysis, and R&D results. As a result of the review, many changes were made, but the bucked design concept was retained because its performance advantage was deemed more important than the less significant difficulties relating to the interface behavior. For the PCAST machine, the radial pressure, at the CS/TF interface is up to twice that of ITER. This is within the range of the bearing material tests done for the bucked version of CIT and IGNITOR. Figure 24 shows some of the R&D results from CIT with the interface pressures indicated.

For ITER, friction analyses for up to 10 pulses have been performed using full 3D global models of the magnet system. These are backed-up by simplified analyses by the Russian Federation which model the CS as a stack of individual disks connected by torsional and vertical springs. The results of these analyses are included in the Appendix B of the most recent ITER Magnet System Design Description Document. Earlier ITER friction analyses are documented in "ITER EDA In-Plane Structural Design, Finite Friction Effects, Central Solenoid Tension, and Compressive Preload", Titus, and Wong, published in the transactions of the 15th IEEE, Hyannis. The last piece of work built confidence in the friction simulation capabilities of ANSYS by showing phenomena that could readily be calculated by hand. One in particular was that the frictional capacity of the CS/TF interface was sufficient to stretch the CS vertically, and develop tension, when the TF was energized. Reports from JET regarding radiation effects on fiberslip are available. If it is acceptable for use on ITER, then it should be acceptable for PCAST .

Figure - 20
Central Solenoid
Shear Stress
Components
In-Plane
(Element Local SXY)
and Torsional
(Element Local SYZ)
Run #5, EOB

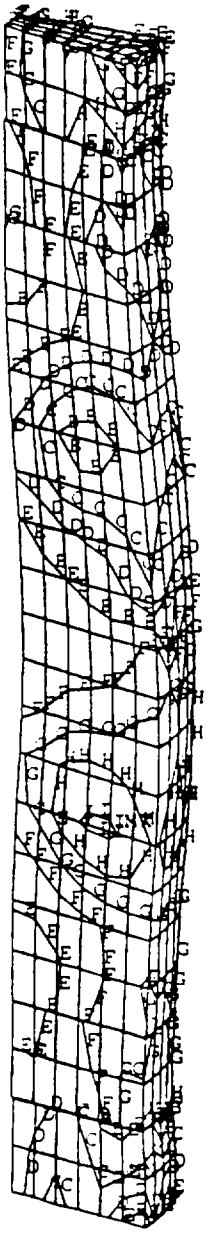

SXY (AVG)
ELEM CS
DMX =0.012275
SMN =-0.346E+08
SMNB=-0.782E+08
SMX =0.294E+08
SMXB=0.658E+08
A =-0.311E+08
B =-0.240E+08
C =-0.168E+08
D =-0.973E+07
E =-0.261E+07
F =0.451E+07
G =0.116E+08
H =0.187E+08
I =0.259E+08

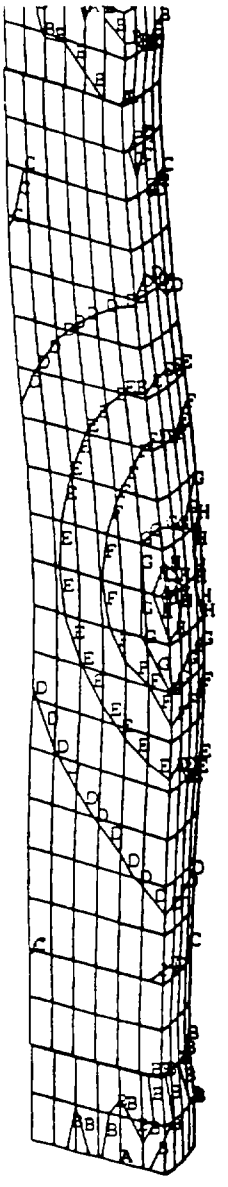

SYZ (AVG)
ELEM CS
DMX =0.012275
SMN =-0.366E+08
SMNB=-0.726E+08
SMX =0.100E+09
SMXB=0.133E+09
A =-0.290E+08
B =-0.138E+08
C =0.141E+07
D =0.166E+08
E =0.318E+08
F =0.471E+08
G =0.623E+08
H =0.775E+08
I =0.927E+08

1

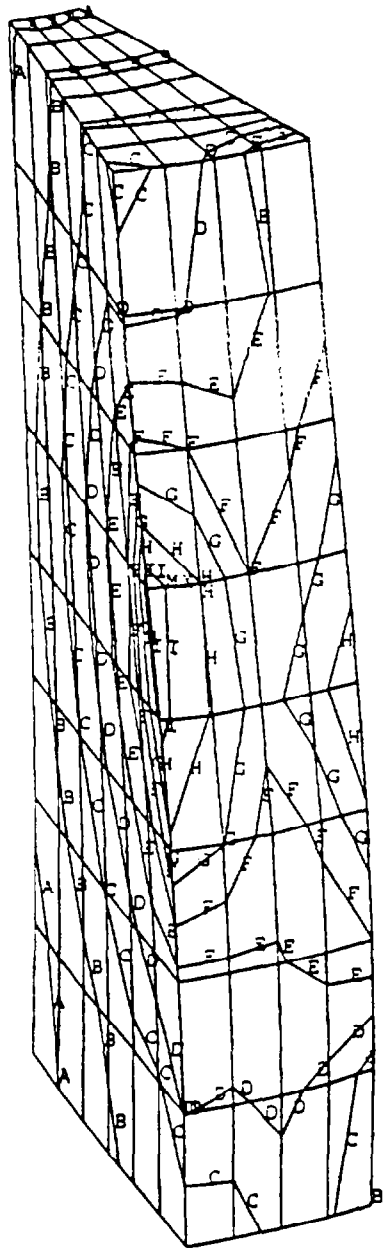

ANSYS 4.4A1
NOV 9 1995
8:44:49
PLOT NO. 1
POST1 STRESS
STEP=7
ITER=30
SYZ (AVG)
ELEM CS
DMX =0.0044
SMN =0.133E-
SMNB=-0.331E-
SMX =0.956E-
SMXB=0.124E-

XV =2
YV =1
ZV =1
DIST=1.7[illegible]
XF =1.1[illegible]
PRECISE [illegible]
A =0.1[illegible]E-
B =0.3[illegible]E-
C =0.3[illegible]E-
D =0.4[illegible]E-
E =0.5[illegible]E-
F =0.6[illegible]E-
G =0.7[illegible]E-
H =0.8[illegible]E-
I =0.9[illegible]E-

R#6 EOB, 190/150 deg tf,220 deg PF1=220,PF2=150, 80 deg structure

Figure - 21
Central Solenoid
"Scuffing"
Shear Stress
(Element Local SYZ)
Run #6, EOB

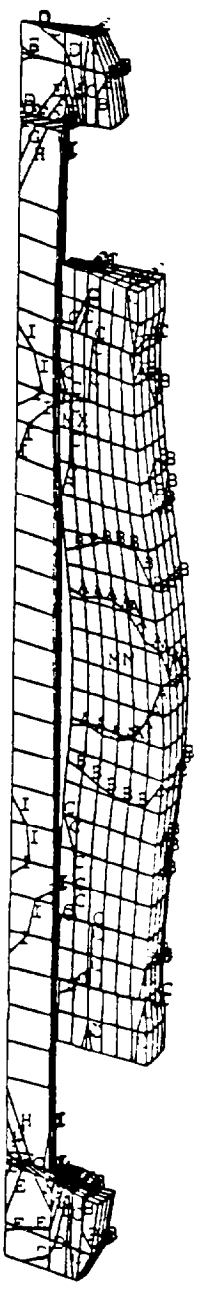

ANSYS 4.4A1
NOV 8 1995
9:49:06
PLOT NO. 10
POST1 STRESS
STEP=8
ITER=30
SY (AVG)
ELEM CS
DMX =0.012275
SMN =-0.228E+09
SMNB=-0.267E+09
SMX =0.471E+09
SMXB=0.681E+09

XV =1
YV =1
ZV =2
DIST=6.777
XF =0.884664
PRECISE HIDDEN
A =-0.189E+09
B =-0.111E+09
C =-0.336E+08
D =0.441E+08
E =0.122E+09
F =0.199E+09
G =0.277E+09
H =0.355E+09
I =0.433E+09

Run #5 EOB
(390 MN preload)

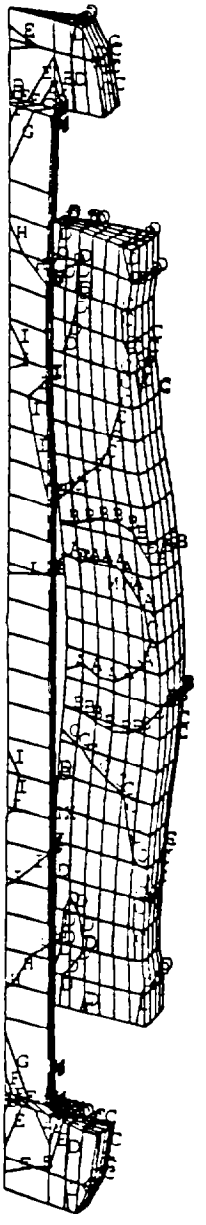

ANSYS
NOV
15:36:05
PLOT NO.
POST1
STEP=7
ITER=30
SY (AVG)
S GLOBAL
DMX =
SMN =
SMNB=
SMX =
SMXB=

XV =1
YV =1
ZV =2
DIST=
XF =
PRECISE HIDDEN
A =
B =
C =
D =
E =
F =
G =
H =
I =

Run #7 EOB
(195 MN preload)

Figure - 22
Tierod and Central Solenoid
Vertical Stress

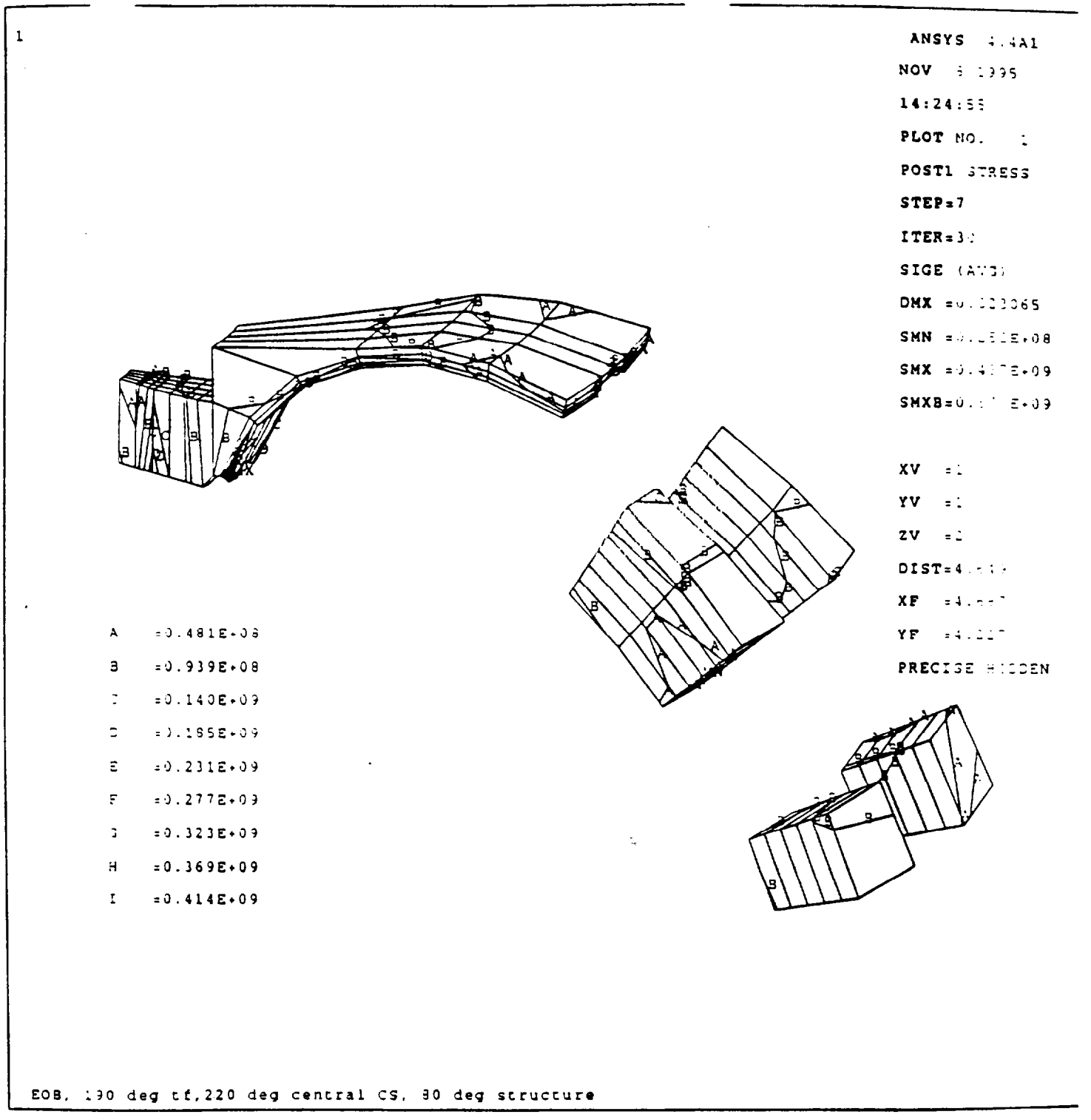

Figure - 23
Crown
Von Mises Stress
Run #5 EOB
(390 MN preload)

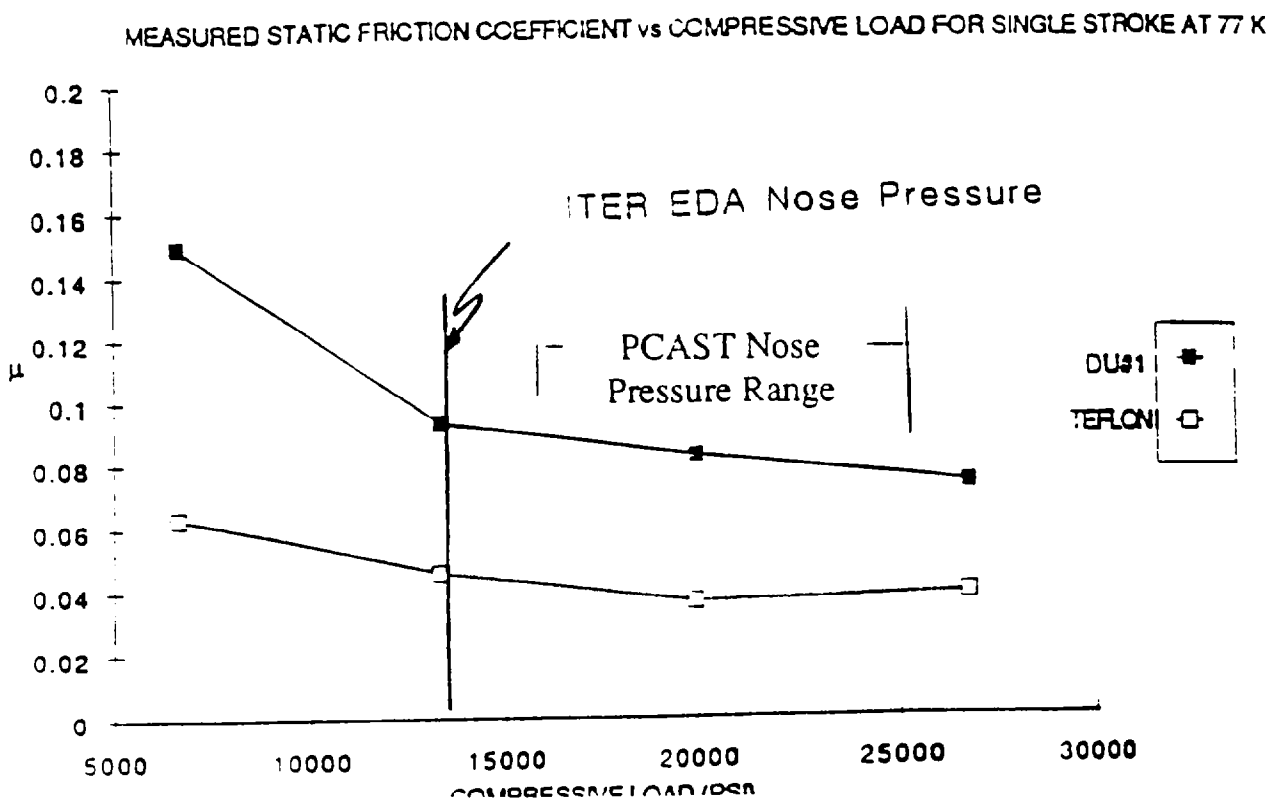

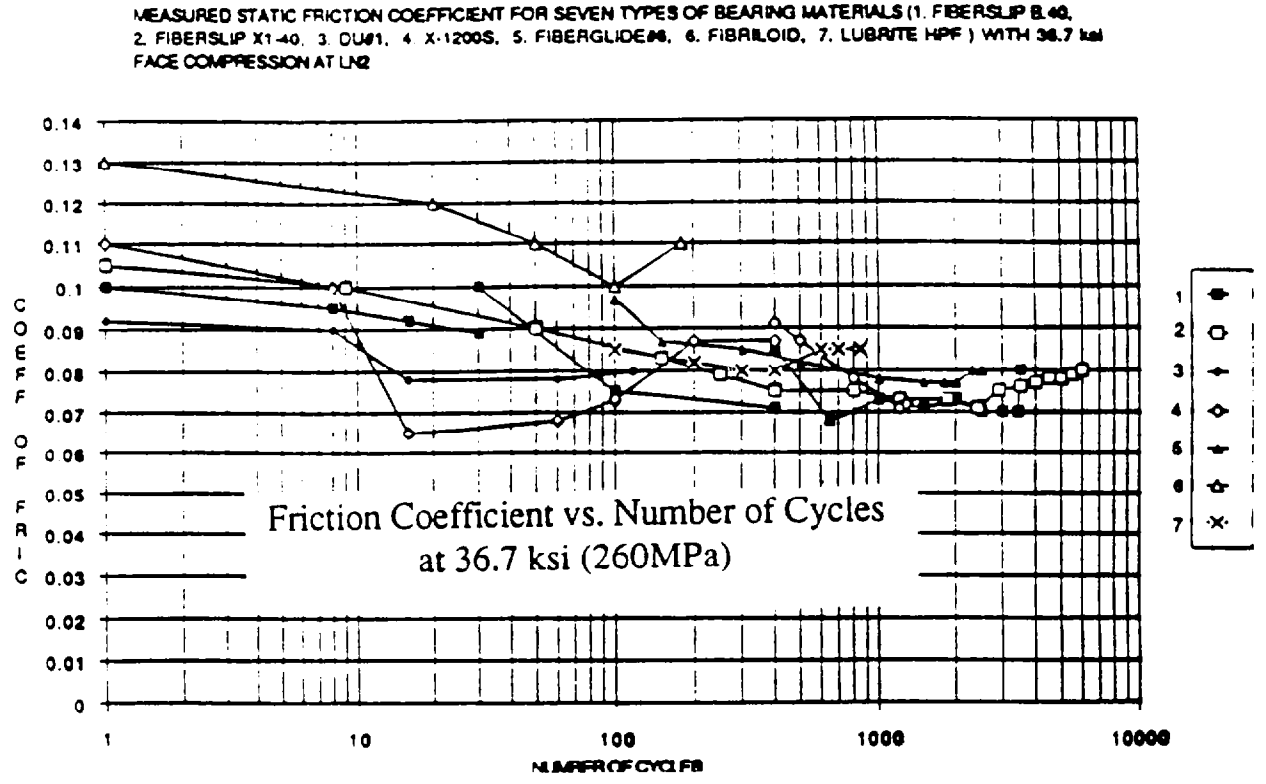

Figure - 24
CIT R&D Program Low Friction
Bearing Material Results

Section 1.5: Vacuum Vessel (J. Spitzer)

1.5.1 Function and Requirements

The vacuum vessel assembly serves as the primary containment for the fusion process providing the high-vacuum environment required for the plasma operations. The vacuum vessel assembly consists of the toroidal vessel shell, ports, vessel supports, and heating and cooling passages.

The vacuum vessel assembly must sustain all electromagnetic, mechanical and thermal loads which occur during vessel conditioning, normal operation and plasma disruptions. It must provide the structural support for all internal hardware including the plasma facing components; provide the capability for heating/cooling of the vessel during bake-out and operation; provide nuclear shielding for the TF and PF magnets; and contribute to passive plasma stabilization while permitting access for plasma heating systems, diagnostics vacuum pumping and maintenance.

1.5.2 Design Description

Configuration

A vacuum vessel assembly has been developed to satisfy the PCAST mission. Figure 1.5-1 shows a plan view of the vacuum vessel assembly. The vacuum vessel consists of eight 45° sectors. Each sector features two large horizontal ports to accommodate plasma heating and current drive systems or diagnostics, as well as horizontal ports above and below the midplane ports for divertor pumping. The vacuum vessel uses double-wall construction with space between the two walls for shielding material and to accommodate the flow of water or steam. Steam is circulated in the vessel jacket during bakeout of the vessel at 350°C. Water is used in the vessel jacket during operation to maintain the vessel walls at a nominal temperature of 150°C, as well as thermalizing fast neutrons and absorption of thermalized neutrons.

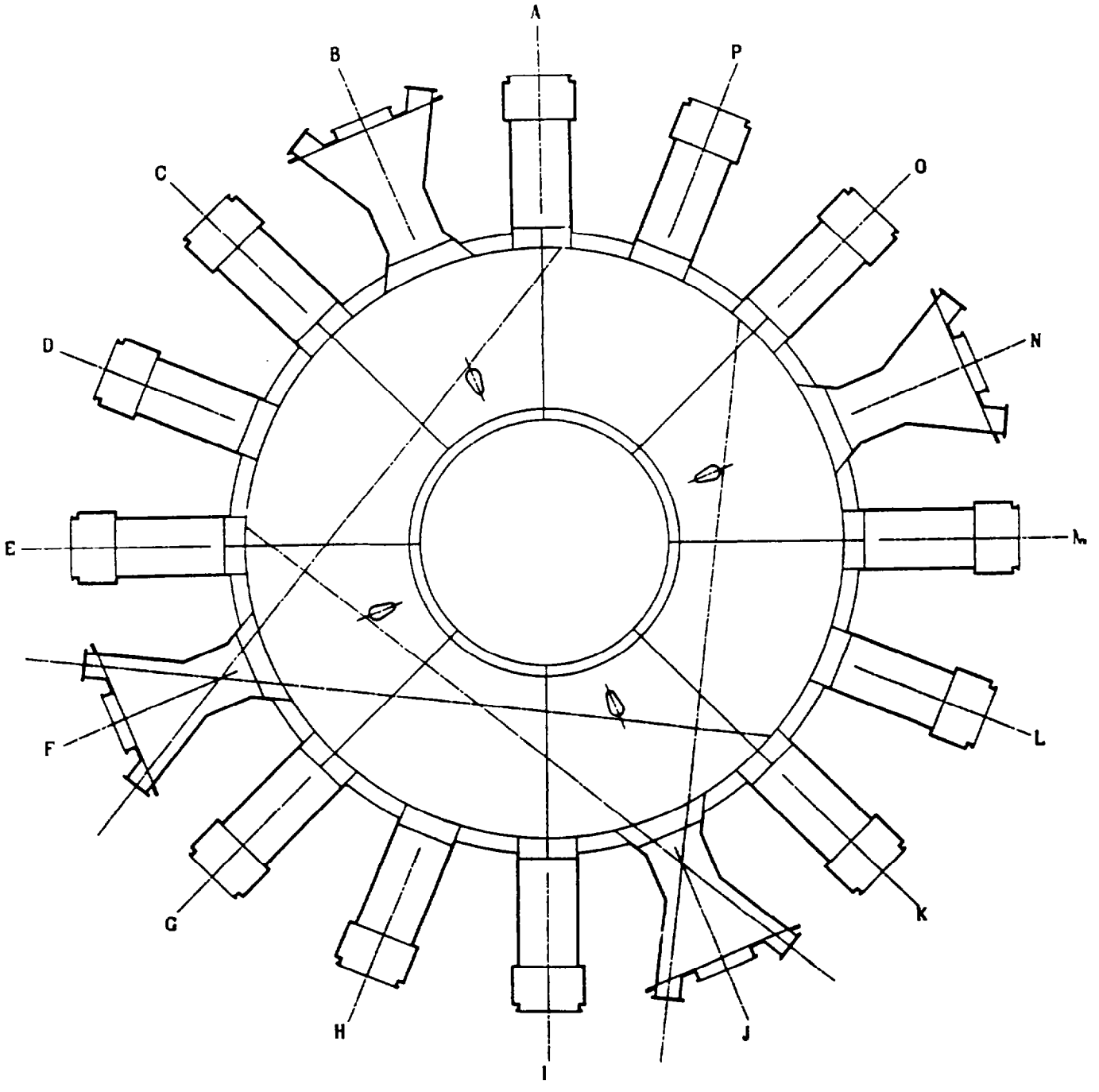

Figure 1.5.1 - Vacuum Vessel Plan View

The vessel cross-section is illustrated in Figure 1.5-2. The vessel has an inside major radius of 2.9 m and an outside major radius of 7.4 m. The overall height of the vessel is 9.7 m. The total thickness of the vessel at the inner wall is 25 cm transitioning to a thickness of 38 cm in the outboard region. The inner and outer walls of the double walled vessel are each 4.45 cm thick. The total weight of the vessel including water and shield material located in the space between the vessel walls is 1375 metric tons.

Design Criteria

A double wall configuration was chosen for the vacuum vessel shell. This type of design is superior to single wall construction in that it is structurally superior in areas where there is bending and the space between the walls automatically provides heating and cooling paths. The double wall configuration also readily lends itself to nuclear shielding. Based on a zero order approximation, the double wall configuration of the vacuum vessel with a 60/40 mixture of stainless steel and water in the inner wall space and the TF case with a nominal thickness of 89 cm provides attenuation of approximately 90-95% of the 320 MW neutron component of the fusion power. The double wall also allows for increases in the wall thickness, if required, without increasing the overall envelope of the vessel.

Stress levels for the PCAST machine vacuum vessel are predicted by scaling results from analysis of the Burning Plasma Experiment (BPX) vacuum vessel. In this instance stress from the dynamic analysis of the BPX vacuum vessel resulting from a fast vertical disruption are used. The scaling procedure is accomplished by developing a ratio of the IxB values for the two machines. In this instance they are nearly identical so the load reduction factor is taken as unity. Since the BPX vacuum vessel used a single wall while the present design uses double wall construction, a wall factor is developed for the various regions of the vessel to account for the effect of the increased moment of inertia on the bending stress intensities. Table 1.5-1 lists the maximum vessel stress intensities from the BPX analysis and the scaled PCAST results.

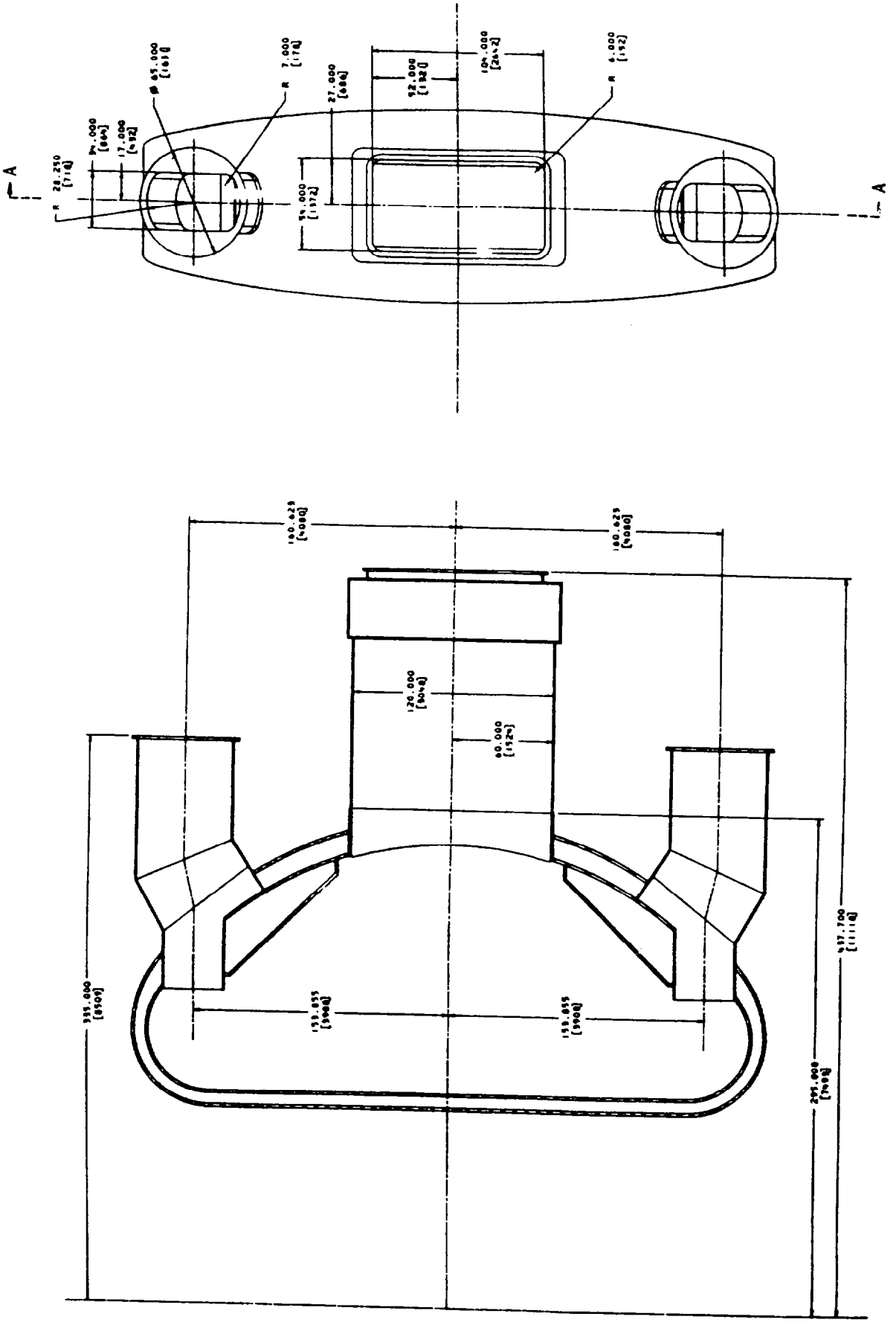

Figure 1.5.2 - Vacuum Vessel Details

Table 1.5-1 - Vacuum Vessel Disruption Stresses Scaled from BPX

BPX Post-CDR	Plasma Parameters		I=11.8 MA, B=9.0 T, IB=106.2		
Vessel Shell	Disruption Load		Fast Vertical Disruption (FS0812T)		
Inconel 625	Vessel Region		Inboard	Top and Bottom	Outboard
	Thickness (in)		2.5	3.5	3.5
	Dynamic Stress Intensity	Mem. Sm (ksi)	22.8	23.9	27.2
		Bend. Sb (ksi)	2.7	8.3	9.5
		Total St (ksi)	25.5	32.2	36.7

PCAST	Plasma Parameters		I=15.0 MA, B=7.0 T, IB=105.0		
	Load Reduction Factor		IB(PCAST)/IB(BPX) = 105/106.2 = .99 ~ 1		
Vessel Shell	Disruption Load		Fast Vertical Disruption (FS0812T)		
Inconel 625	Vessel Region		Inboard	Top and Bottom	Outboard
	Thickness (in)		1.75	1.75	1.75
	Wall Factor		0.17	0.17	0.10
Allowable Stress at 200° C	Dynamic Stress Intensity	Mem. Sm (ksi)	16.3	23.9	27.2
Sm =32 ksi		Bend. Sb (ksi)	< 1.0	1.4	< 1.0
Stot = 48 ksi		Total St (ksi)	17.3	25.3	28.2

Since BPX, improvements have been made in the ability to model halo currents. The quality of the experimental data has also improved dramatically (most notably Alcator C-Mod.) The experimental data base can be used to set the limits for design purposes:

	BPX (1991)	ITER & TPX (1995)
I_{halo}/I_{pl}	0.2	0.33-0.40
Toroidal Peaking Factor	1.0	1.5-2.0

Based on the above data, it can be seen that the ratio of the peak halo current to the plasma current have gone up by a factor of 4, compared to the BPX era. However, modeling studies have shown that disruption scenarios with large

are artificially turned off. The BPX no-halo disruptions, like that used for scaling the PCAST vessel stresses, represent the worst case for the vacuum vessel, since they assume very rapid current decay rates (12MA to zero in 4 ms) in conjunction with the worst attributes of VDE's, namely long vertical drifts. It is expected therefore that the more pessimistic halo current assumptions would not significantly affect the global vacuum vessel design. They would, however, affect the local stresses at the PFC-to-vessel attachments and possibly the vessel support because of the asymmetries. In light of these effects and based on the scaled stress intensities, Inconel 625 was chosen as the vessel material.

Material Selection

Inconel 625 was chosen over SS 316 LN as the material for the vacuum vessel assembly because of the superior material properties of Inconel 625 at elevated temperatures.

At the nominal vessel wall temperature of 150°C during operation, the yield and ultimate strengths of Inconel 625, at 350 MPa and 750 MPa respectively, are 70% greater than that of SS 316 LN. Comparing the predicted maximum vessel stresses to the allowable stress of Inconel 625 (two-thirds of the yield strength at temperature) gives a margin of 25% on the membrane and more than 75% on the total stress intensity. These are considered adequate margins keep the vessel stresses below the allowables when the effects of halo currents as highlighted in the previous section are included.

The lower modulus of elasticity for 316 LN coupled with a higher coefficient of thermal expansion and thermal conductivity would result in thermal stresses on the order of 20% higher than would occur in Inconel 625. The electrical resistivity of Inconel is also higher than SS 316 LN. The toroidal resistance of the vacuum vessel was calculated to be 15 $\mu\Omega$ for Inconel 625 as compared to 9.8 $\mu\Omega$ using SS 316 LN.

The trade-off in selecting Inconel 625 as the vessel material is increased material and fabrication costs. These are offset somewhat by the fact that the lower mechanical properties of SS 316 LN would require an increase in the vessel wall thicknesses and therefore the weight of the vessel. The increased thickness also exacerbates the welding process.

Cooling Requirements

The PCAST machine will generate 400 MW of fusion power. The neutron component of this power is 320 MW which must be absorbed by the vacuum vessel acting as a shield for the TF magnets. Preliminary calculations were made to estimate the vessel cooling requirements to remove 320 MW of nuclear heating.

The vessel is maintained at a nominal 150°C during plasma operations. Water supplied at 50°C provides the vessel cooling. Each quadrant of the vessel is cooled separately. Poloidal ribs between the inner and outer vessel walls form eight coolant channels per quadrant. A flow rate of 380 kg/sec of water would be required to remove a steady-state heat load of 320MW with an outlet water temperature of 100°C. Table 1.5-2 details the vessel cooling calculations.

Thermal Shielding

The vacuum vessel assembly includes a 3.18 cm thick blanket of multi-layer insulation (MLI) for thermal shielding during bakeout at 350°C and operation at 150°C. The MLI is comprised of 100 layers of aluminized Kapton with a separator of Lydall-Manning Cryotherm 233 between layers to minimize conduction through the MLI. Kapton, with a temperature limit of 400°C, was chosen rather than Mylar, to prevent degradation of the insulation during the vessel bakeout. The aluminized Kapton has an emissivity of .05 per layer. The effective emissivity for the MLI system is .05/100 = 0.0005. This value is an idealized number for perfect MLI systems. Studies conducted for TPX demonstrated that with conduction through the layers and small gaps during installation the actual effective emissivity can be as much as a factor of 4 above the idealized value, 0.002. Using this value the heat load from the vessel through the blanket is calculated to be:

Operations -

$$Q_{150} = 5.67e\text{-}8 \times .002 \times 423^4 \times 770\ m^2 = 2.8\ kW$$

Bakeout -

$$Q_{350} = 5.67e\text{-}8 \times .002 \times 623^4 \times 770\ m^2 = 13.2\ kW$$

Table 1.5-2 - Vacuum Vessel Cooling Scoping Study

Q, Heat Load (W)		320.0E+06	
Volume of Vessel Structure (m^3)		71.40	
q''',Volumetric Heat Deposition (W/m^3)	Q/Vvv	4.48E+06	
q''' per quadrant	(Q/Vvv)/4	1.12E+06	
Channel Width- (m)	(Ri*pi/2)/8 channels	0.6000	
Channel Height (m)		0.2286	
Channel Length (m)		182.00	
Acr, Channel Cross Section (m^2)	W*H	0.1372	
Dh, Hydraulic diameter	4*Acr/n	0.3311	
b, Water Flow Rate (kg/sec)	(Q/4)/(Cp*Tdelta)	381.80	
v, Water Velocity (m/sec)	b/(Acr*rho)	2.85	
Re, Reynolds Number	v*Dh/nu	2.40E+06	
ΔP, Pressure Drop (N/m^2) & (psi)	rho*f*L*v^2 /2*D*Gc	71504.99	10.37
Nu, Nusselt Number (R. A.)	.023*Re.^8*Pr^.33	3913.83	
Nu, Nusselt Number (S-T)	.023*Re.^8*Pr^.33*(mub/mus)^.14		4138.65
mu at Tb	(rho*nu)		3.84E-04
mu at Ts (110°C)	(rho*nu)		2.58E-04
h, Film Coefficient (W/m^2-°C)	nu*k/Dh	7851.65	8302.67
ΔT walls and water (°C)	q'''-t/h	6.34	6.00
ΔT through wall (°C)	q'''-t^2/2kw	94.11	94.11
Twmax, Max Wall Temperature (°C)		200.46	200.11
Twnom, (°C)		153.40	153.06
Coolant Properties	English @ Tb		Conversion
Tinlet (°C)	122	50	
Toutlet (°C)	212	100	
Tdelta (°C)		50	
Tb (°C)		75	
k, Conduction Coefficient (W/m-°C)	0.384	0.6642	1.729577
rho, density (kg/m3)	60.99	976.97	16.01846
Cp, Specific Heat (J/kg-°C)	1.0016	4190.69	4184
nu, Kinematic Viscosity (m^2/s)	4.23E-06	3.93E-07	0.09290304
Pr, Prandtl Number	2.42	2.42	1
Wall Properties	English @ Twnom		Conversion
t, Wall Thickness (m)	1.75	4.45E-02	0.0254
kw, Wall Conductivity (W/m-°C)	6.8	11.76	1.729577

1.6 In-Vessel Components (P. Heitzenroeder, D. Hill, E. Hoffmann, G. H. Neilson, L. Sevier, K. Young)

This section addresses the PCAST machine components comparable to those contained in ITER WBS 1.6 (First Wall and Blanket/Shield) and WBS 1.7 (Divertor). These items include the divertors, inboard limiters, outboard limiters and poloidal limiters. In-vessel diagnostics are also overviewed since the first wall design must integrate provisions for them. Also located in the vacuum vessel are fast plasma position control coils, which are detailed in Section 1.9.

Introduction

The PCAST machine's cryogenically cooled copper coils operate at higher fields than ITER's superconducting coils allow. The experimental pulse is shorter than ITER's (100–200 seconds vs. 1000–2000 seconds). Furthermore, the PCAST machine will have no nuclear technology mission (ie, no blankets). The neutron wall load will be <1 MW/m^2 and the fusion power is minimized. All of these choices were made to reduce the size and cost.

In the in-vessel components area, these changes permit consideration of materials which otherwise would not be acceptable. High neutron fluences can result in serious degradation of the thermal conductivity of carbon fiber composites (CFCs). This consideration resulted in beryllium being chosen for virtually all of the first wall of ITER. The reduced neutron fluence in the PCAST device is roughly an order of magnitude lower than in ITER. Consequently, the PCAST device proposes to use carbon fiber composites (CFCs) for all PFCs. CFCs have some advantages relative to beryllium; extensive field experience, good impurity control, and greater tolerance to overheating damage due to misalignment, for example.

The goal of this study is to determine if this approach will appreciably reduce the overall costs. The PCAST PFC design choices were made with this goal in mind.

Configuration and Essential Features

Fig. 1.6-1 shows the location and terminology used to identify the individual first wall components and provides the following essential features:

- All PFCs are made of carbon fiber composites.

- Double null divertors are provided with a short open inner leg and a long slot outer leg.

- Inboard and outboard limiters are provided to protect the vacuum vessel and internal hardware.

- Poloidal limiters are provided for startup and to control conditions for ICRF launcher operation.

- Divertor pumping is provided via ducts to external pumps.

- The close-fitting vacuum vessel wall on the inboard side and re-entrant features of the vessel on the outboard side provide passive stabilization of fast vertical motions of the plasma.

- Two pairs of active control coils (one pair to control vertical motions; one pair to control radial motions) are located within the vessel to control motions of the plasma after initial damping of the motion by passive stabilization. The active coils are powered by feedback controlled power supplies.

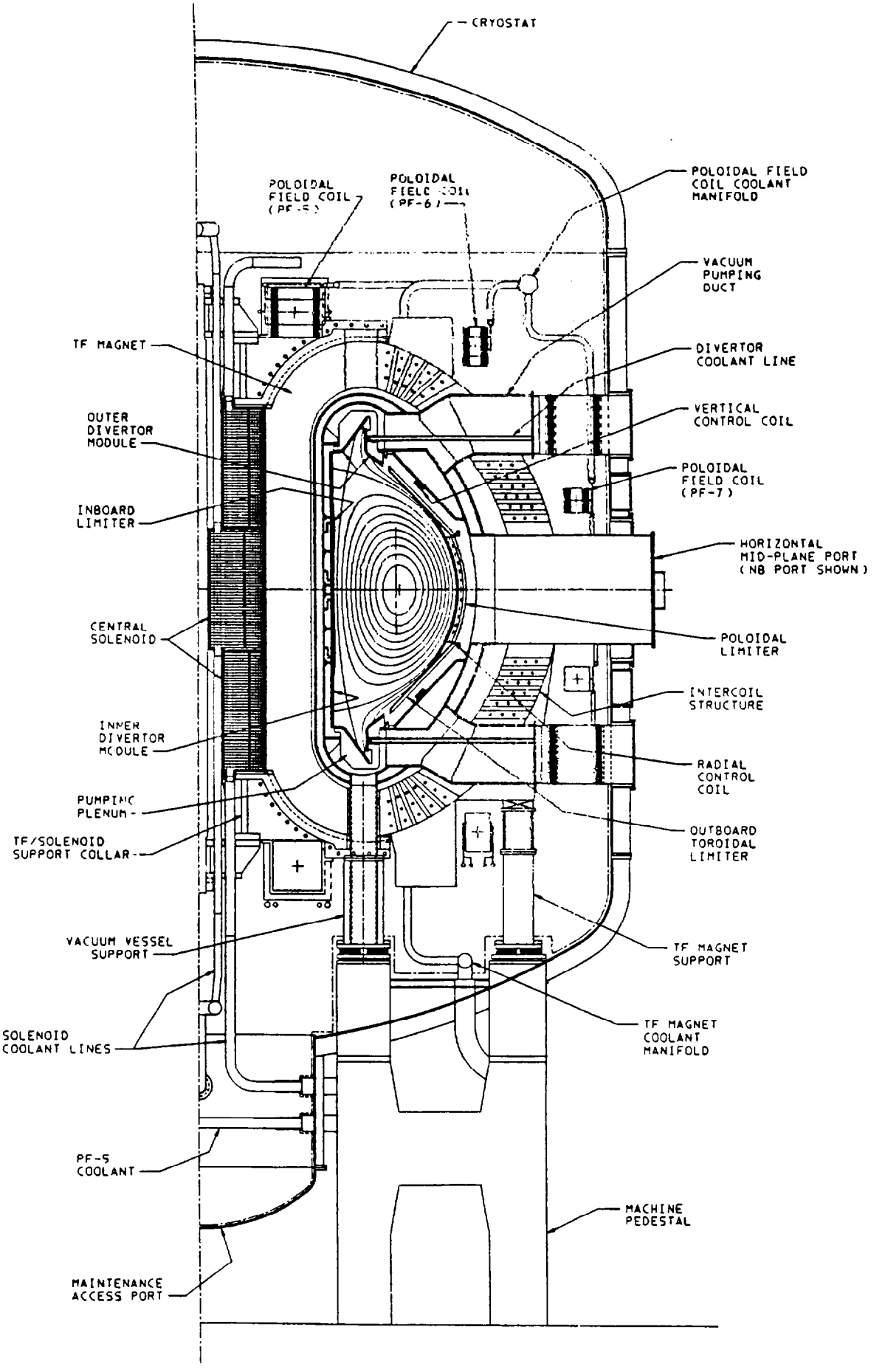

HAFEL-MACH 11-21-95

Figure 1.6-1 Cross-Section of the PCAST Device

Divertors

The PCAST divertor employs a slot geometry for the high heat flux divertor targets with the outer target tilted poloidally to expand the area that intercepts the outboard SOL. Refer to Fig. 1.6-2. Baffles are provided to direct the neutralized plasma exhaust into the pump duct and to limit the leakage of gas and impurities to the main plasma. Auxiliary baffles are positioned between the PFCs and the vacuum vessel to separate the high pressure divertor plenum from the mid plane region of the vacuum vessel. Gas feeding capability is provided to permit gas target/radiative divertor operation. A "macroblock" design approach similar to that developed for TPX is proposed because of the inherent ruggedness and simplicity of this design. Macroblock details are shown in Fig. 1.6-3.

A modular design was chosen for compatibility with remote handling requirements. Each divertor module is further subdivided into outer and inner sections as to reduce the size and weight to facilitate remote handling. Refer to Figs. 1.6-4. and 1.6-5. Each outer divertor module consists of an outboard baffle plate and a primary divertor target. Each inner divertor module is simply the inner divertor target.

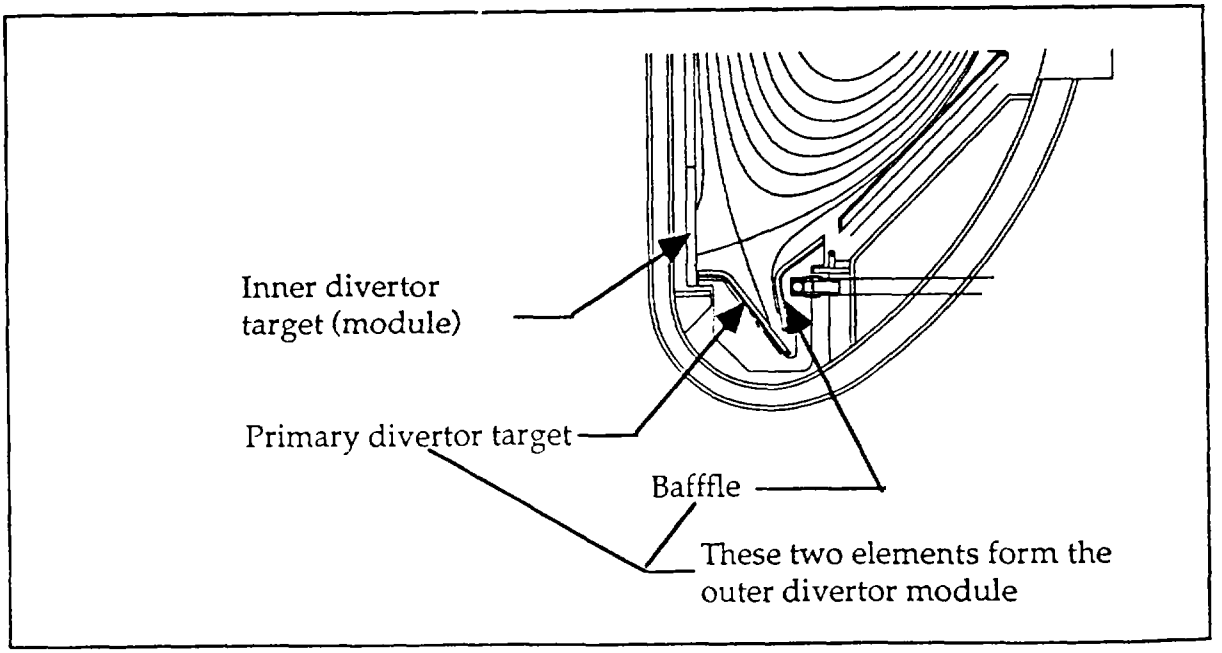

Figure 1.6-2. Divertor Details

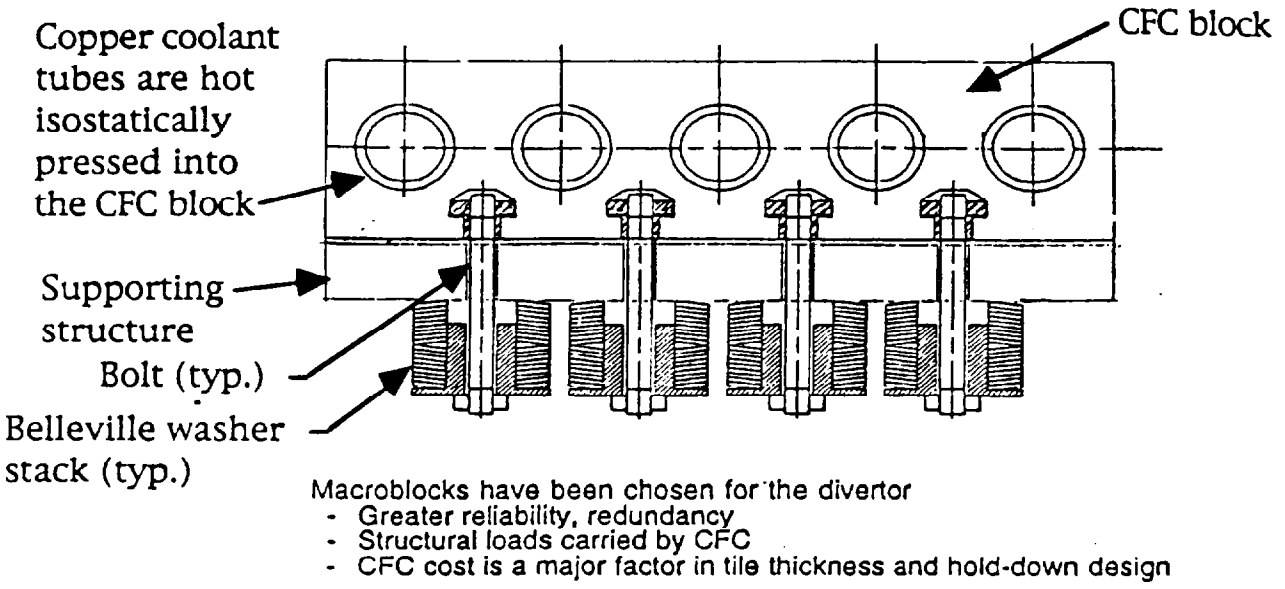

Figure 1.6-3. Macroblock Details

Each outer divertor module has a toroidal extent of 11.25° — meaning 32 modules in the upper ring and 32 modules in the lower ring, each with a toroidal length of 36.12" and a weight of 2200 lbs. The total surface area of all outer divertors — upper and lower — is 127 square meters. An outboard divertor module is illustrated in Figure 1.6-4.

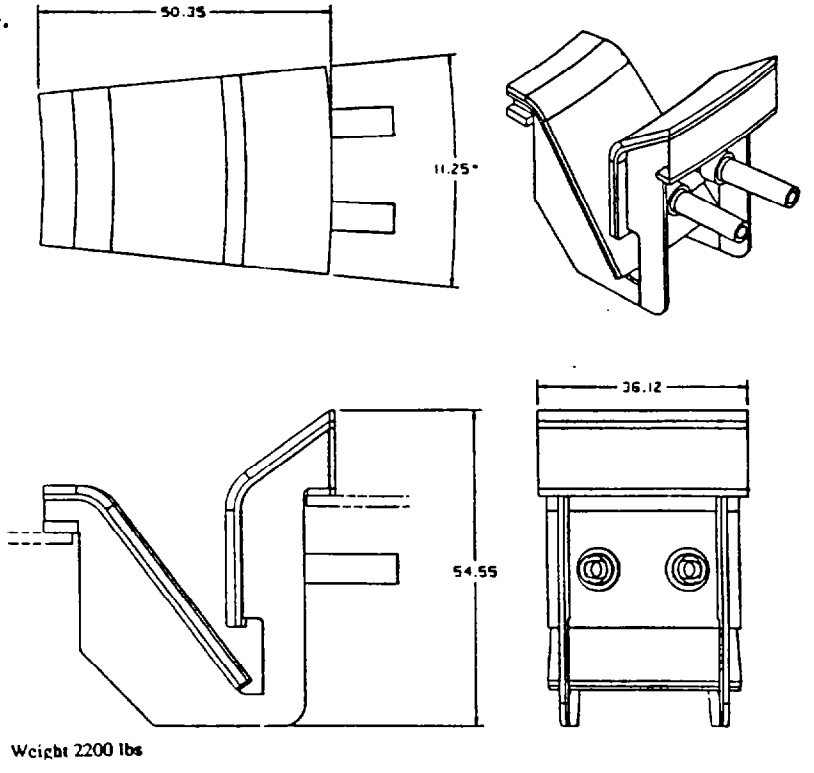

Figure 1.6-4. PCAST Outboard Divertor Module

Each inner target plate makes up an inner divertor module. Each has a toroidal extend of 22.5°, weighs approximately 1300 lbs., and has a surface area of 2.0 square meters. The total surface area of all inner divertors — upper and lower — is therefore 64.0 square meters. Figure 1.6-5 shows one panel of the inner divertor.

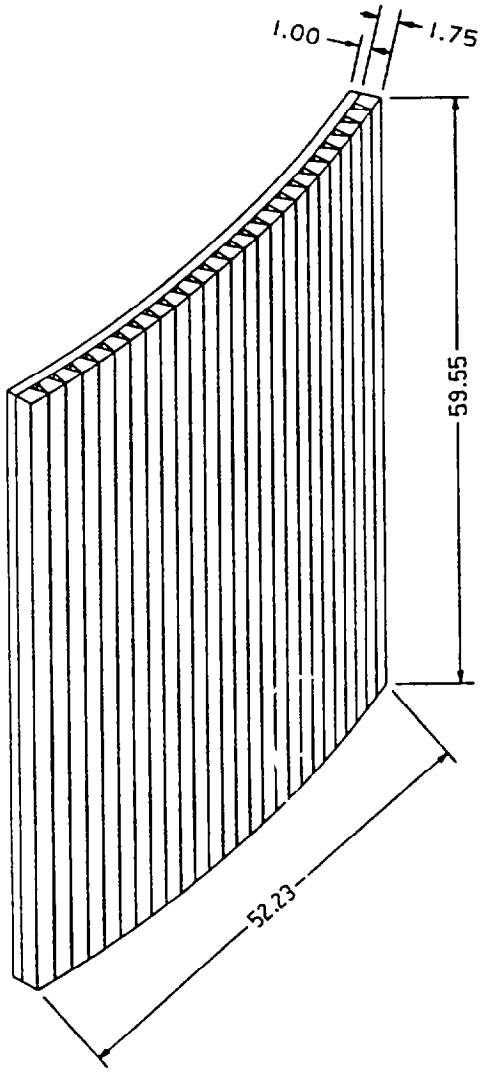

Figure 1.6-5. A PCAST Inner Divertor Module

ITER vs. PCAST Divertor Configuration

The PCAST machine has adopted a deep-vee configuration for the divertor structures. There are three primary differences between it and the ITER divertor configuration: (1) the PCAST divertor length (poloidal X-point to strike-point distance) is shorter than ITER's (0.93 m vs. 1.9 m); (2) PCAST has a horizontal

instead of a vertical target; (3) its configuration is high δ , DN versus low δ, SN. Configuration parameters and key power handling figures of merit are compared in Table 1.6-1. Comparing these figures of merit, it is evident that the divertor power handling in PCAST is more tractable. Refer to the Physics section for further discussion.

	ITER	PCAST
Plasma configuration	Low-triangularity, single-null	High-triangularity, double-null
Structure config.	Long vee, vertical target	Long vee, horizontal target
Length (poloidal, along separatrix)	1.9 m outboard 2.2 m inboard	0.93 m outboard
Depth (vertical)	1.5 m	0.90 m per divertor
Length/minor radius	0.68	0.62
Depth/minor radius	0.54	0.60 per divertor
Plate tilt angle (w.r.t. separatrix)	15 degrees toward vertical (expansion factor 3.9:1)	23 degrees toward horizontal (expansion factor 2.6:1)
Average major radius strike points, R_{avg}	6.3 m (5.4 m inboard, 7.2 m outboard)	4.0 m (outboard)
Wetted area	10 m^2 (per ITER Physics Performance Assessment, p. V-42.) Infer from this an average effective wetted width along targets =0.12 m.	8.0 m^2 based on wetted width =0.16 m (projection of 1.5-cm SOL width on outer target), and two divertors.
P_{loss}	210 MW	75 MW
P_{loss}/A_{wetted}	21 MW/m^2	9.4 MW/m^2
Outer target reduction factor under standard divertor rules	$(1-f_{core\ rad})=0.8\times f_{outer}=0.67$ (remainder to inner) $\_(A_{outer}/A_{wetted})=0.5*7.2/6.3$ =0.57	$(1-f_{core\ rad})=0.8$ $\times f_{outer}=0.8$ (remainder to inner) =0.64
Target heat flux estimate ($=P_{loss}/A_{wetted}$ ×reduction factor)	20 MW/m^2	6.0 MW/m^2
$P_{loss}/2\pi R_{avg}$	5.3 MW/m	3.0 MW/m

Table 1.6-1. Comparison of ITER and PCAST Divertor Configurations

Key Features Common to Both ITER and PCAST Divertors

o **Long-vee shape**: Attenuates recycling neutral flow from divertor to main chamber. Provides flexibility for optimizing the divertor operating scenario and/or structure configuration during the operating phase.

o **Tilted plate:** Increases the "wetted area" on the divertor target to offset the flux compression associated with the long length.

Key Differences in the PCAST Divertor Compared to ITER

o **Length (PCAST=0.93 m, ITER=1.9 m):** (1) PCAST requires less flexibility for divertor optimization than ITER because it requires little or no extrapolation in divertor operating conditions from present machines to handle the power. This can best be seen by comparing simple estimates of outboard target heat flux between the two machines (see table). ITER has 20 MW/m^2 to PCAST's 6.0. The latter is based on an assumed power scrape-off width of 1.5 cm at the mid plane. (2) The neutral attenuation has not been estimated and will have to await divertor modeling. The higher density in PCAST (n_e=1.6x10^{20} m^{-3} vs. 1.3x10^{20} m^{-3}) max. justify a shorter divertor but the optimum length is difficult to determine.

o **Target orientation and tilt angle:** The PCAST high-triangularity plasma (δ_X=0.81) has a nearly-vertical outboard separatrix leg. A horizontal target is needed in order to deflect particles toward the radial pump duct opening. PCAST has a tilt angle (angle between the separatrix and target) of 23 degrees whereas ITER has a tilt angle of 15 degrees. In both cases, tilting is used to spread the heat loads over a larger area.

Limiters

Three types of limiters are provided in the PCAST machine: the inboard toroidal limiter; outboard toroidal limiters; and poloidal limiters. The relatively low steady state heat flux (< 0.2 MW/m^2) deposited on the bulk of the limiter surfaces allows the use of CFC tiles with Inconel cooling plates and support structures.

The inboard toroidal limiter protects the vessel wall and magnetic diagnostics

located on the inboard V.V. wall behind the limiters from energetic particles during normal operation, from plasma radiation heat loads, and from damage during disruptions.

Two outboard toroidal limiters are provided to protect the outboard vessel wall from energetic particle fluxes during normal operation and during startup.

Three poloidal limiters are to provided for startup and to protect equipment in the port region from energetic particle fluxes during normal operation and during disruptions.

Inboard Limiter Modules

Like the divertors, a modular design is used to facilitate remote handling. Each panel has a toroidal extent of 22.5° and a vertical height of 1/2 of the inner limiter (total of 32 panels). Each panel will weigh approximately 1000 lbs. which is well within the capacity of the remote maintenance system.

The inboard limiter modules are made from Inconel sandwich panels protected by CFC tiles attached to the panel by a single central fastener.

The coolant to each panel is supplied through the vacuum vessel wall. The 5 inch space between the vacuum vessel wall and the back side of the inboard first wall armor panels is used to route diagnostics, install structural stand-offs for panel support and coolant supply lines. Each inboard limiter panel has a surface area of 2.5 square meters. The total surface area of all inboard limiter panels is therefore 80 square meters.

Figure 1.6-6 shows a partial cut away panel with supporting stand-offs and coolant carrying corrugations.

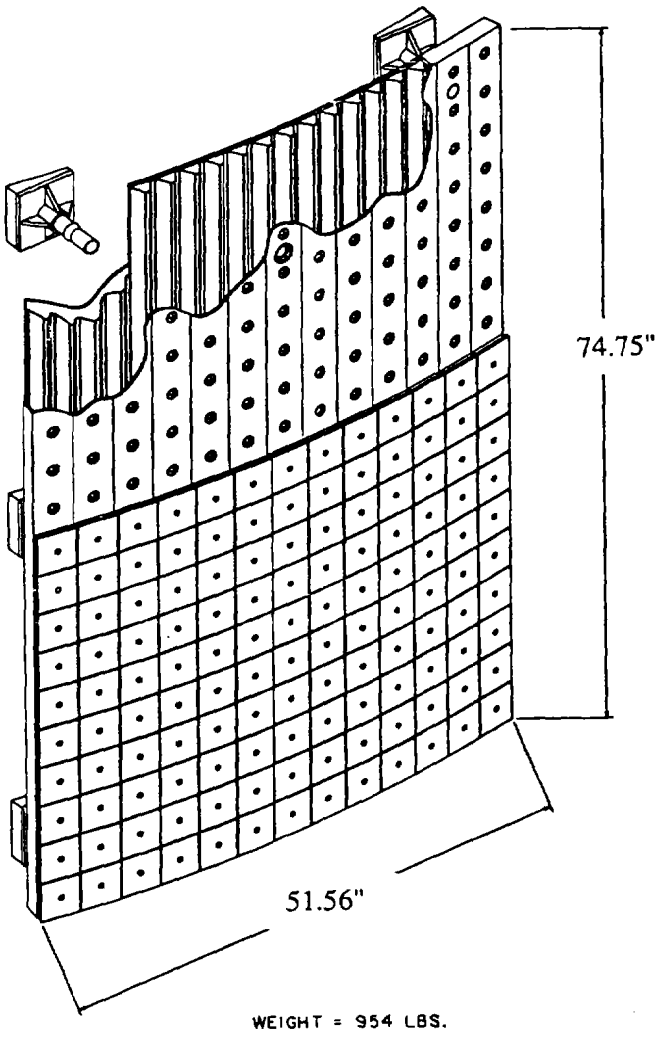

Figure 1.6-6 Inboard Limiter Panel Details

Outboard Limiter Modules

Each outboard toroidal limiter module consists of a water-cooled Inconel sandwich panel plate protected by carbon-fiber-composite tiles attached with one central fastener.

The modules have a conical configuration and are similar in design to the inboard limiter modules. The modules are attached to the vacuum vessel wall by stand-offs and receive their cooling water supply through the same pumping ducts as the divertors.

Each module extends 11.25° toroidally and will fit through a mid plane port without rotation. Each outboard panel has a surface area of 1.84 square meters and weighs approximately 1000 lbs. The total surface area of all outboard limiters — upper and lower — is therefore 117.8 square meters.

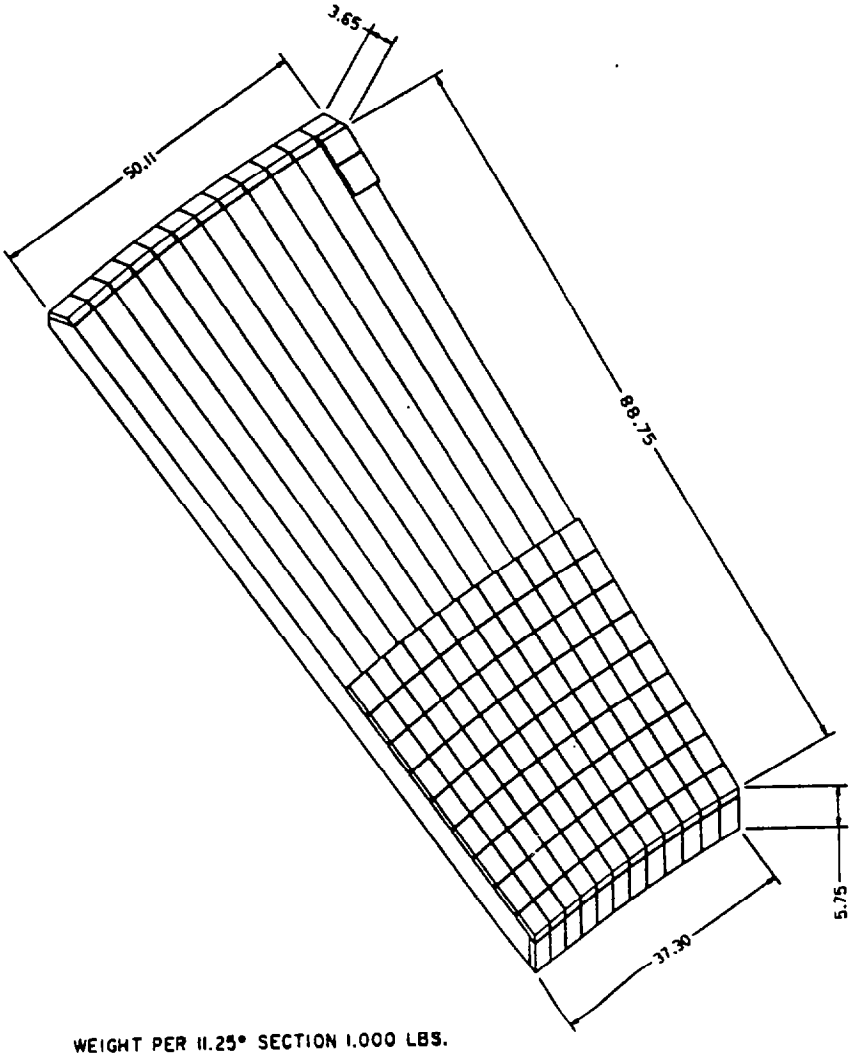

Figure 1.6-7 PCAST Outboard Limiter Module

Poloidal Limiters

The geometry of the three poloidal limiters conform to the geometry of the Faraday Shield on the ICH/FWCD launcher. The limiters consist of water-cooled heat sinks protected by carbon-carbon composite tiles.

In-Vessel Diagnostics

The in-vessel diagnostic components will comprise many magnetic diagnostics in addition to optical components such as mirrors, wave guides and horns, and bolometers. The magnetic diagnostics will generally be attached on the inside of the vacuum vessel wall behind the first wall. Mirrors and wave guides will be mostly brought into the vessel in modules mounted through the access ports, which will also contain necessary shield compensation. Bolometers, probes, periscopes and wave guides may be mounted into divertor modules to provide the necessary measurement capability for the divertor plasmas. There may be mirrors mounted off the first wall structure close to the pumping ports to provide capability for viewing of the first wall and divertor tiles by visible and infra-red cameras.

The magnetic diagnostics have similar measurement requirements to those planned for TPX. The final number of coils and loops will depend on optimization using code analysis. Allowing for some level of redundancy of the coils, the magnetic diagnostics are shown below.

- Flux loops (~50 1-turn coils) are provided to measure one-turn plasma voltage, and, in conjunction with the field probes, to measure plasma position.
- Magnetic field probes are provided in two poloidal arrays (50 - 100 per array) for plasma position & control.
- Two poloidal arrays of Mirnov coils are provided to measure MHD activity.
- Two Rogowski coils spaced 180 degrees apart are provided to measure Ip.
- Four "picture frame" locked mode coils spaced 90 degrees apart are provided to measure MHD activity.
- Two diamagnetic loops spaced at 180 degrees are provided to measure plasma pressure.
- Two poloidal arrays of saddle loops spaced 180 degrees apart are provided to measure differential poloidal flux
- "Halo - current" loops will be specified when the internal divertor and first wall hardware is defined.

Performance and Operational Requirements for PFCs

Power Handling Requirements

The plasma facing components in this machine must reliably dissipate up to a maximum of 100MW of heating power for 120sec, corresponding to the steady phase of a high-Q auxiliary heated discharge (Paux=20MW, Pfus=400MW, Pa=80MW). In this Section, the term "heating power" refers to the total power deposited in the confined plasma, either by auxiliary heating or by fast-alpha slowing. The term "P_{loss}" refers to the power remaining in the plasma after accounting for Bremsstrahlung losses. For the purposes of this study, we have assumed a maximum power deposition of 100MW onto the PFCs for the duration of the discharge.

Power reaches the plasma facing components via radiative processes or by thermal conduction along magnetic field lines in the scrape-off layer plasma. Since each loss channel intercepts different components, the power handling requirements for the PFCs depend on how the energy from the core reaches the walls, and this can vary depending on the operating mode. In order to specify the maximum power handling requirements for each of the PFC subsystems, we consider three possibilities for the global power balance, as shown in Figures 1.6-8, 1.6-9, and 1.6-10. Each case is based on present experimental results extrapolated to the higher power of this device.

Case I, graphically illustrated in Fig. 1.6-8 corresponds to standard high-Q operation with minimal radiative loss from the core plasma and just sufficient scrape-off layer and divertor radiation to reduce the peak divertor heat flux to acceptable levels. In this instance, the outboard divertor targets must dissipate the largest fraction of the heating power. In this case (and in the following Radiative Divertor case) we assume that the power flow into the divertors is up/down asymmetric by 1.2:1, so that one divertor receives 55% of the power flowing in the scrape-off layer (SOL). Furthermore, we assume that 80% of the SOL power flows to the outer divertor. Radiative losses are distributed the same way in each divertor. These power splits are based on experimental data from PDX, ASDEX, and DIII-D operation in the DN configuration and were adopted by the ITER CDA divertor team.

In Case II, called the Radiating Mantle, we assume that 80% of the heating power is dissipated uniformly in all directions by radiative processes in the main plasma, as in Fig. 1.6-9. Such operating conditions are not normally expected, but may occur during experiments aimed at reducing the peak divertor heat flux. This produces maximal radiative loading of the inboard and outboard toroidal limiters and other first wall components not in direct contact with the plasma, such as the Faraday shields on the RF antennae. The radiative losses deposited on a given surface then depend on the fraction of the plasma viewed by the surface and not so much its distance from the plasma. Given a plasma/first wall surface area of about $400m^2$, this uniform heat loading corresponds to $0.2MW/m^2$ for 120sec. Thus, the power handling requirement for a given component is just this number times the exposed surface area times 120 sec.

Finally, in Case III, we consider a Radiative Divertor mode, where the core radiation is minimal and the radiation in the divertor region (x-point and below) is increased as much as possible in order to reduce the power conducted to the targets by the SOL plasma. Figure 1.6-10 shows the power distribution in this case. The exact details of how the radiation is distributed in the divertor is not yet well understood by the edge physics community and cannot be modeled with high confidence, so we have chosen two cases already observed in tokamaks to determine the maximum power loading expected by particular divertor structures. In the first case, the bulk of the radiative losses occur near the x-point (this is the most commonly observed distribution), and in the second, they are spread along the divertor leg. The implications of these assumed distributions will be discussed further in the next section, Surface Heat Loads.

There are actually two more operating conditions which have not been covered and which might have significantly different power loss distributions. These are Start-up and Ramp-down, which are transient phases of each plasma pulse. Both feature direct plasma contact with the limiter surfaces for short periods of time. Ramp-down should not be too different than the steady-state phase, since it mostly consists of letting the energy stored in the plasma dissipate in a controlled manner using the usual divertor configuration. Only when the plasma current has dropped to the minimum controllable level will the discharge shape switch to a limiter configuration, and the power deposition should be small, even when the final collapse of the current channel occurs.

During Start-up, which lasts about 10 sec, the plasma may be operated in the limiter configuration for several seconds until the current channel expands to the point where the PF system can control it Input power during this time will be less than 15 MW, with perhaps 30% of this being radiated and the rest conducted to the outboard toroidal limiters. This total power loading will be much less than would be obtained during radiative divertor operation, but the local heat flux could be high because the power is deposited on leading edges by plasma conduction along field lines. Detailed predictions require a detailed component design plus modeling of the scrape-off layer plasma conditions.

The resulting power handling requirements (peak heat flux) due to radiative loading for the various plasma facing components as determined by each of the operating conditions are summarized in Table 1.6-2. In order to compute these values, we used the power loss trees shown, along with the magnetic and PFC geometry to estimate the plasma emissivity for the edge and divertor plasma regions. In the case of an x-point radiator, a 20 cm diameter gaussian profile was assumed. In the divertor, constant emissivity along the outer leg was used. Note that the peak divertor heat flux due to plasma conduction along the outer leg will be about 6 MW/m^2, which far exceeds any radiative load, thus nothing is in bold print for it. Similarly, the peak heat flux on the poloidal limiter will occur during start up and depends sensitively on the detailed geometry. Maximum values to be used for design purposes are indicated in bold print.

Table 1.6-2. Power Handling Requirements of PCAST PFCs

Component peak heat flux (MW/m^2)	Case I Standard Operation	Case II Radiative Mantle	Case III Radiative divertor (x-point)	Case III Radiative divertor (slot)
inner limiter	0.1	**0.2**	0.1	0.1
outboard limiter*	0.1	**0.2**	0.1	0.1
poloidal limiter*	0.1	**0.2**	0.1	0.1
Faraday shield	0.1	**0.2**	0.1	0.1
Inner divertor target*	0.15	0.2	**0.4**	0.2
Outer target*	0.15	0.2	**0.5**	0.2
Outboard gas baffle	0.12	0.2	**0.5**	0.38

* does not include conducted power

Fig. 1.6-8. Power Loss Tree for High-Q Operation with Minimal Core Radiation.

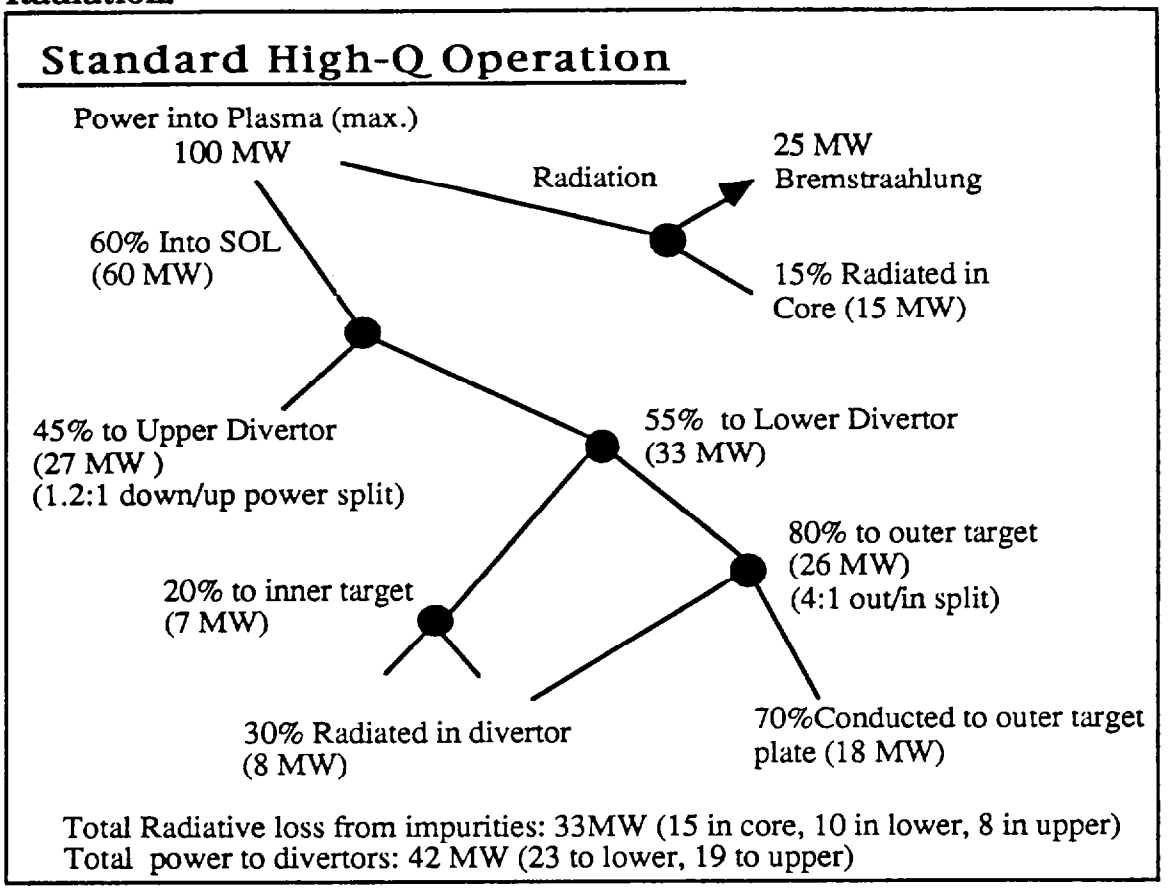

Fig. 1.6-9. Power Loss Tree for Radiative Mantle Operation.

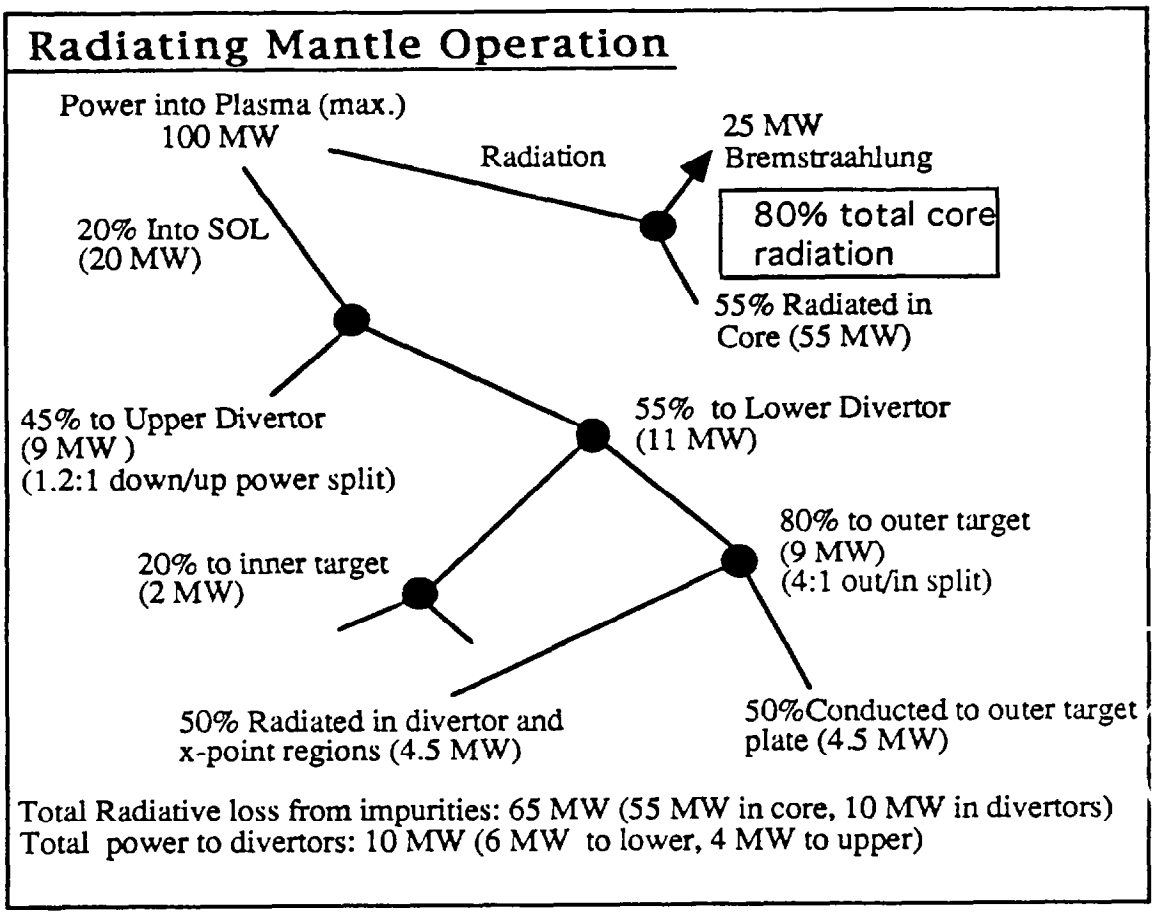

Fig. 1.6-10 Power Loss Tree for Radiative Divertor Operation

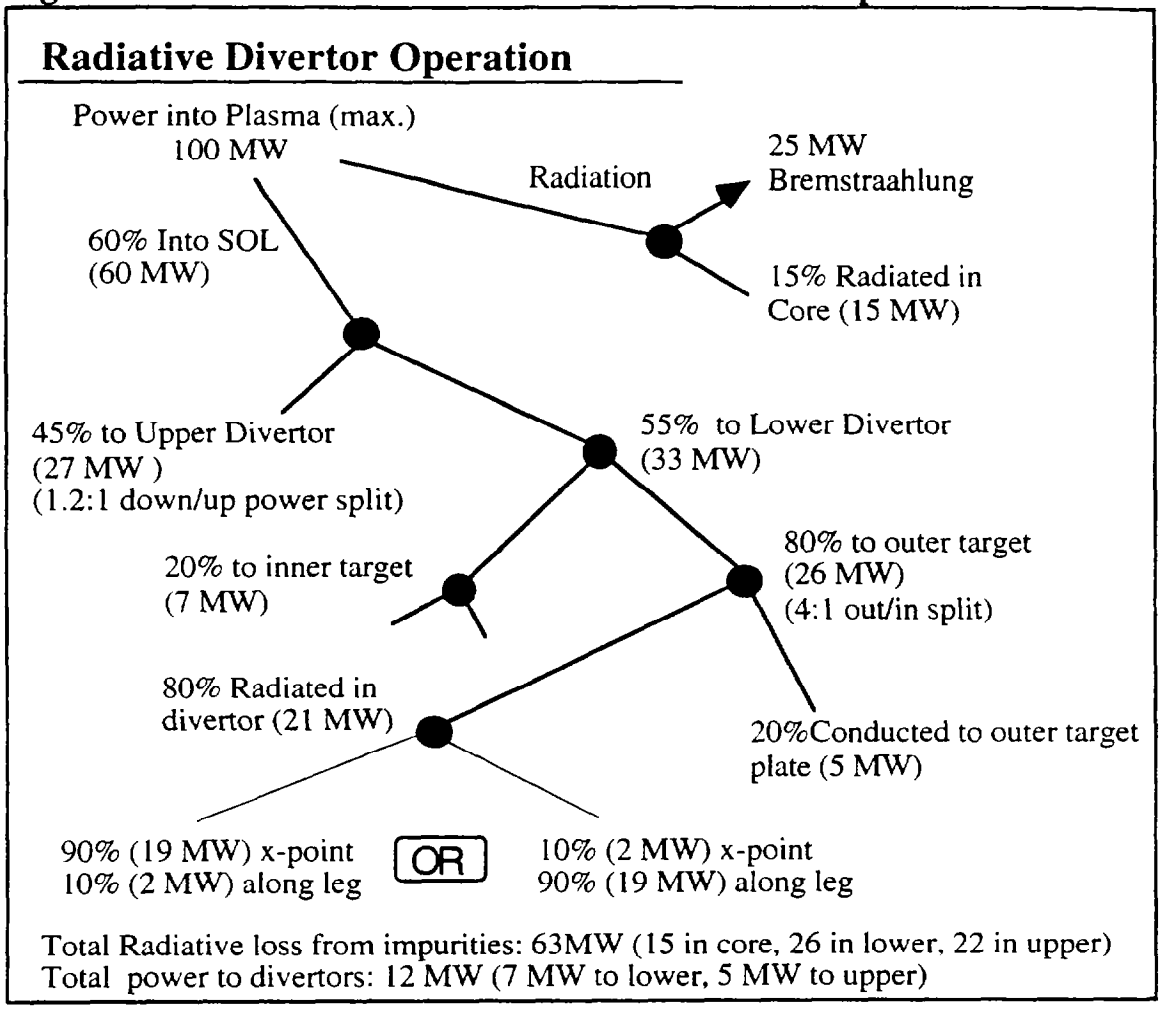

Peak Temperature Limits

The peak temperature limits of all plasma facing materials shall not exceed 1200°C. The maximum toroidally averaged surface temperature shall not exceed 1000°C.

Cooling

All PFCs will be cooled by de-ionized water .

Divertor:

The maximum heat flux on the divertor is 6 MW/square meter. The inlet temperature of the cooling water is 50°C and the inlet water pressure is 2 MPa. To

enhance heat transfer, swirl tape will be used to increase critical heat flux. With a coolant flow velocity of 6 m/s a safety margin of 2 will be achieved and the divertor macro block temperature will be below 1100°C. Fig. 1.6-11 shows a plot of the temperature distribution through a macroblock.

Inboard Limiter:

The maximum heat flux on the inboard limiter is 0.2 MW/square meter. The inlet temperature of the cooling water is 50°C and the inlet water pressure is 2 MPa. The coolant flow velocity will be 3 m/s, which will keep the tile temperature below 200°C in the areas of plasma radiation. The case of neutral beam shine-through needs to be considered later. Fig. 1.6-12 shows a plot of the temperature distribution through a bolted tile.

Total coolant flow required for all PFC systems (except for the unquantified poloidal limiter requirements which are expected to add less than 10% to the total):

1) Inboard Limiters	1555
2) Outboard Limiters	2300
3) Inner Divertor	10367
4) Outer Divertor	23233
	Total: 37455 GPM

Divertor Baffling

To limit core plasma fueling due to leakage from the divertor plenum the leakage conductance from the plenum regions shall be limited according to the following weighted sum over the various leakage paths:

$$\sum_i \varepsilon_i C_i \leq \text{t.b.d. l/s}$$

where the sum is over all leaks i in both divertor regions, C_i is the gas conductance of the leak in question determined according to standard vacuum practice, and the weighting factor ε_i (which reflects the relative core fueling efficiency of gas sources at the different locations) depends on the location of the leakage path, as follows:

1) Through the divertor structures: ε_i=0.01.

2) Through the gap between the outboard divertor structure and the outboard toroidal limiter: ε_i=0.1.

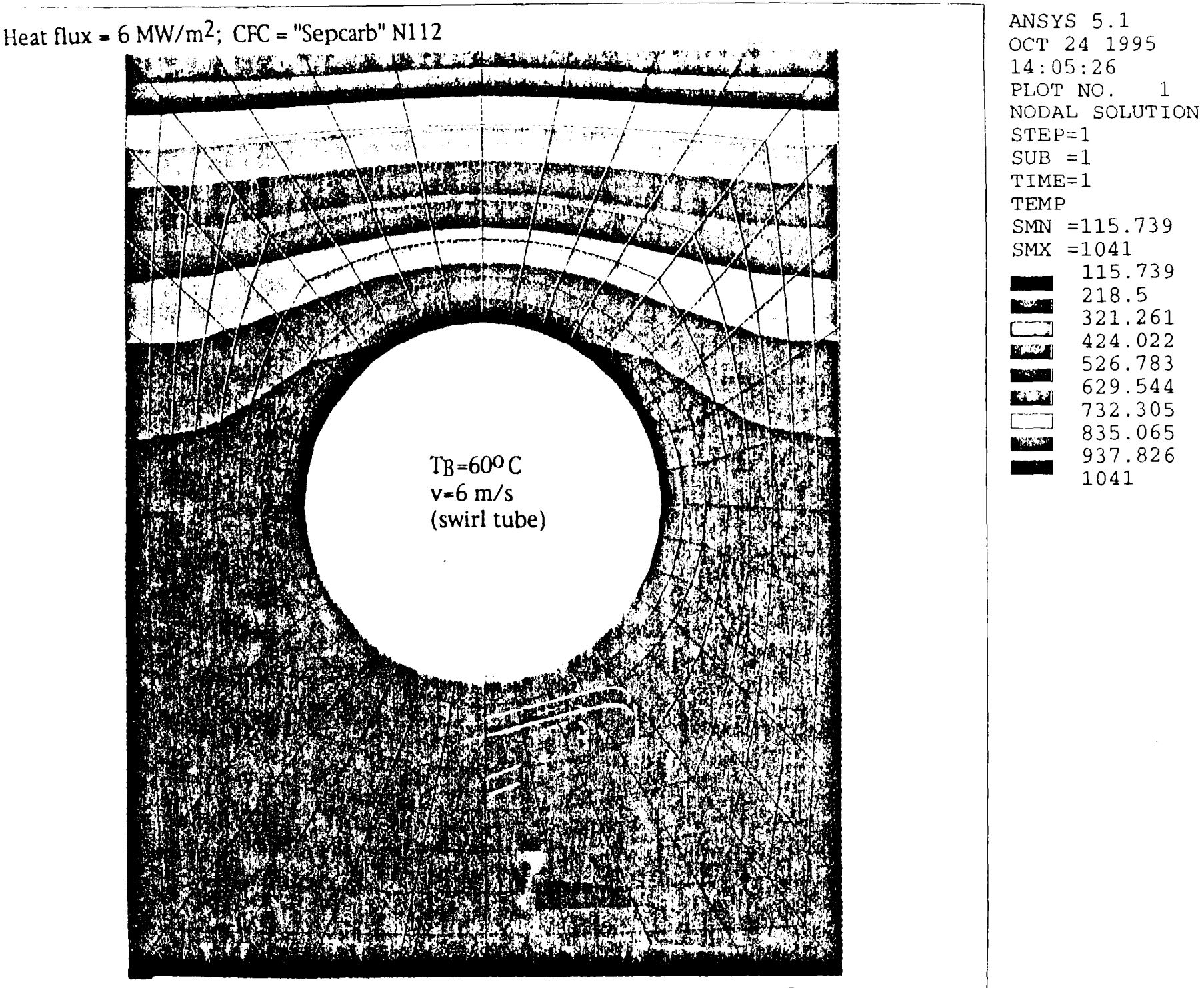

Figure 1.6-11. Temperature Plot for a Divertor Macro Block

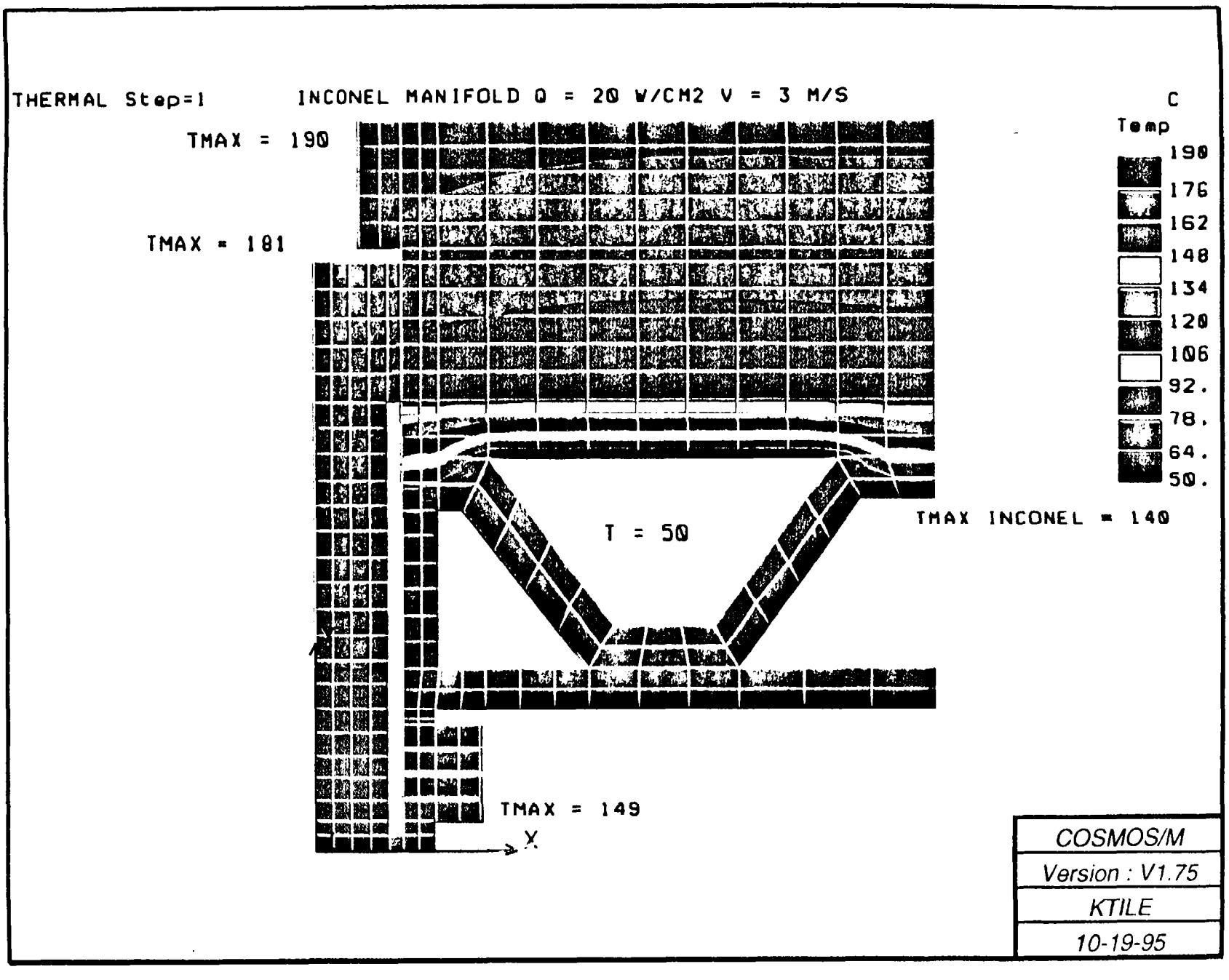

Figure 1.6-12. Temperature Plot for a Bolted PFC Tile

3) Through the auxiliary baffles and the gaps separating the auxiliary baffles, the vessel, and the in-vessel structures: : ε_i=0.2.

The term "leaks" does not include the prescribed gaps between the divertor structures, or the pump duct openings. To limit the degradation in particle exhaust performance due to leakage from the divertor plenum the total leakage conductance from the plenum regions shall be limited according to the following sum over the various leakage paths:

$$\sum_i C_i \leq \text{t.b.d. l/s}$$

Flexibility to re-configure the divertor assemblies shall be provided.

Bakeout

All PFCs will be heated to a temperature of 350°C. During bakeout, the PFC coolant will be drained and the PFCs shall be heated by conduction and radiation from the steam heated vacuum vessel.

Pulse Length & Repetition Rate

The PFCs shall be designed for an operating pulse length of 200 seconds and a maximum repetition rate of 1 pulse per hour.

Maintainability

All PFCs shall be designed in a modular fashion to permit remote removal and replacement.

Glow Discharge Cleaning (GDC)

The PFC designs shall be compatible with GDC for wall conditioning.

Boronization

The PFCs shall be compatible with boronization for wall conditioning

Pre-Shot Temperature

The PFCs will be cooled between shots with de-ionized water with an inlet temperature of nominally 50°C. The PFCs shall be at a temperature greater than

50°C prior to initiation of a shot.

Alignment

Provisions will be made to provide initial alignment and future adjustments, as needed, to minimize hot spots.

Disruption Loads

Electromagnetic loads due to disruption events are the most significant loads seen by the PFCs. The PFCs will be designed to accommodate disruptions characterized by:

- possible vertical displacement
- a thermal quench occuring in 0.1-1 ms
- a current decay with an average time-varying decay rate of 1 MA/ms, and a peak decay rate of 2.0 MA/ms
- a peak poloidal halo curent of 40 % of the maximum plasma current prior to the disruption, with a toroidal peaking factor of 2:1.

Materials

Materials Selection

Carbon fiber composites (CFCs) will be used for all plasma facing surfaces. CFC material will be selected with appropriate considerations of irradiation damage, especially degradation in thermal conductivity. It is possible to use CFCs for the PFCs in PCAST since the maximum neutron dose will be less than 0.1 dpa.graphite. Component lifetime, heat flux, operating temperature with neutron dose, and the remote possibility of limited annealing of damage will determine the initial thermal conductivity that is required for the CFC to be used for each PFC. The thermal analyses presented in the preceeding sections of this report used unirradiated material properties of the CFCs. Future analyses will require consideration of thermal conductivity degradation that varies through the tile thickness as a function of operating temperature.

Copper alloy will be used in the divertor for the coolant tubing that is used in the CFC macroblock design. This copper tubing is not required to resist primary loads due to disruptive instabilities, but must withstand stresses due to differential thermal expansion. The type of alloy selected for use will require further study of possible losses of ductility and stress history. Copper alloy is not required for heat sinks of other PFC components. The relatively low steady state heat flux (< 0.2 MW/m^2) deposited on other PFC components allows use of Inconel support structures.

Low activation has not been a major issue in materials selection at this time. Inconels have been selected as the primary structural material of the plasma facing components. The type of Inconel will be determined from future more detailed stress analysis. Because neutron heating of the Inconel support structure will vary from 12 W/cm^3 on the midplane to 7 W/cm^3 in the divertor region, the Inconel structure will require cooling. The limiters accomplish this cooling through use of a cooled structure of sandwich panel construction. Divertor modules will require a similar type of cooled structural design or use of other cooling techniques.

Neutron Damage

Figure 1.6-11 illustrates that the CFC divertor macroblock is shown to operate between 1040 and 1160 C when a CFC with an unirradiated thermal conductivity of approximately 280 W/m-K is used. At the higher operating temperatures of the macroblock surface CFC's show little degradation in thermal conductivity with neutron dose. But reductions will be greater at lower operating temperatures experienced in the region of the coolant tube. Normalized conductivities (K_{irr}/K_0) are roughly similar for CFCs. A thermal conductivity reduction of roughly 45% is expected at 400 C and 30% at 600 C at full life (0.1 dpa.graphite). This degradation in thermal conductivity is of primary concern in the areas of higher power deposition, i.e.: the divertor. There are three possible approaches to this problem. (1) In the first wall areas where there is sufficient temperature margin, simply allow the higher temperatures that will occur. (2) Use higher thermal conductivity CFC initially. Lastly (3), replace the CFC components in the high heat flux area during the tokamak operating life. Further detailed analysis with considerations of loss of thermal conductivity as a function of dose and temperature must be conducted to determine the appropriate design option.

Copper loss of ductility with neutron dose will need to be investigated on a case by case basis for each alloy under consideration for a maximum of 0.3 dpa.copper experienced in the PFCs.

References

1. C. H. Wu et al., Neutron Irradiation Effects on the Properties of Carbon Materials, Sixth International Conference on Fusion Reactor Materials (ICFRM), 1993, pp 416-420

2. T. Maruyama and M. Harayama, Neutron Irradiation Effect on the Thermal Conductivity and Dimensional Change of Graphite Materials, Journal of Nuclear Materials 195 (1992), pp. 44-50

Section 1.6.3: Miscellaneous Shielding (M. Cole)

1.6.3.1 Functions

Device Shielding Objectives

The primary functions of the device radiation shielding are to:

1. Limit radiation damage to the coil insulation,
2. Limit nuclear heating in TF coils,
3. Reduce neutron induced activation for components needing frequent maintenance,
4. Provide personnel protection against delayed gamma-ray radiation from highly activated tokamak components,
5. Reduce and control neutron activation of test cell air.

Configuration Requirements and Essential Features

The device shielding can functionally be divided into four areas:

1. Torus shielding around the vacuum vessel,
2. Shielding around the vacuum pumping ducts and a biological port plug,
3. Penetration shielding in and around the radial ports,
4. Shielding in the inter-coil structure.

Essential features of the shielding systems are briefly discussed below.

Torus Shielding- The torus shielding is an integral part of the vacuum vessel. The vessel is a double-walled torus made of two 4.45 cm thick Inconel 625 shells. Filling the annuli are steel and water layers arranged to achieve an overall volume ratio of 60:40. This region has a minimum thickness of 16.5 cm. The water is actively circulated to remove the energy deposited in the shielding due to the interaction of the nuclear radiation.

Duct Shielding - Duct shielding is provided to recover the lost shielding effectiveness of the vacuum vessel and to mitigate the effects of neutron streaming so as to reduce the activation of components outside the TF envelope. The shield

thickness required to achieve these goals will depend on the location of the duct and the closest distance that access will be required. In general, about 15 cm of stainless steel/water shield is needed to recover the loss of vessel shielding and 30 cm is needed for making the neighborhood region accessible after machine operations. Lower quality shield materials may be substituted for the SS/water mixture if space around the duct is not a constraint.

Penetration Shielding - Shielding for mid-plane ports is provided for the same purposes as those described above for the ducts. Because these penetrations are at the midplane of the machine, neutron streaming is more severe than that in the pumping duct and diagnostic penetrations. The minimum thickness needed to recover the loss of vessel shielding at the midplane penetration is about 22 cm of stainless steel/water shield. Making neighboring regions outside the TF coil accessible during maintenance requires a shield thickness of 50 cm.

Inter-coil Shielding - Shielding is provided in the inter-coil structure to prevent radiation leakage. These regions have a radial thickness of about 1 m, and will be filled with a mixture of steel and hydrogenous material in a ratio of about 90/10. The hydrogenous materials which have been considered include silicon rubber, grout and epoxy.

Performance and Operational Requirements

Sufficient shielding shall be provided in or around the vacuum vessel and its penetrations to limit the life time radiation dose to the coil insulation to below 30 MGy and the nuclear heat load in the TF to less than 5% of its resistive dissipation. Modifications to penetration shielding required by individual diagnostics will be the responsibility of each diagnostic system.

Design Description

System Design Description

The tokamak radiation shielding includes the neutron and gamma shielding around the torus and penetrations that is required to: 1) limit the nuclear heating of the coils and damage to the coil insulation and 2) limit the activation of components outside the shield. The major shield components

include stainless steel/water between the walls of the vacuum vessel, the 4.45 cm thick walls of the vacuum vessel, the TF coils, and stainless steel/water or hydogenous material in the port plugs, vacuum ducts and inter-coil region.

Torus Shielding

The torus shielding is provided by water and steel plates located within the annulus of the vacuum vessel walls. The water is heated/cooled to maintain the vacuum vessel temperature at a nominal temperature of 150°C during operation and 350°C during bakeout.

The vacuum vessel design provides a 16.51 cm interspace for the steel/water shield on the inboard side of the torus and a 29.21 cm interspace on the outboard side. Multi-layer aluminized polyimide thermal insulation is wrapped around the outside of the torus to insulate the vacuum vessel and reduce the heat loss from the vacuum vessel.

Duct Shielding

The equivalent of 20 cm shielding is required in the area between the coils near the inter-coil region. The shielding in the duct region will be essentially the same as that in the vacuum vessel. Two outer walls of inconel or stainless steel filled with a stainless steel/water or a hydrogenous material with a material ratio of about 60/40. The operating and bakeout temperature of the duct will be the same as the vacuum vessel. Multi-layer aluminized polyimide thermal insulation will be wrapped around the outside of the duct to reduce the heat loss.

Radial Port Plug Shielding

Radial port plug shielding must be provided at all the radial ports. At most ports, large plugs provide the bulk of the shielding and have essentially the same configuration as the vacuum vessel torus. The plugs consist of a box made of inconel plate and are internally filled with stainless steel and water. The plugs are inserted into the radial ports and fit flush with the inside of the vacuum vessel torus wall. The plugs will be supported mechanically by the vacuum vessel and will operate at the same temperature. Diagnostics, fueling,

or other equipment located in the radial ports shall provide the modifications to the shield plugs consistent with the needs of that equipment and with the shield integrity.

TF Coil Structure

The area in the TF Coil structure that can be filled with shielding will be filled with stainless steel and a hydogenous material. This shielding will be 1.12 m thick and conform to any openings or penetrations. This shielding will decrease damage to the coil insulation and decrease the activation of material located outside the TF Coil.

System Performance

Nuclear Heating of Coil Set

The total nuclear heating was calculated as described below. Most of the heating occurs in the vacuum vessel.

Description	Heat Load
Fusion power	400 MW
Neutron power	320 MW
Neutron heating in Coils	<5% of resistive dissipation

Design Basis

Coil Insulation Damage

Samples of laminate-type sheet insulation material, including various combinations of epoxy or polyimide with E-, S- and T-glass were irradiated in a fission reactor during the CIT/BPX design up to 300 MGy. Static and cyclic tests for compressive, shear and flexure strengths showed that it is appropriate to use 30 MGy as the design objective for the organic insulation in the coils.

It has been calculated that, with 400 MW fusion power, the dose rate at the first wall location for the insulation material amounts to 5000 Gy/s. Using 100 s for the nominal pulse length and 5000 pulses as the lifetime run, we expect a total

cumulative dose of 2500 MGy. To meet the 30 MGy objective, a reduction factor of 85 is needed. This may be achieved with 25 cm of stainless steel/water shield (volume ratio 80:20) plus 8 cm of coil case and 2.5 cm of in-vessel component.

TF Coil Heating

The coil heating will be dominated by the copper resistive power dissipation which has been estimated to be about 400 MW when the coils are cooled initially to the LN2 temperature. We stipulate that the additional heat load by the nuclear interaction process shall not be more than 5%. This is achieved if the shield objective for insulation damage is achieved.

Neutron Activation

Material activation has been estimated for major in-vessel components. Typically, the dose rate is expected to be 2.5×10^7 mrem/h after 1 week of cooling for Inconel 625. For SS316, it is 6×10^6 mrem/h. Also, in front of the TF the dose rate is expected to be 4×10^5 mrem/h, and near the cryostat 5×10^4 mrem/h, if there is no shielding in the intercoil structure.

It is desirable to be able to maintain and service most of the machine components outside the TF envelop (around the cryostat). A reasonable working scenario would require an ambient dose rate level < 10 mrem/h after 1 week of cooling. To achieve this level, a reduction factor of 10^6 relative the levels in the vessel is required. This is equivalent to require about 1 m thick stainless steel/water shield. Clearly, such reduction can not be achieved inside the TF envelop. To achieve this for regions outside the TF envelop, the inter-coil space would have to be completely filled and penetration shielding would have to be properly designed. The shielding needed depends on the size an location of penetrations. Multi-dimensional radiation transport analysis will be required to ascertain the adequacy of a design. Preliminary estimates indicated that about 0.5 m of stainless steel/water shielding would be needed for the neutral beam injectors and 0.3 m of similar shielding would be needed for the TVPS.

Section 1.8: Fueling (M. Gouge)

1.8.1 Functions and Design Requirements

The primary functions of the PCAST fueling system are:

(a) to inject DT fuel and impurity gases into the vacuum vessel at the required fueling rate and response time to maintain the fusion power at the required level;

The primary functions of the PCAST wall conditioning system are:

(b) to reduce and control impurity and hydrogenic fuel outgassing from plasma facing components (by wall conditioning) in order to achieve clean and stable plasma operation.

Gas and Pellet Fueling

The Fueling System shall provide "steady state" plasma fueling at a rate which corresponds to a fusion power of up to 400 MW, and "pulsed" fueling to meet the required density ramp-up during the start-up phase.

The steady state core fueling capability must, at a minimum, supply core fueling at the rate of 2.1×10^{21} s^{-1}, or about 30 torr-l/s of D2 or T2. By comparison, the vacuum pumping rate is 100 torr-l/s. This allows an envelope for gas puffing, which is needed for edge control.

The peak core fueling capability should allow the machine to reach operating density in about 15 seconds. This requires a peak fueling rate of 6×10^{21} atoms/sec, or about 85 torr-l/s.

Impurity gases for divertor plasma radiative cooling and wall conditioning gases will also be injected.

Divertor and edge fueling at a rate of 7×10^{21} atom/sec will be provided to control impurity backflow and divertor conditions.

Wall Conditioning

The primary functions of the wall conditioning system are to reduce impurity and hydrogenic fuel outgassing from plasma facing components and reduce the amount of tritium entrained in plasma facing components.

Design Description

The fueling system is assumed to be very similar to that proposed for ITER, but scaled back somewhat to be consistent with the smaller size of the PCAST. It consists of the pellet injector system, the gas puffing system, and the wall conditioning system. The pellet injector system includes a shielded enclosure to allow hands-on maintenance of the injectors and associated components. The fueling system will be capable of tailoring the isotopic mixture of gases to the core and edge of the plasma to reduce the tritium recycling and inventory.

Pellet Injection System

The pellet injection system consists of both centrifugal and pneumatic injectors, housed in a single shielded enclosure located adjacent to the machine. A schematic layout is shown in Figure 1.8-1. The system is capable of higher delivery rates than the requirement stated above in order to make up for any wall pumping effects.

The pneumatic injector is a repeating, single stage light gas gun designed for shallow core fueling. It would be capable of injecting pellets up to 8 mm in diameter at a velocity of up to 1.5 km/s and a frequency up to 2 Hz.

Two centrifugal injection systems are proposed for redundancy to improve the overall availability of the fueling system. The injectors would be capable of injecting pellets of 2 to 4 mm diam at a velocity of ~ 1 km/s and a rate of up to 10 Hz.

The injection room consists of a sealed enclosure sufficiently shielded from the tokamak to allow hands-on maintenance of the injector components. Both the pneumatic and centrifugal injectors are housed in this enclosure, along with

associated instrumentation, vacuum tanks, pumping systems, etc. The torus gas injection system is also located in this room.

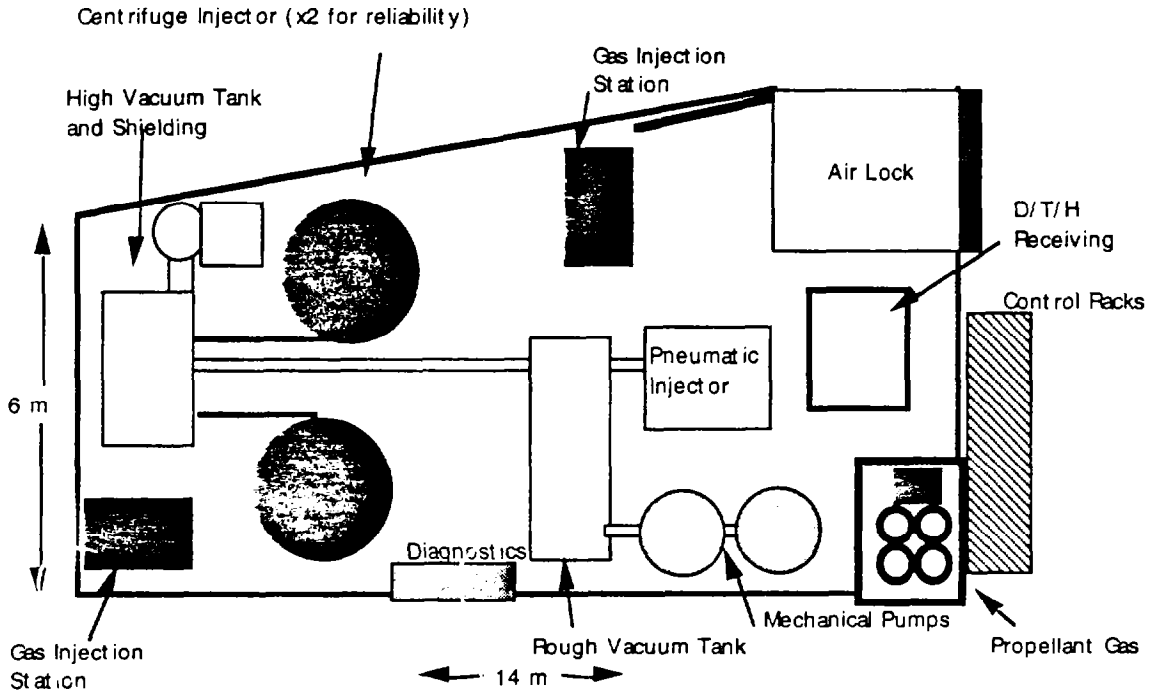

Figure 1.8-1 Fueling Room Schematic

Gas Injection System

The gas puffing system will inject gas in the upper and lower divertor chambers at multiple locations with equal toroidal spacing. In order to improve the response time, the injection valves will be located as close as possible to the machine, but in a location compatible with maintenance requirements.

The injectors will allow the introduction of He, Ne, N_2 and Ar, as well as H_2, D_2, and T_2 in variable ratios. To reduce tritium inventory, the tritium feed line diameters will be minimized.

Wall Conditioning System

The proposed system would be very similar to that proposed for ITER. A Glow Discharge Cleaning (GDC) system will be provided to reduce impurity and hydrogenic outgassing from the first wall and to limit the tritium inventory. However, unlike ITER, the plasma facing components are covered with graphite and carbon - carbon tiles, so the system will be capable of GDC with a He and He:O mixture to chemically remove tritium from the first wall and divertor surfaces.

Issues

The system requirements and design concept described above are very preliminary and the issues are assumed to be similar to those encountered on the ITER system. No major technical problems are expected. The primary assumption is that the fueling room can be located and shielded to provide both the needed access to the tokamak and hands-on maintenance capability for the equipment.

The wall conditioning system has a significant issue associated with the need to limit the tritium inventory in the first wall and divertor tiles, which are composed of carbon/carbon composite. He:O GDC was proposed for the BPX device to solve this problem, and a similar solution may be required for the PCAST device.

Section 1.9: Vertical Stabilization and Plasma Position Control (G. H. Neilson, C. Kessel, P. Heitzenroeder)

The elongation of the nominal plasma is 1.96 at the separatrix, therefore the plasma is vertically unstable to the n=0 axisymmetric mode. Control is provided through a combination of close-fitting conducting structure and fast control coils.

For a given vacuum vessel material, the power required for both vertical and radial position control is significantly reduced if the coils are located as close to the plasma as possible, in a position with a minimum of intervening structure.

Three coil positions were examined for vertical position control:

(1) between the outer limiter plates and vacuum vessel extensions;

(2) between the extensions and the inner vessel wall; and

(3) between the vessel and TF coil.

The resulting peak powers required for a 2 cm. vertical step response were 10, 30, and 300 MVA, respectively, to provide a critically damped trajectory with a rise time of approximately the unstable plasma growth time (35 ms). Based on additional control simulations, it was further decided to use two coil pairs, with one dedicated to vertical control and the second dedicated to radial position control. This further reduced the power requirements.

As a result of these studies the positions chosen for the plasma position control coils are:

- R=5.4 m, Z=+/- 2.4 m for the vertical position control coils.
- R=6.6, Z=+/- 1.4 m for the radial position control coils.

The PCAST plasma position control coils will be fabricated from Inconel vacuum jacketed, MgO insulated water-cooled hollow copper conductor. MgO is chosen as the electrical insulator since it can withstand the elevated temperature bakeout and radiation dose within the PCAST machine. Radiation exposure data for MgO accumulated from accelerator facilities

indicates no apparent effect up to about 10^{10} Gy[1]. This level is at least 4 times higher than the dose expected in the PCAST vessel and permits the coils to be positioned relatively close to the plasma. ITER's dose, on the other hand, would exceed this level since its dose is at least an order of magnitude higher than PCAST due to its longer pulse and operating lifetime. This is probably one of the factors which led to their decision not to use in-vessel plasma position and control coils.

The major characteristics of the Plasma Position Control Coils are given in Table 1.9-1.

Table 1.9-1 Major Parameters of the PCAST Plasma Position Control Coils

	Vertical Position Control Coil	Radial Position Control Coil
Peak kA-t per coil:	100	200
Turns/coil:	2	4
Peak current/turn: (kA)	50	50
Resistive power (MW)	0.73	1.2
Weight (2 coils) (kg)	2500	9000
Max. volts/turn: (v)	100	400

[1] Joel H. Schultz, *Design Practice and Operational Experience of Highly Irradiated, High Performance Normal Magnets* (Journal of Fusion Energy, Vol. 3, No. 2; 1983)

Section 2.2: Assembly (D. Knutson)

2.2-0 Introduction

Neither the time available nor the details of the design permit a bottoms-up analysis and cost estimate of the assembly of the PCAST machine. Instead, the approach adopted was to review the ITER assembly procedures and estimates, and to make comparisons to the PCAST proposal in those areas where differences were expected to be significant. The areas of particular interest included welding, in-vessel components, alignment, tooling, crane usage, complexity, and cryogenic connections. Scaling factors were developed from direct comparisons between PCAST and ITER and from experience on other machines and machine estimates.

2.2-1 Assembly Tasks

Welding

The welding of the vacuum vessel segments to form a toroid, and the welding of the vacuum vessel ports, represents a significant portion of the machine assembly time. TPX manpower estimates indicate that field welding operations on the vacuum vessel were 9.6% of the total assembly labor costs. The PCAST design has 8 vacuum vessel joint locations, compared to 20 joint locations for ITER. The ratio of length of a single weld groove in the poloidal direction, ITER/PCAST is 1.58:1. It was assumed that the welding of ports would scale in proportion to the surface areas of the vacuum vessel or ITER/PCAST equals 2.7:1.

Assembly of In-vessel Components

Cost estimates were available from ITER for the first-wall/blanket system assembly and for the divertor assembly. A blanket system will not be required for PCAST, however other first-wall costs will remain. It was assumed that 75% of the costs associated with the first-wall/blanket system could be eliminated. The remaining first-wall installation could be scaled in proportion to the surface area or ITER/PCAST equals 2.7:1. In the case of the divertors, it was assumed that the reduction in cost would scale roughly with the number of divertors. The ITER

design has 60 divertor cassettes, PCAST requires 32 resulting in a scaling factor of 0.53 applied to the ITER estimate.

Alignment of Major Components

Assembly operations involving the alignment of components represented 7.5% of the total estimated assembly labor cost, excluding the alignment of in-vessel components, for TPX. These figures do not represent a total of the alignment time. However, they do represent the total time of operations where alignment was a significant part. Alignment is an important assembly issue, and is related not only to the number of major components involved, but also to the tolerances required. For the purposes of this study, the alignment precision was assumed to be the same for both ITER and PCAST. In terms of major components, the obvious comparison could be made between the 20 individual coil assemblies (including vacuum vessel segments) of ITER and the 8 two-coil modules and associated vacuum vessel segments for PCAST. The resulting scaling factor would be 0.4 applied to the ITER estimates. Another example is in the outer gravity supports. ITER requires the alignment of 20 individual supports, each weighing 30 metric tons. The PCAST approach would involve the alignment of a single ring weighing approximately 91 metric tons. Other examples exist, but for analyzing alignment differences, the comparison of ITER and PCAST TF coil/vacuum vessel segment quantities probably represents a conservative approach.

Assembly Tooling

The bulk of the tooling estimate would be for the handling, moving, and positioning of the heavy components. Transporters would be required for moving large components from storage areas to the Assembly Hall. Lifting rigs and lifting fixtures would be required for the unloading, moving and positioning of large components in both the Assembly Hall and the Tokamak Hall and Pit. The cost of the transporters and lifting devices would scale with weights. Other special tools and fixtures are necessary for alignment, field machining, welding, installation, temporary supporting, positioning and jacking, to name just a few. It is assumed that the weight of components is a factor in the cost of at least 70% of the assembly tooling. A scaling factor based on weight is applied to 70% of the assembly tooling, the balance of tooling would remain unchanged. The scaling factor based on the

weight of a PCAST TF coil/vacuum vessel module (800 tonnes) compared to an ITER TF coil/vacuum vessel module (1500 tonnes) is 1:1.88 or 0.53.

Crane Usage

During the heavy assembly portion of the assembly operations, that portion involving the installation of the major components, experience has shown that the overhead bridge crane usage during the TFTR assembly was approximately 80%. In fact, crane availability was frequently the major factor impacting the assembly schedule. The assembly of major components in the TPX assembly plan was completed at the end of the vacuum vessel welding and leak checking operation, and consumed an estimated 59% of the assembly labor budget. An additional assumption is that no more than one third of the assembly crew would be actively involved in a crane lift. Applying these factors to the total assembly labor estimate for the ITER machine results in an estimate of the cost of the crane usage for ITER. Generally, cranes rated for heavier lifts operate more slowly, and the lift preparation time, involving installation of heavier lift apparatus and fixturing, is longer. For PCAST, a reduction factor of 10% was assumed due to the lighter weights of lifting rigs and fixturing and consequently shorter lift preparation time.

Design Complexity

The lack of detail in the ITER assembly estimate, and the absence of a bottoms-up PCAST assembly estimate, results in a subjective approach to design complexity. There is a degree of simplicity in the PCAST design that should result in monetary savings in the assembly operations. For example, the gravity support concept for PCAST is simpler, providing a stable platform from which to support the TF structure during assembly. The ITER support concept involves a large number of individual gravity supports necessitating a TF coil assembly sequence to evenly distribute the load. The additional temporary support from the cryostat walls during assembly is further evidence of the inherent instability of the ITER support concept for assembly purposes. Another assembly cost savings is the absence of LN2 panels on the walls of the PCAST cryostat. In addition, PCAST does not require the installation of quench protection instrumentation. There are numerous examples where smaller size, fewer components, and fewer hardware items to be assembled, add up to cost savings at assembly. Applying a global simplicity factor

resulting in a 10% reduction in the PCAST assembly costs compared to ITER would be a conservative and appropriate response.

Materials

Materials primarily represent the consumables required during assembly operations. A scaling factor of 0.70 is applied to the ITER materials estimate for PCAST.

Section 2.3 Maintenance Systems (M. Rennich)

Outline

Introduction

Maintenance Guidelines and Philosophy

2.3.1 General Requirements and Description

General Requirements

General System Description

- General Description
- In-Vessel Maintenance
- In-Cryostat Maintenance
- Ex-Vessel Maintenance
- Mockup and Test Facility

2.3.2 In-Vessel Maintenance System

Requirements

- Functional Requirements
- Design Requirements
- Operational Requirements

Design Description

- System Configuration
- Articulating Booms
- Maintenance Port Enclosures
- Module Handling Fixtures
- Transfer Casks
- Shield Plug Handling Equipment

Operational Description

2.3.3 Ex-Vessel Maintenance Systems

Requirements

- Functional Requirements
- Design Requirements
- Operational Requirements

Design Description

- System Configuration
- Port-Mounted Assemblies
- Boom-Mounted Systems
- Floor-Mounted Systems
- Moveable Casks

2.3.4 In-Cryostat Maintenance Systems

Requirements

- Functional Requirements
- Design Requirements
- Operational Requirements

Design Description

System Configuration
Maintenance Pods
Boom Mounted Manipulators

2.3.5 Viewing and Lighting

Requirements
- Functional
- Design Requirements
- Operational Requirements

Design Description

2.3.6 Tooling

Requirements
- Functional Requirements
- Design Requirements
- Operational Requirements

Design Description
- System Configuration
- Manipulators
- Tools and Connectors
- Pipe Welding and Cutting
- Inspection Tooling

2.3.7 Radiation Hard Components

2.3.8 Control Facilities

Requirements
- Functional Requirements
- Design Requirements

Design Description

2.3.9 Mockup and Test Facilities

Requirements
- Functional Requirements
- Design Requirements

Design Description
- Preliminary Mockup and Test Facility
- Final Mockup and Test Facility

2.3.10 References

Introduction

The Maintenance Systems for the PCAST machine are based on those outlined for the ITER reactor. This reflects similarities of scale, scope, and radiation environments. It also recognizes the use of large scale maintenance tools developed by the NET and ITER teams.

As a consequence of the ITER basis for the PCAST system the ITER Design Description Document 2.3, Remote Handling Equipment was used as the foundation of this analysis. Thus, some of the information and format is used verbatim from that document.

The TPX Maintenance Systems techniques have also been applied in several places to reflect the similarities between the PCAST and TPX with respect to the configuration of the interior component module configurations.

Maintenance Guidelines and Philosophy

The PCAST Fusion Machine will become activated very soon after the beginning of experimental operations. The activation levels will exceed those acceptable for personnel to approach the machine to perform maintenance, consequently machine components will be designed based on proven remote maintenance and remote handling technology to improve the maintainability of the machine and thus increase reliability and availability. Maintenance Systems will provide tools to assist with the operations required to implement the remote operations incorporated into the PCAST operating systems.

The maintainability of all components of the device will be the responsibility of the component designers. The designers will incorporate standardized remote features such as captive fasteners, handling brackets and remotely accessible pipe welds into the elements as necessary. Moreover, all components will be segmented into modular components as determined to be most effective in reducing the maintenance time in or near the PCAST machine.

The design of the Maintenance Systems will focus on the functions required to keep the PCAST machine in operation. Modularization of components and standardization of connectors and handling features will be used to reduce the variety of functions. A classification of the known operations will then be employed to formulate a development plan to verify the design of the complete system.

Based on this classification, the maintenance scenarios such as segmentation of the maintained components and maintenance procedures are established and the requirements for the remote handling equipment design are clarified. This includes determination of the maximum allowable time for maintenance procedures which may have a strong influence on the design of the component to be maintained as well as on the maintenance equipment.

The effectiveness and efficiency of all remote handling operations, component features and tooling must be verified during the design process. This will be

accomplished by full-scale mockup demonstration of complete remote handling scenarios including remote handling equipment/tools, components and procedures.

2.3.1 General Requirements and Description

General Requirements

The PCAST machine has been designed to provide for remote maintenance operations by providing access for tools and through the incorporation of remotely operable features into the machine components.

General System Description

General Description

Maintenance systems will support operations in all areas of the PCAST machine; the interior of the vessel, the interior of the cryostat and the exterior systems. Each of these areas is significantly different in design and function; therefore, the Maintenance Systems are divided into three corresponding categories - In-Vessel Maintenance Systems, Cryostat Interior Maintenance Systems and Ex-Vessel Maintenance Systems.

In addition, four interfacing support systems are provided to complete the overall mission of Maintenance Systems. A Maintenance and Storage Area is provided to facilitate a limited amount of component repair capability and adequate shielded storage for contaminated components awaiting repair or disposal. Viewing systems, including quick deployment systems, are provided for all areas of the machine. A Mockup and Testing Facility will be used to develop maintenance procedures, verify designs and train operators. Finally, a Central Control Facility will be used to operate and coordinate the Maintenance Systems.

Major functions of the maintenance system includes the replacement of all operating components including the Plasma Facing Components (PFC's), Port Mounted Assemblies such as diagnostics and ICRH; magnet systems and coils, and vacuum pumps.

In-Vessel Maintenance

The components inside the PCAST vessel are grouped into a limited number of discrete modules. Each module has been configured to be handled, installed and removed with remote tools. This includes a dedicated handling fixture designed to mate the module to a remotely operated handling boom.

At the equatorial plane there are four maintenance ports set at intervals of 90 degrees. Outside each port is a maintenance cell. Each maintenance port also has an articulated boom permanently mounted in a maintenance enclosure. During machine operations the booms are retracted behind the inner pit shield and isolated with shielded plugs. Each boom can be equipped with either a module handling fixture or a manipulator to operate tools such as wrenches and welding devices.

In-Cryostat Maintenance

The cryostat is a stand alone cylindrical double-walled vacuum vessel with domed ends. The cryostat is located inside a 1.2 m thick cylindrical concrete inner pit shield wall with a detachable roof. The outside diameter of the inner pit shield wall is 28.4 m and over 41 m high.

To enter the annular space between the tokamak and cryostat inner wall, four access ports are provided on the cryostat to which can be mounted a vacuum rated transfer flask containing a maintenance tool. The restricted diameter limits the inspection device to light duty maintenance. The connection to the port is through a vacuum lock or double valve. To access the space between the lower cryostat dome and the bottom of the machine four equally spaced radial ports are provided.

The primary maintenance element inside the cryostat will be the magnetic coils. High reliability is a fundamental requirement for the design of PCAST magnets as they are not expected to fail during the life time of the machine. However, it must be feasible to remotely replace/repair any failed coils, buswork, cryogenic lines or other in-cryostat components so that the plant may continue to operate.

Because the probability of a coil failure is judged to be low, no additional equipment and no specific buildings are provided to accommodate a replacement maintenance activity. However, the building design will not preclude the operation if it is necessary.

Ex-Vessel Maintenance

Ex-vessel equipment is located within the vacuum vessel port ducts or behind the 1.2 m thick cylindrical concrete inner pit shield wall. This equipment includes the ECH, ICRH, NBI, Pellet Injectors, vacuum pumps and diagnostics modules. Because each of these assemblies has different characteristics, each will be provided with unique maintenance scenarios based on standardized maintenance equipment.

The maintenance equipment will be mounted on an array of platforms designed to perform specific types of operations. The overhead bridge crane, floor-mounted vehicles and fixed platforms may be used.

Mockup and Testing Facility

A mockup and test stand facility is essential for the verification tests of remote handling scenarios and equipment from the beginning of the construction phase to the end of PCAST operations. The test stand for remote handling is planned to consist of two stages. The preliminary stage includes tests performed at other facilities during the construction phase; the final stage will involve tests and development in a dedicated on-site Remote Handling Facility building.

Floor-Mounted Systems

Moveable Casks

These are containment boxes, which are transported and attached to a maintenance enclosure before opening the vessel. The equipment necessary to open the port, carry out the replacement task and transfer components is located inside the contained transfer unit. Moveable casks used at the equatorial and divertor port level will not normally provide shielding.

2.3.4 In-Cryostat Maintenance Systems

Requirements

The TF and PF magnetic coils and an array of diagnostic and operating components located inside the cryostat will require maintenance during the life of the machine.

Functional Requirements

- Remote handling of the magnet system, which is composed of 16 TF coils, three pairs of PF coils and a CS coil assemby, is critical because of structural complexity as well as large size and weight (up to 780 tonnes).

- Remote tooling will be required to cut and reweld the vacuum vessel as part of the TF magnet work as well as during vacuum vessel repairs.

- Access by a dexterous manipulator system is required to operate special purpose repair tooling such as remote welders and cutters at the magnet connector junctions.

Design Requirements

- Entry into the cryostat for maintenance operations is gained after warming up to near ambient the coils and associated structures and venting of the cryostat. The conditions are therefore similar to the vessel except that the gamma radiation dose will be several orders of magnitude lower and be dependent upon the actual location within the cryostat.

Pressure	Ambient
Temperature	~ Ambient
Radiation	2 to 4 orders of magnitude lower than in-vessel depending on location [based on ITER estimates]
Magnetic Field	Zero

- Contained access into the Cryostat shall be provided for remote handling operations. For contamination reasons the number of openings through the cryostat during maintenance should be minimized.

Operational Requirements

- Remote handling equipment and tools for in-cryostat use must be composed of radiation hard components (motors, sensors, lubricants, cables, etc.), whose life times are adequate for at least 1000 hours (40 days) continuous operation. The target life time is at least an order of magnitude higher.

- The maintenance equipment will be capable of telerobotic control since most of the expected operations are one-of-a-kind. Each In-cryostat maintenance system will operate independently of each other and the Test Cell transport system.

- Remote handling equipment must be designed to be recovered or rescued in case of failure of the equipment and tools during maintenance. Rescue procedures shall be available for every RH procedure.

- Standardized transporters will be utilized to transfer removed magnet components to the Maintenance Cells and Storage Area. The magnet maintenance system will be able to load and unload the components from these containers.

- Personnel will have no access to the interior of the PCAST cryostat following startup of experimental operations.

Design Description

System Configuration
The Cryostat lid will be removed to provide access to the top sides of the magnetic coils. Access to the lower connections will be through hatches located near the bottom of the cryostat

Special platforms, called Maintenance Pods, will be used to position the manipulators, tooling, lights, cameras and other maintenance systems at established positions near the magnet connector locations. The platforms will be portable with dedicated umbilicals to provide for operation sindependent of other maintenance operations in the Test Cell.

Boom-mounted power arm manipulators will be used to support maintenance operations and inspection functions not addressed by the fixed Maintenance Pods

Maintenance Pods

The platforms will be placed by the overhead bridge crane on the upper side of the magnets.

The platforms will be place by floor mounted transporters on the lower side of the magnets.

Boom-Mounted Manipulators

The Boom Mounted Manipulator system will be the same as that used for Ex-vessel maintenance.

2.3.5 Viewing Systems

Viewing equipment is essential for frequent inspection of the first wall to detect failure of components and to judge the necessity of their repair or replacement..

Requirements

Functional

Requirements for in-vessel viewing equipment are summarized as follows.

- Viewing equipment is to be installed at horizontal maintenance ports
- Viewing equipment must inspect every high heat load area of the PFC's.
- Size (diameter) of the viewing equipment should be designed to minimize neutron streaming and heat loads from the plasma.
- Viewing equipment must be of a diameter sufficient to provide clear viewing information and sufficient stiffness to minimize the deflection and vibration.
- Viewing equipment must be compatible with cooling pipe layout and maint. port design.
- Viewing equipment must be installed behind a shield plug to minimize neutron streaming and heat loads from the plasma.
- Viewing equipment should be designed for its repair or replacement without breaking the vacuum vessel vacuum.
- Viewing or inspection operation will be carried out under vacuum to detect a possible failure of the first wall. Second stage inspection will be required based on the results.

Second Stage (Quantified Inspection)

- After breaking the vacuum of the vacuum vessel, detailed inspection operations such as measuring the surface roughness, erosion effects and the thickness of tiles of the first wall will be carried out by the in-vessel transporter and manipulator/tools. Requirement for repair or replacement of the failed components will be judged based on the results.

Design Requirements

- Routine in-vessel inspection shall be accomplished during non-burn periods under vacuum with the FW components at dwell temperature. The environmental conditions are as follows.

Pressure	UHV
Vent/purge gas	None
Temperature	~200°C
Radiation	~ 3 x 10^4 Gy/h (3x10^6 R/h)
Location/number of RH ports	Maintenance Ports
Magnetic Field	Zero

Operating Requirements

The deployment of the In-Vessel Inspection system must be accomplished within a few hours and a complete inspection campaign must be completed within one day.

The deployment of the Ex-Vessel Inspection system will be accomplished with deployment of the overhead bridge crane system.

Design Description

Two independent viewing systems will be provided for observation of the PCAST system during maintenance shutdowns. The in-vessel system will operate independently of the articulating boom system and will be mounted on dedicated drives which engage cameras and lights. Four viewing systems will be provided, one at each maintenance port. The ex-vessel viewing system will be mounted in a traditional arrangement on the maintenance system booms and manipulators.

2.3.6 Tooling

This section includes all tooling not credited to a component or maintenance subsystem. Generally this includes:

- Manipulators
- Small operating tools such as wrenches
- Pipe cutting and weld tools
- Inspection tools

Requirements

Functional Requirements

Functional requirements will be developed as part of the engineering design process.

Section 2.4: PCAST Machine Cryostat (D. Lang)

2.4.0 Introduction

The PCAST cryostat is a large ~ 20 meter diameter cylindrical vacuum vessel that provides the necessary thermal barrier between the ambient temperature test cell and the cryogenic temperature (80K or 30K) copper magnets. The overall concept is based on the TPX cryostat, a single wall vacuum vessel, and has an overall diameter that is approximately half of the PCAST cryostat diameter. The PCAST cryostat has an outside diameter (OD) that is 60% of the ITER cryostat OD. Due to the smaller size of the PCAST cryostat, a single wall vacuum vessel with reinforcing ribs can be used, rather than the more expensive double wall ITER cryostat. The top and bottom hemisherical heads provide the end closures for the single wall vacuum vessel. Electrical and mechanical penetration elements and attachments for the mechanical support of both the cold mass and the vacuum vessel are included within this WBS element. Specific functions for the cryostat system are to provide:

- the high vacuum barrier around the vacuum vessel and the surrounding cold mass,
- the interfacing hardware between the cryostat and all electrical and mechanical penetrations,
- thermal shielding consisting of the multi-layer insulation required for the cryostat walls and end caps and possibly conventional water cooling panels,
- the attachments to the cryostat for the structural support of the vacuum vessel and the cold mass,
- support of the tokamak components including the cryostat vessel, magnets, magnet structure and vacuum vessel

2.4.1 Performance Requirements

The cryostat design shall satisfy the following performance and operational requirements. Included are:

- design loading pressure the same as ITER, 1 atm external and 2 atm. internal

- base pressure < 10^{-5} torr (cryostat shell with all internals at ambient temperature), subject to a full vacuum pumping system analysis to be done during the preliminary design.
- leak Rate < $2x10^{-4}$ torr-l/s. (The leak rate for the cryostat shell only without internals will be determined during the preliminary design stage.)
- over pressure requirements of an estimated 10 psig (with attendant safety features).
- outgas rate TBD during the preliminary design.
- the cryostat vessel will function at an ambient operating temperature during its operational life.
- the cryostat will be designed to provide for disruptive loads
- the cryostat structure will be designed for and operated at ambient temperatures.
- All penetrations shall accommodate the differential thermal motion between the components and the cryostat.
- The cryostat thermal shields will limit the thermal radiation heat load to the cold mass, primarily the magnet system.

2.4.2 Configuration and Design Description

The cryostat system includes the cryostat vessel, the penetration attachments, attachments for the structural ties of the vacuum vessel and cold mass to the cryostat base structure, mechanical fasteners to attach the nuclear radiation shielding, pressure relief devices, any water cooled heat sinks required to maintain the cryostat vessel at ambient temperature during operation, and seismic restraints both internal and external to the cryostat shell.

Major elements of the cryostat system include:

- the cryostat vessel
- the cryostat penetration and structural attachments
- thermal shielding
- the cryostat support structure
- vacuum and fluid systems

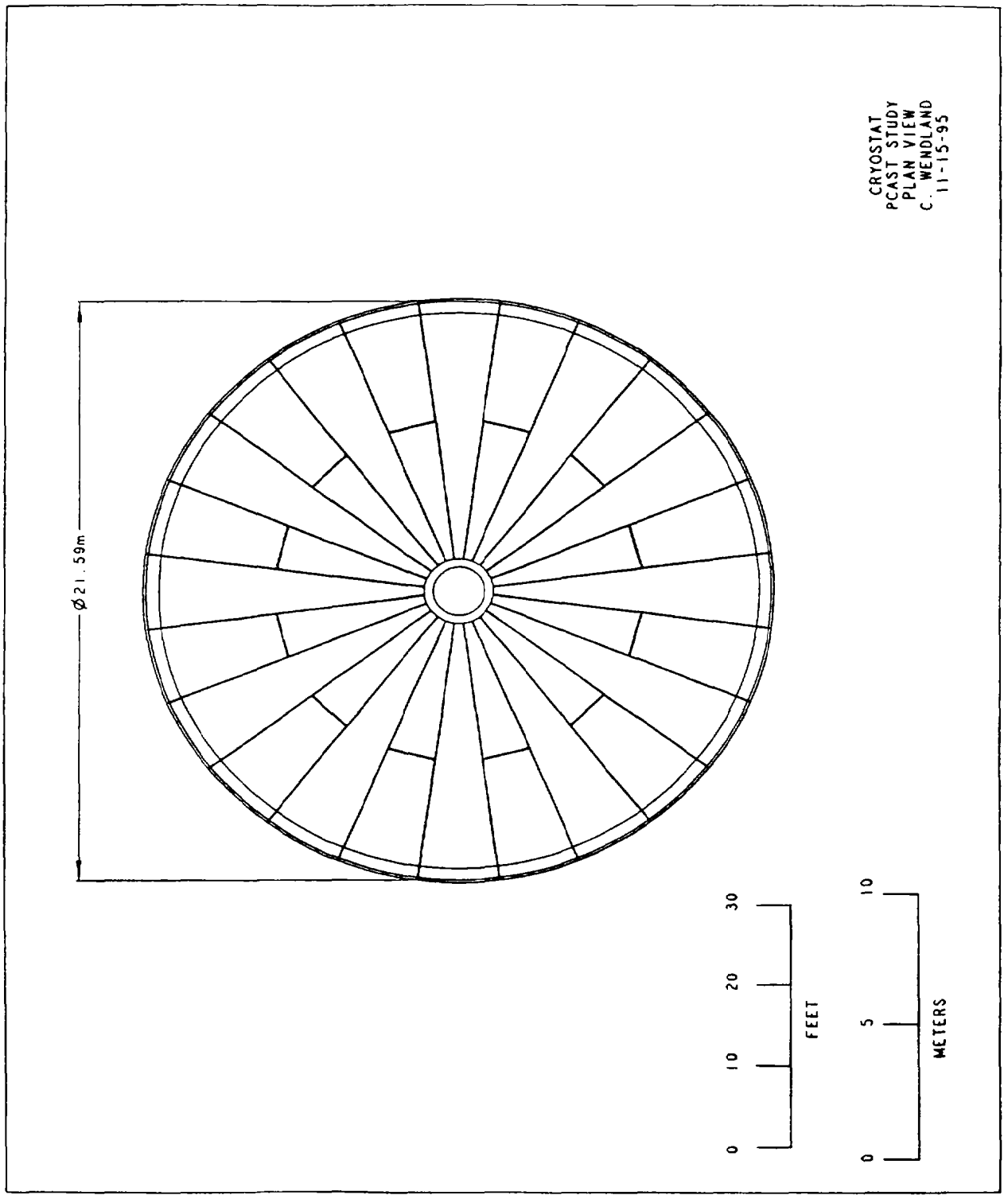

Figure 2.4.2-2 PCAST Cryostat Plan View

The nominal 20m diameter seals for the cryostat sections will use two concentric organic o-rings at each interface. The use of double seals will allow for vacuum leak testing each assembled (large) joint prior to the overall cryostat button-up. All other penetration seals for the cryostat will use single organic o-rings. Viton is the material of choice for o-ring materials. The expected cumulative nuclear radiation dosage for the organic materials in the cryostat system is on the order of TBD rads over the design life of the machine. All organic materials chosen for the cryostat system will have acceptable material properties at these dosage levels. Alternatives for the sealing between sections would be to use a welded lip seal, designed for multiple cutting and re-welding operations.

All loads will be transmitted through the cryostat base in to the cryostat support structure. The vacuum loads are the major determinant for sizing all of the cryostat vessel structures except for the base structure. In addition to the vacuum loads, seismic, gravitational and disruptive EM loads are reacted through and within the base structure.

2.4.2.2 Cryostat Penetrations and Structural Attachments

The bellows and flexible boot configurations described previously are specialty items that may require pre prototype fabrication, and test and evaluation. The largest penetration for the neutral beam injector ports is the most difficult. A glass reinforced silicon rubber flexible boot design concept is envisioned similar to what was proposed for TPX.

Other cryostat attachments include the following:

- internal and external seismic restraints.
- disruption restraints with dielectric interfaces.
- pressure relief devices.
- bearing plates for the vacuum vessel and cold mass support structures.
- optical windows and lighting will be used for visual inspection and monitoring the interior of the cryostat during the operational phase.
- interior walkways and ladders for personnel movement during installation and maintenance operations.

2.4.2.3 Cryostat Thermal Shields

Thermal shielding is used on the cryostat (300K) and on the vacuum vessel to limit the thermal radiation heat load into the cold mass (at 80K and 30K) and onto the cryogenic system. The cryostat thermal shields will cover all cryostat vessel components. The vacuum vessel thermal shield will cover the vacuum vessel and the nozzles that penetrate through the magnet systems until the vacuum vessel connects with the cryostat at the cryostat wall. The cryostat thermal shields will be composed of batts of Multi-Layer Insulation (MLI). MLI is made by alternating layers of reflective coating material and spacer material. The intent is to use 2 batts, each with 20 layers of aluminized mylar with separating spun material sheets. Only these passive radiation shields are currently planned, no actively cooled shields are required. The surface area of the cryostat is estimated at 1,965 square meters, and this value is used for the area of cryostat thermal shields. Thermal shielding for the cryostat system includes the following;

- Aluminized mylar multi-layer insulation including that located on the cryostat walls, located between the cryostat warm surfaces and the cold mass (magnets and magnet structure, as well as cryogenic piping inside the tokamak)
- ambient temperature water cooled sinks on the cryostat structure.

2.4.2.4 Cryostat Support Structure

The cryostat support structure consists eight stainless steel structures that support the tokamak from the experimental vault floor. These "H" shaped structures must support approximately 8,430 tonnes, the weight of the cryostat, magnets, vacuum vessel and magnet structure. These 8 structures are assumed to have 2 legs, each of which is a box beam approximately 1.25m square, with 2.5 cm thick walls. The weight of this structure is 160 tonnes.

2.4.2.5 Vacuum and Fluid Systems

Elements in this area include:

- requirements to others for cryogen's, inert gases, vacuum pumping, water cooling etc.

• the valves and tubulation associated with the above at the cryostat shell interface

Design Basis - Codes and Standards

ASME Boiler and Pressure Vessel Code

American Welding Society Standards

American Vacuum Society Standards

2.4.2.5 System Assembly, Installation, and Testing

The cryostat system design also has those features necessary to enable the following tests to be performed during the construction and or operational phase of the TPX machine, including:

- vacuum leak checking.
- vacuum outgas and rate of rise testing.
- pressure testing (only during the construction phase of the cryostat).
- resonant frequency test. (Optional test, with cold mass and vacuum chamber installed for confirmation of seismic and disruptive load resonant frequencies).
- heating tests (to determine the integrity of all installed thermal shielding materials).
- cool down tests (to determine the integrity of all installed thermal shielding materials; some of these tests will be done in conjunction with the heating tests).

2.4.3 System Facility Requirements

The cryostat system design will accommodate all dead, live, and environmental loads. The use of high permeability materials is not allowed (the relative permeability for all materials will be <1.02). Organic materials chosen for use in the cryostat system will be compatible with the integrated TBD dosage level.

The cryostat system will meet or exceed all performance and operational requirements over the design life of the facility.

Materials for the cryostat and structure are 304 stainless steel

2.4.4 Cost Estimate and Costing Methodology

The cryostat is costed on a $/kg basis, it has been estimated to have the following weights:

Cryostat System Weights

Cryostat Section	Weight
Shell with ribs	800 tonnes
Ports and flanges	120 tonnes
Structural attachments	160 tonnes
Support structure	160 tonnes
Total Weight	**1,240 tonnes**

Section 2.5: Heating and Cooling System (D. Kungl)

This section describes the PCAST heating and cooling requirements, it covers the scope equivalent to ITER WBS elements 2.6, 3.3, 3.5, and 3.6.

The PCAST Heating and Cooling System supports the following loads:

A) TF and PF Magnet Refrigerator Cooling
B) Plasma Facing Components Heating and Cooling
C) Hardware Bakeout
D) Vacuum Vessel Heating and Cooling
E) Auxiliary Systems Cooling including:
    NINB including Power Supplies
    ICH including Power Supplies
    Diagnostics
    Vacuum Pumping
F) Motor Generator Sets
G) Power Conversion Equipment
H) Balance of Plant
I) FPPC Coils

Descriptions include loads and special conditions such as water chemistry by subsystem. The PCAST Heating and Cooling System includes the following subsystems:

1) 50°C - 1 M-Ohm Subsystem
2) 350°C Bakeout Subsystem
3) 35°C Tower Water Subsystem
4) 27°C - 1 M-Ohm Subsystem
5) H&C Subsystem Utilities

Hardware is grouped by common heating and/or cooling requirements. It is assumed that the vacuum vessel and all in-vessel hardware will be at 50°C at plasma initiation.

The method used to arrive at a system description and a cost estimate is to:

1) obtain the heating and cooling requirements for the PCAST Machine,

2) calculate the major system and hardware parameters to meet the PCAST heating and cooling requirements,

3) use the recent TPX Heating and Cooling subsystem hardware designs and cost estimates compared to the PCAST designs and scale the PCAST cost estimate. Since PPPL site available hardware was included as credit for the TPX estimate that type hardware cost is added over and above the PCAST estimate scaled from TPX.

The PCAST experiments are anticipated to be ~120 seconds in pulse length with a repetition rate of 5 pulses per 24 hours or one pulse every 4.8 hours. The noted pulse length and repetition rate are the basis for the calculations made to determine the parameters of PCAST heating and cooling system hardware. For systems such as the magnets that are required to be energized longer than 120 seconds, the longer pulse length has been used.

The PCAST cost estimate for this hardware utilized the recent cost estimate made for the TPX Heating and Cooling System. Respective PCAST subsystem heating and/or cooling requirements are compared to the appropriate TPX subsystem and the heating or cooling load, flow, storage versus steady capacity and chemistry parameters were compared. PCAST costs were then determined by scaling.

PCAST Estimate by H&C Subsystems

The PCAST H&C System includes 5 subsystems. Four subsystems provide heating and cooling to the PCAST loads while the 5th supplies utilities for the other 4 subsystems. The subsystems are described below.

1) 50°C 1 M-Ohm Subsystem: This subsystem will provide heating and/or cooling for the Vacuum Vessel, PFC's and the Fast Plasma Position

Control (FPPC) Coils. The 50°C water will be sufficient in quantity to bring the VV, PFC's and FPPC Coils to 50°C for experiment initiation. The VV cooling water will see an outlet temperature of 100°C (50°C rise). The Vacuum Vessel requires the storage of 75,000 gallons of 50°C water for each pulse. The total water through the FPPC Coils during the pulse is 435 gallons and will be provided as a once-through coolant as will all water in this subsystem. The PFC's require a flow of 37,500 GPM for 3 minutes or 115×10^3 gallons.

2) 350°C Bakeout Subsystem: The 350°C argon Bakeout Subsystem is a scale-up of the TPX Bakeout Subsystem. The basic PCAST bakeout subsystem will consist of electric heaters, blowers, argon gas supply tanks, a tank for holding compressed argon gas and a compressor. The ratio of PCAST mass to be baked out to the TPX mass to be baked out is 1606 Tons/79 Tons or a factor of 20. The TPX estimates were scaled by this factor.

3) 35°C Tower Water Subsystem: This system provides cooling for the LN2 and Helium Refrigeration Plants, the 4 Motor Generator sets and the Balance of Plant (plant utilities). A set of cooling towers provide 35°C cooling water. The refrigeration plant cooling will be provided by 2 cooling towers while a 3rd tower will provide cooling for the 4 motor generators and the balance of plant loads. The refrigerator plant and balance of plant are steady state loads and the 4 MG's are also assumed as steady state loads for this estimate.

4) 27°C Chilled Water 1 M-Ohm & 17 M-Ohm Subsystem: The 27°C Chilled Water Subsystem will provide 1 M-Ohm and 17 M-Ohm cooling water to the NINB, ICH, Diagnostics, Vacuum Pumping and Power Conversion Equipment. The larger loads in this subsystem are the NINB, ICH and Power Conversion Equipment, which are 94% of the load, while the Diagnostics and Vacuum Pumping are only 6%. The provision of 27°C cooling water will require 120 Tons of chiller capacity and the storage of 30×10^3 gallons of cooled water to be used during the pulse.

5) Heating and Cooling System Utilities Subsystem: The Heating and Cooling System subsystems require utilities to setup, maintain and operate the subsystems as specified. The Utilities Subsystem includes all of the equipment required to provide this capability. The parts of this subsystem

are makeup water (including deionizing equipment), argon gas blanket and drainage including quench and drain tanks. These utilities on TPX, with the exception of the quench and drain tanks, are estimated at 15.3% of the other subsystem's estimated cost. The quench and drain tanks were sized to accommodate the water volume of the 50°C 1-Meg-Ohm system (200,000 gallons) and an allowance was made for associated pumps and piping. Not included in the TPX design is a filter vent system. The filter vent system has been scaled to the building sizes, a factor of 0.67 was applied to the ITER cost estimate for this system.

Table 2.5-1 below compares parameters of the ITER and PCAST machines that affect the scale of the equipment required to provide the heating and cooling function.

Table 2.5-2 summarizes the loads on the PCAST H&C subsystems.

Table 2.5-1 PCAST/ITER PARAMETER COMPARISONS

DESCRIPTION	ITER	PCAST	ITER/PCAST
Fusion Power/Pulse	1500MW	400MW	3.75
Pulse Length	≥1000s	120s	8.33
Rep Rate	2000s	17280s	8.64
Input Energy/Pulse	9600 GJ	1260 GJ	7.62
Cycle Time	2000s	420s	4.76
Pulses/Day	12	5	2.4
Operating Time/Day	24000s	2100s	11.42
Aux Syst Oper Pwr	210MW	160MW	1.32
Aux Syst Energy	7584GJ	8597GJ	0.88
Fusion Energy/Day	18000GJ	240GJ	75

TABLE 2.5-2

		PCAST HEATING AND COOLING SYSTEM PARAMETERS					
H&C SUBSYSTEM	LOAD DESCRIPT	LOAD MW	LOAD BTUX10^6	PULSE WIDTH (SEC)	FLOW RATE (GPM)	KGAL H2O STORED	ITER WBS
1) 50°C-1 MEG OHM	VAC VESS	320	40	180	24,400	75	2.6
	FPPC COILS	4	1	180	193	1	PRIMARY
	PFC"S	100	17	180	37,500	115	
2) 350°C BAKEOUT	VAC VESS INTRNL CMP	1,606 TONS		SIMILIAR TO TPX PROFILE			ITER B/O INCL IN WBS 2.6
3) 35°C - COOLING TOWER	MAG REFRIG	80		STEADY STATE	27,527		3.5
	BAL PLANT	20		STEADY STATE	6,900		HEAT SINKS
	MG SETS	14		STEADY STATE	4,800		
4) 27°C- CHILLED WATER	NINB			135			3.3
	ICH			135			SECONDARY
	DIAG	51	7	135	13,300	30	
	VAC PMP'G			STEADY STATE			
	PWR CONV			180			
5) H&C UTILITIES	SERVE ABOVE SYSTEMS	• MAKEUP WATER, GAS BLNKT, DRAINAGE SYSTEMS ESTIMATED AT 15.3% OF THE OTHER SUBSYSTEMS					3.6 CVCS

Section 3.1 Vacuum Pumping Systems (K. St. Onge)

3.1.1 Vacuum Pumping Requirements

General Requirements

The vacuum pumping systems shall provide vacuum services for torus evacuation, cryostat evacuation, divertor pumping, and glow discharge cleaning. The vacuum pumping systems shall provide vacuum pumping ducts to connect the torus to the vacuum pumps and to the gas handling and detritiation systems. The vacuum pumping systems shall provide roughing and foreline pumping services to the neutral beam systems, RF heating systems, pellet fueling systems, and diagnostic systems. The vacuum pumping systems shall provide instrumentation to assist in the detection of leaks in the primary vacuum system boundary.

Divertor Pumping Speed

The total volumetric pumping speed at the divertor plena shall not be less than 50 m3/s for tritium deuteride (DT, mass 5) at 50 C and 2 mTorr.

Divertor Pumping Throughput

The vacuum pumping systems shall be able to accommodate a divertor throughput of 100 Torr-l/s of tritium deuteride (DT, mass 5) and 2 Torr-l/sof helium at 50 C and a total pressure of 2 mTorr when operating on the standard schedule of 145 s shots on 180 minute intervals.

Control of Divertor Pumping Speed and Throughput

The vacuum pumping systems shall provide a means of adjusting the divertor pumping pressure-throughput curve by altering the conductance and/or the volumetric pumping speed of the divertor pumping system. This feature shall, at a minimum, provide the capability to operate with constant throughput

while the pressure in the divertor plena is varied throughout the range from 2 mTorr to 10 mTorr.

Torus Base Pressures

The torus base pressure for species with Z > 2 shall not be greater than 10-9 Torr. The torus base pressure for other species shall not be greater than 10-7 Torr. Reference gas loads are TBD.

Torus Surface Conditioning

The vacuum pumping systems shall be capable of indefinitely supporting torus glow discharge cleaning with hydrogen, deuterium, helium, or a mixture of helium and oxygen at a temperature of 350 C and at pressures of 10 to 20 mTorr. The total volumetric pumping speed at the divertor plena during glow discharge cleaning shall not be less than TBD m3/s for helium at 350 C and 10 mTorr.

Leak Detection Systems

The vacuum pumping systems shall provide a means of detecting leaks in the primary vacuum boundary. The sensitivity threshold shall not be greater than 10-9 Torr-l/s.

Neutral Beam Vacuum Services

The vacuum pumping systems shall provide vacuum pumping services for the neutral beam systems. At this writing the specific requirements for both PCAST and ITER are TBD, so this report scales the neutral beam pumping parameters from TFTR.

RF Heating Vacuum Services

The vacuum pumping systems shall provide roughing and foreline pumping for the RF heating systems. The specific requirements are TBD, but the pumping speed and throughput are expected to be low enough that RF

vacuum pumping will not require a dedicated pumping system. Ergo this report treats RF pumping as one of the diagnostic systems.

Pellet Fueling Systems Vacuum Services

The vacuum pumping systems shall provide roughing and foreline pumping for the pellet fueling systems. The specific requirements are TBD, depending on whether a pneumatic injector is needed in addition to the centrifugal injectors. Although pellet fueling system vacuum pumping is expected to require dedicated roughing and backing pumps that will probably be in the scope of the vacuum pumping systems, this report includes their description and cost estimate in the section on pellet fueling. Refer to that section for information on pellet fueling vacuum pumping.

Diagnostics Systems Vacuum Services

The vacuum pumping systems shall provide roughing and foreline pumping for miscellaneous diagnostic systems. Specific requirements for each system are TBD, but only one -- the neutral beam diagnostic -- is expected to have requirements that will have a significant impact on the vacuum pumping system. This report assumes that the neutral beam diagnostic will have pumping requirements similar to that of a IFTR neutral beam.

Cryostat Vacuum Services

The vacuum pumping systems shall provide vacuum pumping services for the cryostat. The specific requirements are TBD, so this report scales the ITER cryostat pumping requirements.

3.1.2 System Description

Torus and Divertor Vacuum Pumping

The torus vacuum pumps will be located outside the biological shield in order to facilitate hands-on maintenance. A set of sixteen nominally radial

vacuum pumping ducts -- eight equally spaced at the top of the machine and eight equally spaced at the bottom of the machine -- will connect the torus and the divertor plena to an array of turbomolecular pumps that will be used for torus evacuation, divertor pumping, and glow discharge cleaning. The torus will be pumped through the divertors. There will be three large turbopumps at the end of each duct; each pump will have a volumetric speed of 5 m3/s for nitrogen at 300 K and 1 mTorr. The total volumetric pumping speed at the divertor plena will be 50+ m3/s for tritium deuteride (DT, mass 5) at 50 C and 2 mTorr, resulting in a divertor throughput capability of 100+ Torr-l/s at 2 mTorr for indefinite periods. A throttling gate valve will be installed at the inlet to each of the high speed turbopumps; the valves will be used to control pumping speed and to isolate the torus.

At each of the sixteen pumping stations there will be a smaller turbomolecular pump with a volumetric speed of approximately 0.2 m3/s. This pump will be used to forepump the larger turbopumps during torus baking and evacuation, thus dramatically increasing the compression ratio for the lightgases. This small turbopump will not be used for divertor pumping and discharge cleaning operations; a valve and bypass line will permit directing the exhaust from the larger turbopumps around this pump and straight to the roughing and backing system.

Since all of the torus turbomolecular pumps can be used simultaneously, the torus pumping system will be extraordinarily tolerant of leaks and outgassing. The conductance from the torus through the divertors is TBD, but with a total speed at the divertor plena of 50+ m3/s for mass 5 at 50 C, the speed at the torus volume is expected to be 30+ m3/s, so the system could theoretically reach a partial pressure of 10-7 Torr with a light gas load as large as 3 mTorr-l/s. The system will be correspondingly tolerant of impurity gas loads.

There are no completely sealed and dry high speed turbomolecular pumps available at this time, so the 5 m3/s torus pumps described in this report will suffer tritium contamination of the bearing oil. Nevertheless, the advantages of continuous high speed pumping without accumulating a significant tritium inventory seem to outweigh the liability of the contaminated oil. Techniques for contaminated oil replacement and disposal have been developed for existing

tokamaks. The smaller second stage turbomolecular pumps are currently available as sealed and dry units.

Torus Vacuum Pumping Ducts

The vacuum pumping ducts will be single-walled from the torus to the cryostat wall. From that point outward it is assumed that all ducts will be double-walled to provide a redundant tritium containment barrier. There is no plan at present to install a redundant containment boundary around individual vacuum pumps.

Torus Roughing and Backing Pumping

This report assumes that a three-stage array of dry sealed scroll pumps will be used for roughing and forepumping. There is not much data on scroll pumping performance with the light gases, and the data that is available seems to show that the pumping speed drops precipitously in the low viscous regime. If the data is correct, scroll pumps would be unable to provide the required pumping speed, and roots pumps or some other type of low viscous pumps will be used in their place. Since dry sealed scroll pumps are relatively expensive, the assumption regarding the use of scroll pumps produces a conservative construction cost estimate.

Three first stage pumps will be used. Each pump will have a nominal volumetric pumping speed of 0.36 m3/s. These pumps will be backed by two second stage pumps; each of the second stage pumps will have a speed of 0.17 m3/s. The second stage pumps will be backed by two third stage pumps that have a speed of .017 m3/s per pump. All of the scroll pumps will be completely sealed and dry.

Cryostat Vacuum Pumping

This report assumes that the cryostat pumping system will be completely conventional except that the effluent will be monitored for tritium contamination and will be directed to the gas cleanup system if contamination is found. The concept described here is based on an arbitrary requirement to pump the

cryostat from 760 Torr to 10-5 Torr in 48 hrs (ITER is 100 hrs). Like the torus pumps, the cryostat vacuum pumps will be located outside the biological shield in order to facilitate hands-on maintenance. Cryostat pumping ducts will be installed to connect the pumps to the cryostat. At the pumping station there will be six 5 m3/s pumps like those used on the torus pumping system. A smaller turbomolecular pump with a volumetric speed of approximately 0.2 m3/s will be used to forepump the larger turbopumps, thus increasing the compression ratio for the light gases. The high vacuum pumps will be backed by two 3 m3/s roots pumps andtwo 0.6 m3/s rotary mechanical pumps.

Neutral Beam Pumping

This report scales the neutral beam pumping requirements from TFTR. Each TFTR neutral beam enclosure has a volume of about 50 m3, and the estimated volume of a beam enclosure is 100 m3, so the pumping on each beam is scaled up from TFTR by a factor of approximately two. Thus each enclosure will probably require about 10 m3/s of turbomolecular pumping.

Like the torus pumps, the neutral beam vacuum pumps will be located outside the biological shield in order to facilitate hands-on maintenance. Neutral beam pumping ducts will be installed to connect the pumps to the beam enclosures and to the beam cryopumping modules. High vacuum pumping will be provided by two 5 m3/s pumps like those used on the torus pumping system. At each of the beam pumping stations there will be a smaller turbomolecular pump with a volumetric speed of approximately 0.2 m3/s. This pump will be used to forepump the larger turbopumps, thus increasing the compression ratio for the light gases.

This report assumes that a three-stage array of dry sealed scroll pumps will be used in the neutral beam roughing and backing system, but roots pumps or some other type of low viscous regime pumps might be required for the reason discussed in Section 3.1.2.3. The original TFTR neutral beam roughing pump skid had about 1.6 m3/s of low viscous (roots) pumping speed; scaling up by a factor of two would mean that PCAST could require about 3.2 m3/s, but this speed would require the installation of nine 0.36 m3/s scroll pumps, which seems excessive and would be expensive. Therefore, this report assumes that first-

stage roughing and backing will be performed by three 0.36 m3/s scroll pumps, which should be sufficient to allow regeneration between shots on 180 minute intervals. Second- and third-stage roughing and backing pumping will be respectively performed by two 0.17 m3/s pumps and two 0.017 m3/s pumps.

RF Systems Pumping

Refer to **Diagnostics Systems Pumping**

Diagnostic Systems Pumping

Diagnostic systems roughing and foreline pumping will be provided via one or two vacuum manifolds at TBD locations around the PCAST machine. Vacuum Pumping Systems will provide a high vacuum isolation valve -- installed at the manifold -- for each diagnostic system that requires pumping. The diagnostic systems will supply their own high vacuum pumps (preferably oil-free turbomolecular pumps) and their own roughing and forepumping lines to connect to the manifold. This report assumes that the manifold pumping will be done with the torus roughing and backing system.

The exception to this approach is the neutral beam diagnostic, which has TBD requirements at this writing. Therefore, this report assumes that the pumping requirements are similar to those of a TFTR neutral beam injector and that pumping will be performed with the PCAST Neutral Beam Pumping System.

Leak Detection Systems

This area has not been investigated as part of this study, so this report assumes that leak detection is similar to ITER but is significantly smaller -- approximately 50% -- in scale.

Section 3.2: Tritium Plant (B. Nelson and K. St. Onge)

3.2.1 Functions and Design Requirements

The Tritium Plant for PCAST is envisioned to have very similiar functional requirements to those considered for ITER (Ref. ITER DDD, WBS 3.2 Tritium Plant, and ITER DDD, WBS 1.8 Fueling), except on a somewhat smaller scale. It consists of systems and equipment to:

- supply deuterium and tritium mixtures for torus fueling,
- process the plasma exhaust streams to recover tritium and deuterium
- detritiate cooling water
- reduce tritium in air, gases, and liquids that are discharged to the environment

These functions are distributed among several sub-systems as follows:

Tokamak Exhaust Processing

This system separates deuterium and tritium from the torus exhaust for direct recycle to the torus, for enrichment, or for storage. This system further detritiates the exhaust stream to levels that permit venting to the atmosphere. Typical parameters of interest are shown for ITER and PCAST in Table 1.

Table 3.2-1. ITER and PCAST fueling and tritium handling parameters

Quantity	Unit	ITER	PCAST
Maximum Burn Duration	seconds	1,000	120
Maximum torus fueling rate	Pa-liter/sec	100,000	~10,000
Cycle time between shots	seconds	1,200	~17,000
Maximum average exhaust rate during burn	Pa-liter/sec	1×10^5	$\sim 1 \times 10^4$
Fraction of HDT recycled directly to torus after removal of non-hydrogen impurities,	%	>60 to 100	0 to 100

HDT Isotope Separation

This system separates the hydrogen isotopes to produce deuterium and tritium mixtures for feeding the fueling system and produces an HD stream for release to the atmosphere. The tritium content of the released stream is $<10^{-6}$mol %.

Fuel Storage and Delivery

This system stores deuterium and tritium until required by the fueling system.

Water Detritiation

This system detritiates cooling water to levels that are acceptable for operating personnel and detritiates waste water to levels suitable for release to the environment. The maximum tritium content in the effluent is limited to 1 microCurie/kG (37 Mbq/kg).

Atmosphere Detritiation

This system removes tritium from air that is to be discharged to the environment during normal operation, maintenance, and accidental conditions within ALARA objectives. Detritiation will be provided for all areas normally contaminated with tritium, such as gloveboxes and hot cells, as well as areas where release of tritium is possible during an accident.

Analytical Facilities

These facilities provide the necessary instrumentation to assay the gas and liquid streams for process control.

Control Systems

These systems provide monitoring and controls to keep process operations within operating and safety limits.

General safety considerations

The PCAST tritium system will be designed similiar to the ITER tritium system from the safety standpoint. All tritium containing systems will have confinement/containment barriers consistent with the quantities of tritium contained. Where required, secondary and tertiary confinement will be used. The systems will be segmented to keep the releasable inventory in any one loop within acceptable limits.

3.2.2 Design Description

The PCAST tritium plant would be very similiar to the ITER tritium plant (Ref. ITER DDD, WBS 3.2 Tritium Plant). The main features of the various systems are as follows:

Tokamak Exhaust Processing

The Tokamak Exhaust Processing system processes plasma exhaust or glow discharge cleaning (GDC) exhaust to recover hydrogen mixtures for recycle directly back to the fueling system, for isotopic enrichment, or for storage until required for fueling. Hydrogen isotopes are separated from impurities by permeation through a palladium/silver alloy membrane. Two permeator stages are used. The impurity stream then passes through another process, such as a permeator membrane reactor (PMR), to remove the rest of the tritium. Buffer tanks are used to keep the flowrate relatively constant, regardless of the operating state of the tokamak.

Isotope Separation System

The Isotope Separation System (ISS) uses cryogenic distillation of the HDT gas mixture to separate individual isotopes from streams. These streams include those from the plasma exhaust, impurity processing, NBI gas source, and water detritiation.

Fuel Storage and Delivery

The Hydrogen Storage and Distribution System provides for storage and distribution of the DT working inventory during processing and when operations and systems are shut down and for the unloading, storage, and transfer of all tritium received from offsite when needed for fueling.

The systems consists of multiple uranium beds, each of which is connected to the two stage permeator, the ISS and the fueling system. Tanks are used to premix and store gases in the ratios required by the various components of the fueling system (centrifugal injectors, pnuematic injectors, or gas puffing).

Water Detritiation

Two processes are envisioned for water detritiation, the water distillation (WD) process and the vapor phase catalytic exchange (VPCE). The VPCE operates at high concentrations, while the WD process operates over a wide range of tritium content, down to the level that can be released to the environment. The throughput of the water detritiation plant for ITER is estimated to be 120 kg/h, while the PCAST plant would be perhaps 10% of this capacity, or ~10 kg/h.

Atmosphere Detritiation

The atmosphere detritiation system comprises several units with specific functions. These include the emergency atmosphere detritiation system (ADS), the vent detritiation system (VDS), the plasma chamber maintenance detritiation system, the hot cell ADS, the heat transport vault dryer and the secondary confinement detritiation system. Each unit consist of a combination of catalytic oxidation and molecular sieve beds. At least two sets of beds will be required to provide continuous operation. The capacities of the various subsystems for ITER and PCAST are shown in Table 2.

Table 2 Atmosphere Detritiation System capacities

System	ITER capacity (m^3/h)	PCAST capacity (m^3/h)
Emergency atmosphere detritiation system	3500	~1000
Vent detritiation system	500	~100
Plasma chamber maintenance	3500	~1000
Hot cell dedicated ADS	-	
Heat transport vault dryer	500 *	~100
Secondary confinement detritiation system	50 for each	same

* +200 m^3/h for separate VDS

Analytical Facilities

Instrumentation is provided to determine the composition of process streams and the contents of storage vessels. For ITER, the gas composition will be measured using mass spectrometry, gas chromatography, or Raman laser analysis. Calorimeters will be used to find the tritium content of storage beds.

3.2.3 Issues

The technology associated with handling tritium has been developed through fusion R&D projects such as the TSTA and in conjunction with other programs. The primary unknown associated with the PCAST tritium plant is the total amount of tritium that can be contained in the system, which is site specific and determines the need for direct recycling, the real-time throughput, and the accuracy of the tritium accounting system.

Section 3.4: Cryogenics System

(D. Lang, B. Felker and D. Slack)

Contents:

3.4.0 Introduction

The PCAST device study proposes to use cryogenically cooled copper magnets operating at higher fields than ITER to reduce the overall size of a long pulse burning plasma device. The experimental pulse is shorter than ITER's (100-200 seconds vs. 1000-2000 seconds), and therefore can be accomplished using the cryogenically cooled copper magnets. The cryogenic system supplies the refrigeration required to initially cool for a plasma pulse, and then recool the magnets between pulses. The cryogenic system lowers the magnets to 80K for the toroidal field (TF) coils and for the poloidal field (PF) coils, PF2-7 U&L, and to 30K for the PF1 U&L coils. The cryogenics plant includes both nitrogen and helium systems, and will include a warm helium gas storage system, purification systems, compressors, refrigerators, distribution systems and high-pressure helium primary cooling loops.

One of the dominant engineering considerations for cryogenically cooled copper coils of this scale, is the size of the refrigerators. The largest modules currently produced in industry for air liquefaction plants are of 500 ton per day (1 MW of refrigeration at 80K) capacity, and would probably be paralleled to achieve the PCAST needed 8.2 MW (refrigeration at 80K) capacity for re-liquefaction of nitrogen. The PCAST Machine requirement would be equivalent to a plant which would produce 4,100 tonnes per day of liquid nitrogen, and would be approximately two and a half times larger than the largest currently operating US plant.

Operation of a plant of this scale would be of major concern if the cryogenic gasses boiled off during the pulse were released rather than being re-liquefied. With the cooling strategy we have selected, the cryogenic fluid is used only for pre-cooling and not for active heat removal during the pulse; the nitrogen gas can therefore be continuously re-liquefied. Environmental and safety impacts are substantially reduced, as re-liquefying the gas is a much more benign process, and large volumes of cryogenic liquid do not have to be transported or stored.

3.4.1 Performance Requirements

The primary requirement is to refrigerate the coils to 80K for the TF coils and the PF2-7 U&L coils and 30K for the PF1U&L coils. This includes the initial cooldown as well as the heat removal between shots. The largest heat load is by far the ohmic heating that occurs when the copper magnets are energized. The total amount of energy on a per pulse basis is shown in

Table 3.4.1-1. Radiation and conduction heat loads, pumping losses, and similar heat losses are accounted for in the other heat loads (+30% value). The plan is to take 5 shots per day. For the purposes of this report we have assumed that the shots would be evenly spread over a 24 hour day. If the shots are taken over a shorter period, the refrigeration requirements will increase. The ability to have a storage capacity to store refrigeration is limited due to the very low specific heat at these temperatures.

Table 3.4.1-1 PCAST Baseline Cryogenic Heat Loads Per Pulse

Source	**80K Load**	**30K Load**
Ohmic Heating Loads:		
TF coils	76.7 GJ	NA
PF 1 U&L coils	7.0 GJ	1.0 GJ
PF 2-7 U&L coils	16 GJ	NA
Subtotal	**99.7 GJ**	**1.0 GJ**
Other loads:		
Pumping losses, Rad, etc.	30 GJ	0.3 GJ
Total	**129.7 GJ**	**1.3 GJ**

Table 3.4.1-2 PCAST Primary Cooling Loop Requirements

Description	**80K Primary Loop**	**30K Primary Loop**
Supply Pressure	5 atm	5 atm
Return Pressure	4 atm	4 atm
Flow Rate Maximum	34 kg/s of helium	7.4 kg/s of helium
Supply Temperature	80 K	30 K
Return Temperature	80 to 244 K	30 to 216 K

3.4.2 Configuration and Plant Design Description

80 K Nitrogen System

The primary purpose of the nitrogen system is to cool the coils from 300K to 80K. In addition the nitrogen system will provide liquid nitrogen to the helium system. The nitrogen system is shown in Figure 3.4.2-1 The system consists of a LN plant (a reliquifier) and a helium gas primary cooling loop. The nitrogen system is primarily a reliquifier, that will be initially filled using trucked in nitrogen. The heat is removed from the coils by the primary helium gas cooling loop. This loop is then cooled by the heat exchanger in the liquid nitrogen dewar. The heat is absorbed by the vaporization of the liquid nitrogen, and then the cold vapor is returned to the reliquifier. The nitrogen system will provide a thermal barrier or heat sink for components in the PCAST Machine. For the helium system it will limit the heat input to the cold box, storage dewars, and vacuum jacketed lines. For the cold box, the nitrogen will provide an auxiliary stage of precooling that occurs before the first helium expansion turbine.

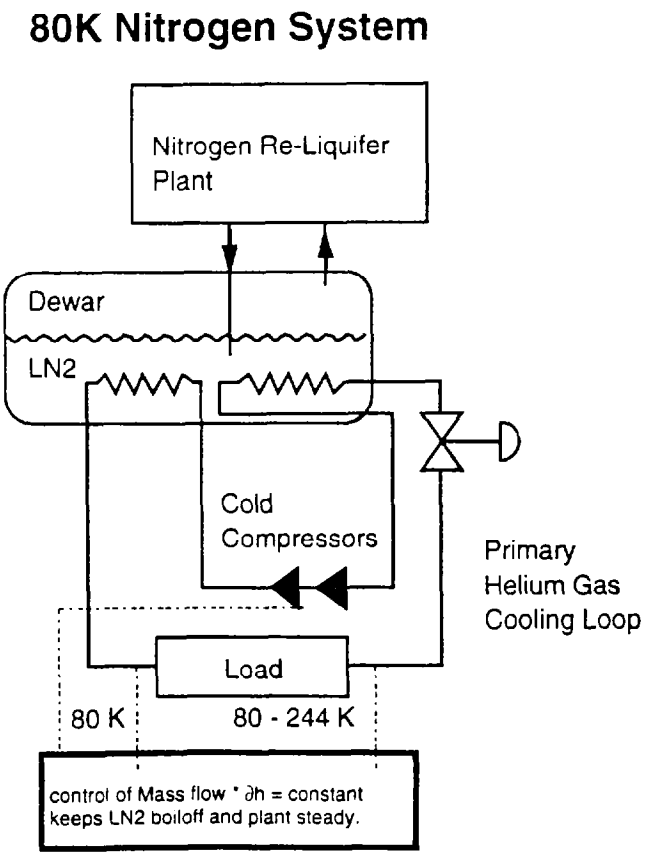

Figure 3.4.2-1 Nitrogen System Schematic

Liquid Nitrogen Storage

Limited liquid nitrogen storage will be required as the heat load is rejected to the re-liquifier. The heat exchanger dewar will provide the primary liquid nitrogen storage.

Liquid Nitrogen Controls I /C

Controls will allow for local subsystem control and subsystem optimization outside of the Central I&C. Once in an operational ready mode the cryogenics controls will be driven from a Centralized Control System. Fully automatic operation with interlocks to the Facility and Personnel Safety Systems will be possible from local or Central I&C.

Liquid Nitrogen Distribution

The distribution system will consist of the main supply, return, vent, auxiliary supply, ambient helium lines and cryogenic operational control valves. The main supply and return lines will be vacuum jacketed lines allowing for cooling or warming. Vent lines will be appropriately placed along the distribution system.

Helium System

There are two separate primary helium cooling loops. The first loop is used to cool the TF coils and PF coils 2 through 7. These coils are cooled to 80°K prior to each shot. The maximum temperature reached by any of the coils on this loop is 244°K in the TF coils. This cooling loop is cooled by a heat exchanger in the liquid nitrogen system. See Figure 3.4.2-1. The mass flow rate of this loop is controlled so that the product of mass flow and enthalpy change is constant and therefore provide a constant heat load to the system.

The second primary cooling loop is for PF 1 which is cooled to 30°K before each shot and reaches a maximum temperature of 216°K during the shot. The direct cooling of this coil is provided by a high pressure, primary

cooling loop driven by cold pumps. The cooling from 300K to 85K of this primary cooling loop is provided by the liquid nitrogen system, via a heat exchanger in a LN dewar, with LN supplied from the nitrogen system. For cooling from 85K to 30K this primary cooling loop is cooled by a heat exchanger that is supplied with helium at 30K directly from the helium refrigerator, and the liquid nitrogen dewar is valved out. The heat load into the helium system is held constant by regulating the mass flow in the high pressure cooling loop in accordance with the difference in temperature seen at the inlet and outlet of the heat exchanger. Large helium refrigerators require relatively constant heat loads, as it takes a long time for the overall system to come into proper flow balance, between the various heat exchangers and expansion turbines. The helium system is shown in Figure 3.4.2-2

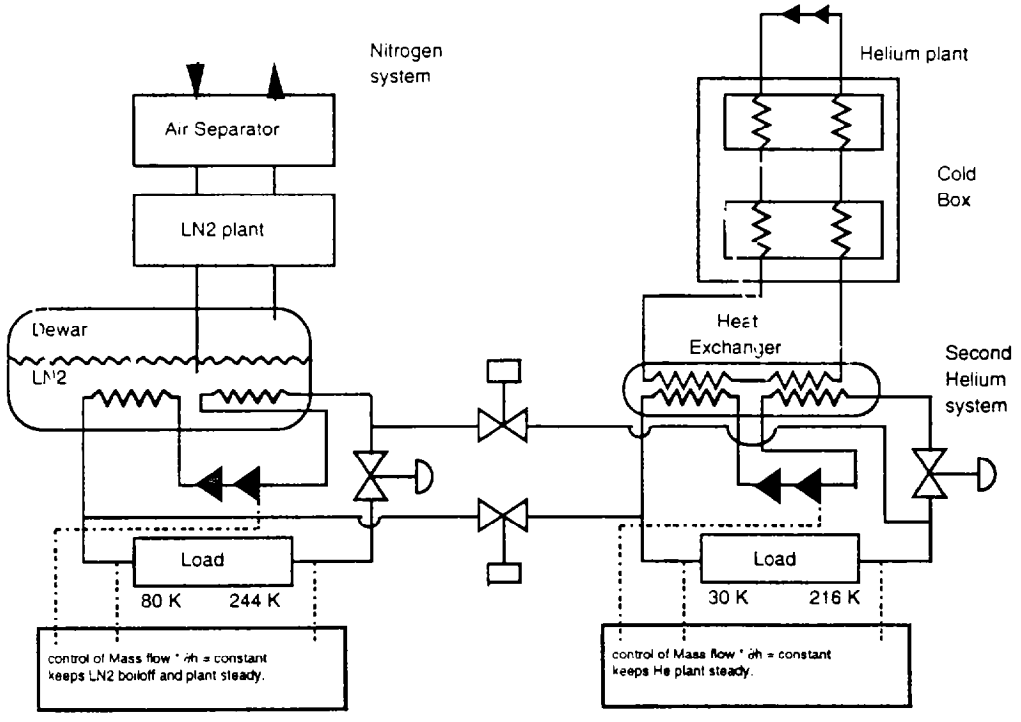

Figure 3.4.2-2 Cryogenics System

Table 3.4.2-1 Baseline Cryogenic System

	Baseline System	
	NITROGEN SYSTEM, Refrigeration from 300K to 80K	HELIUM SYSTEM, Refrigeration from 85 K to 30 K
Description	80K TF & PF2-7	30K PF1
	(adiabatic heat absorption)	
	Heat Load, GJ	Heat Load, GJ
TF (Note 1)	85	
PF 1 U/L (note 2)	7	1.1
PF 2-7 U/L (note 2)	17	
Total per pulse	109	1.1
Total 5 pulses/day	545	5.5
[Mega-Watts refrig.] required to cool based upon 24 hour per day operation.	8.2	0.083
Refrigeration temp K	80	30
Number of plants	8.2	1.38
Size	LN plants of 1 MW size (500 ton/day)	MFTF-B plants of 60 kW size (note 3)
Electrical power of a single plant[1 MW]	10.00	4.10

Notes:

(1) TF Heat loads per Neumeyer Table dated 11/3/95, temperature distribution per A. Brooks
(2) PF heat loads per C. Neumeyer table dated 11/3/95, temperature distribution per A. Brooks.
(3) A rough Equivalence is 11 kW @ 5 K is = approx. 60 kW @ 30 K.

Helium Refrigerator

Refrigerators are often evaluated in terms of their thermodynamic performance. Care should be taken when comparing the various efficiencies,

coefficient of performance and ideal power requirements. For the PCAST machine the helium refrigerator has been estimated based on the performance of the 11kW at 4.5K MFTF-B helium refrigerator. This refrigerator would produce about 60kW at 30K, and is of the largest sized helium refrigerators built to date. The required electrical power has been estimated using the actual installed horsepower of the MFTF-B helium refrigerator.

The Helium Refrigerator is comprised of two sections, a Warm Compressor section and a Cold Box section (Refrigerator). The compressors take the room temperature helium, either from gas storage or from the cold box return and raise its pressure to approximately 2 MPa before entrance into the cold box. The cold box is comprised of several subsets of heat exchangers and expansion turbines which utilize the helium supplied for dual purposes. Liquid nitrogen is used to provide cooling of the incoming helium stream, and reduce the overall refrigeration requirement. A portion of the helium stream is diverted through an expansion turbine and into a heat exchanger to cool the incoming helium stream. Multiple stages are diverted to accomplish this reduction in temperature of the incoming helium gas stream. The helium stream which remains is sub cooled by passing through heat exchangers and finally a Joule-Thomson valve.

Gas Storage

The gas storage system for the helium will consist of commercially available tanks that are commonly utilized for ambient temperature storage of propane. A high rate of storage can be attained by designing the compressor output pressure as the maximum storage pressure. Storage pressures near 2 MPa are typical for these tanks. This pressure allows for usage of the refrigerator compressors as the storage compressors.

The storage tanks will be piped such that the helium will flow through the tanks and insure a clean gas supply by constant purging of the storage system. An on-line gas analysis system will monitor the helium gas stream at several locations to insure the helium purity.

Controls I/C

Controls will allow for local subsystem control and subsystem optimization outside of the Central I&C. Once in an operational ready mode the cryogenics controls will be driven from a Centralized Control System. Fully

automatic operation with interlocks to the Facility and Personnel Safety Systems will be possible from local or Central I&C.

Helium Distribution

The Distribution system will consist of the main supply, return, vent, auxiliary supply, ambient helium lines and cryogenic operational control valves. The main supply and return lines will be vacuum jacketed lines allowing for cooling or warming. Vent lines will be appropriately placed along the distribution system. Secondary helium lines will provide for purging before cool down and continuous gas analysis of the helium system.

Helium Primary Cooling Loop

The primary cooling loop will be a 5 atm helium gas cooling loop, that will be circulated by cold pumps through the coils and also through a heat exchanger. The heat removed from the coil will be rejected into the 30K helium supplied from the refrigerator in the heat exchanger.

3.4.3 Operating Scenario

The assumption used for this study was that the magnet shots (up to 5 per day) would be equally spaced over a 24 hour day. This allows the minimum sizing for the cryogenic system which would be operated continuously at its rated capacity.

3.4.4 System Facility Requirements

The primary requirements for the cryogenic system are for buildings, electrical power and cooling water. The requirements are as shown in Table 3.4.4-1

Table 3.4.4.1 Cryogenic Facility Requirements

Building Area - Helium Bldg.	1,400 m^2
Nitrogen Bldg.	5,700 m^2
Electrical Power	88 MW
Cooling Water	88 MW

3.4.5 System Options Considered

30 K TF Magnet Option

One of the options that was considered was to precool the TF coils to 30K, and thereby lower the overall heating of the coils, as well as reduce the electrical power requirements. Table 3.4.5-1 shows the heat loads that would occur if the TF coils were cooled to 30K, in addition to the PF1 U&L. Table 3.4.5-2 show the resulting cryogenic system configuration for this option.

Table 3.4.5-1 PCAST 30K TF Option Cryogenic Heat Loads Per Pulse

Source	**80K Load**	**30K Load**
Ohmic Heating Loads:		
TF coils	9.8 GJ	18.2 GJ
PF 1 U&L coils	7.0 GJ	1.0 GJ
PF 2-7 U&L coils	16 GJ	NA
Subtotal	**32.8 GJ**	**19.2 GJ**
Other loads:		
Pumping losses, Rad, etc.	10 GJ	5.8 GJ
Total	**42.8 GJ**	**25 GJ**

Table 3.4.5-2 PCAST 30K TF Cryogenic System

TF 30K Option System		
	NITROGEN SYS. Refrigeration from 300K to 80K	HELIUM SYSTEM, Refrigeration from 85 K to 30 K
Description	80K PF2-7	30K TF & PF1
	(adiabatic heat absorp.)	
	Heat Load, GJ	Heat Load, GJ
TF (Note 1)	10	18
PF 1 U/L (note 2)	7	1
PF 2-7 U/L (note 2)	16	0
Total per pulse	33	19
Total 5 pulses/day	166	96
Total Load per 24 hr With 30% pumping losses	215	125
[Mega-Watts refrig.] required to cool based upon 24 hour per day operation.	2.49	1.44
Refrigeration temp.	80°K	30°K
Number of plants	2.5	24.1
Size	LN plants of 1 MW size (500 ton/day)	MFTF-B plants of 60 kW size (note 3)
Electrical power of a single plant[MW]	10.00	4.10

Notes:

(1) TF Heat loads per Neumeyer Table dated 11/3/95, temperature distribution per A. Brooks
(2) PF heat loads per C. Neumeyer table dated 11/3/95, temperature distribution per A. Brooks.
(3) A rough Equivalence is 11 kW @ 5 K is = approx. 60 kW @ 30 K.

Trucking in Liquid Nitrogen Option

The option of trucking in liquid nitrogen was considered for the baseline 80K TF design heat loads. This option would require delivery of over 190 truckloads of liquid nitrogen per day. The existing liquid nitrogen capacity in any area in the U.S. is not adequate to supply this rate. The cost of trucking this nitrogen in would exceed $354K for just the nitrogen. An unloading station that could continuously unload 9 trucks would also be required. The cost of the warming and dispersion towers required to warm the enormous clouds of cold nitrogen vapor are not included but would be required in order to deal with the oxygen deficiency problems that would otherwise occur. Significant environmental impacts would also have to be considered.

Section 4.0 : Power Systems (C. Neumeyer)

Introduction

The PCAST machine uses cryogenically cooled copper magnets operating at high fields with a low duty cycle (120 second burn, five pulses per 24 hour period). The power and energy demands are large, and require maximum utilization of utility grid power along with the addition of a supplemental pulsed energy storage power system. However, the technologies and design approaches used on existing tokamak devices (TFTR, JET, JT-60) are applicable and can be readily scaled to the PCAST machine, and the required supplemental energy storage system is of similar scale to existing systems.

The PCAST Power Systems consist of the following major elements:

WBS 4.1 *Coil Power Supply and Distribution System*

- Utility Grid Interface
- Substation
- Energy Storage System
- Reactive Power Compensation System
- AC Distribution
- Toroidal Field (TF) AC/DC Converters and DC Circuit Components
- Poloidal Field (PF) AC/DC Converters and DC Circuit Components

WBS 4.2 *Auxiliary Heating Power Supply System*

- Auxiliary Heating AC/DC Converters

WBS 4.3 *Steady State Electric Power Network*

- Auxiliary Power System

WBS 4.4 *Fast Plasma Position Control (FPPC) Power Supply System*

• Fast Vertical Position Control (FVPC) AC/DC Converters and DC Circuit Components

• Fast Radial Position Control (FRPC) AC/DC Converters and DC Circuit Components

In order to develop a design concept and determine the required electrical power sources and component ratings, a simulation of the operation of the power systems was developed. The PF scenario was described by a set of breakpoints based on the desired plasma start up and equilibria. Given this scenario and the geometry of the PF coils the time evolution of the PF coil currents and voltages was determined. Similarly, the time evolution of the TF coil current and voltage was determined. A conceptual design for the PCAST power system was developed based on which the time evolution of the total active and reactive power demands from the grid and energy storage system was determined via the simulation. The key design driver was the constraint on active power available from the grid, which was set equal to the value on which the ITER design is based.

4.1 Requirements and Assumptions

4.1.1 Limitations on Grid Power

The ITER project has investigated the availability of grid power at various sites around the world and has developed a set of assumptions which guide their design[1], and which shall applied also to the study described herein. Table 4.1.1-1 lists the constraints on power available to the Experimental Loads (TF, PF, FPPC, and Heating).

Table 4.1.1-1: Limitations on Grid Experimental Power

Parameter	Maximum Value
Active Power	650MW
Reactive Power	500MVAR
Active Power Step	60MW
Active Power Ramp	200MW/sec

[1]ITER Design Description Document (DDD), Coil Power Supply & Distribution System (WBS 4.1), Issue 3: June 2, 1995, Appendix B

Although the duty cycle of the ITER load is higher than that of the PCAST machine, both load scenarios are of sufficient duration to initiate the inertial, governor, and Automatic Generation Control (AGC) response of the grid. Therefore the imposition of the same constraints is appropriate.

In addition to the above, the ITER design[2] assumes that up to 250MW and 166MVAR will be available from a separate interface with the grid for the purposes of supplying power to the Auxiliary (balance of plant) Loads, which shall also be assumed for the PCAST machine.

In practice the availability of grid power is highly site dependent and the response of the grid to the specific loads imposed by any proposed design would have to be analyzed in detail, taking into account the local grid characteristics at the prospective site.

4.1.2 Toroidal Field Coil Requirements

Main parameters assumed are given in Table 4.1.2-1.

Table 4.1.2-1: TF Coil Parameters

Parameter	Value
Bmax @ Radius R	7.0 Tesla
Radius R	5.0 m
Number of TF Coils	16
Number of Turns per Coil	50
Current per Turn @ Bmax	218.75 kA
Inductance	1.435 Henries
Initial Temperature	80K
Resistance @ 80K	3.3 mΩ
Flat top duration	160 seconds

The flat top of the TF current is required to begin at the time of PF precharge current maximum (Start of Initiation, SOI) and continue to the end of the plasma current flat top (End of Flat Top, EOF).

---

[2]ITER Design Description Document (DDD), Steady State Power Network (WBS 4.3), 3 March 1995

An equation for the resistance of the TF coil as a function of $\int i^2(t)dt$ was derived based on data from finite element simulations of the TF coil behavior[3] and was used as the basis for the resistance calculation in the simulation. For simplicity the magneto-resistivity effect was not considered in the simulation. Comparison of finite element simulations (with linear ramp-up and ramp-down current profile) with and without the inclusion of this effect show that it increases the power demand at the end of flat top by a few percent. Future work should include consideration of this effect.

4.1.3 Poloidal Field Coil Requirements

Coil geometry is given in Table 4.1.3-1.

Table 4.1.3-1: PF Coil Geometry

PF Coil	R (m)	ΔR (m)	Z (m)	ΔZ (m)	Turns	Fill
1	1.16	1.009	0.75	1.4481	294	0.886
2	1.16	1.009	2.25	1.4481	294	0.886
3	1.16	1.009	3.375	0.6975	98	0.884
4	1.16	1.009	4.125	0.6975	98	0.884
5	2.483	1.2348	6.858	1.232	240	0.893
6	7.036	0.6239	6.012	0.9707	120	0.872
7	9.566	0.6239	2.204	0.6253	60	0.871

The corresponding mutual inductance matrix is given in Table 4.1.3-3.

Table 4.1.3-3: PF Coil Mutual Inductances (mHenries)

PF Coil	1	2	3	4	5	6	7	Pls	VV
1	311.7	86.78	10.53	6.026	13.23	23.52	18.08	0.339	0.347
2		249.7	36.97	16.61	19.41	27.22	17.15	0.264	0.260
3			357.0	21.63	10.07	9.215	5.311	0.060	0.596
4				35.61	15.38	9.68	4.980	0.049	0.049
5					586.0	114.4	40.41	0.234	0.235
6						820.3	17.29	0.670	0.666
7							395.4	0.662	0.654
Pls								0.009	0.022
VV									0.005

[3]R. Pillsbury (MIT), e-mail of 26 October 1995

The plasma and vacuum vessel were each modeled as single conducting filaments.

The 20C room temperature resistance and initial temperature of the coils is given in Table 4.1.3-4.

Table 4.1.3-4: PF Coil Room Temperature Circuit Resistances & Initial Temperature

PF Coil	1	2	3	4	5	6	7
R (mΩ)	16.78	16.78	3.876	3.876	22.80	41.54	21.96
To (K)	30	80	80	80	80	80	80

Equations were developed for the simulation which account for the variation in specific heat and resistivity with temperature, based on OFHC copper with RRR=100. The magneto-resistivity effect was not considered. This effect could be significant in the case of PF1 and should be considered in future work.

Scenarios for start-up and the plasma equilibrium states were provided by Wang[4] and Bulmer[5]. The following states are defined:

SOP - Start of Pulse (Start of current flow in PF coils)
SOI - Start of Initiation (Time of insertion of discharge resistors for start-up loop voltage)
SOD - Start of Discharge (Start of plasma current)
EOI - End of Initiation (Time of exclusion of discharge resistors)
SOX - Start of X-point (Time of X-point formation)
SOF - Start of Flat Top (Start of plasma current flat top)
SOB - Start of Burn (Start of burn of fully heated plasma)
EOB - End of Burn
EOD - End of Discharge (End of plasma current)
EOP - End of Pulse (End of current flow in PF coils)

The baseline scenario is given in Table 4.1.3-5.

[4]"Startup calculation with 15 V breakdown voltage for PCAST machine", P. W. Wang (MIT), 18 October 1995..

[5]"Fiducial States for Inertially Cooled Option", R. Bulmer (LLNL), 23 October 1995

Table 4.1.3-5: PF Scenario

	SOP (PF5)	SOP (PF1-4, PF6-7)	SOI	SOD	EOI	SOX	SOF	SOB	EOB	EOD	EOP
Time	-45.0	-25.0	0.0	0.388	0.688	15.688	25	40	160	185	195
IPF1 (kA)	0.0	0.0	89.5	82.3	78.2	-61.7	-130.6	-123.7	-131.7	8.6	0.0
IPF2 (kA)	0.0	0.0	87.4	93.5	94.6	55.4	10.7	7.3	-9.1	8.6	0.0
IPF3 (kA)	0.0	0.0	175.5	145.9	144.8	70.0	50.7	45.2	33.2	12.3	0.0
IPF4 (kA)	0.0	0.0	165.3	140.8	140.8	63.2	51.2	46.2	36.5	12.3	0.0
IPF5 (kA)	0.0	49.3	110.8	103.3	102.5	97.6	92.3	88.0	75.2	11.1	0.0
IPF6 (kA)	0.0	0.0	4.8	2.0	0.336	-38.1	-58.2	-53.8	-53.7	0.000	0.0
IPF7 (kA)	0.0	0.0	6.4	5.4	5.3	-46.8	-76.2	-89.3	-90.3	0.667	0.0
Ipls (MA)	0.0	0.0	0.0	0.0	0.1	10.0	15.3	15.3	15.3	0.0	0.0

As indicated above, the precharge ramp rate of PF5 was decreased in order to avoid the power supply requirement being driven by this non-critical phase.

4.1.4 Fast Plasma Position Control Requirements

The Fast Plasma Position Control (FPPC) system is assumed to consist of separate vertical (Fast Vertical Position Control, FVPC) and radial (Fast Radial Position Control, FRPC) circuits. Requirements are summarized in Table 4.1.4-1.

Table 4.1.4-1: FPPC Requirements

Parameter	Vertical Control	Radial Control
Number of Turns per Coil	2	4
Number of Coils	2	2
Current (kA-turn) per Coil	+/- 100	+/-200
Current per Turn (kA)	+/- 50	+/-50
Voltage per Turn (V)	100	400
Voltage per Coil (V)	200	1600
Voltage (V)	400	3200
Peak Power (MW)	20	160

Detailed requirements for the profiles of the voltage and current have not been developed at this stage of the design. Therefore the following assumptions will be made:

a) The average power is low;
b) The frequency response of a anti-parallel circulating current converter constructed of 6-pulse bridges fed at normal power frequency is adequate for the application.

4.1.5 Heating System Requirements

Main assumptions are given in Table 4.1.5-1.

Table 4.1.5-1: Heating System Requirements

Parameter	ICRF	500kV NINB
Power to Plasma, heating phase (SOF SOB)	30MW to	30MW
Power to Plasma, burn phase (SOB to EOB)	10MW	10MW
Efficiency	50%	50%

4.1.6 Auxiliary System Requirements

Main assumptions are given in Table 4.1.6-1.

Table 4.1.6-1: Auxiliary System Requirements[6]

Parameter	30K Cryogenic Refrigerator	80K Cryogenic Refrigerator	Balance of Plant
Power Requirement	5.8MW[1,2]	82.1MW[1]	20MW
Efficiency	1/68.3	1/10	n.a.
Power Factor	0.8	0.8	0.8

Note 1: The cryogenic refrigeration plants are assumed to operate on a continuous (24 hr/day) basis so that the plant size and peak load on the grid are minimized. The average power requirement is thus computed based on the average refrigeration power needed to remove the losses due to 5 pulses per 24 hours, with a 30% pumping loss included in the total heat load.

Note 2: The 30K refrigeration system must remove only the heat associated with PF1 in the range of 30 to 85K.

[6]"PCAST Cryogenic System Scoping", D. Lang (LLNL), 6 November 1995

4.1.7 Other Assumptions

a) Power system efficiency

The overall efficiency of the power system in the delivery of units of active and reactive power from the AC grid to the DC terminals of the AC/DC conversion system was taken as 95%. The losses in the DC bus bar systems were accounted for separately as described in a subsequent paragraph.

b) Energy Storage System Characteristics

The use of motor-generator (MG) sets with characteristics identical to those used on TFTR was assumed, since performance models were available for inertia, windage loss, friction loss, eddy and hysteresis loss, motor drive power characteristics, etc., and since costs are known. As discussed in a subsequent paragraph, however, the power to energy ratio of the TFTR units does not ideally match the PCAST requirements.

c) Thyristor Converter Characteristics

A conventional phase controlled thyristor converter topology is assumed. Modular AC/DC converter unit characteristics were adopted as indicated in Table 4.1.7-1.

Table 4.1.7-1: AC/DC Converter Characteristics

Parameter	TF	PF	FVPC	FRPC
AC Input Voltage (AC rms line-line volts)	600	750	600	750
DC Output Voltage (average volts, no load)	810.28	1012.85	810.28	1012.85
Regulation (% voltage drop @ full load current, 60Hz)	20	20	20	20
DC Output Current (kA DC, full load)	25	25	25	25
Maximum Inversion Voltage (% of no load (+) voltage)	65	65	65	65
Range of operation	2-quadrant	4-quadrant	2-quadrant	2-quadrant

When the PF and FPPC converters are supplied from the variable frequency Energy Storage System the voltage drop under load was adjusted according to the frequency. The basic converter unit is 6-pulse, but always arranged in pairs so that the net harmonic content of the system contains the characteristic 12-pulse harmonics. The ability of the converter to "freewheel" or "bypass" when not needed as a power source is essential in order to reduce the reactive power consumption of the TF and PF systems. This could be accomplished using an external bypass thyristor array or by circulating the current within the bridge as planned for the ITER AC/DC converters.

4.2 Conceptual Design

4.2.1 AC Power Systems

A conceptual one-line diagram of the AC power systems is given in Figure 4.2.1-1. As concluded in the ITER site power studies, an EHV transmission line with voltage 345kV or higher would service the Experimental Power Substation. The Auxiliary Power Substation is fed by a separate interface with the grid with voltage 230kV or higher. The designs for the Auxiliary and Experimental Power substations are essentially identical to ITER. Drive power for the MG sets is taken from the Auxiliary Power Substation.

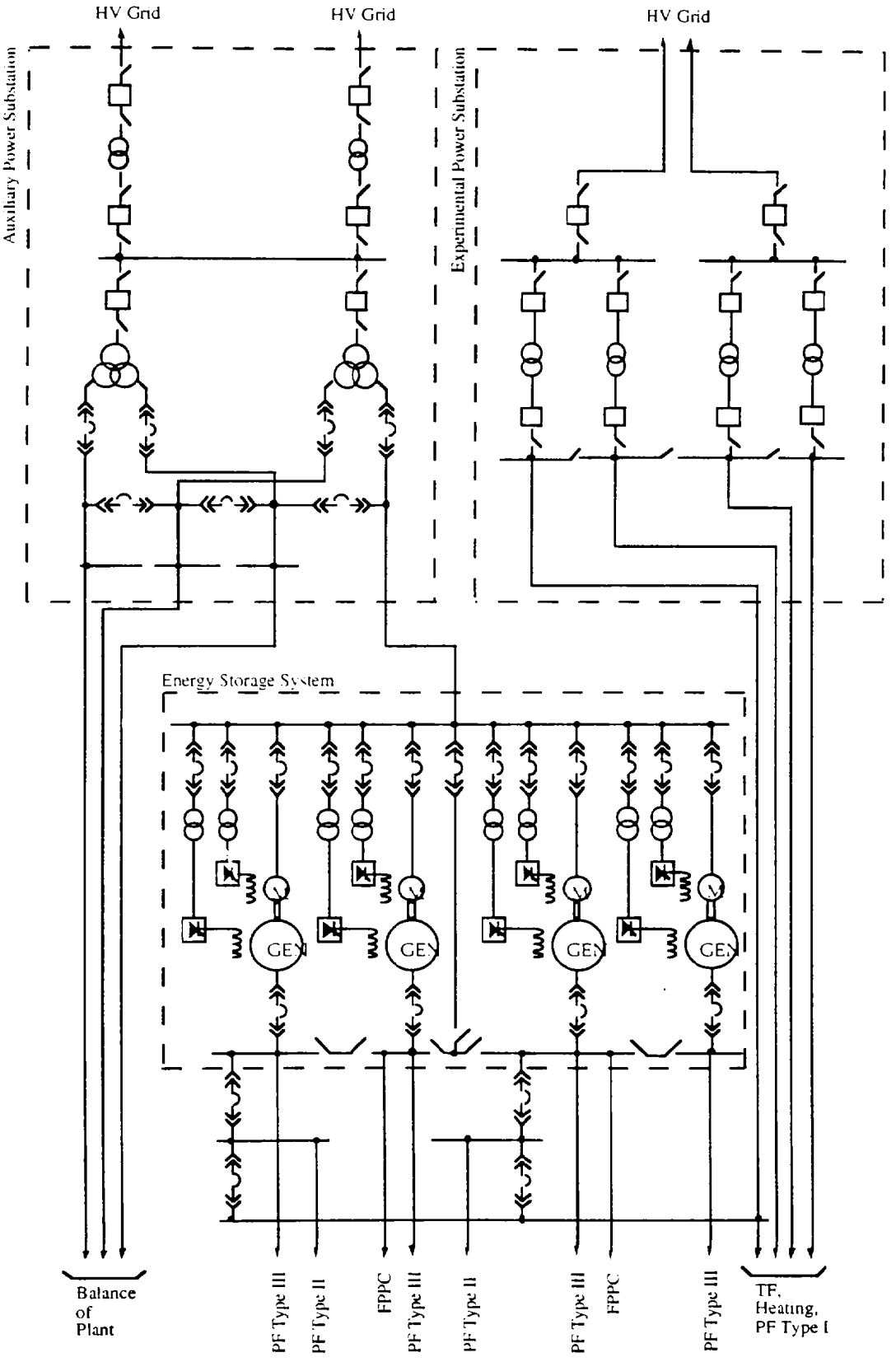

Figure 4.2.1-1: Conceptual One Line Diagram of AC Power Systems

4.2.2 TF Power Supply System

A conceptual schematic of the TF Power Supply System is given in Figure 4.2.2-1. An array of 4 series x 10 parallel 6-pulse, 800V/25kA, 2-quadrant converters is required for the PCAST TF load. The TF converters are fed entirely from the grid using 60Hz AC power. Inductors are included in each branch of the converter to limit the rate of rise of fault current. This facilitates the reduction of the maximum fault current as seen by a fault outside of the converter array as well as inside the converter array. The latter can be especially problematic when a large number of parallel branches could potentially feed into a single faulty branch. In the case of a fault inside the converter array on one branch, it is assumed that the other branches, except perhaps for one, suppress their thyristor firings and enter a bypass mode so that they do not all contribute their full prospective fault current to the single faulty branch.

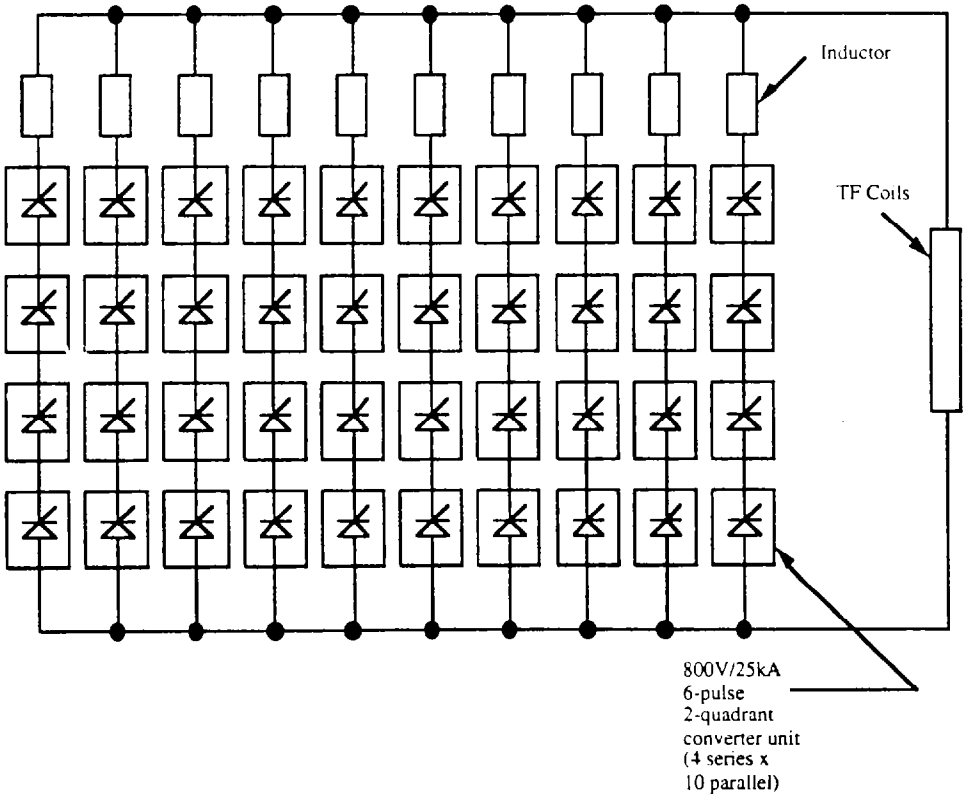

Figure 4.2.2-1: TF Converter Topology

Eight parallel 1" x 12" copper bars per pole, 100 meters per pole, are assumed for the TF bus bar system. Peak bus bar power consumption at maximum current is 2.7MW. Temperature rise per pulse is ≈ 15 deg C.

4.2.3 PF Power Supply System

A conceptual schematic of a typical PF Power Supply System is given in Figure 4.2.3-1. An array of series and parallel 6-pulse, 1kV/25kA, 4-quadrant converters is utilized. Three classes of converters exist as follows:

Type I: Continuously fed from grid 60Hz AC supply; active during entire pulse

Type II: Subject to bus transfer from variable frequency MG AC supply to 60HZ grid AC supply, and vice-versa, during a pulse; may be active during entire pulse

Type III: Continuously fed from variable frequency MG AC supply; subject to brief pulses of operation

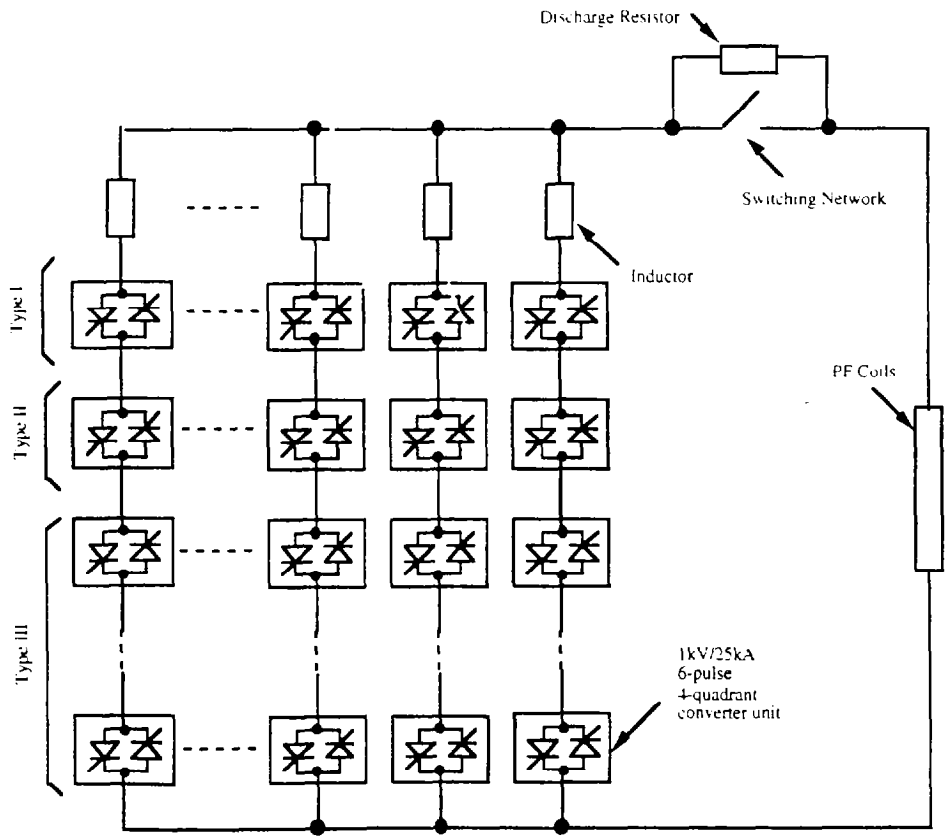

Figure 4.2.3-1: Typical PF Converter Topology

Since the grid AC power supply is power limited whereas the MG AC power supply is energy limited, the large fluctuations in power during PF precharge, plasma start-up, and plasma ramping are best provided by the MG source whereas the long duration low power demand during plasma burn is best provided by the grid source. To reduce the total inventory of AC/DC converters, the Type II converters are introduced which can switch between the grid and MG AC power sources. Such switch over can be readily and rapidly accomplished by placing the Type II converter momentarily into the bypass mode and performing a bus transfer operation on the AC side.

Per the ITER concept the 4-quadrant converter operation is achieved by back-to-back connection of (2-quadrant) thyristors in each bridge leg. During high current operations all parallel converter branches are operating with an equal share of the current. Near current zero one half of the converter branches are suppressed, after which the opposite polarity thyristors in those converters are fired to establish the anti-parallel circulating current converter mode. In this mode a smooth zero crossing is achieved without reversing switches. Once away from current zero in the opposite polarity the opposite procedure is followed to exit the anti-parallel mode and re-establish the parallel mode.

A Switching Network (consisting of a DC Circuit Breaker and discharge resistor) is included to provide a high loop voltage during the plasma initiation process. Although the peak PF currents are large compared to the TFTR/JET/JT-60 experience they are in the same range as that being considered for the ITER Central Solenoid (CS) circuit ($\approx$ 170kA) for which an R&D program is underway to develop DC circuit breakers. For PCAST the high interruption currents occur in PF-3, 4, and 5 and could probably be lowered by increasing the number of turns, since the rms current density in these coils is not extremely high.

One, two, three , and in some cases four parallel 1" x 12" copper bars, 100 meters per pole, are assumed for the various PF bus bar systems. Peak bus bar power consumption in any circuit at maximum current is 4.6 MW. Maximum temperature rise is $\approx$ 15 deg C.

4.2.4 FPPC Power Supply System

A conceptual schematic of the Fast Plasma Position Control converters (FRPC for radial control, FVPC for vertical control) is given in Figure 4.2.4-1.

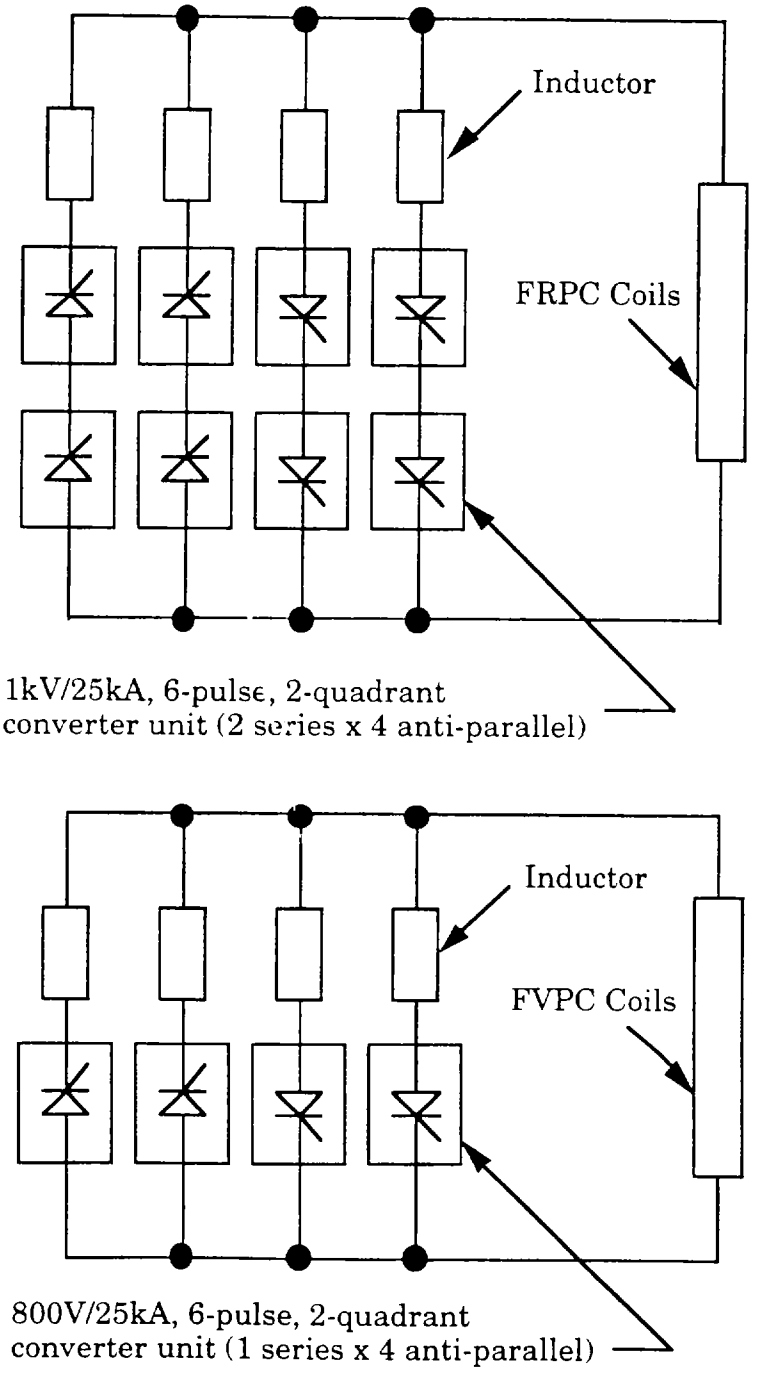

Figure 4.2.4-1: Fast Vertical and Radial Control Converter Topology

Both the FRPC and FVPC converters supply bipolar current and are arranged in the anti-parallel configuration for fast and unlimited zero crossings. A scheme similar to the PF, consisting of 4-quadrant converters with ability to transition from parallel to anti-parallel modes near zero crossing was not considered because the time delays associated with the transition between modes might be excessive. Since the pulsed power is high but the average power is small, the FPPC converters will be supplied by the MG sets.

4.3 Simulation

4.3.1 Simulation Methodology

The simulation is performed using the following steps:

a) the PF coil voltage, current, power, and energy are computed, based on the given scenario of current, the mutual inductance matrix, and the computation of resistance as a function of the coil heating.

b) the PF power supply performance is simulated in response to a), including the computation of number of active converter units (comprised of Type I, II, and III above) required as a function of time (sequential control), total active and reactive power from grid and MG sources, MG drive power/energy extraction/speed simulation, and power and energy of discharge resistors during plasma initiation procedure.

c) a simulation of the TF scenario is performed based on the application of maximum available power supply voltage during current rise to determine the current rise time requirement, coil heating, and active and reactive power demand.

d) the TF scenario is aligned with the PF scenario so that the start of the TF flat top coincides with the end of the PF precharge scenario, and the composite active and reactive power demand of the system is computed. The demand of the heating system is included. This result comprises the total Experimental Systems power demand from the grid.

e) the Auxiliary Systems power demand is taken as the sum of the demands of the 30K and 80K refrigeration systems' 24 hour average power requirement (based on the losses in the coils calculated in the simulation) plus the balance of plant power plus the power (calculated in the simulation) required to drive the MG system.

f) The FPPC converters are not included in the simulation. Their power consumption would add to the PF load on the MG sets, as would their energy. However, the average power is expected to be small and therefore not significant.

To limit the power demand on the grid the following steps are taken during the simulation:

a) at a selected time near the end of the TF current rise the TF voltage is reduced by dropping one series layer of converters; this increases the headroom available for the power demand of the PF-1 Type I converters which are fed from the grid.

b) at SOF the Type II converters are switched from the MG power source to the grid, and the Type III converters are excluded (bypassed).

c) at selected times near the end of the burn phase the Type II converters are switched (one or more PF circuits at a time) from the grid back to the MG power source; this increases the headroom available for the TF and PF-1 converters fed from the grid as their power demand increases due to the temperature (and resistance) increase, and minimizes the energy taken from the MG sets.

4.3.2 Simulation Results

Simulation results are depicted in Figures 4.3.2-1 through 4.3.2-10 and summarized in Table 4.3.2-1. Note that the high negative peak voltage and power associated with the plasma initiation procedure are clipped from figures 4.3.2-2 and 4.3.2-3 so as to enlarge the more important regions outside of this interval.

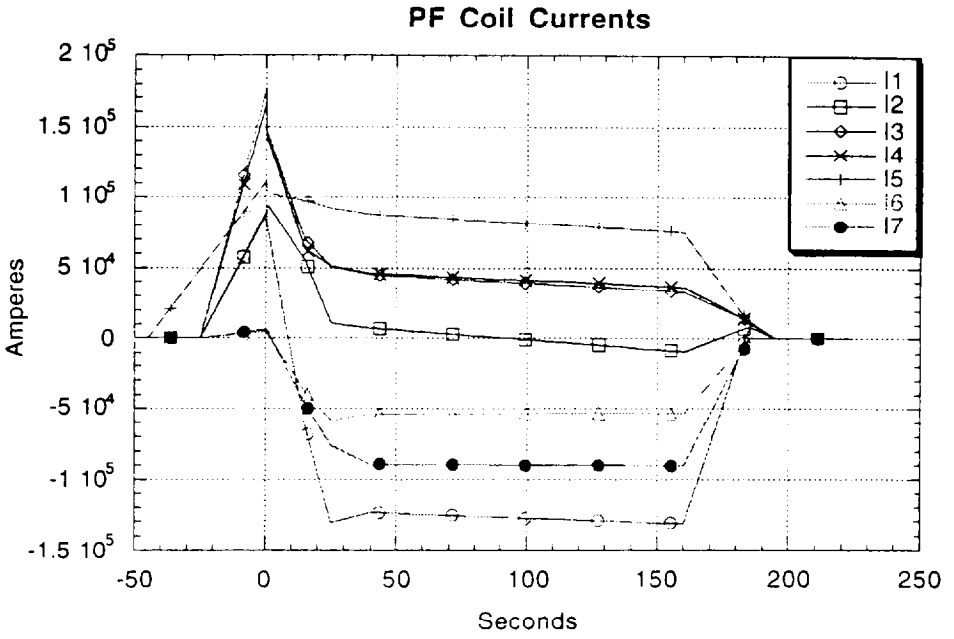

Fig. 4.3.2-1: PF Coil Currents

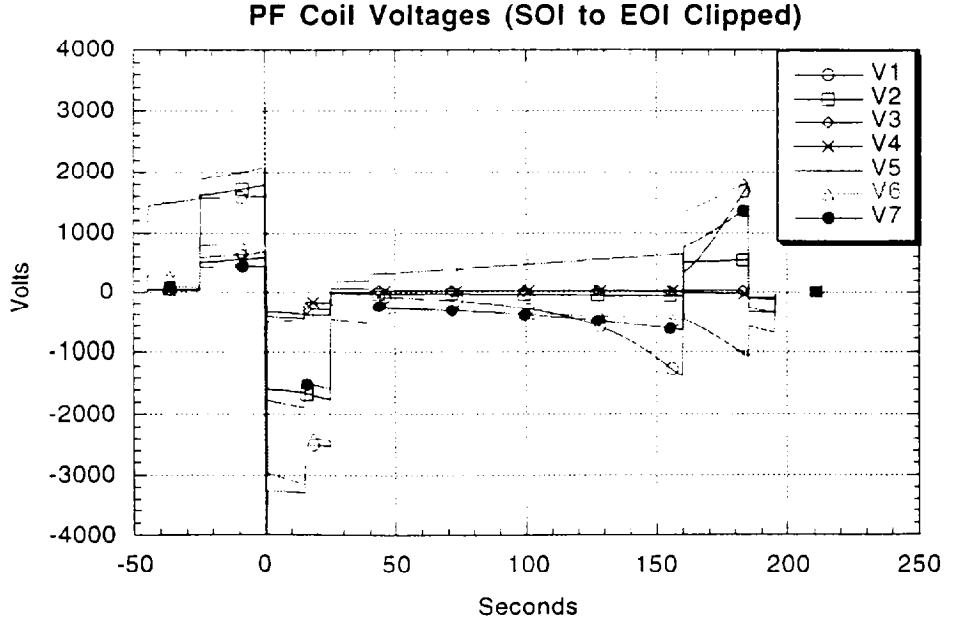

Fig. 4.3.2-2: PF Coil Voltages

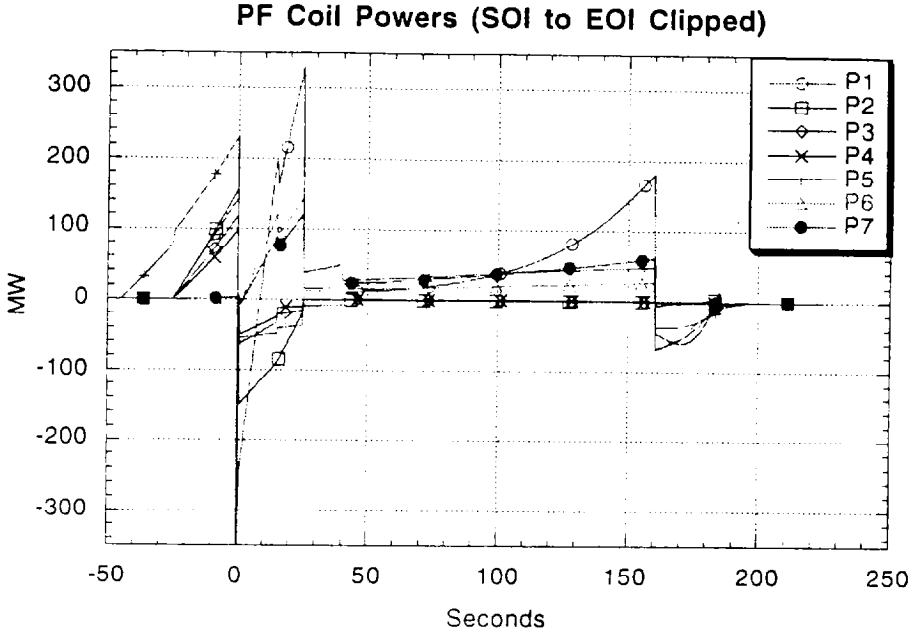

Fig. 4.3.2-3: PF Coil Powers

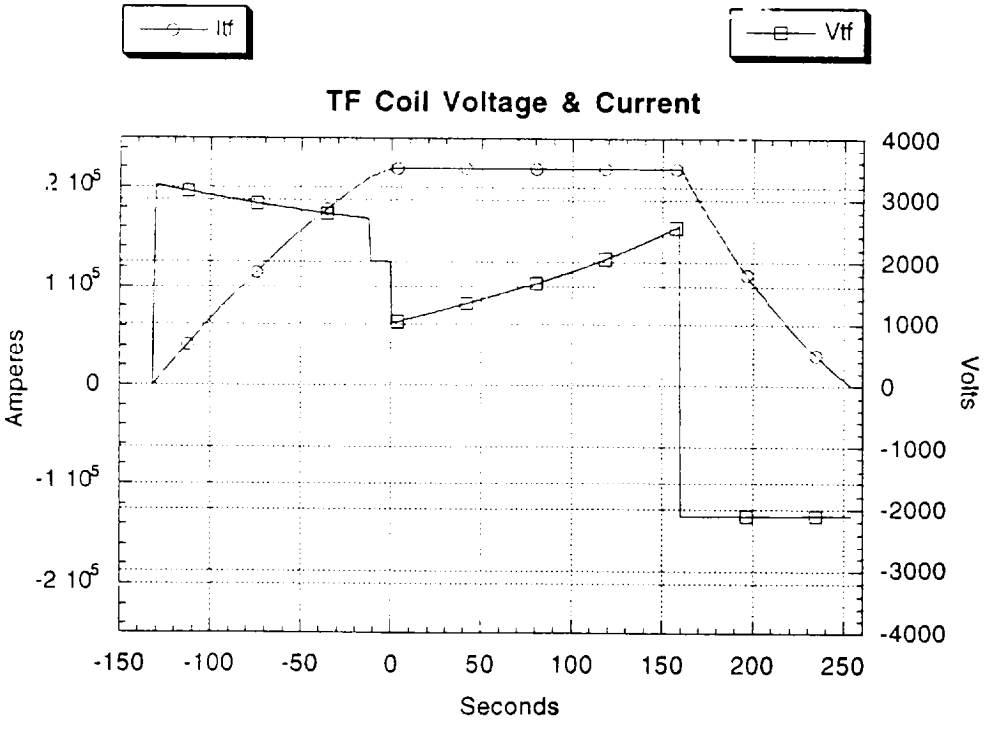

Fig. 4.3.2-4: TF Coil Voltage & Current

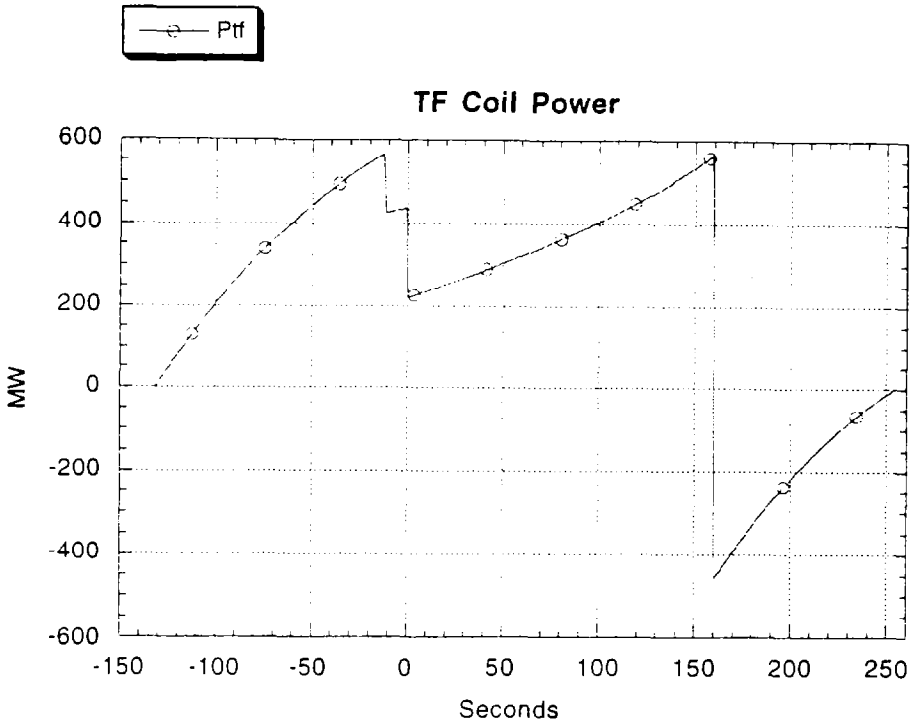

Fig. 4.3.2-5: TF Coil Power

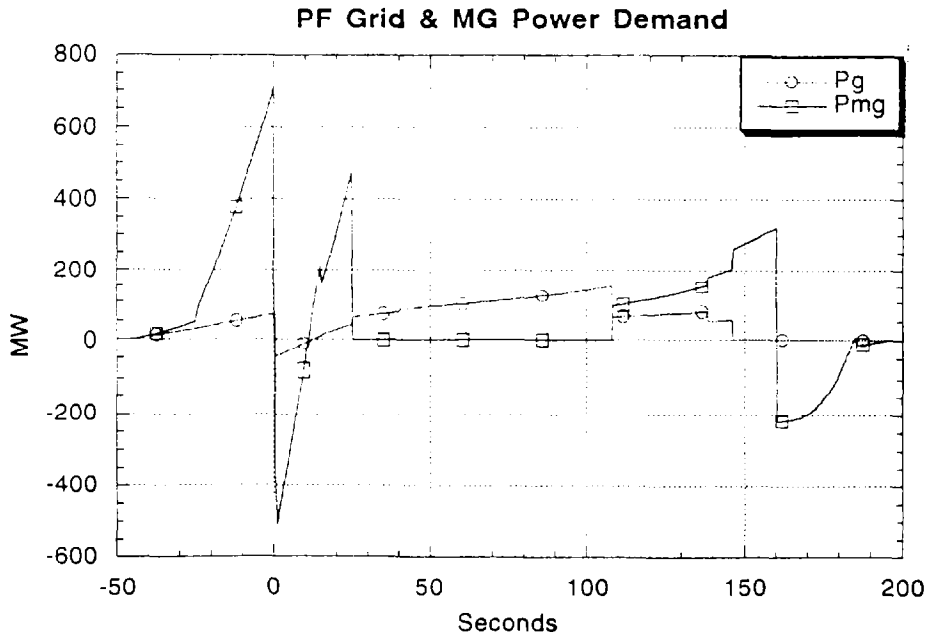

Fig. 4.3.2-6: PF Power Demand

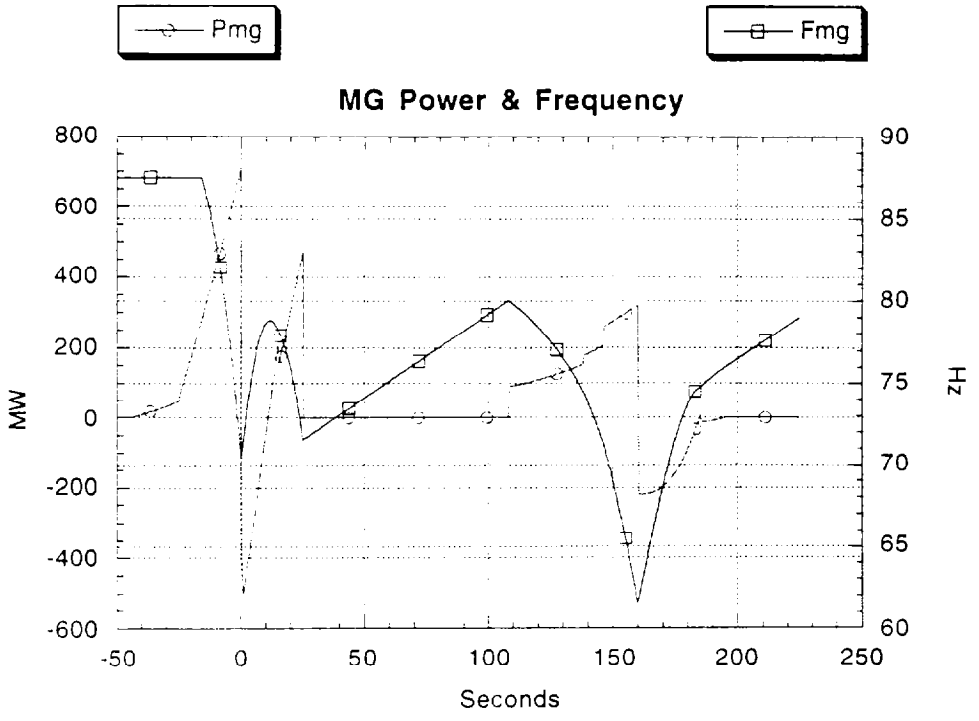

Fig. 4.3.2-7: MG Power & Frequency

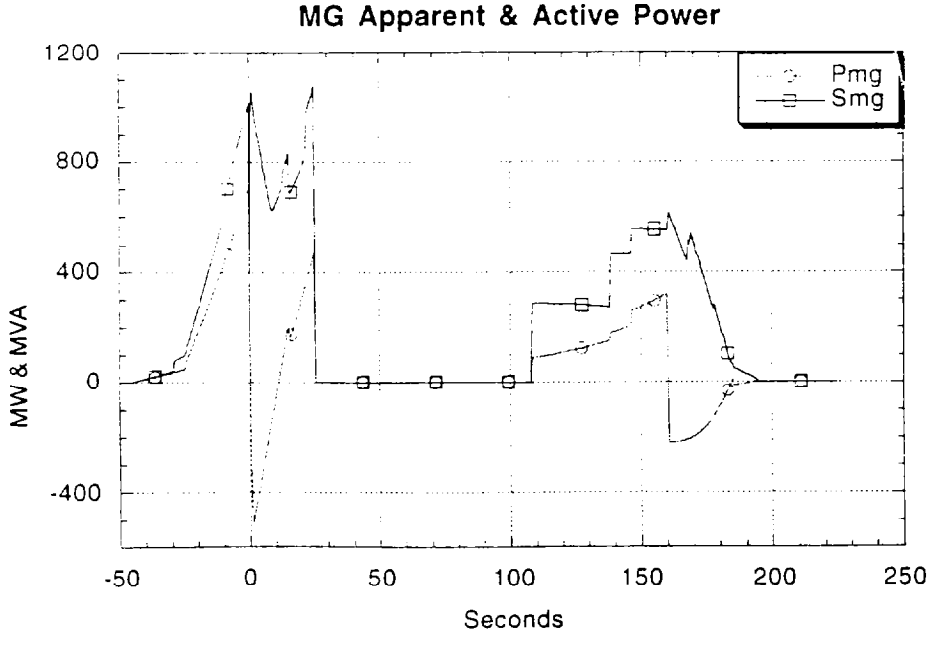

Fig. 4.3.2-8: MG Power

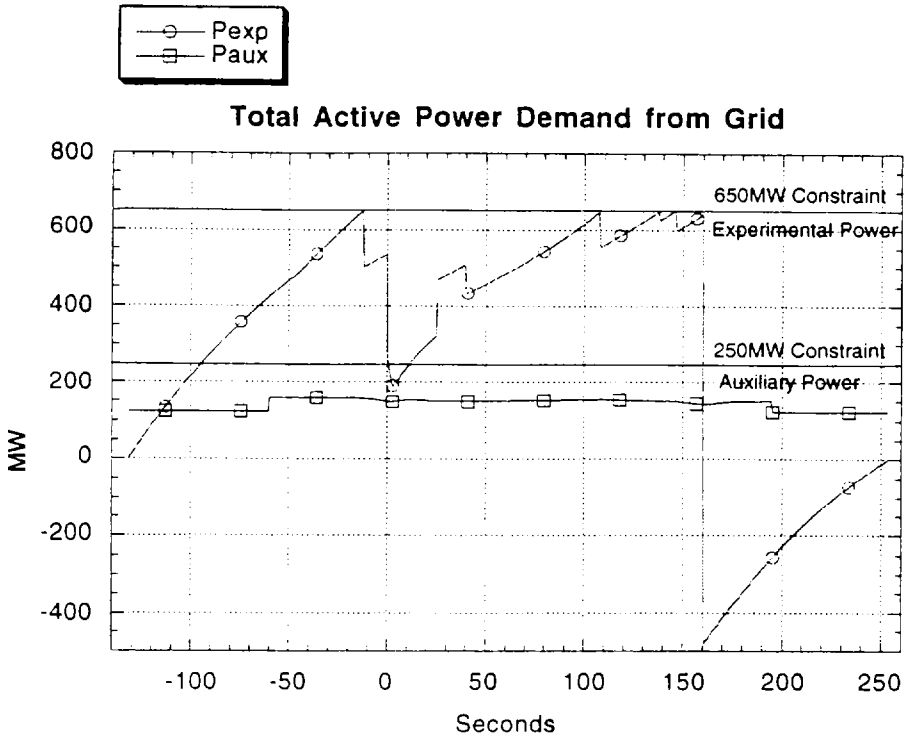

Fig. 4.3.2-9: Total Active Power Demand on Grid

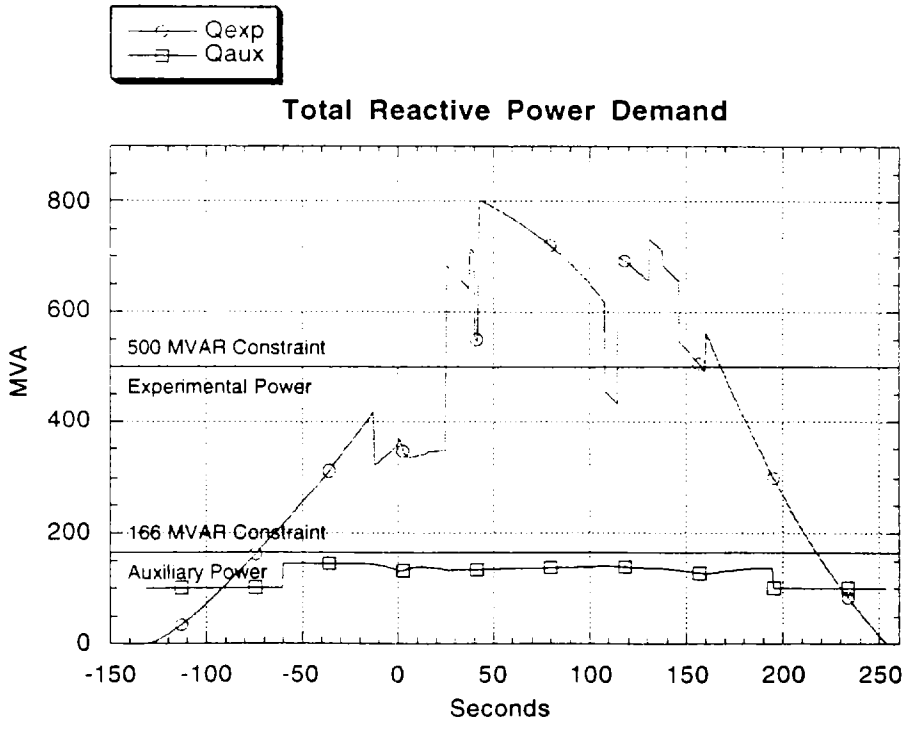

Fig. 4.3.2-10: Total Reactive Power Demand on Grid

It is worth noting that the MG energy delivery reaches two peaks, the first occurring at SOF and the second during the latter part of the burn phase. It is note that the second peak drives the requirement on MG energy. If the burn period were to end at t = 145 seconds (105 seconds into the burn phase which lasts 120 seconds at present) the MG requirement would be dramatically reduced.

The reactive demand of the Experimental Power System exceeded the 500MVAR limit established by ITER, which implies that a 300MVA Reactive Power Compensation System would be required.

While the ITER limit of 650MW and 200MW/sec was respected, the 60MW maximum power step was not during several of the scenario events (e.g turn on/turn off of heating, inversion of the TF). This was due mainly to the lack of a power step limiting strategy in the simulation. Power step limiting and/or staggering of the turn on of components could easily be implemented to overcome this deficiency without significant impact on the final results and conclusions.

Several aspects of the design would require further study to find an optimal design, including the following:

a) selection of optimum converter unit voltage rating (TF and PF Type I, II, and III).

b) distribution of PF loads on grid and MG power sources

c) inertia constant of MG system

d) number of coil turns

e) PF coil and plasma current ramp rates

f) plasma initiation scenario and discharge resistance values

4.4 Trade Studies

A study was undertaken concerning the trade-off between the TF electric power requirements and the cryogenic refrigeration requirements to determine whether sub-cooling the TF from 80K down to 30K would result in a net cost savings.

Electrical System Aspects

The selection of initial TF coil temperature dramatically affects its resistance, and hence the optimal power supply voltage selection, the power supply cost, and the energy dissipated in the coil.

Figures 4.4-1 through 4.4-4 show the relationship between the TF open circuit voltage and:

1) the ratio between power demand at the end of the current ramp (P_S) and EOFT (P_e)
2) the peak power demand during the pulse
3) the total energy dissipated at the end of the pulse
4) the total cost attributable to the TF power supply system in 1995 US dollars

The analysis was performed for the inertial cooled cases with initial temperatures of 30K, 50K, and 80K initial temperature, and for the active cooling case. For inertial cooling the resistivity vs. I2T is based on data provided by R. Pillsbury (MIT); magnetoresistivity effects are not included. For the active cooling case a constant bulk average temperature of 100K was assumed, and a constant resistance.

The assumed flat top time is 160 seconds (the TF flat top begins at the time of the PF precharge peak), and extends through the plasma current ramp time from SOI to SOF for 25 seconds, the heating phase from SOF to SOB for 15 seconds, and the burn from SOB to EOB for 120 seconds.

The power supply no-load voltage is constant during current rise, although the voltage drop due to the internal impedance of the power supply is included.

Cost scaling was obtained using the ITER power supply costing basis[7] , which includes design, fabrication, installation, and commissioning. The ITER specific cost for the substation, AC distribution system, AC/DC conversion system amounts to 98.6 $K/MVA in 1995 US dollars.

---

[7]Coil Power Supply and Distribution (WBS 4.1), Cost Assessment Document, ITER JCT, Naka JWS, Issue 1: 19 April 1995

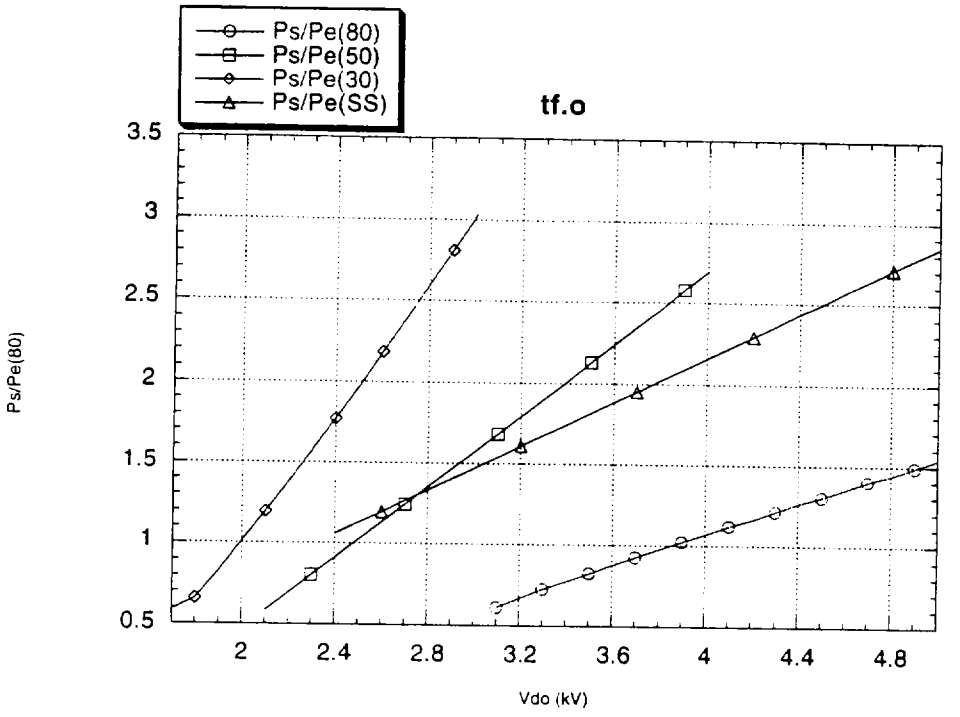

Figure 4.4-1: Ratio of Power at the end of the current ramp (P_S) to Power at the End of Flat Top (P_e) vs. Open Circuit Voltage

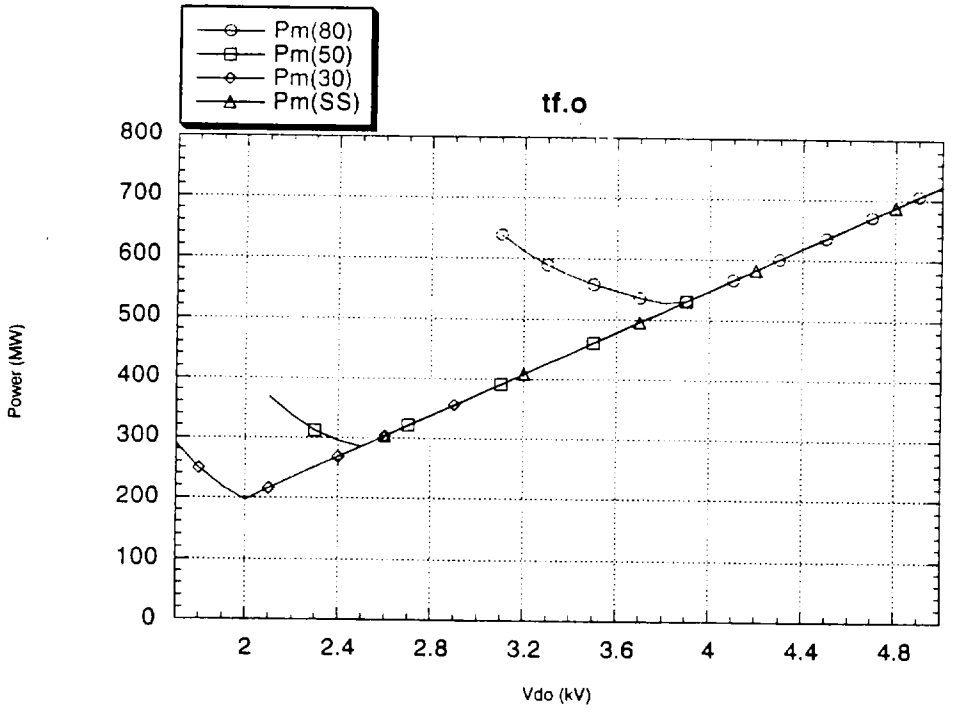

Figure 4.4-2: Maximum Peak Power Required vs. Open Circuit Voltage

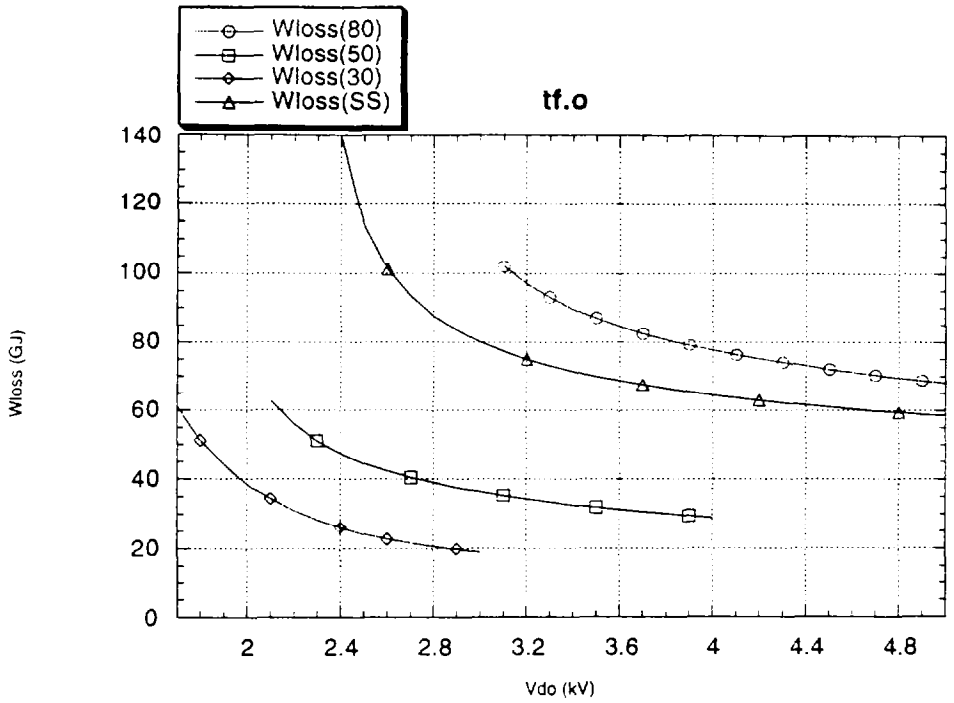

Figure 4.4-3: Energy Dissipation vs. Open Circuit Voltage

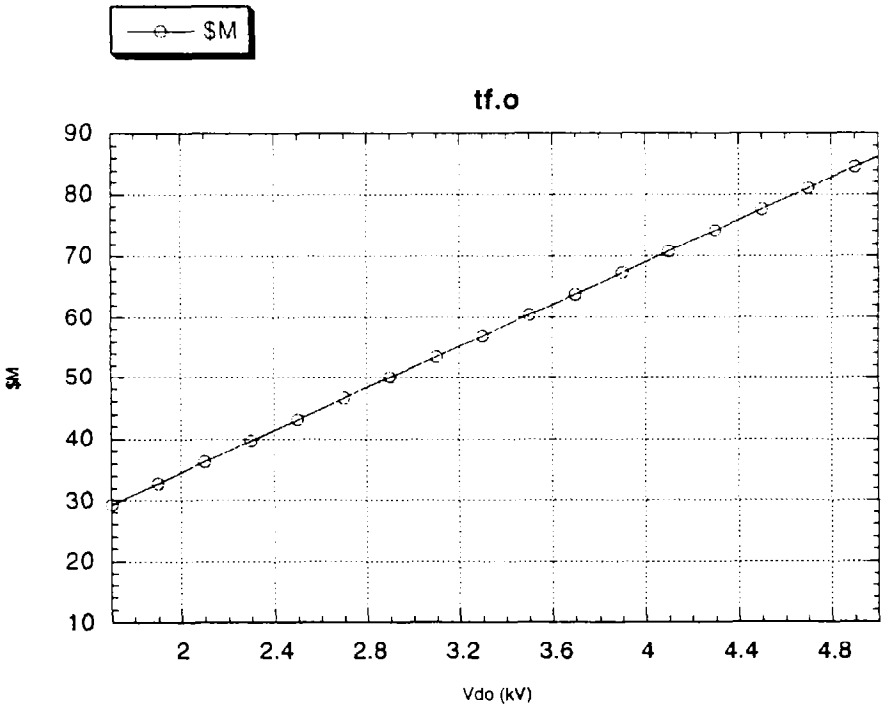

Figure 4.4-4: Cost vs. Open Circuit Voltage

Cryogenic System Aspects

Studies by A. Brooks (PPPL) indicate that in a scenario which uses a 30K initial TF coil temperature, 28GJ of heat must be removed in cooling the TF coil system between pulses, and that a two stage refrigeration system involving the temperature ranges 300-85K, and 85-30K, would have to remove 10 and 18 GJ, respectively, out of the total 28GJ.

Studies by D. Lang[8] (LLNL) resulted in the following observations:

1) 30% pumping losses need to be added to the heat load due to the I^2 R losses
2) A liquid nitrogen refrigeration plant may be characterized as follows:

- 10 watt AC input power per watt refrigeration power
- $13.6/watt of refrigeration power, including AC power system costs

3) A 30K helium refrigeration plant may be characterized as follows:

- 68.3 watt AC input power per watt refrigeration power
- $100.0/watt of refrigeration power, including AC power system costs

Tradeoff

The cases of 80K and 30K initial temperature are compared in Table 4.4-1.

The power supply costed is based on the energy loss (per the previous set of curves, 28GJ loss, 30K initial temperature corresponds to a 2.2kV supply, 260MW max power, whereas 77GJ loss 80K initial temperature corresponds to a 3.8kV supply, 540MW max power).

Cost reductions in the MG system are accounted for, since the size of the PCAST MG system could be reduced if the peak TF power was reduced.

---

[8]"PCAST Cryogenic System Scoping", D. Lang (LLNL) 6 November 1995

The conclusion of the study is that the use of 30K initial temperature does not result in a significant cost savings. Furthermore, if one includes the additional losses due to magnetoresistivity the cost advantage of the 80K initial temperature would prevail. The approximate impact of magnetoresistivity (which have not been analyzed for the TF current profile now being considered) is indicated in the second part of the spreadsheet.

Table 4.4-1: Cost Comparison of 30K and 80K TF Systems

80K vs. 30K Initial TF Temperature (w/o Magnetoresistivity Considerations)....

		80K TF	30K TF	ΔCryo Cos	ΔPS Cos	ΔCost
TF Energy Dissipation	GJ	77.0	28.0			
TF Peak Power	MW	540.0	260.0			
PS Cost	$M95	67.0	42.0		-25.0	-25.0
MG Cost	$M95	80.1	38.6		-41.5	-41.5
30K TF Loss	GJ	0.0	18.0			
80K TF Loss	GJ	77.0	10.0			
Pulses per day		5.0	5.0			
Pumping loss multiplier		1.3	1.3			
Avg 30K Cryo Power	MW	0.0	1.4			
Avg 80K Cryo Power	MW	5.8	0.8			
30K Watt AC/Watt Cryo		68.3	68.3			
80K Watt AC/Watt Cryo		10	10			
Avg 30K AC Power	MW	0.0	92.5			
Avg 80K AC Power	MW	57.9	7.5			
Tot Avg AC Power	MW	57.9	100.1			
30K Cost/Watt	$95/Watt	100.0	100.0			
80K Cost/Watt	$95/Watt	13.6	13.6			
30K Cryo Cost	$M95	0.0	135.4	135.4		135.4
80K Cryo Cost	$M95	78.8	10.2	-68.6		-68.6
Delta Costs	$M95			66.9	-66.5	0.3

Example of Magnetoresistivity Effect on TF (180s ramp up/down, 120s flat top)....

	30K		50K		80K	
	R	P	R	P	R	P
w/o MR	2.94E-03	90.1	5.88E-03	180.1	1.45E-02	443.7
w/MR	4.85E-03	148.4	7.22E-03	221.1	1.54E-02	470.3
ΔP(EOFT)%		64.7		22.8		6.0

Summary and Conclusions

A preconceptual design has been developed for the PCAST machine, and a simulation of the performance of the system was used to determine the required ratings of the Power Systems components. The constraint on available grid power established by ITER was applied to the PCAST machine. The power consumption of the PCAST machine exceeds that of ITER due to 1) the use of copper instead of superconducting magnets and 2) the faster ramping of the TF and PF currents. In order to supply the extra power and energy a supplemental Energy Storage System is required for PCAST, but not for ITER.

The quench protection discharge circuits required for the ITER superconducting magnets are not required for PCAST. However, PCAST still requires a (relatively small) Switching Network for plasma initiation.

PCAST uses internal control coils, whereas ITER does not.

The cost basis of the ITER Power Systems is well developed and documented, and was used to arrive at a comparable estimate for the PCAST Power Systems. The PCAST costs for the Experimental Power Systems are slightly less than those of ITER, owing mainly to the fact that the increase in power and energy demand due to the use of copper instead of superconducting magnets on PCAST is offset by the absence of requirements for complex quench protection discharge circuits on PCAST. The Auxiliary Power Systems cost is less due to the smaller demand of the PCAST machine.

Section 4.5: CODAC and Section 4.6: Interlocks (S. Davis)

Introduction

The Command Control and Data Acquisition (CODAC) system is responsible for the central instrumentation and control for the PCAST machine. Its major responsibilities include the Supervisory Control System, the Machine Control System, the Diagnostic Control System, the Data Management System, the Synchronization System, the Network and Communication System, and the Supervisory Interlock System.

The basic design requirements for central instrumentation and control are high duty cycle, safe and reliable operation using robust, redundant, standardized systems, and efficient operation, both locally at the tokamak site and at remote sites. In addition, there must be near real-time access to a variety of plasma parameters.

The cost estimate depends most heavily on assumptions about; 1) the total data load and the characterizations of the various types of data to be acquired, 2) the networking capacity that will be required, and 3) projections of cost/capacity trends within the rapidly changing computer industry.

This PCAST estimate is based on the previous cost estimate developed for ITER (1, 2) and takes into account primarily the reduced pulse length and duty cycle.

Data Management

Quantities of experimental, control and plant monitoring data, including video sources, are described in Table I, along with the data compression ratios which have been used in extrapolating the total acquisition and storage load. Intelligent front-end processors located at the data sources are assumed to do most of the compression before forwarding the data over a network to the data management system.

The maximum length of one shot is assumed to be 160 seconds with a maximum of 5 such shots per day providing a maximum daily machine duty cycle of 800 seconds per day. Some data, such as plant monitoring data, will be acquired continuously, for 86,400 seconds per day.

Table I - PCAST Data Requirements

Physics Data	**110 GB/day**
Slow Data Fast Data	5000 channels @ 1 KHz, 3:1 compression, during entire shot
Burst	1000 channels, rates from 100 KHz - 100 MHz, (aggregate limit of 8 GB/ shot) No compression
Trending	1000 channels, 1K snapshot, 30 times per second, Exceedingly compressible, assume wavelet 30:1
Diagnostic Video	20 cameras, 30 frames/sec, 200x200 pixels/frame Good compression, 10:1
Plant Data	**36 GB/day**
Plant Monitoring	90,000 monitor points, 1 sample per second, Day and Night
Site Video	100 cameras, 1 frame/sec, 640x480 video frame; Day and Night , Mostly similar pictures, 20:1 compression (Real-time full 30 frame/sec video sent over Video network; this quantity is only the amount to archive)
Plasma Control	500 points @10 KHz, During the shot only; 3:1 compression
Results Data	**21 GB/day** Estimated as 10% of raw data, not compressible
Total Data	**167 GB/day (w/compression)**

It is further assumed that data acquired at rates of less than about 1 KHz will be archived and available forever.

To accommodate diagnostic data with sampling rates from 10 KHz to 200 MHz, or higher, three different strategies have evolved. Each system is

assumed to sample continuously at its base sampling rate (a 'typical' rate of 100 MHz is used for the calculations of data quantity).

The first method is 'trending'. A snapshot of 1,000 samples will be forwarded 30 times per second, to drive continuous data displays. This data will also be archived, heavily compressed, as a low-resolution record of the data.

The second and third methods fall under the category of burst mode capture. The second method is event-driven, in which preprogrammed and plasma-event-driven triggers cause the data to be archived in narrow windows at the full base sampling rate.

The third method is interactive. Since each subsystem will have the local capacity to store many seconds of data, any of the trending data that is interactively selected will automatically become 'interesting' data, and fully archived throughout the region of interest.

To provide estimates for long term storage requirements, we have assumed that 1 years worth of data will required on-line and ten years worth of data will be required to be accessible within 5-15 minutes (from a tape silo).

Engineering and Diagnostic Systems

At the time of this estimate, limited information is available about the requirements for either engineering or diagnostic subsystems. However, the subsystem I&C costs are not historically included in the central I&C cost estimates. The main effort associated with these systems is in defining interfaces and providing tools for subsystem development and testing. The effort also include roughly one console per subsystem. This effort scales somewhat with the number of subsystems, but is not related to the size of the machine or data load, and is unchanged from the earlier estimate.

Conceptual Design

Given the limited scope of the study reported herein, and the similarity of the poloidal field control task to that of ITER, studies of the PCAST poloidal control system were not performed except that preliminary analyses of the basic scenario, start up, and fast control requirements were undertaken in order to formulate a design basis for the PF and FPPC coils and power systems. These are discussed in detail in the Physics chapter and are summarized as follows.

a) Several iterations on the fiducial static equilibria were performed and a baseline scenario was adopted which satisfies the thermal and stress criteria.[1] The feasibility of the scenario was confirmed using the Tokamak Simulation Code (TSC).

b) An initiation sequence was examined[2] in which the plasma is centered at Ro = 6 m with 0.5 m minor radius and a breakdown voltage of 15 V is applied with an initial flux bias of 108 V-s. A total of 7.3 V-s is consumed during the sequence. The field null quality specifications, $|Bp| < 2.5$ mT, were met within the circle of 0.5 m radius centered at Ro = 6.0 m during the breakdown.

c) Vertical Stability, Vertical Position Control, and Radial Position Control were examined[3]. With due consideration of the effect of the vacuum vessel the growth time for vertical motion was found to be consistent with reasonable requirements for vertical position control. Several control coil locations were examined, and a baseline consisting of separate coil pairs for the vertical and radial control functions was adopted. A location of R=5.4, Z=+/-2.4m was chosen for the vertical control coil pair, and R=6.6m, Z=+/-1.4m for the radial control coil pair. For vertical control, assuming the least stable plasma configuration at SOF, and a 1 cm RMS random displacement with a 60 ms time-scale, the required peak current and voltage were determined to be 100kA-turn and 100V/turn (total peak power of 20MW). Similarly for radial control, assuming the flat top plasma at full

---

[1] "Fiducial States Satisfying Thermal Criteria", R. Bulmer (LLNL), 18 October 1995
[2] "Startup Calculation with 15V Breakdown Voltage for PCAST Machine", P. W. Wang (MIT), 18 October 1995
[3] C. Kessel write-ups provided to H. Neilson

beta, and a 20% thermal drop every 500 ms the required peak current and voltage were determined to be 200 kA-turn and 400 V/turn (total peak power of 160MW).

Since the scope and scale of the Poloidal Control Systems for PCAST would be very similar to those of ITER, the ITER cost estimate is applied equally to the PCAST machine.

Section 6.2: Facilities (D. Knutson)

6.2 INTRODUCTION

The smaller configuration of the PCAST machine and the use of liquid nitrogen cooling for the TF and PF coils are two significant factors to be considered in comparing the cost of the PCAST and ITER facilities. Since the siting of neither of these machines has been determined, the facilities for the PCAST machine must be based on the same assumptions used to develop the design and cost estimates for ITER. The designs of individual ITER buildings were based on stated requirements, however the "green field" siting involved certain additional assumptions. For example, seismic characteristics, meteorological characteristics, capacity to dissipate heat to the environment, sufficient steady state electric power, sufficient supply of water, availability of a trained workforce, an industrial socioeconomic infrastructure, access to all forms of transportation, etc., were among the considerations.

The approach to be used in estimating the cost of facilities for the PCAST machine will simply consist of reviewing the ITER facilities to determine what effect the smaller configuration and other differing requirements will have on the ITER cost estimate. Scaling factors will be applied on an individual basis to the various buildings in the ITER complex. A number of buildings will not be affected by the PCAST requirements. For example, the Tokamak Control Building, the Site Services Building, and the Emergency Power Generating Building would not be expected to change as a result of adopting the PCAST design. Two new buildings will be required for PCAST, an MG power supply building and a liquid nitrogen refrigeration building. The cost of these buildings will be independently estimated and added to the PCAST estimate.

6.2 .1 THE ITER FACILITIES

The ITER building layout, shown in Fig. 6.2.1-1, occupies an area of 73.4 hectares (≈ 181.4 acres). The buildings and other areas have been numbered according to the key on the layout drawing. The buildings can be grouped according to function as follows:

Tokamak Building Group
- Tokamak Building: Tokamak Hall (1), Assembly Hall (2), Laydown Hall (3)
- Tritium Building (5)
- Electrical Termination Building (7)
- Tokamak Services Buildings (6)

Cryoplant Group
- Cryoplant Compressor Building (10)
- Cryoplant Cold Box and Dewar Building (11)

Assembly Support Group
- Poloidal Field Coil Fabrication Building (25)
- Magnet Cold Test Building (26)
- Assembly Laydown and Storage Building (28)

Magnet and Heating Power Supply Group
- Power Conversion Buildings (13)
- Magnet Power Supply and Switching Network Building (12)
- Neutral Beam Power Conversion Building (15)
- RF Auxiliary Heating Power Conversion Building (14)

Hot Cell and Radwaste Group
- Hot Cell Building (4)
- Low Level Radwaste Building (8)
- Personnel Building (9)

Operations Building Group
- Tokamak Control Building (23)
- Emergency Power Generating Building (21)

Site Infrastructure Group
- Laboratory Office Building (22)
- Site Services Building (24)
- Remote Handling Mockup Building (27)
- Site Improvements:
  Switchyards, Utility Tunnels, Fences, Roadways, Outdoor Structures and Lighting, Cooling System Basins, etc.

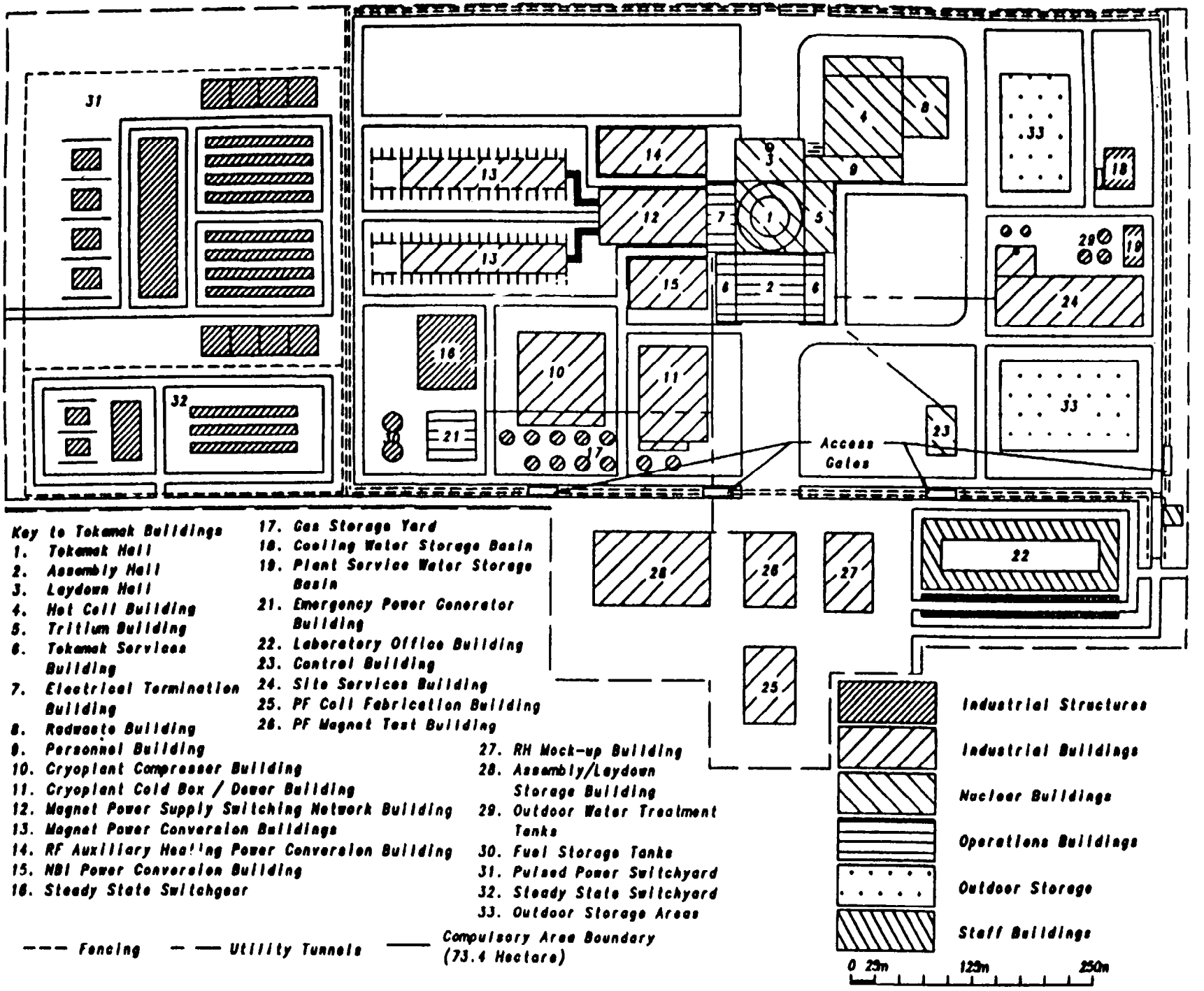

ITER BUILDING LAYOUT

FIG. 6.2.1-1

The adoption of the PCAST design would affect all of the ITER Facility Groups with the possible exception of the Hot Cell and Radwaste Group. The Tokamak Building, consisting of the Assembly Hall, the Tokamak Hall, and the Laydown Hall, is one of the more complex buildings and one of the primary ITER areas that will be affected by the PCAST design. Drawings of the ITER Tokamak Building are shown in Plan View (Fig. 6.2.1-2), North-South Section (Fig. 6.2.1-3), and East-West Section (Fig 6.2.1-4). A second major area affected by the PCAST design is the Cryoplant Group. The Cryoplant Compressor Building and the Cryoplant Cold Box and Dewar Building, however, are comparitively simple and will be affected largely in floor area. Consequently, drawings have not been included in this report for the ITER Cryoplant Group and other ITER Groups affected by the PCAST proposal.

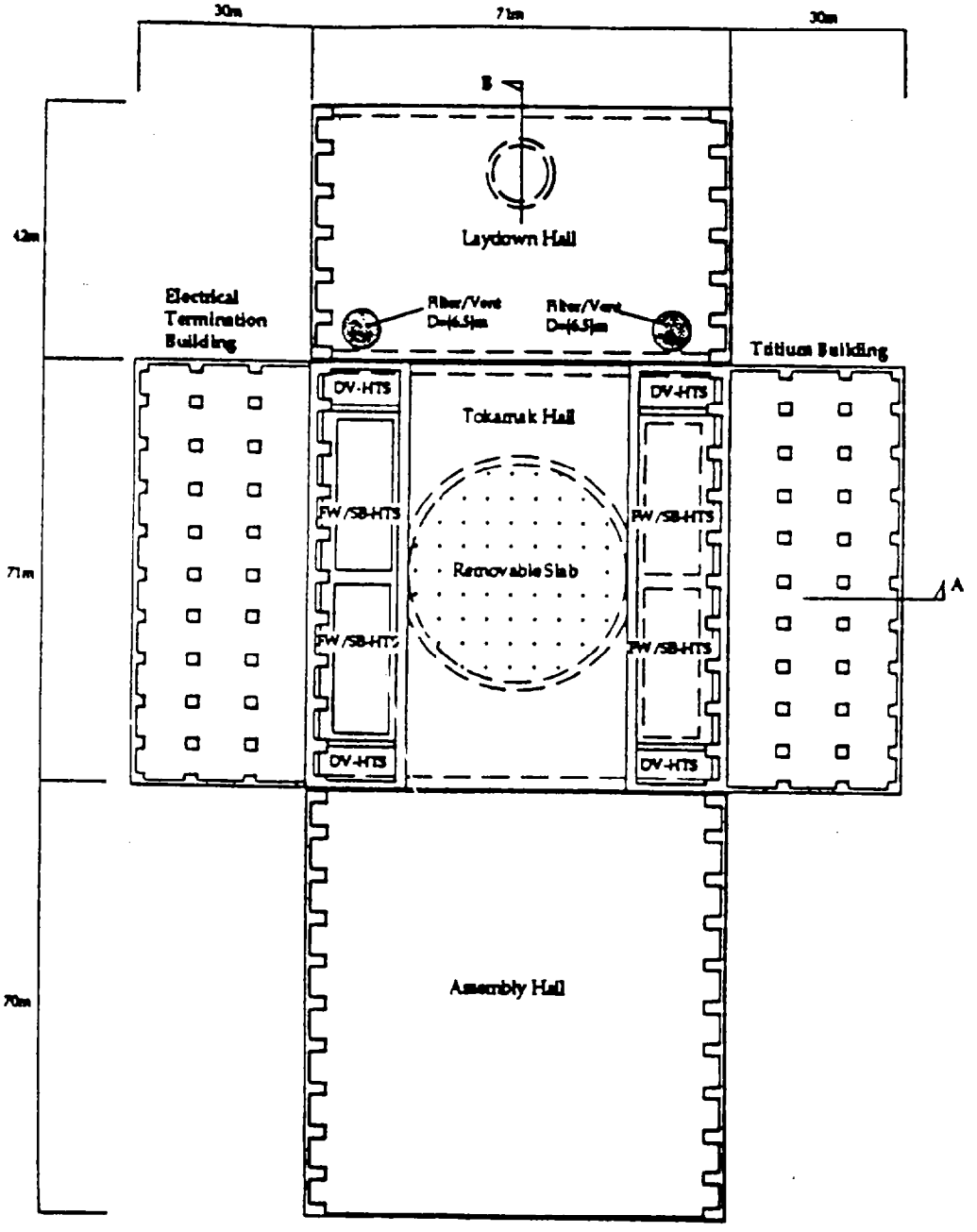

ITER TOKAMAK BUILDING
PLAN VIEW AT GRADE ELEVATION

FIG. 6.2.1-2

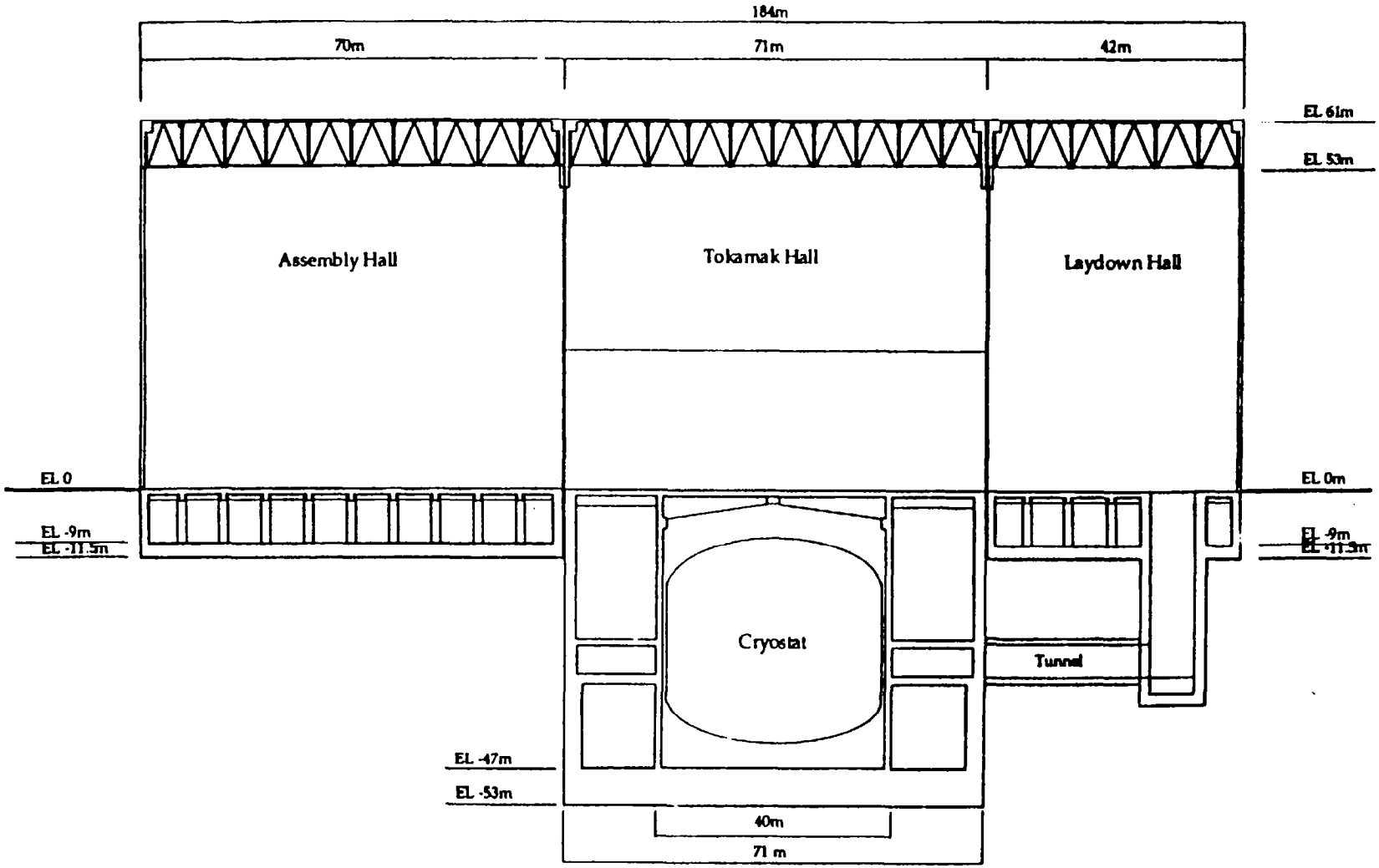

ITER TOKAMAK BUILDING
NORTH-SOUTH SECTION

FIG. 6.2.1-3

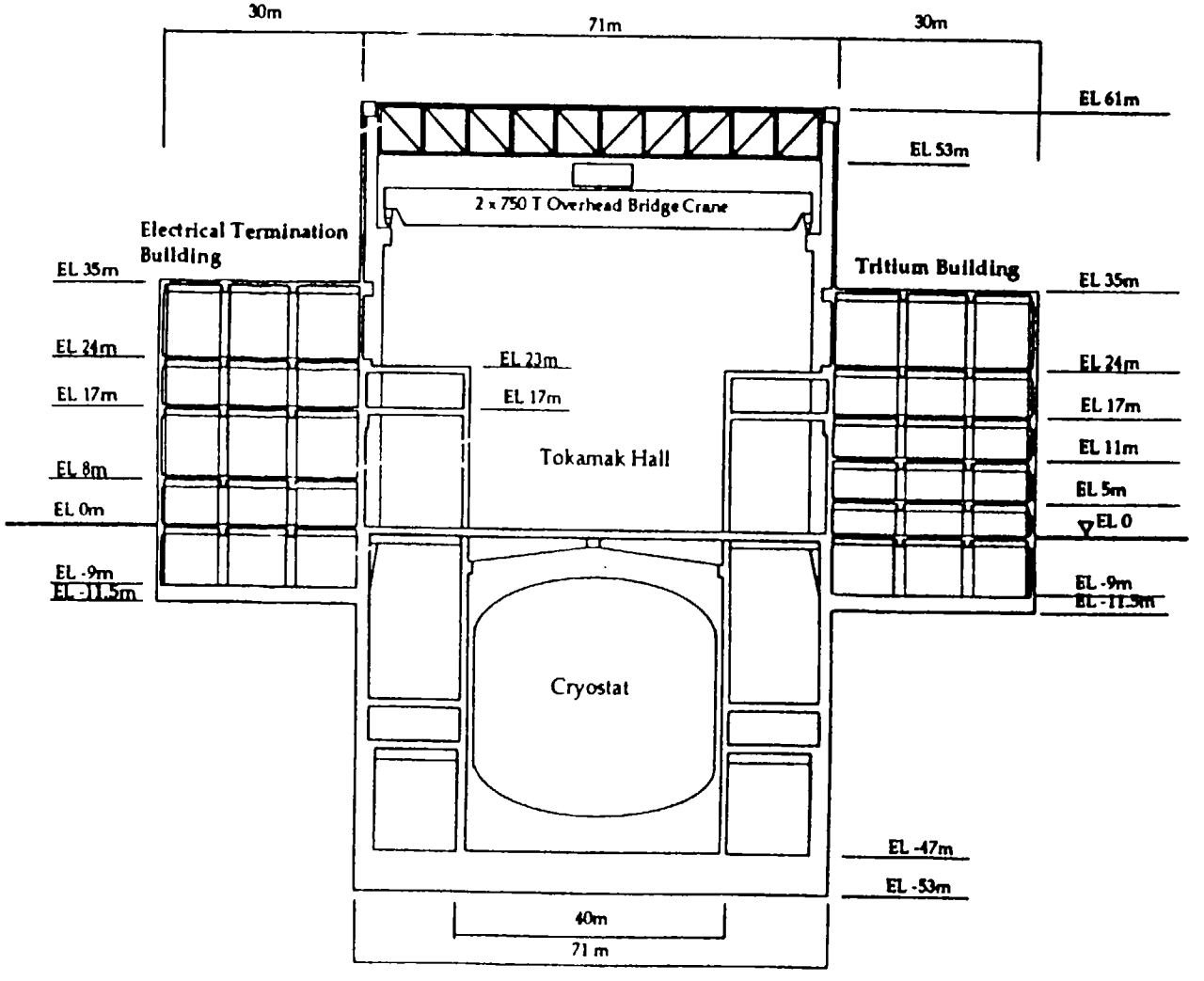

ITER TOKAMAK BUILDING
EAST-WEST SECTION

FIG. 6.2.1-4

6.2 .2 ITER FACILITY COST ESTIMATE

The cost estimate for theITER buildings is shown in Table 6.2.2-1. The buildings are keyed to the ITER building layout, Fig. 6.2.1-1. Parameters include the building footprint, gross volume, structural steel and concrete, and the floor area. The cost of the ITER facility totals $891M in FY89 dollars. It should be noted that these costs include the A/E Title I and Title II costs. Engineering and design of the buildings would be subcontracted to industry.

PARAMETERS						ESTIMATE '89 MS's)		
Bldg. #	Footprint	Gross Volume	Structural Concrete	Structural Steel	Floor Area		UNIT COSTS	
	m2	m3	m3	tonnes	m2	M$	$/m2	$/m3
1,2,3	13,060	1,060,000	160,370	18,980	35,790	363	27,894	343
4	8,000	164,800	50,500	0	20,800	92	11,492	558
5	2,130	89,460	21,810	2,500	12,780	44	20,824	496
6	2,804	117,600	6,400	2,500	11,200	35	12,655	302
12,13,14,15	25,250	396,200	24,510	5,630	37,700	71	2,810	179
Stack	100	na	na	na	na	2	na	na
8,9	5,260	50,000	10,750	0	6,480	16	3,066	323
22	8,460	70,270	10,480	1,800	17,570	23	2,669	321
10,11	15,600	381,800	12,830	2,000	15,550	62	3,981	163
23	2,600	34,800	9,890	0	5,760	12	4,652	348
21	2,500	17,500	3,370	0	2,500	6	2,258	323
24	8,100	103,000	8,100	2,070	8,100	19	2,290	180
28	9,000	108,000	9,000	1,500	9,000	15	1,613	135
25	4,030	69,000	4,030	850	4,030	10	2,602	152
26	4,030	84,900	4,030	1,020	4,030	13	3,202	152
tunnels	na	na	na	na	na	31	na	na
31,32	na	na	na	na	na	7	na	na
7	2,130	89,460	21,010	2,300	10,650	35	16,659	397
27	4,000	228,160	10,910	2,300	5,950	35	8,871	156
Bldgs. total	117,054	3,064,950	367,990	43,450	207,890	891		

Number Key:

Tokamak building	1,2,3
Hot Cell Building	4
Tritium Building	5
Tokamak Service Building	6
Auxiary Building	12,13,14,15
Plant Effluent stack	stack
Radwaste and Personnel Building	8,9
Laboratory Office Building	22
Cryoplant Building	10,11
Control Building	23
Emergency Power Building	21
Site Services Building	24
Assembly laydown storage building	28
Poloidal Field Coil Fab Building	25
Magnet Test Building	26
Utility Tunnels and site improvement	tunnel
Switch yard and Misc Buildings	31,32
Electrical Terminations Building	7
Remote Handling Mockup Building	27

ITER FACILITY PARAMETERS & COST ESTIMATE

TABLE 6.2.2-1

6.2. 3 EFFECT OF PCAST ON ITER FACILITIES

Tokamak Building (1, 2, 3)

The Tokamak Building has undergone a major change as a result of the PCAST configuration and consequently has been redrawn as shown in Plan View (Fig. 6.2.3-1), East-West Section (Fig. 6.2.3-2) and North-South Section (Fig. 6.2.3-3). The Tokamak Hall in the center of the structure includes the tokamak pit in which the cryostat containing the tokamak is located. The pit has been reduced in size reflecting the smaller dimensions of the PCAST cryostat. The annular space surrounding the cryostat biological shield contains several levels and is used for neutral beams, RF launchers, remote maintenance and auxiliary equipment. It was assumed that this equipment would basically occupy the same radial dimension and therefore the radial dimension of the annular space was not reduced for PCAST. The upper portion of the Tokamak Hall was reduced in area and height to reflect the new pit dimensions and reduction in cryostat height.

The adjacent Assembly Hall located south of the Tokamak Hall was reduced to reflect the reduction in size of the machine components. The area in the basement of the Assembly Hall contains a neutral beam test cell and some neutral beam power supply equipment. This area is also available for diagnostic operations. The Laydown Hall to the north of the Tokamak Hall is intended for storage of machine components. Since the individual components are not expected to differ appreciably in size, the area underwent a relatively smaller reduction than the Assembly Hall. The space in the Laydown Hall basement is dedicated to remote handling operations, and is connected to the annular space around the cryostat biological shield by means of a vertical shaft and tunnel providing a passageway for the transfer of components requiring remote maintenance. Remote maintenance control and actuation systems are also located in the Laydown Hall basement.

The new dimensions of the PCAST Tokamak Building result in a scaling factor of 0.71 in the floor area when applied to the ITER design.

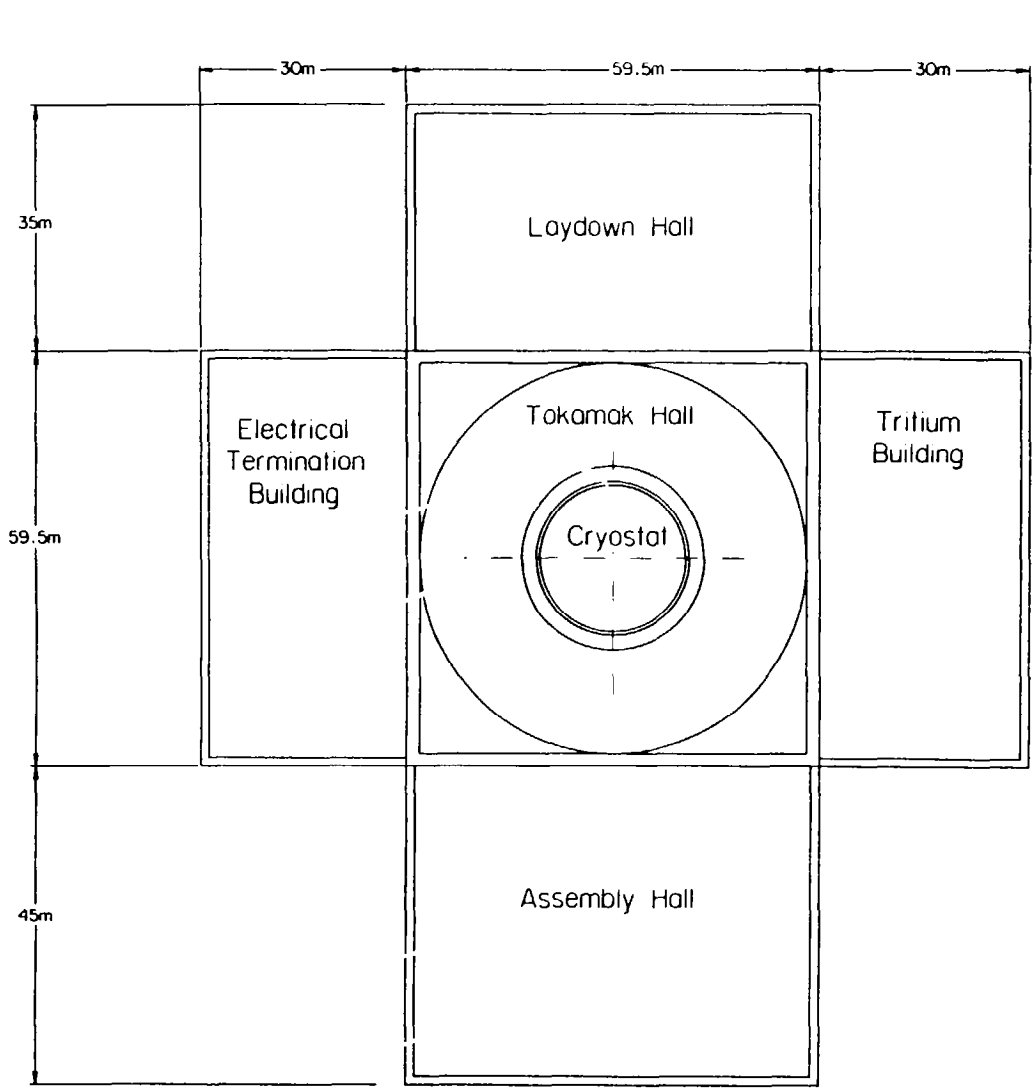

PCAST TOKAMAK BUILDING
PLAN VIEW AT GRADE ELEVATION

FIG. 6.2.3-1

TOKAMAK BUILDINGS
PCAST STUDY
PLAN VIEW
C. WENDLAND
11-15-95

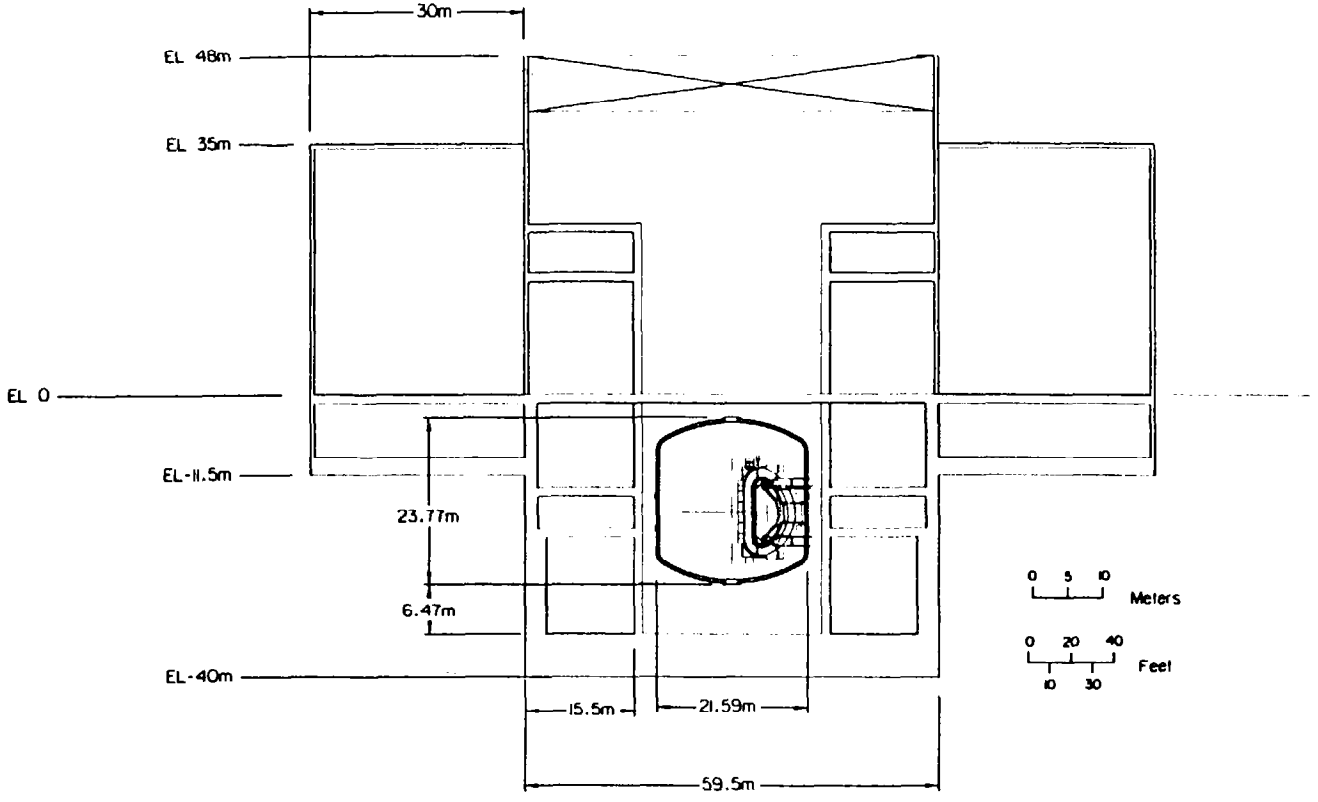

PCAST TOKAMAK BUILDING
EAST-WEST SECTION

FIG. 6.2.3-2

TOKAMAK HALL
PCAST STUDY
EAST-WEST SECTION
C. WENDLAND
11-15-95

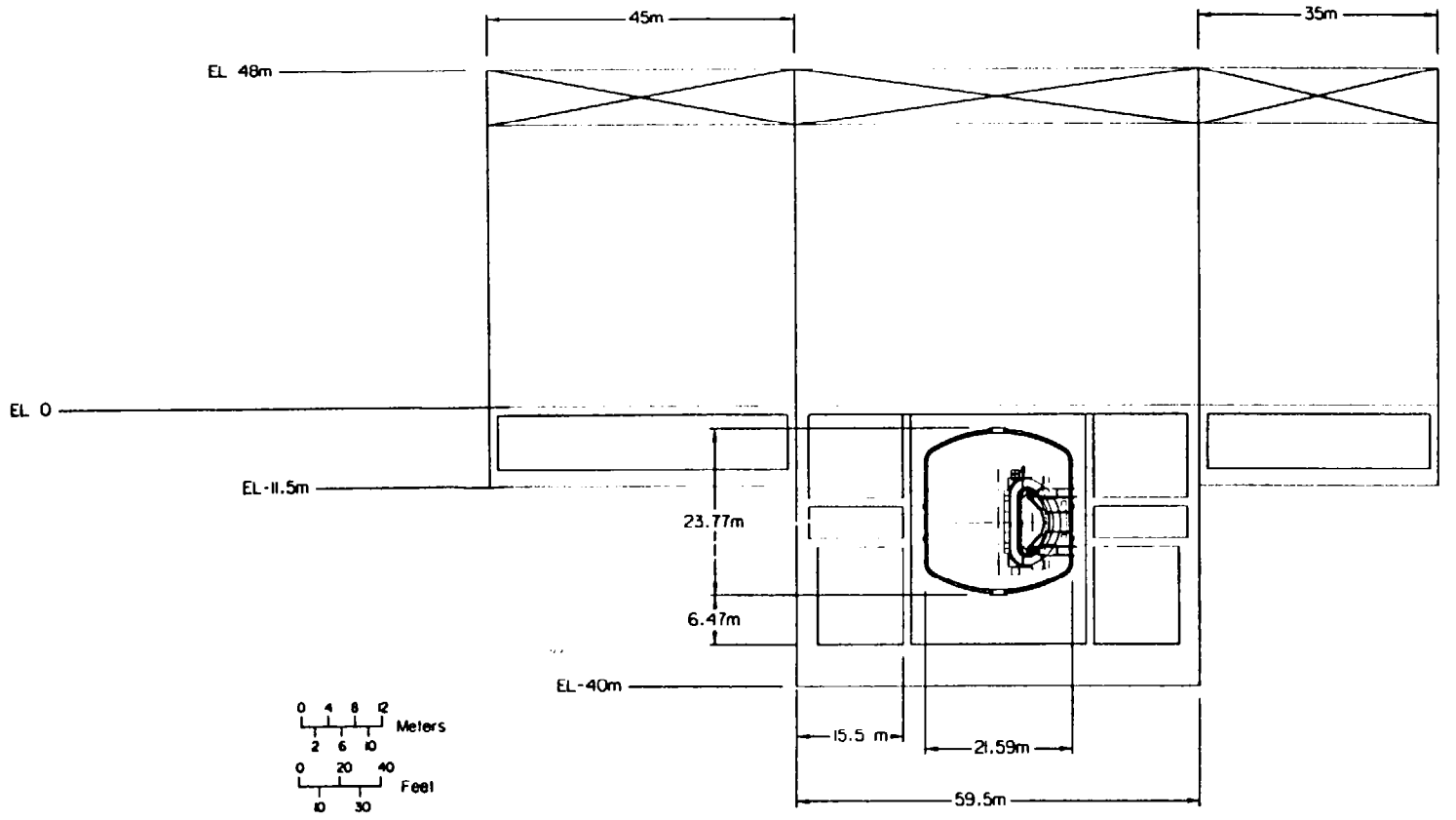

PCAST TOKAMAK BUILDING
NORTH SOUTH SECTION

TOKAMAK HALL
PCAST STUDY
NORTH-SOUTH SECTION
C. WENDLAND
11-15-95

FIG. 6.2.3-3

Hot Cell Building (4)

The Hot Cell Building provides space for decontamination and waste processing. In particular the building is designed for the reprocessing of divertor cassettes. Based on an evaluation described in section WBS 6.3 of the report, a scaling factor or 0.50 is applied to the floor area.

Tritium Building (5)

The Tritium Building houses the tritium storage and processing facilities including the Exhaust Gas Processing System, the Fuel Cleanup System, the Isotope Separation System, the Fuel Storage System, the Water Detritiation System, and the Atmosphere Detritiation System. It is estimated that the PCAST machine will require 1.4E23 tritons or 6700 curies per pulse. At 5 pulses per day this equates to 33,500 curies. ITER has ~ 5 times the volume and ~ 8 times the pulse length of PCAST, so its requirements would be a factor of 40 higher. The Tritium Building provides space for the vacuum pumping system, a tritium laboratory, changing areas for personnel, maintenance areas, and areas to accommodate a control system and a DT storage and distribution system. A scaling factor of 0.40 is applied to the floor area.

Tokamak Services Building (6)

The Tokamak Services Building actually consists of two buildings similar in size and located east and west of the Assembly Hall. The building houses the secondary heat transfer system for the first wall and divertor, for plasma heating, for diagnostics, and for the test module. In addition, the building provides space for the chilled water distribution system. Work areas for maintenance functions must abe accommodated. It is assumed that the Tokamak Services Buildings would scale with the linear dimension of the Assembly hall but maintain the same width. This would result in a scaling factor of 0.70 applied to the floor area.

Auxiliary Buildings (12. 13, 14, 15)

The Auxiliary Buildings consist of five independent structures. A magnet power supply switching network building (12), two power conversion buildings (13), an ICRF/ECRF power supply building (14), and a power supply building for neutral beam (15).

The Magnet Power Supply Switching Network Building (12) basically provides quench protection for superconducting coils. This building would not be necessary for PCAST. The scaling factor is therefore 0.00.

The TF/PF Power Conversion Buildings (13) would be larger than ITER because the PCAST TF/PF coils are not superconducting. The scaling factor applied to the floor area will be 1.48 for PCAST.

The ICRF/ECRF Power Conversion Building (14) and the Neutral Beam Power Conversion Building (15) can be scaled based upon the power generated. ITER power to the plasma is 100 MW. ITER assumes an efficiency of 33-1/3%, therefore power generated is 300 MW. PCAST power to the plasma is 60 MW. PCAST assumes an efficiency of 50%, therefore power generated is 120 MW. The resulting scaling factor is 120/300 or 0.40 applied to the floor area.

An MG Building will be required for PCAST. This will be a new building and will house 4 MG sets similar in size to TFTR. TFTR has 2 MG sets (950 MVA), therefore a building twice the size of the TFTR MG complex would be required for PCAST. The present TFTR MG building floor area is 42,000 ft^2 or 3716 m^2. Four MG sets of the TFTR size would require a floor area of 7432 m^2. Based on actual building costs corrected to FY89, the cost of a new MG building would be $20 M.

Plant Gaseous Effluent Stack

The primary function of the Plant Gaseous Effluent Stack is to provide an elevated release point for all gaseous effluents which may contain radioactive or hazardous materials. It is assumed that there would be little change in the requirements for PCAST. The resulting scaling factor is 1.0.

Radwaste & Personnel Buildings (8, 9)

The building provides space for the liquid waste processing system, the dry waste processing system, shipping and receiving activated and processed material, an analytical chemistry laboratory and change areas and other amenities of personnel. It is assumed that the reduction in neutron fluence and the smaller size of the PCAST machine would affect the amount of radwaste material produced in the lifetime of the machine. The neutron load in ITER is 1.0 MWa/m^2 compared to 0.01 MWa/m^2 for PCAST, a factor of 100 less. The major radius of PCAST is approximately 60% that of ITER. The PCAST Radwaste & Personnel Building floor area has been taken as 33% of the ITER building area.

Laboratory Office Building (22)

The primary function of the Laboratory Office Building is to provide office space for the scientists, engineers, administrators and support personnel assigned to the ITER site. The building is designed for offices, computer network equipment, meeting rooms, a library, and amenities for an occupancy of 750 personnel. The size of the Laboratory Office Building will be reduced to reflect an anticipated 25% reduction in staff for PCAST. The reduction in staff will result in a scaling factor of 0.75 applied to the floor area.

Cryoplant Buildings (10, 11)

The ITER cryoplant consists of two buildings. The Cryoplant Compressor Building houses the compressor portion of the liquid helium refrigeration and supply system, and the Cryoplant Cold Box/Dewar Building houses the expander portion of the liquid helium refrigeration system including liquid helium circulation pumps and tanks for volume control of the liquid and gas phases of cryogenic helium. The refrigeration capacity for the PCAST machine will require 83KW of gaseous helium at 30°K plus 8200KW of liquid nitrogen at 80°K. Scaling from the MFTF-B 11KW refrigerator, the size required for the PCAST helium system would be approximately 1200 m^2, or a factor of 0.08 relative to ITER. Based on MFTF-B experience, the helium refrigeration capacity of the cryoplant at 30°K is approximately 6 times higher than the capacity at 4.5°K. The 150KW ITER cryoplant is therefore capable of producing 900KW of helium at 30°K. Since only 83 KW is required, a scaling factor of 83/900 or 0.09 can be applied to the ITER facility for helium. As this is a slightly more conservative value, it will be used for scaling, and it results in an estimated area layout of 1,400 m^2 for the helium building. An 8200 KW liquid nitrogen plant will require a floor area of 5700 m^2. This is based on the scaling of the MFTF-B 500KW reliquifier, as well as using current manufacturer's estimates for the amount of space required for each 1 MW 80K refrigerator. The building cost per square meter of the liquid nitrogen plant would be comparable to the ITER costs.

Tokamak Control Building (23)

The Tokamak Control Building provides space for the CODAC (Control and Data Acquisition) system, the plasma control supervisor system, interlock system, vacuum pumping control system, diagnostic data acquisition system, radiation monitoring system, etc. In addition, the area will house the on-line computer control system. It is assumed that the PCAST control building will provide space for similar systems and personnel, therefore a scaling factor of 1.0 will be applied.

Emergency Power Supply Building (21)

The Emergency Power Supply Building is designed to accommodate the emergency generator units which provide emergency power to the loads on the emergency power buses within the ITER plant. In addition, the building provides space for the electrical power control room, maintenance shops, and fire fighting equipment. The functions and the space required would be similar for PCAST therefore a scaling factor of 1.0 will be applied.

Site Services Building (24)

The Site Services Building houses a variety of site services including potable water, deionized water plant, chilled water, low pressure steam generation,

compressed air, non-toxic storage, maintenance, etc. Similar services will be required for PCAST therefore a scaling factor of 1.0 will be applied.

Assembly Laydown and Storage Building (28)

The Assembly Laydown and Storage Building is designed to house and provide storage of large tokamak components which require a protected environment prior to installation. Since the PCAST components are smaller, the length and width of the building were reduced by 5/8 but with the same height. The resulting scaling factor is 0.40 applied to the floor area.

Poloidal Field Coil Fabrication Building (25)

The Poloidal Field Coil Fabrication Building has to accommodate the equipment and systems used to fabricate the ITER PF coils. The largest PCAST PF coils (~ 20.4 m in diameter) are smaller than the largest ITER coils (~ 32 m in diameter), but still too large to be shipped to the site. The working area of the ITER Poloidal Field Coil Fabrication Building has been reduced proportionally. Offices and machine shop areas were not reduced. The resulting scaling factor is 0.60 applied to the floor area.

Magnet Coil Test Building (26)

The PCAST design specifies copper coils which should not require a pre-test, therefore the Magnet Coil Test Building would not be required. The scaling factor is 0.00.

Utility Tunnels and Site Improvements

It is assumed that the cost of utility tunnels and site improvements will be the same for ITER and PCAST. The resulting scaling factor is 1.0.

Switchyards and Miscellaneous Structures (31, 32)

There are two switchyards in the ITER facility layout. One is the Pulsed Power Switchyard and Miscellaneous Structures (31), and the other is the Steady State Switchyard and Miscellaneous Structures (32), Miscellaneous structures are also provided for the Cryoplant, Emergency Power Supply, Site Services area and the Cooling Towers. Basemats are provided for power supply equipment such as towers, transformers, etc. The Pulsed Power Switchyard (31) would remain the same for both ITER and PCAST as the power from the grid is equal. The Steady State Switchyard (32) for PCAST would be 70% of the size and cost required for ITER. Since the two switchyards are essentially equal in cost, the combined scaling factor is 0.85.

Electrical Termination Building (7)

The Electrical Termination Building is a five story building designed to accommodate the electrical feed equipment including the cabling and

switchgear up to the point at which the current leads become superconducting. The building is also designed to accommodate the auxiliary cold boxes and cold terminal boxes. In addition, space for diagnostics is provided as well as for the vacuum vessel air-cooled heat exchanger. The requirements for PCAST are different with LN2 and gaseous helium replacing LHe, however, the scope of the equipment is somewhat comparable. For PCAST the length of the Electrical Termination Building has been scaled to agree with the length of the Tokamak Hall. The width and height of the building have not been changed. The resulting scaling factor is 0.63 applied to the floor area.

Remote Handling Mockup Building (27)

The Remote Handling Mockup Building is a facility to perform verification tests of remote handling equipment, including preparation of the equipment for initial assembly operations and to develop equipment for ITER decommissioning. A test stand (mockup) will contain 3 segments of the vacuum vessel. In addition, the building will provide space for a control room and associated offices. For PCAST the length and width of the mockup itself can be reduced in proportion, however, the work area surrounding the mockup would remain about the same as ITER, and the area of the control room, office, and machine shop would also remain the same. The result is a scaling factor of 0.66 applied to the floor area.

Section 6.3; Waste Treatment and Storage (M. Rennich)

1. Item 6.3C includes two types of remote maintenance equipment; a series of machines to refurbish divertors and a multipurpose maintenance cell. The divertor refurbishment system would not be required for PCAST because the divertors are assumed to be replaced rather than repaired. The multipurpose maintenance cell(s) would be retained for the reasons stated in the ITER DDD 6.3 including cutting, welding, disassembly and reassembly of large components.

2. All other items in WBS 6.3 are required to perform waste management functions such as decontamination, storage, packaging and waste concentration and reduction. The quantity and scale of equipment required for these operations is estimated to be approximately 50% of that required for ITER. This estimation is based on a reduced low level waste volume due to fewer cleaning requirements, reduced component waste volume due to the smaller machine size and reduced storage because contaminated divertors modules are not recycled.

Section 6.5 LIQUID DISTRIBUTION SYSTEM (D. Knutson)

6.5.0 INTRODUCTION

The ITER Liquid Distribution System is basically a system of pumps, piping, valves, heat exchangers, steam generators, chillers, storage tanks, etc., for the distribution of potable water, demineralized water, steam, hot water, fire protection water, and chilled water to meet the requirements of the buildings and various systems on site. Included in the Liquid Distribution System is the monitoring, treatment and discharge of sewerage effluent and industrial waste water from the buildings and structures on site.

6.5.1 COST ESTIMATE

It is obvious that the same or similar systems will be required for PCAST. In the absence of any available detail in this area, and the time required to generate a bottoms-up estimate without the specific requirements, an attempt will be made to apply a scaling factor to the ITER estimate in order to arrive at a reasonable estimate for PCAST. There are two areas that would affect the Liquid Distribution System in a global sense; 1) the reduction in personnel staff required for PCAST, and 2) the reduction in area over which the distribution would take place.

There are no figures available for the staffing level required to operate the ITER complex, with the exception of the Laboratory Office Building where a reduction in administrative and professional personnel of 25% has been assumed (Ref. 6.2.3). There are other areas where buildings have been eliminated, or their operations greatly curtailed. For example, the reduction in the amount of decontamination and radwaste should result in a reduction of staff handling that function. Although a reduction in personnel would result in a reduction of some of the services provided by the Liquid Distribution System, no attempt is being made to develop a scaling factor reflecting this reduction.

The elimination of certain buildings and the reduction in size of many of the remaining buildings has resulted in an overall reduction in floor area (Ref. Table 6.2.4-1). The site layout would be more compact with reductions in the distances over which the distribution system must operate. The ITER floor area is 203,090 m^2 and the PCAST floor area is 131,302 m^2 resulting in a reduction ratio of 1.55:1 or a scaling factor of 0.65.

Section 6.6 GAS DISTRIBUTION SYSTEM (D. Knutson)

6.6.0 INTRODUCTION

The ITER Gas Distribution System basically supplies compressed air for a variety of applications throughout the ITER complex. It consists of compressors, receivers, dryers, storage tanks, and distribution systems. It also provides for storage of non-radioactive gases such as argon, nitrogen, etc., including distribution systems. Speicalty gases such as SF_6 are provided at the point of consumption. Breathing air systems are also included as part of the responsibility the ITER Gas Distribution System.

6.6.1 COST ESTIMATE

The same or similar systems will obviously be required for PCAST. Available detail is absent in this area, and time does not permit generating a bottoms-up estimate. In the absence of specific requirements, an attempt will be made to apply a scaling factor to the ITER estimate in order to arrive at a reasonable estimate for PCAST. There are two areas that would affect the Gas Distribution System in a global sense; 1) the reduction in personnel staff required for PCAST, and 2) the reduction in area over which the distribution would take place. In this sense it can be compared with the approach used in estimating the costs for WBS 6.5.

There are no figures available for the staffing level required to operate the ITER complex, with the exception of the Laboratory Office Building where a reduction in administrative and professional personnel of 25% has been assumed (Ref. 6.2.3). There are other areas where buildings have been eliminated, or their operations greatly curtailed. For example, the reduction in the amount of decontamination and radwaste should result in a reduction of staff handling that function. Although a reduction in personnel would result in a reduction of some of the services provided by the Gas Distribution System, no attempt is being made to develop and apply a scaling factor reflecting this reduction.

However, the elimination of certain buildings and the reduction in size of many of the remaining buildings has resulted in an overall reduction in floor area (Ref. Table 6.2.4-1). Consequently the site layout for PCAST would be more compact with reductions in the distances over which the distribution system must operate. The ITER floor area is 203,090 m^2 and the PCAST floor area is 131,302 m^2 resulting in a reduction ratio of 1.55:1 or a scaling factor of 0.65.

Section 6.7 General Test Equipment (J. Sinnis)

This WBS element for ITER includes the vacuum vessel/cryostat for testing the CS coil and PF coils 3,4,5,6,8, the vacuum system to evacuate the vessel/cryostat, power supply and quench protection equipment and monitoring and I&C equipment for the test.

The PCAST Machine would not require the same equipment as ITER but would require vacuum pumping and leak checking equipment to verify the field welds of the cryostat and vacuum vessel. This would include temporary blank-off flanges and special fixtures to isolate sections of the vessel and cryostat for testing as the welding proceeds.

The PCAST Machine coils would undergo acceptance testing at the vendor's plant before shipping. This would include ground plane insulation integrity tests (meggar and hi-pot), partial discharge tests and turn-to-turn testing. At the assembly site, a sub-set of these tests would be repeated to verify the quality of the insulation after assembly.

The leak checking fixtures and temporary blank-off flanges are estimated at 10% of the cost of the component being tested.

An allowance is made for the coil test equipment.